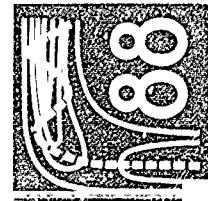


AD-A223 307	DTIC ACCESSION NUMBER		PHOTOGRAPH THIS SHEET		/																																																																		
		LEVEL	DTIC FILE COPY		INVENTORY																																																																		
		<div style="font-size: 18pt; font-weight: bold; margin-bottom: 5px;">R/D 5836-CH-02</div> <div style="font-size: 10pt; margin-bottom: 5px;">DOCUMENT IDENTIFICATION</div> <div style="font-size: 18pt; font-weight: bold;">29 JULY 1988</div>																																																																					
		DISTRIBUTION STATEMENT Approved for release Distribution																																																																					
DISTRIBUTION STATEMENT																																																																							
<table border="1" style="width: 100%; border-collapse: collapse;"> <tr> <td colspan="6" style="font-size: 8pt;">ACCESSION FOR</td> </tr> <tr> <td style="width: 15%;">NTIS</td> <td style="width: 15%;">GRA&I</td> <td colspan="4" style="text-align: center;"><input checked="" type="checkbox"/></td> </tr> <tr> <td>DTIC</td> <td>TAB</td> <td colspan="4" style="text-align: center;"><input type="checkbox"/></td> </tr> <tr> <td colspan="2">UNANNOUNCED</td> <td colspan="4" style="text-align: center;"><input type="checkbox"/></td> </tr> <tr> <td colspan="6">JUSTIFICATION <i>per form 8</i></td> </tr> <tr> <td colspan="6" style="height: 20px;"></td> </tr> <tr> <td colspan="6" style="font-size: 8pt;">BY</td> </tr> <tr> <td colspan="6" style="font-size: 8pt;">DISTRIBUTION /</td> </tr> <tr> <td colspan="6" style="font-size: 8pt;">AVAILABILITY CODES</td> </tr> <tr> <td colspan="2" style="font-size: 8pt;">DIST</td> <td colspan="4" style="font-size: 8pt;">AVAIL AND/OR SPECIAL</td> </tr> <tr> <td colspan="2" style="height: 40px; vertical-align: bottom; font-size: 18pt; font-weight: bold;">A-1</td> <td colspan="4"></td> </tr> </table>						ACCESSION FOR						NTIS	GRA&I	<input checked="" type="checkbox"/>				DTIC	TAB	<input type="checkbox"/>				UNANNOUNCED		<input type="checkbox"/>				JUSTIFICATION <i>per form 8</i>												BY						DISTRIBUTION /						AVAILABILITY CODES						DIST		AVAIL AND/OR SPECIAL				A-1					
ACCESSION FOR																																																																							
NTIS	GRA&I	<input checked="" type="checkbox"/>																																																																					
DTIC	TAB	<input type="checkbox"/>																																																																					
UNANNOUNCED		<input type="checkbox"/>																																																																					
JUSTIFICATION <i>per form 8</i>																																																																							
BY																																																																							
DISTRIBUTION /																																																																							
AVAILABILITY CODES																																																																							
DIST		AVAIL AND/OR SPECIAL																																																																					
A-1																																																																							
DISTRIBUTION STAMP		DATE ACCESSIONED																																																																					
		DATE RETURNED																																																																					
		REGISTERED OR CERTIFIED NO.																																																																					
DATE RECEIVED IN DTIC <div style="float: right; font-size: 18pt; font-weight: bold; margin-top: -20px;">1986</div>																																																																							
PHOTOGRAPH THIS SHEET AND RETURN TO DTIC-FDAC																																																																							



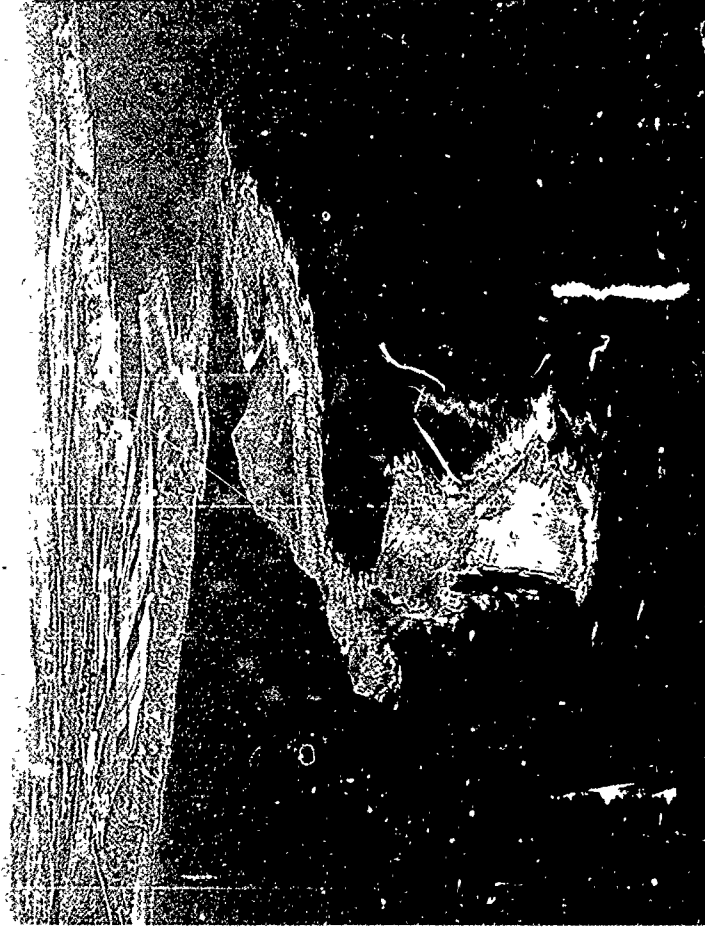
Tenth International Symposium on Gas Kinetics

University College of Swansea 24-29 July 1988

AD-A223 307

THE 10TH & 11TH INTERNATIONAL SYMPOSIUM GROUP (TNS)

U.S. GOVERNMENT PRINTING OFFICE: 1988

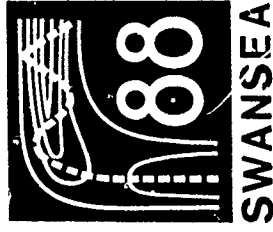


ABSTRACTS

TENTH INTERNATIONAL SYMPOSIUM ON GAS KINETICS

R/D 5836-CH-02

DATA 45-88-m-01D



University College of Swansea

24 - 29 July 1988

ABSTRACTS OF PAPERS

Organised by the Gas Kinetics Group, of the Faraday
Division of the Royal Society of Chemistry.

Local Organising Committee

Professor J. H. Purnell;
Dr. R. M. Marshall
Dr. R. S. Mason

Programme Committee

Dr. G. Hancock (Oxford)
Dr. R. M. Marshall (Swansea)
Dr. R. S. Mason (Swansea)
Professor J. P. Simons (Nottingham)
Professor I. W. M. Smith (Birmingham)

Sponsorship

We gratefully acknowledge sponsorship of the Symposium by the following companies and organisations

British Council
British Gas Corporation
British Nuclear Fuels
British Petroleum
Coherent (U.K.)
Dow Corning
European Research Office, United States Army
I.C.I.
Kodak
Lamb's Physik
Leybold
* London Research Office, United States Navy
Shell
Swansea City Council
University College of Swansea
Welsh Development Agency
West Glamorgan County Council

* The information in this book does not necessarily reflect the position or the policy of the United States Government and no official endorsement should be inferred

CONTENTS

<u>Scientific programme</u>	Pages (i) to (xi)
<u>Abstracts</u>	
Polanyi Memorial Lecture	
Oral presentations,	1 to 55
Poster Session A,	A1 to A56
Poster Session B,	B1 to B59
<u>Author Index</u>	

SCIENTIFIC PROGRAMME

Monday, 25th July

Morning

09 00

Opening

09 10 1 Plenary lecture by Prof. R. N. Zare (Stanford)
"State-to-state bimolecular reaction dynamics:
 $O + HX (v, J) \rightarrow OH (v', N') + X$ ".

09 50 2 "Study of CN radical kinetics"
J. L. Durant, Jr. and F. P. Tully (Livermore).

10 10 3 "Thermal and state-to-state kinetics in
reactions of the CN radical studied in pulsed
laser photolysis time resolved laser induced
fluorescence experiments"
I. R. Sims and I. W. M. Smith, (Birmingham)

10 30

COFFEE

11 10 4 "Fast-flow studies of atomic carbon kinetics at
300 K"
B. Barrere, Ph. Caubet, G. Dorthe and
J. Marchais (Gordeaux).

11 30 5 "The chemistry of the alkali metals in the
mesosphere: rates of formation and
photodissociation of the alkali superoxide
molecules"
J. M. C. Plane and B. Rajasekhar (Miami).

11 50 6 "On the preparation of highly vibrationally
excited molecules by UV multiphoton excitation"
M. Damm, H. Hippler, C. Kiehn and J. Troe,
(Göttingen).

12 10 7 "Measurements of the vibronic excitation
function and rate constants for reaction
between $I_2(v_0, v', n)$ and Xe "
R. J. Donovan, A. J. Holmes, P. R. R.
Langridge Smith and T. Ridley, (Edinburgh)

12 30

End of Session

Afternoon

14 00 8 Plenary lecture by Dr. M. J. Pilling (Oxford)
"The temperature and pressure dependences of
association reactions".

14 40 9 "Study of methyl recombination at ambient
temperature in the range 0.2 to 2.0 mbar"
D. Waller, H.-H. Grotheer and Th. Just,
(Stuttgart).

15 00 10 "Experimental and theoretical study of the
kinetics of the reaction between ethyl radicals
and molecular oxygen"
I. R. Slagle, and D. Gutman, (Illinois) and
A. F. Wagner, (Argonne)

15 20

TEA

16 00 11 "Angular momentum effects in the fall-off
regime"
R. G. Gilbert and S. C. Smith, (Sydney)

16 20 12 "Collisional energy transfer and evolution of
molecular distribution in highly vibrationally
excited toluene"
K. Luther, K. Reihls and A. Symonds,
(Göttingen)

16 40 13 "In situ radical detection under VIB
conditions using REMPI: a study of the kinetics
of CF₃ radicals"
P. M. Golden, R. M. Robertson, and
M. J. Rossi, (SRI).

17 00 14 "Formation of hydrogen in ethylene pyrolysis at
900K"
I. S. Jayaweera and P. D. Pacey, (Dalhousie)

17 20 15 "Unimolecular reaction rate in the weak
collision limit: an approximate analytical
solution to the 2D master equation"
E. E. Nikitin, and S. Ya. Umanski, (Moscow).

17 40

End of Session

Tuesday, 26th July

Morning

09.00 Announcement

09.05 16 Plenary lecture by Prof. A. Dalgarno (Harvard)
"The chemistry of interstellar space".

09.45 17 "Deuterium fractionation in interstellar molecules via ion-molecule reactions"
M. Henrichman, (Brandeis), E. E. Ferguson (Orsay), A. Hansel, R. Richter, and W. Lindinger, (Innsbruck), J. Paulson, (Hanscom AFB), N. G. Adams and D. Smith, (Birmingham).

10.05 18 "Product formation in the reaction of N atoms with methyl radicals"
G. Marston, F. L. Nesbitt and L. J. Stief, (NASA).

10.25 COFFEE

10.55 19 "Translational energy dependences of rate constants for ion-molecule reactions as a function of temperature: rotational energy effects"
R. A. Morris, J. F. Paulson, and A. A. Viggiano, (Hanscom AFB).

11.15 20 "Modelling of the thermal decomposition of ethane"
M. D. U. Gonzales, and D. J. Norfolk, (CEGR)

11.35 21 "Laser induced fluorescence measurements in plasma etching processes"
J. P. Booth, G. Hancock, N. Perry and M. Toogood, (Oxford)

11.55 22 "Time-resolved studies of the kinetics of SiH₂ radical reactions"
J. E. Baggott, H. M. Frey, K. D. King, P. D. Lightfoot, R. Walsh and I. M. Watts, (Reading)

12.15 23 "High-temperature reactor studies of isolated elementary reactions"
A. Fontijn, (Rensselaer).

12.35 End of Session

Afternoon

14.00 24 Plenary lecture by Prof. P. Gray (Leeds).
"Oscillations and ignitions in exothermic reactions".

14.40 25 "Experimental study of the high temperature reaction schemes accounting for the auto-ignition of alkanes"
F. Baronne, G. Scacchi and Y. Simon, (Nancy).

15.00 26 "Reaction mechanisms for pyrolysis and oxidation of hydrocarbon fuels of intermediate size over extended temperature ranges"
W. J. Pitz and C. K. Westbrook, (Livermore).

15.20 TEA

16.00 27 "The formation of formaldehyde and acetylene in a methane-oxygen flame"
R. Le Bec, G. M. Come, P. M. Marquaire and M. P. Martin, (Nancy).

16.20 28 "Analysis of the structure of flames: experimental and modelling approaches"
M. Carlier, P. Devolder, J.-F. Pauwels and L.-R. Sochet, (Villeneuve D'Ascq)

16.40 29 "Novel thermokinetic oscillations in hydrogen oxidation"
D. L. Baulch, J. F. Griffiths, A. J. Pappin and A. F. Sykes, (Leeds)

17.00 30 "The ignition behaviour in gaseous thermal explosions"
A. Moise, H. O. Pritchard, and L. Thang, (Canada)

17.20 End of Session

Evening

20.00 22.00 POSTER SESSION A

Wednesday, 27th July

Morning

- 09 00 31 Plenary lecture by Prof. K. Morokuma (Osaka)
"Potential energy surfaces and dynamics of some
gas phase reactions".
- 09 40 32 "Exact 3D quantum reactivity of the $\text{Li} + \text{HF}$
reaction"
A. Lagana, (Perugia), R. T. Pack, (Los Alamos)
and G. A. Parker (Oklahoma).
- 10 00 33 "Classical trajectory studies of the addition
and dissociation reaction $\text{H} + \text{CO} \rightleftharpoons \text{HCO}$ "
R. Steckler, and A. F. Wagner, (Argonne)
- 10 20 34 "Non-equilibrium H_2 kinetics"
C. Bowes and H. Telleba, (Ottawa)
- 10 40 COFFEE
- 11 05 POLANYI MEMORIAL LECTURE, Prof. J. C. Polanyi
(Toronto)
"Probing the transition state".
- 12 15 End of Session

Thursday, 28th July

Morning

09 00 Announcements

- 09 05 35 Plenary lecture by Prof. A. R. Zewail
(Cal. Tech.)
"Femtosecond real-time dynamics of reactions".
- 09 45 36 "Photofragment vector correlations in single
photon and vibrationally mediated
photodissociation"
M. Brouard, M. T. Martinez, J. O'Mahony and
J. P. Simons. (Nottingham).
- 10 05 37 "State selective photodissociation dynamics of
A state ammonia"
M. N. R. Ashfold and R. N. Dixon. (Bristol),
G. Ahlers, J. Biesner, L. Schneider and
K. H. Welge (Bielefeld) and X. Xie. (Bielefeld
and China).

10 25 COFFEE

- 10 55 38 "Reactions of spin-orbital excited chlorine
atoms ($Cl(^2P_{1/2})$)"
S. A. Chasovnikov, A. I. Chichinin and
L. N. Krasnoperov. (Novosibirsk)
- 11 15 39 "Molecular beam studies of ionization reactions
in collisions of excited rare gas atoms with
molecules"
B. Brunetti and F. Vecchiocattivi. (Perugia)
- 11 35 40 "State-to-state excitation functions by time
profiles of crossed beam chemiluminescence"
T. Contreras, A. González Ureña, E. Verdasco
and V. Sáez Rabanos. (Madrid).
- 11 55 41 Plenary lecture by Prof. S. Stolte (Nijmegen).
"Scattering of oriented molecules".

12 35 End of Session

Afternoon

- 14 00 42 Plenary lecture by Prof. J. I. Brauman
(Stanford).
"Complex ions: transition states and
intermediates in gas phase ionic reactions".
- 14 40 43 "A study of the mechanism of proton transfer to
 C_6H_5F and $CH_3C_6H_4F$ using Tandem Mass
Spectrometry"
R. Mason. (Swansea)
- 15 00 44 "Energy uptake in the collision of massive ions
with inert gas atoms"
P. J. Derrick. (Warwick).
- 15 20 45 "Charge transfer excitation and fragmentation
of molecular ions in association with argon
clusters"
D. M. Bernard, N. G. Gotts and A. J. Stace.
(Sussex)
- 15 40 TEA
- 16 15 46 "Heterogeneous chemistry related to antarctic
ozone depletion: reaction of $ClONO_2$ and N_2O_5 on
ice surfaces"
D. M. Golden, M. J. Rossi and M. A. Tolbert.
(SRI)
- 16 35 47 "Interactions of gas molecules with water
surfaces"
P. Davidovits, J. M. Van Doren, J. Gardner, J.
Jayne, and L. Watson. (Boston), and E. Kolb, D.
R. Worsnop and M. S. Zahniser. (Aerodyne
Research).
- 16 55 48 "Laboratory studies of sticking coefficients
and heterogeneous reactions important in the
stratosphere"
M.-T. Leu and L. F. Keyser. (Pasadena).

17 15 End of Session

Evening

20 00-22 00 POSTER SESSION B.

Friday 29th July

Morning

09.00	Announcements
09.05	Plenary lecture by Dr. A. R. Ravishankara (Boulder) "Antarctic ozone hole, acid rain and atmospheric chemical kinetics".
09.45	Reversible adduct formation in the reactions of Cl(P ₁) with CS ₂ , COS and O ₂ : kinetics and thermodynamics J. M. Nicovich, C. J. Shackelford and P. H. Wine, (Georgia).
10.05	Kinetics and UV spectrum of the methylperoxy radical F. Simon, W. Schneider, and G. K. Moortgat, (Mainz), and M. Jenkin, (Harwell).
10.25	COFFEE
11.00	Kinetics of the gas-phase reactions of NO ₃ radicals and N ₂ O ₅ with organic compounds J. N. Pitts, S. M. Aschmann and R. Atkinson, (Riverside).
11.20	Kinetics and mechanisms of reactions of organic peroxy radicals and HO ₂ R. A. Cox, and M. E. Jenkin, (Harwell).
11.40	An experimental and computational study of the reactions of NO ₃ radicals with Cl and HO ₂ F. Ewig, A. Hoffman and R. Zellner, (Göttingen)
12.00	Flash photolysis kinetic study of peroxyacetylnitrate formation I. Bridier, R. Lesclaux and B. Veyret, (Bordeaux)
12.20	Closing remarks.

END OF SYMPOSIUM

- A1 "A new approach to weak-collision factor β "
W. Forst, (Nancy)
- A2 "Kinetic paths for elementary chemical reactions: the hyperspherical perspective"
V. Aquilanti, S. Cavalli and G. Grossi, (Perugia)
- A3 "Collision processes through rydberg states of molecules in the field of strong infrared radiation"
G. K. Ivanov, A. S. Vortazaryan, and G. V. Golubkov, (Moscow).
- A4 "On dynamics of the elementary multiphoton processes in gases"
A. V. Ivanova, (Moscow).
- A5 "Competing reactions of the acetone cation-radical: RRKM-QET calculations on an ab initio potential energy surface"
C. Lifshitz and F. Louage, (Jerusalem) and N. Heifrich and H. Schwarz, (Berlin)
- A6 "Properties of activation barriers from forward and reverse rates of hydrogen atom transfers"
H. Furue and P. D. Pacey, (Bathouste).
- A7 "Dynamical studies on exoergic indirect exchange reactions $A + BCD \rightarrow AB + CD$ "
M. T. Rayez, J. C. Rayez, P. Halvick and B. Duguay, (Bordeaux).
- A8 "Molecular formation by radiative association in radical-radical and ion-molecule collisions"
I. W. M. Smith, (Birmingham).
- A9 "Kinetic measurements by pulsed photolysis and time-resolved infrared laser absorption"
J. Brunning, M. J. Frost and I. W. M. Smith, (Birmingham)
- A10 "Rearrangement of channels in reaction of $O(^3P)$ atoms with ethylene"
E. N. Aleksandrov, V. S. Arutyunov, V. I. Vedenev, V. D. Enjazez and S. N. Kozlov, (Moscow)
- A11 "The first step of N atoms interaction with methane, ammonia and hydrogen"
V. Ya. Rasevich, and V. I. Vedenev, (Moscow).
- A12 "Rate constants for abstraction of hydrogen from ethylene by methyl and ethyl radicals relative to abstraction from propane and isobutane"
S. I. Abonkhail, X-H Lin and M. H. Back, (Ottawa).
- A13 "Study of the self-reactions of propylperoxy radicals in the gas phase"
S. Föörgeteg, B. László and T. Bérces, (Budapest).
- A14 "Study of oxetane decomposition by the variable encounter method"
L. Zolotai, T. Bérces and F. Márta, (Budapest).
- A15 "Reaction kinetics of $Mg(3P_1)$ with hydrocarbons"
F. Beitia, F. Castano and E. Martínez, (Bilbao).
- A16 "Reaction kinetics and spectroscopy of CHF radical with some hydrocarbons"
F. Castano, A. O. de Zárate and E. Martínez, (Bilbao).
- A17 "Study of the $SO_2 + H_2$ reaction"
J. Chamboux, F. Jorand, V. Viossat and K. Sahetchian, (Paris) and C. Chachaty (Gif sur Yvette)
- A18 "Study of some reactions of n-alkoxy radicals"
K. A. Sahetchian, A. Heiss and R. Rigny, (Paris)
- A19 "OH vibrational energy distribution in reactions of $O(^1D)$ atoms"
S. G. Cheskis, A. A. Iogansen, P. V. Kulakov, I. Yu. Razuvaev, O. M. Sarkisov and A. A. Titov (Moscow)
- A20 "Observation of new absorptions of the C_2H_3 (vinyl) radical and some of its chemistry"
A. Fahr and A. H. Laufer, (N.B.S.).
- A21 "Reactions of vinyl and phenyl radicals with ethyne, ethene and benzene"
A. Fahr and S. E. Stein, (N.B.S.).
- A22 "Rate constants for the reactions $t-C_4H_9 + DX \rightarrow t-C_4H_9D + X$ ($X = Br, I$); the heat of formation of t -butyl"
W. Müller-Markgraf, M. J. Rossi and D. M. Golden, (SRI).
- A23 "Kinetic studies of the reactions of $CH_3C_2H_5$, $i-C_4H_9$, and $t-C_4H_9$ with HBr and HI and the heats of formation of the alkyl radical"
J. J. Russell, J. A. Seetula and D. Gutman, (Illinois)

- A24 "The N.B.S. chemical kinetics data center databases and computational programs for use on personal computers" J. T. Herron and W. G. Mallard. (N.B.S.).
- A25 "Design and implementation of a chemical kinetics database" W. G. Mallard and J. T. Herron. (N.B.S.).
- A26 "Bimolecular reactions of fluorine atoms with halogenated ethane in the gas phase" U. Wördsörfer and H. Heydtmann. (Frankfurt/Main).
- A27 "Direct measurements of elementary radical reactions at various energies studied by UV-LIF" A. Jacobs, M. Wahl, R. Weller and J. Wolfrum. (Heidelberg)
- A28 "Discharge-flow kinetic study of the reaction $\text{CH}_3\text{S} + \text{NO}_2$ " J. L. Jourdain, A. Mellouki and G. Le Bras. (Orléans). 2
- A29 "Kinetic study of the reactions of NO_3 radicals with Br, BrO and HBr" G. Poulet, A. Mellouki and G. Le Bras. (Orléans) and R. Singer, G. Moortgat and J. Burrows. (Mainz).
- A30 "Kinetics of the combination reactions of chlorofluoromethylperoxy radicals with NO_2 in the temperature range 233-373 K" F. Caralp, R. Lesclaux, M. T. Rayez and J. C. Rayez. (Bordeaux) and W. Forst. (Nancy).
- A31 "Product distribution of the elementary $\text{C}_2\text{H}_5 + \text{O}$ reaction in the p = 0.7 - 5 torr range at T = 300 and 600 K" J. Peeters and D. Mees. (Lieven).
- A32 "Kinetics and computer modelling of reactions of N (^4S) with hydrocarbons" C. S. Blatt, S. G. Roscoe and J. M. Roscoe. (Wolffville, Nova Scotia).
- A33 "Effects of pressure in OH-alkene reactions" F. P. Tuily. (Livermore).
- A34 "A new low temperature source of non-volatile metal atoms" C. Vinckler, J. Corthouts and S. de Jaegere. (Lieven)
- A35 "Time-resolved studies of the kinetics of the reactions of dimethylsilylene" J. E. Baggott, M. A. Blitz, H. M. Frey, P. D. Lightfoot and R. Walsh. (Reading).
- A36 "248 nm Laser photolysis of gaseous fluorine/alkyl iodide mixtures" D. Raybone, T. M. Watkinson, J. C. Whitehead and F. Winterbottom. (Manchester)
- A37 "Kinetics of the reactions of $\text{C}_2\text{H}_5\text{S}$ with NO_2 , NO and O_2 at 296 K" G. Blaca and L. E. Jusinski. (SRI) and R. Patrick. (LSI Logic).
- A38 "Tropospheric oxidation of aromatic hydrocarbons: rate constants of the reactions of OH with benzene and toluene by the discharge flow method" N. Bourmada, P. Devolder, J-F. Pauwels, and J-P. Szwarysyn. (Villeneuve D'Ascq).
- A39 "Kinetics and mechanism for the reaction of hydroxyl radicals with nitrogen containing compounds" M. Donlon, D. O'Farrell, J. Treacy and H. W. Sidebottom. (Dublin) and O. J. Nielsen. (Roskilde).
- A40 "The reaction of CH_3OH with O_2 , NO and NO_2 " C. Anastasi and V. J. Simpson. (York) and J. Munk and P. Pagsberg. (Roskilde).
- A41 "NO chemistry in electrical discharges" C. Anastasi, J. Harrison and M. Stark. (York).
- A42 "Rate of reaction of the hydroxymethyl radical with nitric oxide from 230-373K" L. J. Stief, F. L. Nesbitt and W. A. Payne. (NASA).
- A43 "Pre-exponential temperature dependences of bimolecular reaction rate coefficients predicted by transition state theory" N. Cohen. (Aerospace Corporation).
- A44 "The reaction of $\text{O}(^3\text{P})$ with NO_2 " C. E. Canosa-Mas, P. J. Carpenter, S. J. Smith and R. P. Wayne. (Oxford)
- A45 "Temperature study of the reactions of NO_3 with alkanes and alkenes" S. J. Smith, S. J. Waygood, C. E. Canosa-Mas and R. P. Wayne. (Oxford).

- A46 "Some recent gas kinetic studies involving silylenes"
M. P. Clarke, I. M. T. Davidson, M. Dillon and G. Eaton.
(Leicester).
- A47 "The $\text{HO}_2 + \text{HO}_2$ reaction at elevated temperatures"
R. Ilescaux, P. D. Lightfoot and B. Veyret. (Hordeaux).
- A48 "Kinetics of the reaction of CH_2S with O_3 "
G. S. Tyndall and A. R. Ravishankara. (Boulder)
- A49 "Theoretical Study of the recombination reaction $\text{CH}_3 + \text{CH}_3 \rightarrow \text{C}_2\text{H}_6$ "
A. F. Wagner. (Argonne) and D. M. Wardlaw. (Kingston, Ont.)
- A50 "Kinetics of the reaction of CF_3ClO_2 with NO_2 "
S. B. Moore and R. W. Carr. (Minnesota).
- A51 "The energy transfer processes in R-MX mixtures (R=Ar, Kr, Xe)"
A. Jowko, E. Bartkiewicz, M. Symanowicz, K. Wojciechowski.
M. Rosa and M. Forys. (Siedlce).
- A52 "A laser photolysis/cw-laser absorption study of the reactions of phenyl radicals with NO , NO_2 , O_2 , CCl_4 and selected hydrocarbons"
M. Freidel and R. Zellner. (Göttingen).
- A53 "Kinetic and mechanistic studies of the photo-oxidations of aliphatic ethers under tropospheric conditions"
P. J. Bennett and J. A. Kerr. (Birmingham).
- A54 "Kinetics of the reaction of atomic chlorine with methane at 294 ± 1 K by mass spectrometry"
J. P. Sametyn, P. Devolder, B. Meriaux, and A. Tighezza.
(Villeneuve D'Ascq).
- A55 "High precision determination of rate constants for the reactions of alkenes with OH at 300 K, using a smog chamber technique"
W. Behnke, F. Nollting and C. Zetzsch. (Hannover)
- A56 "A laser flash photolysis/resonance fluorescence study of halogen atom/hydrocarbon molecule reactions"
M. J. Pilling and P. W. Seakins. (Oxford)

poster session B

- B1 "Open shell atomic beam scattering and the spin orbit dependence of potential energy surfaces"
V. Aquilanti, R. Candori and F. Pirani (Perugia) and G. Liuti. (Siena).
- B2 "Accurate atom-diatom intermolecular potentials from high resolution crossed molecular beam scattering experiments"
L. Benerenti, P. Casavecchia and G. G. Volpi. (Perugia).
- B3 "C + NO → CN + O reaction dynamics studied with pulsed crossed supersonic molecular beams"
M. Costes, C. Naulin and G. Dorthé. (Dordeaux)
- B4 "Computer simulation of the state-resolved reactions of O(³P) with HCl and HBr"
P.-A. Elofson and L. Holmlid. (Gothenburg).
- B5 "Energy distribution by direct deconvolution: experimental test, energy transferred by collision in methylcyclobutane/cyclobutane, and the CH₂(¹A₁) heat of formation"
J. M. Figuera, M. Fuentes and J. C. Rodriguez. (Madrid).
- B6 "Energy transfer reactions of N₂(A₂⁺)"
M. F. Golde, G. Ho, R. F. Sperlin and W. Tao. (Pittsburgh)
- B7 "Time resolved infrared emission in the O + CF₂ reaction"
G. Hancock and D. Heard. (Oxford)
- B8 "Resonance-enhanced two-photon ionization spectra of benzene in the third channel region"
T. Ichimura. (Tokyo) and H. Shinohara and N. Nishi. (Okazaki).
- B9 "Chemiluminescence and rotational polarisation in the reactions Mn + O₂, NO₂, SO₂, CO₂, N₂O"
M. R. Levy. (Newcastle upon Tyne).
- B10 "A laser induced fluorescence study of the B(O₂⁺) and A(O₂⁺) states of tellurium dimers"
E. Martinez, F. Castanc, M. T. Martinez, P. Puyuelo and F. J. Bast rrechea. (Bilbao)
- B11 "Measurements of state-to-state energy transfer rate coefficients for OH(A₂⁺, v=0)"
A. Jorg, U. Meier, K. Kohse-Holtinghaus and Th. Just. (Stuttgart)
- B12 "Photodissociation of jet-cooled N-nitroso-methylcyanamide in the near-UV"
P. A. Giovannacci, M.R.S. McCoustra and J. Pfab. (Heriot-Watt).
- B13 "Trace analysis of NO by high resolution jet spectroscopy"
V. M. Young, A. H. Yates, M. R. S. McCoustra and J. Pfab. (Heriot Watt).
- B14 "The 355 nm photodissociation of jet-cooled alkyl thionitrites"
P. A. Giovannacci, M. R. S. McCoustra and J. Pfab. (Heriot Watt).
- B15 "Dehalogenation of α, ω-dihalogenopolymethylenes using alkali metal vapors. Gas phase generation and reactions of diradicals"
A. Al-Yahya, E. A. Volina and L. E. Gusei'nikov. (Moscow).
- B16 "Direct infrared spectroscopic evidence for allyl radical and definition of the initiation step in thermal decomposition of cycloalkanes"
L. E. Gusei'nikov, V. V. Volkova and L. V. Shevelkova. (Moscow) and G. Zimmermann and U. Ziegler. (Leipzig).
- B17 "Selfignition of combustible gases promoted by difluoramine radicals"
A. A. Borisov, V. M. Zamanski, V. V. Lisiyanski, S. A. Rusakov and G. I. Skachkov. (Moscow).
- B18 "Matrix designed studies in chemical kinetics"
C. Anastasi and J. Anderez-Alvarez. (York).
- B19 "The self reactions of methylperoxy radicals in the gas phase"
C. Anastasi, P. J. Couzens and D. J. Waddington. (York) and M. J. Brown and D. B. Smith. (British Gas).
- B20 "Spectrum and kinetics of a OOH species"
C. Anastasi and M. Foxon. (York) and P. Genske and P. Pagsberg. (Roskilde).
- B21 "The decomposition of methane"
R. W. Barnes and G. L. Pratt. (Sussex).

- B22 "Modelling of the gas-phase oxidation of cyclohexane"
S. E. Kiaf and F. Baronnet, (Nancy).
- B23 "Kinetic modelling of n-butane oxidation"
A. Chakir, M. Cathonnet, J. C. Boettner and F. Gaillard,
(Orléans)
- B24 "An expert system for the design of simplified reaction
mechanisms"
J. C. Giniasty, V. Bucci, E. Demange, C. Müller, G. Scacchi
and G. M. Come, (Nancy).
- B25 "Very low conversion pyrolysis of 1,2-dichloroethane"
M. Salouhi, P. M. Marquaire and G. M. Come, (Nancy)
- B26 "High temperature reaction between methane and chlorine"
M. Chumbon, P. M. Marquaire and G. M. Come, (Nancy).
- B27 "Computer modelling of the thermal decomposition of
3-methylpentane at 420°C and 133 mbar"
F. Billaud, K. Eiyahysoul, P. Malacarne, and F. Baronnet,
(Nancy).
- B28 "The interaction of carbon monoxide and carbon dioxide with
the homogeneous reduction of nitric oxide by ammonia"
H. F. Hemminger and J. Wolfrum, (Heidelberg).
- B29 "High temperature oxidation of methyl chloride and vinyl
chloride"
G. Achhammer, M. Schneider and J. Wolfrum, (Heidelberg).
- B30 "Persistent luminescence as an indicator of the endpoint of
chemiluminescent titrations"
M. Kaufman, (Atlanta).
- B31 "Simulation of P-T explosion limits and auto-ignitions in
the $\text{CO} - \text{CH}_2\text{O} - \text{H}_2 - \text{O}_2$ system"
U. Maas and J. Warnatz, (Heidelberg).
- B32 "The mechanism of chain propagation in the reaction of
methane oxidation"
V. I. Vedenev, A. A. Mantashyan and M. A. Teitelboim
(Moscow and Yerevan).
- B33 "Kinetic modelling of high pressure oxidation of rich
methane-oxygen mixtures"
V. I. Vedenev, M. A. Teitelboim, M. Ye. Goldenberg, M. I.
Gorban and A. A. Kernaikh, (Moscow).
- B34 "Thermal decomposition of dimethylnitramine by pulsed laser
pyrolysis"
P. H. Stewart, S. E. Ngenda, J-M Zellweger, J. B. Jeffries,
D. M. Golden and D. F. McMillen, (SRI).
- B35 "Pyrolysis and infrared laser photolysis of silane"
A. Mele and D. Stranges, (Rome) and A. Giardini-Guidoni and
R. Teghil, (Potenza).
- B36 "Heterogeneous factors and the phenomenon of the negative
temperature coefficient of the maximum rate of
propionaldehyde oxidation"
Em. A. Oganesyan, A. P. Lusparyan, I. A. Vardanyan and A. B.
Naibandyan, (Yerevan).
- B37 "The regularities of nonisothermal processes in systems with
branching chain reactions"
A. N. Peregudov and V. T. Gontkovskaja, (Chernogolovka).
- B38 "A master equation study of the approach to equilibrium in
isomerisation and addition/dissociation reactions"
N. J. B. Green, P. J. Marchant, M. J. Pilling and
S. H. Robertson, (Oxford).
- B39 "A detailed chemical kinetic study of the oxidation of n-
pentane"
W. J. Pitz and C. K. Westbrook, (Livermore)
- B40 "The pyrolysis of propylene"
I. Wyrie, C. S. Rebeiro and J. M. Roscoe, (Wolfville,
Nova Scotia).
- B41 "Oxidation reaction of hydrogen near the second ignition
limit: evidence for pressure pulses"
K. Sahetchian, F. Jorand, J. Chamboux and V. Viossat,
(Paris)
- B42 "Kinetic and mechanistic investigations of the reactions of
aromatic hydrocarbons with atomic oxygen"
V. Schliephake, M. Tappe and H. Frerichs, (Göttingen).

- B13 "Kinetics and chemiluminescence in the reaction of methane with oxygen atoms from the thermal decomposition of ozone"
S. Tóby and F. S. Tóby, (Rutgers).
- B14 "Reduction of large reaction mechanisms"
T. Tutányi and T. Bárcas, (Budapest).
- B15 "Role of nitric oxide in the H_2-O_2 flame"
J. Blan, J. Vandoreen and P. van Tiggelen, (Louvain-la-Neuve).
- B16 "The high pressure, high temperature hydrogenation of benzene"
S. W. Wood, (British Gas).
- B17 "Bicolor Laser IR + UV Photodissociation of CF_3Cl "
C. Lalo, J. Masanet, J. Deson and J. Tardieu de Malleissye, (Paris).
- B18 "Chlorine oxides in the low temperature photolysis of ClO_2 "
A. Reimer and F. Zabel, (Wuppertal).
- B19 "Kinetics of the gas phase reaction of Cl atoms with Organic Species"
T. J. Wallington, L. M. Skowes, W. O. Siegl, C. H. Wu and S. M. Japar, (Ford Motor Company).
- B20 "ICl catalysed decomposition of ditertiary butyl peroxide - unimolecular reactions of a surrogate hydroperoxy alkyl radical"
L. Batt, M. A. Khan and T. J. Mitchell (Aberdeen) and C. Morley, (Shell Research).
- B21 "Direct observation after IR multiphoton absorption of the dynamics of excited molecules near to the dissociation threshold"
B. Abel, R. Herzog, H. Hippler and J. Troe, (Göttingen).
- B22 "Collisional energy transfer between highly excited N_2^0 molecules"
H. Teitelbaum, (Ottawa) and J. Troe, (Göttingen).
- B23 "An oscillatory reaction in the gas phase the kinetics of homogeneous cluster formation"
Z. Cheng and H. Teitelbaum, (Ottawa).
- B24 "Infrared multiphoton dissociation of dimethylnitramine"
Y. Lazarou and P. Papagiannakopoulos, (Crete).
- B25 "Comparison of ab initio calculations, transition state theory and experiment for the recombination of methyl radicals"
K. Darvesh, R. Boyd and P. D. Pacey (Dalhousie).
- B26 "Cross-combination ratios of methyl and C_4-C_6 aliphatic hydrocarbon radicals"
L. Seres, A. Nacs, T. Körtvélyesi and M. Görgényi, (Szeged).
- B27 "Gas phase iv_2 photochemistry of NF_3 : dynamics and kinetics of both $NF(X^2\Sigma)$ and $NF(a^4\Delta)$ radical products"
H. Hevajian, R. F. Heidner III, J. S. Holloway and J. B. Koffend, (Aerospace Corporation).
- B28 "Electronic quenching of excited diatomic hydrides"
R. A. Browarzik, F. Rohrer, F. Stuhl, R. D. Kenner and P. Heinrich, (Bochum) and Y. P. Vlahoyannis, E. Hontzopoulos, A. Vagiri, S. C. Farantos and C. Fotakis, (Crete).
- B29 "The branch chain reaction $NF_2 + O_3$ and the promotion of H_2CO and CH_4 oxidation by NF_2 "
Y. M. Gershenzon and V. B. Rozenshtein, (Moscow).

POLANYI MEMORIAL LECTURE

PROBING THE TRANSITION STATE

John C. Polanyi

Department of Chemistry, University of Toronto,
Toronto M5S 1A1, CANADA

Since one is unconscious in initial and final states, introspection naturally focuses on the transition state. I shall talk at the outset about Michael Polanyi's career transitions, to the extent that I understand them. From the achievements of H. Eyring, M.G. Evans and H. Polanyi in their pursuit of the reactive transition state the story moves on to recent attempts to probe transition states directly in both emission and absorption, by time-independent and time-resolved techniques, for half-collisions and for reactions as fundamental as

$H + D_2 \rightarrow HD_2^{\ddagger} \rightarrow HD + D$. In closing an account will be given of attempts to reduce the range of reactive transition states through restriction of angles-of-approach, reactant separations and impact parameters, achieved by inducing reaction in van der Waals complexes, or between species co-adsorbed on single crystal surfaces.

PLENARY LECTURE

-State-to-state bimolecular reaction dynamics:
 $O + HX(v,J) \rightarrow OH(v',N') + X''$

R. N. Zare

Department of Chemistry, Stanford University,
Stanford CA 94305, U.S.A.

Abstract not available

STUDY OF CN RADICAL KINETICS*

J. L. Durant, Jr. and F. P. Tully

Combustion Research Facility
Sandia National Laboratories
Livermore, CA 94550

Chemical reactions of the CN radical are important in a wide variety of combustion environments. Despite their importance, there is a decided lack of kinetic data on CN-radical reactions, especially as functions of temperature and pressure. Perhaps the most important CN reaction is that with O_2 . However, there is an almost complete lack of data on the temperature dependence of this reaction; indeed, recent determinations of this rate coefficient at room temperature are scattered over a factor of four. To remedy this situation, we have undertaken a study of the CN + O_2 reaction between 298 and 800 K using the laser photolysis/laser-excited fluorescence technique (LP/LEF).

Of central importance to our successful implementation of the LP/LEF technique was the development of an intense cw dye-laser operating at 387 nm. In initial experiments, we used the dye Polyphenyl 1 to excite the (B-X) transition in CN. While LEF signal levels were sufficient to perform kinetic studies, we found the dye laser difficult to maintain over an extended period. In discussions with Exciton Chemical Co., we learned of an experimental dye, Exalite 392E, that might be suitable for ultraviolet, cw-laser operation.

We obtained a sample of the dye, and characterized its cw operation in a Spectra-Physics 375 dye laser tuned by a three plate birefringent filter.¹ Figure 1 displays the dye-laser tuning curve we obtained for a 1.6 mM solution of Exalite 392E pumped by 3.5 W of all-lines-UV output from an Ar⁺ laser. The laser output is greater than 250 mW at 392 nm, and it significantly exceeds that from a Polyphenyl 1 dye laser throughout the 375-408 nm tuning range. The fractional absorption of the 1.6 mM dye solution is only 0.45, suggesting that one could obtain even higher dye-laser output powers by further increasing the dye concentration. However, the CN (B-X) transition is easily saturated, and we typically use laser powers <20 mW in our studies.

Figure 2 shows a typical CN decay profile obtained by pumping the P(4) line of the (0-0) (B-X) transition in CN and monitoring fluorescence in the (0-1) (B-X) transition at 420 nm. To obtain this decay, 0.3 microns of C₂N₂ is photolyzed by 300 μ l of unfocused 193 nm laser light. Our Exalite 392E probe laser power was 12 mW. The excellent signal/background ratio allows us to easily follow the decay through eight 1/e-lifetimes. Clearly, the accuracy of the rates obtained by this method is defined by uncertainties in gas handling, mixture concentrations and pressure measurement, but not by the quality of the decays collected. The current status of the CN-radical kinetic studies is discussed.

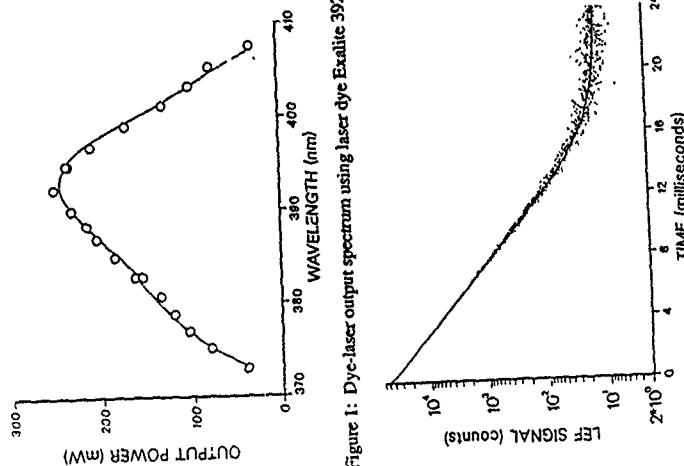
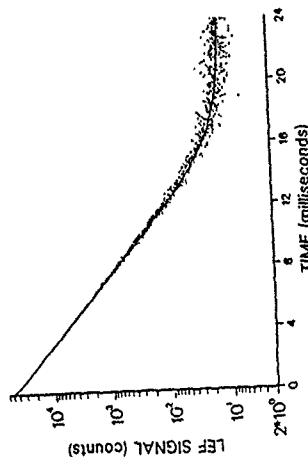


Figure 1: Dye-laser output spectrum using laser dye Exalite 392E.

Figure 2: Typical [CN] profile obtained in kinetic study of the CN + O_2 reaction.

*Research sponsored by the U. S. Department of Energy, Office of Basic Energy Sciences, Division of Chemical Sciences.

1) F. P. Tully and J. L. Durant, Jr., Applied Optics, in press.

THERMAL AND STATE-TO-STATE KINETICS IN REACTIONS
OF THE CN RADICAL STUDIED IN PULSED LASER
PHOTOLYSIS TIME RESOLVED LASER INDUCED
FLUORESCENCE EXPERIMENTS

Ian R. Sims and Ian W.M. Smith

Department of Chemistry
University of Birmingham
P.O. Box 363
Birmingham
B15 2TT
England

The results of a series of experiments on reactions of the CN radical will be reported. The experiments combine (i) creation of the radicals by pulsed photolysis of NCNO with the frequency-doubled output of a Nd:YAG laser, with (ii) observation of the pseudo-first-order decays of the radical concentrations by laser-induced fluorescence (LIF) using a tunable dye laser to excite lines in the CN(B-X) system. The experiments are direct, accurate and state-specific, and they yield information about the temperature (and pressure) dependence of the processes removing CN(v=0) and CN(v=1), since the photolysis produces a small fraction of CN radicals in (v=1).

The reactions of CN with O₂ (producing NCO + O) and CN with NO (producing NCNO) are proto-typical radical-radical reactions with rates which decrease with temperature.¹ In neither case is there any evidence for the alternative 'four-centre' reaction channel (to CO + NO or CO + N₂). With NO, removal of CN(v=0) is relatively slow and the rate depends on total pressure and decreases steeply as the temperature is raised. On the other hand, removal of CN(v=1) is rapid ($k_{795} = 7.6 \times 10^{-11}$ cm³ molecule⁻¹ s⁻¹) and the rate is independent of pressure and only decreases slowly with temperature. This observation is consistent with vibrational relaxation of CN(v=1) in collisions in which an (NCNO) complex is formed. We shall describe measurements on these reactions down to unusually low temperature. (ca 100 K) and will compare our results with theoretical predictions.

We shall also report kinetic data for the reactions of CN(v=0) and CN(v=1) with H₂, D₂, HCl, HBr, HI and NH₃ for temperatures between 205 and 768K. At 295 K, the rate constants (k/cm³ molecule⁻¹ s⁻¹) for these reactions are: 2.40×10^{-14} , 8.4×10^{-15} , 5.9×10^{-15} , 8.8×10^{-15} , 7.0×10^{-11} , and 2.7×10^{-11} , respectively. For all species and all

temperatures, the rate constants for removal of CN(v=1) are very similar to those for reaction of CN(v=0), indicating that vibrational relaxation is unimportant and that the reactions are not accelerated by the presence of excess energy in the vibration of the CN radical. The small or insignificant effect on the rates of reaction indicates that the CN group is effectively a 'spectator' during the changes in structure and bonding which occur during the reactive collisions.

Finally, we expect to report on the influence of HCl vibrational excitation on the rate of the reaction:



For these experiments, a pulsed HCl chemical laser is added to the apparatus to excite the HCl reagent immediately prior to the formation of CN radicals by pulsed photolysis.

1. I.R. Sims and I.W.M. Smith, J.C.S. Faraday 2, to be published May, 1988
2. I.R. Sims and I.W.M. Smith, Chem. Phys. Letters, submitted May, 1988.

FAST-FLOW STUDIES OF ATOMIC CARBON KINETICS AT 300 K

B. Barrère, Ph. Caubet, G. Dorthé and J. Marchais

Laboratoire de Photochimie et Photochimie Moléculaire
Université de Bordeaux I, 33405 Talence, France

Atomic carbon is believed to play an important role in interstellar chemistry and in combustion processes. As far as we know, only flash photolysis technique has been used to determine its reactivity at 300 K. For most experiments, 2.5 atomic carbon was produced from the vacuum ultraviolet photolysis of C_3O_2 by a flash lamp. In a very recent study, the multiphoton dissociation of CH_2Br_2 by an excimer laser was used. Such studies were restricted to reactant molecules not too seriously affected by the flash. In particular the $C + OCS$ reaction was not studied.

We have shown in previous flow experiments that this reaction exhibits a strong ultraviolet chemiluminescence from the CS transition $a^3\Pi_u \leftarrow X^1\Sigma_g^+$ + $h\nu$ despite the rather long radiative lifetime of a $3\Pi_u$ state. The direct production of $CS(a^3\Pi)$ from reactive collisions between C and OCS has been recently confirmed in our pulsed crossed molecular beam apparatus.

For our kinetical study, atomic carbon was obtained from microwave dissociation of CO diluted in He and then mixed $25cm$ downstream to OCS also diluted in He . The vibronic band intensities of $CS(a^3\Pi_u \leftarrow X^1\Sigma_g^+)$ transition varied in the same way along the distance from the mixing point, i.e. keeping exactly the same relative distribution. This indicated that vibrational relaxation between vibrational levels of $CS(a^3\Pi)$ was negligible with respect to collisional removal of these levels due to electronic quenching. From this feature it could be deduced that once $CS(a^3\Pi_u)$ vibrational levels have reached steady state their concentration remained proportional to that of atomic carbon provided that $[OCS] = \text{constant} = [OCS]_0 \gg [C]_0$. That latter condition results also in a pseudo first order $C + OCS$ reaction with an exponential decay of any band intensity. We chose that of the $(0,0)$ band which is the most intense.

The bimolecular rate constant of the homogeneous $C + OCS$ reaction was extracted from the different exponential decays with distance by the resolution of the complete differential continuity equation of atomic carbon in the flow under different

flow velocities from 20 to $35 m s^{-1}$ and for helium pressures of 2 and 3 Torr. A value of $(9.3 \pm 0.4) \times 10^{-11} cm^3 \text{ molecule}^{-1} s^{-1}$ was found. The addition of NO or O_2 to a fixed $[OCS]_0$ value allowed the determination of the rate constants of the $C + NO$ and $C + O_2$ reactions found to be respectively equal to $(2.6 \pm 0.4) \times 10^{-11}$ and $(1.5 \pm 0.3) \times 10^{-11} cm^3 \text{ molecule}^{-1} s^{-1}$. The plug flow approximation leads to apparent rate constants much lower and with slightly greater relative uncertainty range for example $(5.6 \pm 0.4) \times 10^{-11} cm^3 \text{ molecule}^{-1} s^{-1}$ for the $C + OCS$ reaction.

References

- 1- W. Braun, A.M. Bass, D.D. Davis and J.D. Simmons, Proc. Roy. Soc. A312, 417 (1969)
- 2- D. Husain and L.J. Kirsch, Trans. Faraday Soc., 67, 2025 (1971)
- 3- D. Husain and A.N. Young J. Chem. Soc. Faraday Trans II, 71, 525 (1975)
- 4- K.H. Becker, K.J. Brockmann and P. Wiesen J. Chem Soc., Faraday Trans II 84 (1988) to be published
- 5- G. Dorthé, J. Caillie and S. Burdinski, J. Chem. Phys. 78, 594 (1983)

THE CHEMISTRY OF THE ALKALI METALS IN THE MESOSPHERE:
RATES OF FORMATION AND PHOTODISSOCIATION OF THE ALKALI
SUPEROXIDE MOLECULES

John M.G. Plane and B. Rajasekhar

Rosenstiel School of Marine and Atmospheric Science
Division of Marine and Atmospheric Chemistry
4600 Rickenbacker Causeway
Miami, Florida 33149-1098

We have developed a new experimental system^{1,3} for determining the absolute rate coefficients for reactions of metal atoms at temperatures characteristic of the mesosphere (200-240 K). It is in this part of the atmosphere, about 90 km in altitude, that a number of metals including the alkali atoms Na, K and Li, are ablated from meteors.

The technique employs the entrainment of an alkali halide vapour in a fast flow from a heat-pipe, followed by rapid expansion into a central chamber which can be varied in temperature from 230 - 1150 K. The alkali atoms are then produced by pulsed photolysis of the halide, and monitored by laser induced fluorescence. We will report studies of the reactions



The recommended rate coefficients/cm⁶molecule⁻²s⁻¹ are:

$$k(Li+O_2+N_2, 267-1100 K) = (4.30 \pm 1.36) \times 10^{-30} (T/300 K)^{-(1.02 \pm 0.06)}$$

$$k(Li+O_2+He, 267-1100 K) = (1.25 \pm 0.48) \times 10^{-30} (T/300 K)^{-(0.38 \pm 0.08)}$$

$$k(Na+O_2+N_2, 233-1100 K) = (2.88 \pm 0.70) \times 10^{-30} (T/300 K)^{-(1.30 \pm 0.04)}$$

We have used the kinetic decays obtained at 1100 K to estimate the lower limit for the bond energies of both LiO₂ and NaO₂. These are substantially greater than the currently accepted values, and are in reasonable accord with ab initio calculations we have performed on both molecules:

Bond Energies/ kJmol ⁻¹					
Current Value	Expt. HF/6-31G	MP4/6-31G	HF/6-311G	MP4/6-311G	
NaO ₂ 146 ± 21	≥ 208	179.3	199.7	169.9	185.5
LiO ₂ 220 ± 20	≥ 310	267.5	297.6	268.8	296.1

Atmospheric models indicate that the alkali superoxides are the major sink for the alkali atoms immediately below the layer of free metal atoms at about 90 km. We are presently measuring the absolute photolysis cross-sections of NaO₂ and LiO₂ in order to discover the degree to which daytime photolysis limits their effectiveness as alkali atom sinks. In these studies, the superoxide molecules are produced by combining a flow of the metal vapor from a heat-pipe oven with a flow of O₂ and are then photolyzed at excimer laser wavelengths between 193 and 308 nm. So far, we have obtained the following cross-sections for NaO₂ + hν → Na(2S) + O₂: σ(193 nm) = (3.0 ± 1.5) × 10⁻¹⁸ cm², σ(248 nm) = (1.8 ± 0.9) × 10⁻¹⁸ cm², with negligible photolysis at longer wavelengths and no evidence of the production of NaO and O. This is in accord with an ab initio calculation on the 2A₂ → 2B₁ transition of NaO₂ corresponding to λ ≈ 200 nm.

There is good evidence in our system that the molecule NaO₂ is rapidly produced from the reaction NaO₂ + O₂. It appears to have a substantially greater cross-section, σ(248 nm) ≥ 3 × 10⁻¹⁷ cm², which may be of greater atmospheric significance.

1. J.M.G. Plane, J. Phys. Chem. (1987), **91**, 6552.
2. J.M.G. Plane and E.S. Saltzman, J. Chem. Phys. (1987), **87**, 4606.
3. J.M.G. Plane and B. Rajasekhar, J. Chem. Soc., Faraday Trans. II, (1988), **84**, 273.

ON THE PREPARATION OF HIGHLY VIBRATIONALLY
EXCITED MOLECULES BY
UV MULTIPHOTON EXCITATION

M. Damm, H. Hippler, C. Riehn, and J. Troe
Institut für Physikalische Chemie
der Universität Göttingen, Ramannstraße 6
D-3400 Göttingen, West Germany

Absorption of UV photons followed by internal conversion allows to produce large concentrations of vibrationally highly excited polyatomic molecules. The repetition of this process in a well defined manner gives access to very high vibrational excitation energies which are difficult to reach by other methods. The vibrational excitation may exceed the ionization energy without that ionization sets in.

This novel UV multiphoton excitation technique serves to study weak energy dependences of properties of vibrationally highly excited molecules. In a first application to azulene¹⁾, the pressure- and pumping intensity-dependent yield of isomerization to naphthalene was measured and interpreted in terms of the energy dependences of the isomerization, the collisional energy transfer, and the UV absorption of two-photon excited molecules. The experimental results can be interpreted using a careful modeling of the excitation dependence of the UV absorption spectrum of azulene which is based on shock wave experiments of the high temperature spectrum. Likewise, shock wave experiments of the thermal isomerization of azulene to naphthalene serve for a construction of specific rate constants of the isomerization. The experimental data are consistent with the assumption of an energy-independent average energy transfer per collision $\langle \Delta E \rangle$ in the energy range $E > 30\,000\text{ cm}^{-1}$. However, the interpretation is still somewhat uncertain because of the uncertainties of the various input parameters. Unambiguous conclusions require more direct experiments with time-resolved observations after picosecond-excitation. Such experiments are in preparation in our laboratory²⁾.

Analogous experiments in the cycloheptatriene/toluene system are also described³⁾. There is evidence, for a strong competition between C-H and C-C bond splits in toluene at high excitation energies. This results in complicated radical reaction mechanisms after the laser pulses. Therefore, again observations of the reaction yield directly after very short intense laser pulses are required.

- 1) M. Damm, H. Hippler, and J. Troe, J. Chem. Phys., in press.
- 2) K. Luther, M. Sander, and J. Troe, in preparation.
- 3) H. Hippler, C. Riehn, and J. Troe, in preparation.

Measurement of the vibronic excitation function and rate constants for reaction between $I_2(O_g, v'=n)$ and Xe

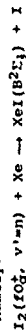
R.J. DONOVAN, A.J. HOLMES, P.R.R. LANGRIDGE-SMITH
and T. RIDLEY

Department of Chemistry, University of Edinburgh,
West Mains Road, Edinburgh EH9 3JJ.

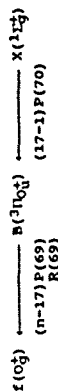
It is now well known that the study of fluorescence excitation and emission spectra of halogen/rare gas mixtures can yield valuable information on the dynamics of rare gas-halide formation. In particular, the use of tunable ultraviolet radiation to excite the halogen partner to an ion-pair state allows the electronic and vibrational state dependence for the reaction to be measured. The reactions of Cl_2 with Kr and Ar have been studied using synchrotron radiation and clearly show that excitation of the $Cl_2(2I_1^+)$ ion-pair state in Cl_2 /rare gas mixtures gives rise to formation of $RgCl^+$. Extensive studies of the reactions of ICl , I_2 and IBr ion-pair states with Xe have also been carried out. These experiments show that there is no barrier in the entrance channel for reaction involving the halogen ion-pair states. To date there has been little information reported on the rates for these processes. Ishiwata et al. have measured the rate constant for the reaction:



to be $3.0 \pm 0.5 \times 10^{-10} \text{ cm}^3 \text{ molecule}^{-1} \text{ s}^{-1}$, following laser excitation of Cl_2/Xe mixtures [5]. We present kinetic measurements from a state selected study of a similar reaction, namely:



The I_2 molecules were excited to the $f(O_g)$ ion-pair state using the optical-optical double resonance technique (OODR) as follows:



Using this technique we have successfully excited specific rovibronic levels of the $f(O_g)$ state from $v'=0$ up to $v'=107$, corresponding to an energy range of ca. 9000 cm^{-1} . This highlights the versatility of OODR for selecting the energy available in the entrance channel for the reaction. Dispersed fluorescence spectra collected following excitation of $I_2(O_g, v'=88, J'=70)$ are shown in Figure 1.

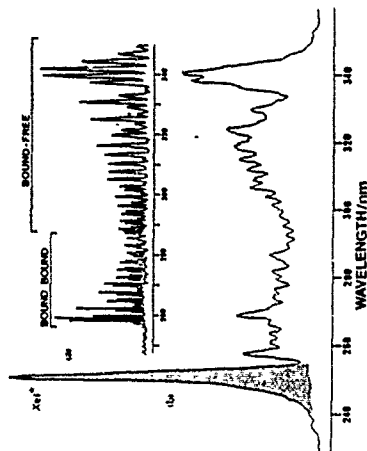


Figure 1. Dispersed fluorescence spectra following excitation of $I_2(fO_g, v'=88, J'=70)$

- (a) High resolution spectrum of the $f(O_g)$ state
+ $B^3O_u^+$ system [$p(I_2) = 1.46 \times 10^{-2} \text{ kNm}^{-2}$]
(b) Low resolution spectrum of the $I_2f(O_g)$ state
+ $B^3O_u^+$ and $XeI(B^2E_1) + (X^2I_1)$ systems
[$p(I_2) = 1.46 \times 10^{-2} \text{ kNm}^{-2}$, $p(Xe) = 1.87 \text{ kNm}^{-2}$]

PLENARY LECTURE

THE TEMPERATURE AND PRESSURE DEPENDENCE OF
ASSOCIATION REACTIONS

M.J.Pilling

Physical Chemistry Laboratory, South Parks Road,
Oxford OX1 3QZ, U.K.

Association reactions such as radical/radical recombination and atom/molecule addition reactions show a complex pressure and temperature dependence. Experimental data, especially for reactions containing small numbers of atoms, are generally determined in the fall-off region, at comparatively low temperatures. Extrapolations are therefore required both to the high pressure limit, k^∞ , for comparison with results of canonical models and to high temperatures for incorporation in simulations of complex processes such as combustion. The techniques available for fitting experimental data and for performing such extrapolations will be discussed¹⁻³, along with their application to reactions recently studied in this laboratory^{3,4-6}. Several anomalies occur and there is a need for a general "hypothesis free" method of data fitting.

We have recently exploited relaxation to equilibrium, in reactions of the type⁷:



to determine equilibrium constants and thermodynamic parameters. Such experiments also provide, in principle, data on the forward and backward rate constants, k_1 and k_{-1} . The relationship between these rate constants and those measured and/or calculated under irreversible conditions has been questioned by Quack⁸, for isomerisation reactions. We have extended this investigation to association reactions in an attempt to determine the value of the kinetic, as distinct from the thermodynamic, data available from relaxation studies.

References

1. R.G.Gilbert, K.Luther and J.Troe, Ber.Bunsenges.Phys.Chem., 1983, 87, 169
2. A.F.Wagner and D.Wardlaw, J.Phys.Chem., in press
3. M.Reiffer, M.J.Pilling and M.J.C.Smith, J.Phys.Chem., 1987, 91, 6028
4. P.D.Lightfoot and M.J.Pilling, J.Phys.Chem., 1987, 91, 3373
5. I.R.Slagle, D.Gutman, J.W.Davies and M.J.Pilling, J.Phys.Chem., in press
6. M.Brouard, M.T.Macpherson and M.J.Pilling, J.Phys.Chem., submitted for publication.
7. M.Brouard, P.D.Lightfoot and M.J.Pilling, J.Phys.Chem., 1986, 90, 445.
8. M.Quack, Ber.Bunsenges.Phys.Chem., 1984, 88, 94.

STUDY OF METHYL RECOMBINATION AT AMBIENT TEMPERATURE IN THE RANGE 0.2 TO 2.0 MBAR

Dieter Walter, Horst-Henning Grotheer and Thomas Just
Institut für physikalische Chemie der Verbrennung,
DFVLR, Pfaffenwaldring 38 - 40, 7000 Stuttgart 80,
West Germany

The recombination of methyl radicals has been studied as a function of pressure at ambient temperature to obtain more detailed knowledge of the kinetics of this reaction in the unimolecular falloff region. We used the mass spectrometer discharge flow technique. By dealing with diffusion and viscous pressure effects we were able to extend the pressure range of our flow reactor down to 0.2 mbar. The fast reaction $\text{F} + \text{CH}_3 \rightarrow \text{CH}_3 + \text{HF}$ served as radical source. The methyl radicals were monitored with a TOF mass spectrometer at $m/e = 15$ amu with low electron energies (below 15 eV), in order to avoid fragmentation of the CH_3 molecules in the ion source.

The title reaction was measured in an initial concentration range of $1 \cdot 10^{-11} \text{ cm}^{-3} < [\text{CH}_3] < 6 \cdot 10^{-10} \text{ cm}^{-3}$. The measured decays are of second order. Heterogeneous loss of CH_3 radicals turned out to be small. The initial methyl concentrations were determined by scavenging the radicals at the end of the flow tube via the fast reaction $\text{CH}_3 + \text{NO} \rightarrow \text{CH}_3\text{O} + \text{NO}$ and absolute determination of the product NO. Under our conditions the NO yields were not interfered by subsequent reactions. The limited spatial resolution of the method is accounted for by applying a suitable calibration procedure.

Our results yield at room temperature a falloff curve covering a substantial part of the falloff region, which has not been accessible in prior studies [2] and references therein. In the overlapping pressure regime our data are in accord with [2], however beyond 1 mbar we measured lower rate coefficients by factors 1.3 to 1.7 than predicted by [3].

Our data can be fitted to the expression

$$k(M) = \frac{k_0[M]}{1 + \frac{k_0[M]}{k_{\infty}}} \cdot F_C \cdot (1 + [\log(k_0[M]/k_{\infty})]^2)^{-1}$$

by using

$$k_{\infty} = 5.29 \cdot 10^{-11} \text{ cm}^3/\text{s}$$

$$k_0 = 9.0 \cdot 10^{-27} \text{ cm}^6/\text{s}^2$$

$$F_C = 0.6$$

An extension of our measurements to higher temperatures is underway.

References

- 1.) F. Yamada, I. R. Slagle, D. Gutman, Chem. Phys. Letters **83** (1981) 409
- 2.) I. R. Slagle, D. Gutman, I. W. Davies, M. J. Pilling J. Phys. Chem. to be published 1988
- 3.) A. F. Wagner, D. M. Wardlaw, J. Phys. Chem. to be published 1988

EXPERIMENTAL AND THEORETICAL STUDY OF THE KINETICS OF THE REACTION BETWEEN ETHYL RADICALS AND MOLECULAR OXYGEN

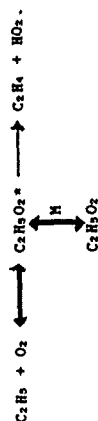
I. R. Slagle, and D. Gutman

Department of Chemistry, Illinois Institute of Technology, Chicago, Illinois 60616, U. S. A.

A. F. Wagner

Chemistry Division, Argonne National Laboratory, Argonne, Illinois 60439, U. S. A.

The kinetics of the $C_2H_5 + O_2$ reaction has been studied from 295 - 905 K. The behavior of this reaction throughout this temperature range (which includes the low-temperature addition process, the $C_2H_5 + O_2 \rightleftharpoons C_2H_5O_2$ equilibrium near 600 K, and the high-temperature process (which has the net reaction $C_2H_5 + O_2 \rightarrow C_2H_4 + HO_2$)) has been quantitatively characterized by experiment and completely accounted for by a comprehensive mechanism which has the basic form,



(The final step, $C_2H_5O_2^* \rightarrow C_2H_4 + HO_2$, represents the irreversible conversion of $C_2H_5O_2^*$ into C_2H_4 and HO_2 via a cyclic transition state, a transformation which could involve the formation of an additional intermediate such as $C_2H_5O_2H^*$).

Experiments were conducted using a tubular reactor coupled to a photoionization mass spectrometer.¹ C_2H_5 was produced by the 248nm photolysis of C_2H_5Br . Concentration profiles of C_2H_5 and C_2H_4 were recorded in time-resolved experiments. The information obtained on the $C_2H_5 + O_2$ reaction includes rate constants for the addition process below the ceiling temperature (falloff curves at 298, 385, and 473 K), phenomenological $C_2H_5 + O_2$ rate constants above the ceiling temperature (750 and 850 K), and C_2H_4 yields as a function of temperature (296, 373, and 473 K) and density ($3-24 \times 10^{-6}$ molecule cm^{-3}).

The theoretical study involved obtaining rate constants for all steps in the above mechanism using RRKM Theory (variational RRKM theory in the case of the initial addition step). A special effort was made to incorporate current knowledge of relevant potential energy surfaces as well as of structures and internal motions of reactants, intermediates, and transition states (the latter from ab initio calculations). For this reason few empirically-derived parameters were required in the kinetic model.

The ability of this theoretical model to reproduce the broad spectrum of kinetic observations which have been reported on the kinetics of the $C_2H_5 + O_2$ reaction is interpreted as strong evidence that the chosen mechanism is correct. These observations include, in addition to the results of the current study, prior determinations of falloff curves for the $C_2H_5 + O_2$ rate constant and $C_2H_4 + O_2 \rightleftharpoons C_2H_5O_2$ equilibrium constants obtained in our laboratory,^{2,3} measurements of C_2H_4 yield below the ceiling temperature by Plumb and Ryan⁴ and by Miki et al.,⁵ and phenomenological $C_2H_5 + O_2$ rate constants (593-753 K) obtained by McAdam and Walker.⁶

The mechanism is not in accord with interpretations of the kinetic studies of the reverse reaction, $HO_2 + C_2H_4$.⁷ The nature of this disagreement and its possible origins will be presented.

1. Slagle, I. R.; Gutman, D. J. Am. Chem. Soc. 1985, 107, 5342.
2. Slagle, I. R.; Feng, Q.; Gutman, D. J. Phys. Chem. 1984, 88, 3648.
3. Slagle, I. R.; Nataszczak, E.; Gutman, D. J. Phys. Chem. 1986, 90, 402.
4. Plumb, I. C.; Ryan, K. R. Int. J. Chem. Kinet. 1981, 13, 1011.
5. Miki, H.; Maki, P. D.; Savage, C. M.; Breitenbach, L. P. J. Phys. Chem. 1982, 86, 3825.
6. McAdam, K. G.; Walker, R. W. J. Chem. Soc. Faraday Trans. 2, 1987, 83, 1509.

ANGULAR MOMENTUM EFFECTS IN THE FALL-OFF REGIME

Robert G. Gilbert and Sean C. Smith

Chemistry School, University of Sydney, NSW 2006, Australia

A new technique has been developed for calculating the pressure dependence of rate coefficients for reactions (such as radical recombinations and ion-molecule associations) with a simple-fission transition state and therefore where the fall-off behavior shows strong effects due to angular momentum (J) conservation. Older techniques such as the Wase-Rabinovich method are inapplicable, since they rely on the strong collision treatment, which is grossly inaccurate. The new method (a generalization of one recently published^{1,2}) is applicable to any pressure, to any form for the collisional rotational energy transfer probability distribution function $P(R,R')$, and to any ratio of the moments of inertia of transition state (I^\ddagger) and reactant (I). It thus extends our previous solution¹ which was valid only when $P(R,R')$ was independent of R' (an approximation which is excellent for most reactions involving only neutral species, but unacceptable when $I^\ddagger/I > 6$, which includes most ion-molecule association reactions). The method starts with the full two-dimensional master equation:

$$-k_{uni}g(E,J) = \omega \int [P(E',J')g(E',J') dE dJ] - [k(E,J)\omega]g(E,J) \quad (1)$$

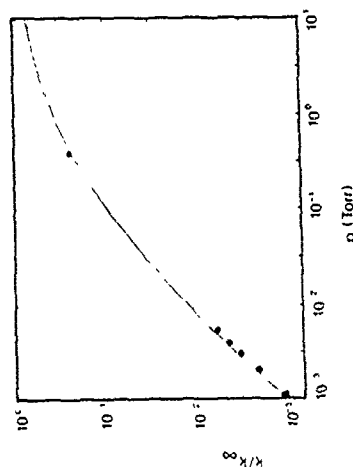
where E = energy, $P(E',J',J)$ = collisional transfer probability, $k(E,J)$ = microscopic reaction rate, k_{uni} = overall rate coefficient and ω = collision frequency. Eq. 1 is reduced to an ordinary one-dimensional master equation (i.e., in E alone), with the $k(E)$ therein an average over J of $k(E,J)$ which, while complicated in form, is straightforward to evaluate from RRKM theory for other modes such as SACM). One can then evaluate k_{uni} by conventional means for solving the master equation, with computational resources comparable to those required for ordinary RRKM/master equation solutions. Recombination (association) rates are found from k_{uni} by microscopic reversibility. In the low-pressure limit, our solution is proved to be an exact upper bound to k_0 or Troe's approximate solution for k_0 is found to exceed this upper bound by as much as a factor of 2. It is shown that this is because of approximations in Troe's factorizing k_0 into terms involving into F_{rob} etc.; Troe's $k(E,J)$ is found to be accurate. Amendments to Troe's solution have been

found which give results within 10% of our exact upper bound.

The new method is used to fit data⁴ on the association of CH_3^+ with HCN in He bath gas (see figure). These data cannot be fitted by either one-dimensional master equation or inefficient strong collision treatments. The fitting employs a $k(E,J)$ calculated by canonical variational theory, which leads to a high-pressure rate in accord with experiment. The fit to the data gives values for the average downward energy transfer for both internal and rotational energy of 125 cm^{-1} ($\pm 25\%$), which is in accord with values expected from trajectory calculations.⁵

The new technique thus enables one, either analytically or numerically, to fit and/or predict fall-off data for any reaction system (neutral or ion-molecule) with a simple-fission transition state, wherein J -conservation effects are most important. Computational requirements are modest.

- ¹S. C. Smith and R. G. Gilbert, *Int. J. Chem. Kinet.* **20**, 307 (1988).
²S. C. Smith and R. G. Gilbert, *Quantum Chemistry Program Exchange* 1988 [an update of QCPE 3, 64 (1983)].
³J. Troe, *Z. Phys. Chem.* **154**, 73 (1987); see also A.J. Penner and W. Forst, *Chem. Phys.* **13**, 51 (1976).
⁴P.R. Kemper, L.M. Bass and M.T. Bowers, *J. Phys. Chem.* **89**, 1105 (1985); J.S. Knight, C.G. Freeman and M.J. McEwan, *J. Am. Chem. Soc.* **108**, 1404 (1986).
⁵E.g., N. Dale, W.L. Hase and R.G. Gilbert, *J. Phys. Chem.* **88**, 5135 (1984).



COLLISIONAL ENERGY TRANSFER AND EVOLUTION
OF MOLECULAR DISTRIBUTION IN HIGHLY
VIBRATIONALLY EXCITED TOLUENE

K. Luther, K. Reihs and A. Symonds
Institut für Physikalische Chemie
der Universität Göttingen, Tammannstrasse 6
D-3400 Göttingen, West Germany

The kinetics of many chemical reactions depend strongly on the collisional energy transfer properties of highly vibrationally excited molecules. So far the direct experimental characterization of collisional deactivation over wide energy ranges has been limited to determinations of $\langle \Delta E \rangle$, the average amount of energy transferred per collision. The corresponding various techniques all have in common that they observe time resolved average signals from a whole relaxing sample and hence determine the energy dependence of $\langle \Delta E \rangle$ as ensemble averages $\langle \Delta E(E) \rangle$.

In a quite different approach we use our recently developed KCSI detection method ("kinetically controlled selective ionization")¹⁾. Thus we observe the time evolution of the molecular population in a preselected narrow energy interval during the course of the vibrational deactivation of a molecular sample. This energy resolved method allows to determine $\langle \Delta E \rangle$ in a non ensemble-averaged way, with a particular sensitivity to the energy dependence $\langle \Delta E(E) \rangle$. Most important

however, the measurements give an direct experimental access to the evolution of the molecular energy distribution of an ensemble during the relaxation, and values of the parameter $\langle \Delta E^2(E) \rangle$ can be determined.

We report experiments of this type with toluene^{2,3)} initially prepared by laser excitation, internal conversion and isomerization at ν : energy of 49300 cm⁻¹. KCSI data from observations at various wavelengths are presented, and the resulting $\langle \Delta E(E) \rangle$ dependence, $\langle \Delta E^2(E) \rangle$, and the evolution of the molecular energy distribution are discussed.

- 1) H. G. Löhmannsröben and K. Luther, Chem.Phys.Lett. **144**, 473 (1988)
- 2) K. Luther and K. Reihs, Ber. Bunsenges. Phys. Chem. **92**, 442 (1988)
- 3) K. Luther, K. Reihs and A. Symonds, in preparation.

IN SITU RADICAL DETECTION UNDER VLP CONDITIONS USING REMPI:
A STUDY OF THE KINETICS OF CF₃ RADICALS

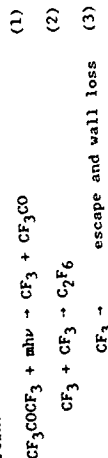
Michel J. Rossi, Robert M. Robertson and David M. Golden

Department of Chemical Kinetics, Chemical Physics Laboratory
 SRI International, Menlo Park, CA 94025 - USA

Absolute rate constants for fast radical reactions (recombination and metathesis) have been measured in the last few years using the Very Low Pressure Reactor technique such as VLP, VLP Φ and VLP/S. The stable reaction products resulting from radical-radical and radical-molecule interaction were usually monitored by electron impact mass spectrometry, and the presence of the free radical was inferred from the identity of the free radical precursor and the reaction products rather than established by direct observation.

The subject of this work is the study of the CF₃ kinetics under VLP Φ conditions based on the direct observation of the CF₃ free radical inside the Knudsen cell using Resonance Enhanced Multiphoton Ionization (REMPI) detection of free radicals. At a given time interval after the pulsed IR photolysis of an appropriate precursor, the density of free radicals is interrogated by REMPI. In order to quantitatively measure the free radical decay kinetics, which is a composite of first order (escape and wall loss) and second order (radical recombination) processes, we calibrate the REMPI signal by measuring the steady state depletion of the mass spectrometric radical precursor signal upon pulsed photolysis in a manner that is independent of subsequent chemistry (at short delay times (μ s)).

We have validated this new development by studying the recombination kinetics of CF₃ under VLP Φ conditions by comparing the results obtained using the new REMPI technique with the results from steady state mass spectrometric recombination studies and found good agreement. The pertinent reaction system is as follows:



Under our pulsed IR-irradiation conditions CF₃CO does not undergo secondary photolysis proposed in the literature. REMPI spectra of CF₃ have been taken immediately after the IR laser pulse and at variable intervals after photolysis in the range 450 to 485 nm. These spectra reveal the cooling process of the nascent CF₃ upon wall collisions with the gold coated vessel walls. The REMPI spectrum of the thermalized CF₃ agrees with the one obtained by Hudgens and coworkers under very different conditions. [DHW 82]

The time dependent REMPI signal increases within 2.5 μ s of the start of the CO₂ laser pulse, after which a rapid decay followed by a slower decay occurs. The first component of the decay corresponds to diffusional mixing of the originally irradiated volume into the plenum of the reactor. The second, slower component corresponds to "chemistry" of interest, that is competing uni- and bimolecular processes and extends to the beginning of the next IR laser pulse. Increasing the CF₃ density by either increasing the CF₃COCF₃ (HFA) pressure at constant HFA pressure, or conversely, increasing the IR fluence at constant HFA pressure, makes the bimolecular process (2) more important than the unimolecular processes (3). Using expression (4) we are able to separate k_2 from k_3 .

$$[\text{CF}_3]_0/[\text{CF}_3] = \exp(k_3 t) + (2k_2/k_3)[\text{CF}_3]_0(\exp(k_3 t) - 1) \quad (4)$$

In expression (4), t corresponds to the delay, after which an initial density of CF₃, [CF₃]₀, decays to [CF₃]. Plots of the ratio [CF₃]₀/[CF₃] as a function of [CF₃]₀ reveal k_2 and k_3 at given specific delays t .

We have studied the etching reaction of CF₃ radical on SiO₂ and Si surfaces in terms of sticking coefficients and stable reaction products using the REMPI technique. We will present the results on the sticking coefficients of 1 atom, SiH₂ and SiH₃ free radicals on surfaces of interest using the REMPI technique outlined above. The 1 atoms were generated using IR-MPD of CF₃I, SiH₂ was generated from secondary IR photolysis of n-C₄H₉SiH₃ and SiH₃ was produced via 193 nm photolysis of SiH₄. The REMPI spectrum of SiH₂ around 500 nm will be presented for the first time.

[DHW82] Michael J. Duignan, Jeffrey W. Hudgens and Jeffrey R. Wyatt, J. Phys. Chem. 1982, 86, 4156-4161.

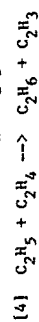
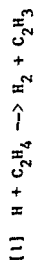
@This work was supported by USAFOSR Contract No. F49620-86-K-0001.

FORMATION OF HYDROGEN IN ETHYLENE PYROLYSIS AT 900K

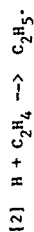
Indira S. Jayaweera and Philip D. Pacey

Department of Chemistry
Dalhousie University
Halifax, NS CANADA B3H 4J3

L-1 has been pyrolyzed at 900K in a flow system. The products ethane and hydrogen have been analyzed by gas chromatography. The results are consistent with a mechanism in which these products are initially formed as follows:



Reaction [1] occurs only 1 to 2% as often as the addition reaction,



The latter reaction is close to equilibrium. Taking the rate constant, k_2 , and the equilibrium constant, K_2 , from the literature and making small adjustments for minor processes, k_1 is found to be $(9 \pm 3) \times 10^7 \text{ L mol}^{-1} \text{ s}^{-1}$. Here the uncertainty is intended to encompass errors in the present work and in the literature parameters. Previous estimates of k_1 have differed by as much as an order of magnitude. It is suggested that, in some of these cases, reaction [2] was studied instead of reaction [1].

A secondary source of hydrogen was also observed. Its dependence on ethylene concentration was consistent with formation from an intermediate with six carbon atoms, such as cyclohexene.

UNIMOLECULAR REACTION RATE IN THE WEAK COLLISION LIMIT: AN
APPROXIMATE ANALYTICAL SOLUTION TO THE 2D MASTER EQUATION.

E.E. Nikitin, S.Ya. Umanski.
Institute of Chemical Physics, Academy of Sciences
Moscow, V-534

An approximate analytical solution to the 2D diffusion master equation which describes the vibrational and rotational collisional activation of a polyatomic molecule in a heat bath is presented. Limiting cases of a weak and strong correlation between VT and RT channels are studied, and a possibility of a partial transfer of the rotational energy into the vibrational one between successive collisions is considered. An expression for the low-pressure rate constant is arrived in which the collision efficiency β_c is expressed via the diffusion coefficients in the E_{vib} , E_{rot} space. The inversion problem, that of extracting information on vibrational relaxation paths in polyatomic molecules from experimental rate constants is briefly discussed.

THE CHEMISTRY OF INTERSTELLAR SPACE

A. DalgarnoHarvard-Smithsonian Center for Astrophysics
60 Garden Street, Cambridge, MA, 02138, USA

Interstellar space offers a diverse range of physical conditions in which molecules are formed. The molecules provide powerful diagnostic probes of the environments in which they are detected by the emission and absorption of radiation. Their presence modifies substantially the thermal and ionization balance and the evolution of the regions in which they exist.

The chemistry of cosmic gas in diffuse and dense clouds and in regions subjected to slow non-dissociative and fast dissociative shocks will be presented with an emphasis on recent developments and unanswered questions. A brief discussion will be given of molecular formation in the expanding envelope of Supernova 1987a.

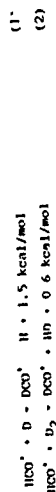
DEUTERIUM FRACTIONATION IN INTERSTELLAR MOLECULES VIA ION MOLECULE REACTIONS

A. Hansel, R. Richter, U. Lindinger, E. E. Ferguson*, M. Henchman**,
J. F. Paulson***, D. Smith**** and M. G. Adams*****

Institut für Ionophysik der Universität Innsbruck,
Technikerstrasse 25, A-6020 Innsbruck, Austria

Of the seventy or so species that have been identified in interstellar clouds, eleven contain deuterium. The relative abundance D/H is marked in excess of the cosmic n(H) ratio of 2×10^{-5} . Thus the measured D/H ratio ranges from 10^{-3} to 10^{-2} . This fractionation is found for complex and simple species alike -- and for species of high chemical potential, such as C_3H_2 . Any model for the formation of interstellar molecules must also be able to account for the deuterium exchange via ion-molecule reactions. Extensive investigation of isotope exchange reactions, such as $HCO^+ + D_2$, are facile; yet many exothermic reactions, such as (1) , are not.

as (1) , are facile; yet many exothermic reactions, such as (2) , are not.



This finding violates the accepted belief that exothermic ion-molecule reactions are facile... that hypersurfaces, whose dominant features are basins, show no restrictive energy barriers

A simple mechanism accounts for the failure of exothermic reactions such as (2) . That distinguishes (1) from (2) are the cross features of the reaction hypersurfaces -- one deep basin (Figure 1) as compared to two shallow basins (Figure 2) -- these being a consequence of the electronic states of the reactants. Thus (1) involves an unfilled-shell reactant and a filled-shell reactant, while (2) involves two filled-shell reactants. The intermediate in (1) is a strongly bound chemical intermediate; the system falls into the basin and pops out again. The intermediates in (2) are weakly bound by electrostatic forces -- for isotope exchange to occur by H/D shuttling, the second intermediate must be energetically accessible -- $\Delta E < 0$. For (2) , the wide difference in the proton affinities of CO and H_2 ($\Delta E = 1.8 \text{ eV}$) renders the second basin ($D \rightarrow \sim 0.5 \text{ eV}$) inaccessible

* Physico-Chimie des Rayonnements, Université Paris-Sud, Orsay, France
** Chemistry Department, Brandeis University, Waltham, MA 02254, USA
*** Air Force Geophysics Laboratory, AFGL/ID, Hanscom AFB, MA 01731, USA
**** Dept. of Space Research, Birmingham University, Birmingham B15 2TT, UK

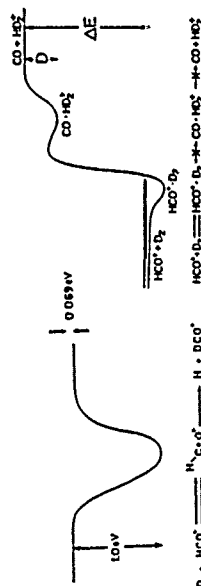
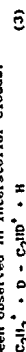


FIGURE 1

FIGURE 2

This model accounts successfully for the observed occurrence and non-occurrence of isotope exchange reactions involving the species D , HD and D_2 , according to (1) and (2) . Since deuterium atoms are the most abundant deuterium species in interstellar clouds, reaction (1) should provide an efficient synthesis for the production of deuterated ions -- provided that the intermediate is strongly bound. Such considerations led us to propose the following syntheses for CCD and C_3HD , two deuterated species that have recently been observed in interstellar clouds. (1)



We now report laboratory measurements of the rate constants for the reactions (3) and (4) using the Innsbruck Selected Ion Flow Drift Tube (SIFT) at a temperature of 300K, using helium as the buffer gas in the pressure range $0.15 - 0.35 \text{ torr}$. Both reactions are efficient: $k_3 = 2 \times 10^{-10}$ and $k_4 = 5 \times 10^{-10} \text{ cm}^3/\text{molec s}$. While the temperature dependence was not studied, the negative temperature dependence found for reaction (1) would be expected. In that case, at the temperature of interstellar clouds, the reaction would be even more efficient.

On the basis of the evidence currently available, isotope exchange with D atoms constitutes an efficient route for deuterium fractionation. It is a one-step synthesis: the efficiency should be independent of the complexity and the reactivity of the ionic reactant; and it uses as deuterating agent the most abundant deuterated species.

In "Rate Coefficients in Astrochemistry", T. J. Millar and D. A. Williams, eds (Reidel/Dordrecht, 1988) in press.

(1) M. Henchman, J. F. Paulson, D. Smith, M. G. Adams and U. Lindinger, Williams, eds (Reidel/Dordrecht, 1988) in preparation.

(2) A. Hansel, R. Richter, U. Lindinger and E. E. Ferguson, in preparation.

PRODUCT FORMATION IN THE REACTION OF N ATOMS
WITH METHYL RADICALS

George Marston, Fred L. Nesbitt and Louis J. Stief

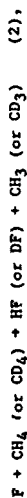
Astrochemistry Branch, Code 491,
NASA/Goddard Space Flight Center, Greenbelt, MD 20771 USA

The reaction $N(^4S) + CH_3$ is a potentially important source of HCN in the atmosphere of Titan and active nitrogen/hydrocarbon laboratory experiments. There are three thermodynamically accessible channels:



Although channel (1a) is favored energetically, it is forbidden by both spin and orbital symmetry (assuming a transition state of C_s point group) correlation rules. Both of the other channels are allowed by these rules.

We have recently measured the rate constant for reaction (1) at 300 K and obtained the result $k_1 = (8.6 \pm 2.0) \times 10^{-11} \text{ cm}^3 \text{ s}^{-1}$, where the quoted errors include both statistical (2 σ) and systematic (10-15%) errors. At present we are using a DF-MS system to study the product distribution of reaction (1). N atoms are generated by passing $h\nu$ through a microwave discharge and CH_3 (or CD_3) are formed by the reaction



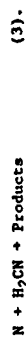
F atoms being formed by passing CF_4 through a microwave discharge.

Our results at room temperature are summarized below:

Product	Fraction	Method of Determination
HCN + H_2 (1a)	0.1	Detection of D_2 at mass 4
HCN + 2H (1b)	<0.1	Comparison of D-atom profiles with computer simulation
$H_2CN + H$ (1c)	0.9	Same as channel (1b) and detection of H_2CN and D_2CN

The results can be rationalized in terms of the symmetries and energetics of the different product channels

We have also measured the rate constant for the reaction



H_2CN was generated in reaction (1) and we obtain $k_3(300K) = (6.6 \pm 2.2/1.4) \times 10^{-11} \text{ cm}^3 \text{ s}^{-1}$. In excess N we found overall yields for the conversion of CH_3 to HCN of close to unity, suggesting that the major channel for reaction (3) is that leading to HCN + NH.

TRANSLATIONAL ENERGY DEPENDENCES OF RATE CONSTANTS FOR
ION-MOLECULE REACTIONS AS A FUNCTION OF TEMPERATURE:
ROTATIONAL ENERGY EFFECTS

Robert A. Morris, A. A. Viggiano, and John F. Paulson

Ionospheric Physics Division, Air Force Geophysics Laboratory
Hanscom AFB, MA 01731

A technique is presented by which the dependence of the rate constant on the rotational energy of the neutral can be obtained for certain ion-molecule reactions. Application of the method is limited to monatomic ions and to neutrals with vibrational energies in excess of thermal energy. These are the first reported measurements of the rotational energy dependence of an ion-molecule reaction rate constant. The apparatus employed is a temperature variable selected ion flow drift tube (SIFDT).¹

When a reaction involving a monatomic ion is studied in a drift tube, varying the electric field results only in changing the ion translational energy and therefore the center-of-mass collision energy. Thus the translational energy dependence of the rate constant at a particular temperature of reactant neutral is obtained. The temperature of the reactant neutral is equal to the bath gas temperature, defining the rotational energy of the neutral. For neutral species with vibrational modes not appreciably excited at the temperatures used in the experiment, the only significant internal energy of the reactant neutral is that of rotation. By comparing rate constants measured at a given collision energy but at different temperatures, we obtain the dependence of the rate constant on the rotational energy of the neutral.

The rate constant for the reaction $O^+ + N_2O$ has been measured as a function of ion translational energy from 205 to 450 K and the results are shown in Figure 1. Here the rate constant appears to be insensitive to the N_2O internal energy since the data obtained at different temperatures fall approximately on the same curve.

In contrast, Figure 2 shows that at a given center-of-mass collision energy, the rate constant for the $O^+ + CH_4$ reaction depends on the temperature of the CH_4 and therefore on the CH_4 rotational energy. The CH_4 rotational energy dependence for this reaction is expressed approximately as $T^{-0.5}$.

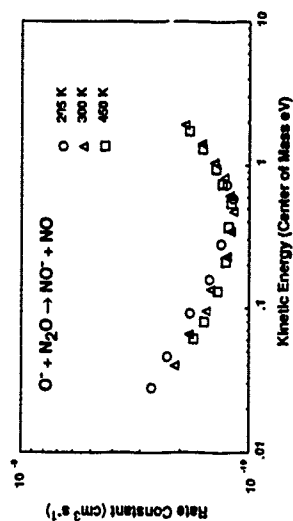


Figure 1. Rate constant for the reaction $O^+ + N_2O$ as a function of center-of-mass collision energy measured at 205, 300 and 450 K.

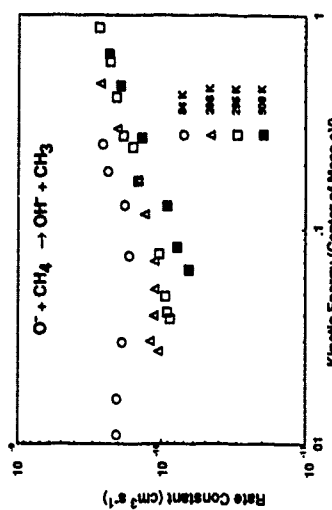


Figure 2. Rate constant for the reaction $O^+ + CH_4$ as a function of center-of-mass collision energy measured at 84, 208, 295 and 500 K.

Reference:

- 1 D. Smith and N.G. Adams, *Adv. At. Mol. Phys.*, **23**, 1988.

MODELLING OF THE THERMAL DECOMPOSITION OF ETHANE

Mark D U Gonzales and David J Norfolk

CEGB Research Division, Berkeley Nuclear Laboratories,
Berkeley, Gloucestershire GL13 9PB, UK

1. INTRODUCTION

The presence of CO and CH_4 in the CO_2 coolant of Advanced Gas-Cooled Reactors (AGRs) produces minor organic intermediates of high carbon potential. These may decompose to form unwanted carbon deposits on metal surfaces. To help predict this behaviour, a computational model of the gas-phase chemistry is being developed [1,2], based on literature kinetic data. However experiments show that the unsaturated intermediates - principally C_2H_4 - take part in surface reactions other than simple decomposition to carbon. Relevant kinetic data are not available for these reactions.

Pyrolysis of C_2H_4 in He produces many of the hydrocarbon species present in AGRs, but without irradiation. It therefore forms a simple experimental system for studying these surface reactions. This paper reports initial work without hot metal surfaces: these will be included later. The results are again analysed using a computational model based on the kinetics of the elementary species involved.

2. EXPERIMENTAL AND MODEL

The reaction vessel was a simple flow reactor comprising an externally-heated silica tube of internal diameter 40mm, through which was passed helium containing 20.5ppm C_2H_4 at close to 1 atmosphere total pressure. The effluent mixture was analysed by gas chromatography. Data were obtained at constant mass flow rate at reactor temperatures between 450 and 800°C.

The model contains 20 fundamental gas-phase reactions of 9 species describing the pyrolysis of C_2H_4 to C_2H_2 , CH_4 , C_2H_6 and H_2 via CH_3 , C_2H_5 , C_2H_3 and H. It was implemented assuming plug flow, using the Harwell FACSIMILE code [3].

3. RESULTS AND DISCUSSION

The results are summarised in Figure 1; apparent variations in carbon balance are due to calibration errors.

Initial comparison with the model predictions showed that C_2H_4 destruction below 710°C was much less than expected. This was accounted for by postulating that H atoms were lost from the gas phase by adsorption on the silica vessel. When this was allowed for, predicted and observed yields were in good agreement

throughout the temperature range (e.g. Figure 2). The hypothesis was checked by adding extra silica surface: as expected, C_2H_4 destruction was further suppressed.

[1] Norfolk, D.J. et al, 1983, Radiat. Phys. Chem. 21 (3) 307.

[2] Burns, H.G. et al, 1988, Nucl. Energy 27 (2) 109.

[3] Curtis, A.R. et al, 1985, UKAEA Report AERE-R 11771.

This paper is published by permission of the Central Electricity Generating Board. ©CEGB 1988.

Figure 1:

Observed
Effluent
Distribution at
Constant Mass
Flow Rate

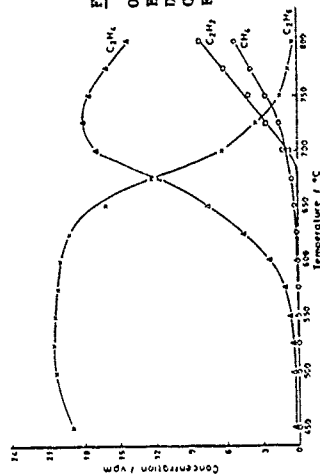
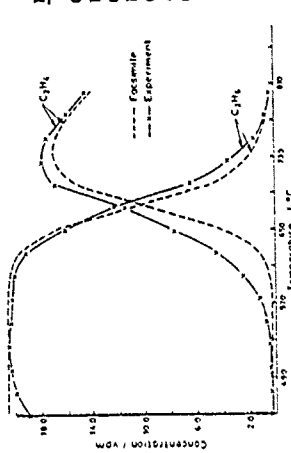


Figure 2:

Comparison of
Predicted and
Observed
Effluent
Concentrations
of C_2H_4 and
 C_2H_2

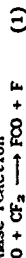


LASER INDUCED FLUORESCENCE MEASUREMENTS IN PLASMA ETCHING PROCESSES

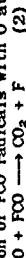
J. P. Booth, G. Hancock, N. Perry, & M. Toogood
Physical Chemistry Laboratory, South Parks Road,
Oxford, OX1 3QZ.

We report the results of a laser induced fluorescence study of the CF and CF₂ radicals in fluorocarbon plasmas used for the etching of Si and SiO₂ features in integrated circuit manufacture. In pure CF₄ at a pressure of 50 mTorr and at an RF power of 100 W delivered to a volume of ~2.2ℓ, the ground state fluorocarbon radicals are relatively unreactive in the gas phase. Physical removal, either by pumpout or reaction on the surface of the etching reactor, dominates the loss processes for CF and CF₂. These processes are examined by measurement of the spatial variations of the radicals' concentrations within the reactor, and also by their temporal variation after the discharge is rapidly switched off. The measurements are consistent with a sticking probability of 4x10⁻² for CF₂ radicals on the reactor surfaces.

The increased rate of etching of Si in a CF₄ plasma to which O₂ is added results from the increased concentration of F atoms produced. Both ground state CF and CF₂ concentrations show marked decreases in the presence of O₂, which for the latter is explained by the gas phase reaction



the rate constant for which has been measured in our laboratory as 1.75x10⁻¹¹ cm³molecule⁻¹s⁻¹. This reaction, together with the subsequent fast reaction of FCO radicals with O atoms



contributes to the observed increases in F atom concentration. It is, however, the reduction in the F atom recombination rate with CF₂, due to the removal of CF₂ by reaction with O, that is responsible for the significant increase in concentration that is observed. Fig. 1 shows the measured and calculated CF₂ and CF concentrations as a function of pressure of O₂, the calculated values resulting from modelling the electron impact production processes and the chemical and physical loss processes in the reactor.

The presence of an excess of O atoms increases the measured loss rates of CF₂ and CF following plasma turn off due to chemical removal by reactions such as (1), to the extent that diffusion and wall loss no longer dominate. This has been

exploited to extract the spatial variation of the radicals' production rate from the measured spatially and temporally resolved LIF signals.

LIF is in principle a quantitative technique, but in practice it is very difficult to estimate the sensitivity of a given detection system, and the method is generally used to measure relative concentrations. We have developed a calibration procedure for LIF measurements in which the intensity of the LIF signal from CF and CF₂ is compared with that obtained using LIF from a known concentration of a stable molecule (NOX², v⁻¹=1) at a similar wavelength near 234 nm. The concentration of CF_x radicals relative to that of the NO calibrant is given in terms of the absolute cross-section for absorption, the Franck-Condon factors in both emission and absorption, the fluorescence quantum yields, and the LIF signals integrated in time over the fluorescence pulse. The absorption cross-section was obtained from measurements of the radiative lifetimes of the appropriate upper states (26.1 ns for CF and 49 ns for CF₂) which we have undertaken. The measured ground state CF and CF₂ concentrations in a 100 W rf discharge in 50 mtorr of CF₄ were 3.4x10⁻¹¹ cm⁻³ and 3x10⁻¹² cm⁻³ respectively.

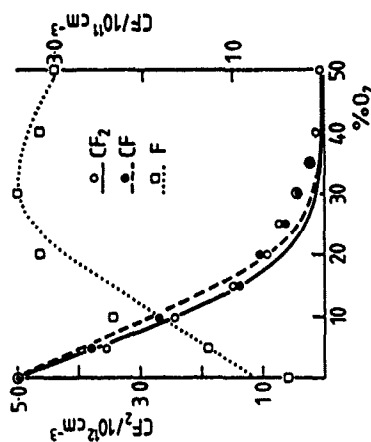


Fig. 1. Variation of ground state CF₂ and CF as a function of added O₂ for a CF₄ RF plasma. Points are experimental observations; lines are model calculations.

TIME-RESOLVED STUDIES OF THE KINETICS OF SiH_2 RADICAL REACTIONS

J.E. Baggott, R.M. Frey, K.D. King,* P.D. Lightfoot,** R. Walsh
and I.M. Watts

Department of Chemistry, University of Reading, Whiteknights,
P.O. Box 224, RG6 2AD, U.K.

1. Introduction.

The current interest in the gas-phase chemistry of silylenes derives from the role of these reactive intermediates in the chemical vapour deposition of thin films of amorphous silicon,¹ their involvement in the decomposition mechanisms of organosilanes,² and their kinetic behaviour in contrast to the corresponding carbenes which highlights the similarities and the differences between organosilicon and hydrocarbon chemistry. We have developed new time-resolved laser absorption techniques to determine absolute rate constants for SiH_2 and SiMe_2 radical removal processes, and report here some of our latest findings for SiH_2 .

2. Experimental.

High concentrations of SiH_2 radicals were generated by 193 nm (ArF exciplex) laser flash photolysis of typically 1.5 mtorr phenylsilane in either static or slowly flowing gas mixtures. The radical concentrations were monitored in real time using a multipass c.w. laser absorption technique. The monitoring light source was provided by a single mode ring dye laser operating at 17259.52 cm^{-1} , corresponding to the $^2\text{Q}_{3/2}(5)$ rotational line of the $\text{SiH}_2 \text{ } ^2\text{A}_1(0,2,0) \leftarrow \text{X}^1\text{A}_1(0,0,0)$ vibronic transition. Concentration-time profiles were determined from the transient attenuation of the monitoring light intensity incident on a fast photodiode. In the work described here, the decay profiles were single exponentials reflecting the kinetics of SiH_2 removal with various substrates under pseudo-first-order conditions.

3. Results and Discussion.

At the Symposium, we will communicate our latest results on the room-temperature insertion reactions of SiH_2 with silane, disilane and the methylsilanes. These results will be compared with previous time-resolved studies³ and the implications for silane decomposition kinetics will be discussed. We have recently reported the results of our studies of the temperature dependence of the rate coefficient for removal of SiH_2 in the presence of D_2 .⁴ These studies, which extend over the temperature interval 268 - 330 K,

are summarised in Fig. 1. We are currently extending these studies to higher temperatures, and will report our new results at the Symposium. These results will be discussed in terms of the decomposition kinetics of silane and the revised silylene heat of formation, RRKM modelling of the decomposition and insertion reactions, deuterium isotope effects, and the contrasts with the kinetics of the reaction of singlet methylene with hydrogen

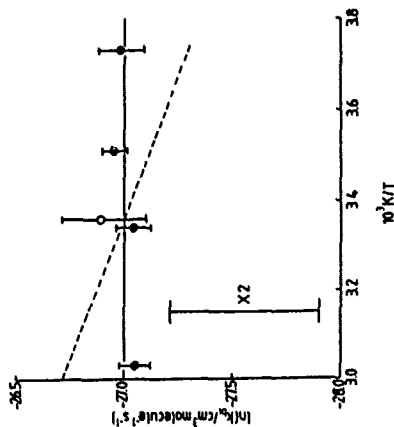


Fig. 1. Arrhenius plot for the bimolecular rate coefficient for SiH_2 removal by D_2 . (o), this work, (•) earlier work of Jasinski and Chu. The expected temperature variation for a reaction with an A-factor of $2 \times 10^{11} \text{ cm}^3 \text{ molecule}^{-1} \text{ s}^{-1}$ and an activation energy of $1.57 \text{ kcal mol}^{-1}$ is indicated by the dashed line.

4. References and Notes.

- * Permanent address: Department of Chemical Engineering, The University of Adelaide, Box 498, G.P.O. Adelaide, South Australia 5001.
- ** Present address: Laboratoire de Chimie Physique A. Université de Bordeaux I, 33405 Talence Cedex, France.
1. J.M. Jasinski, E.S. Meyerson and B.A. Scott, *Ann. Rev. Phys. Chem.*, **38**, 109 (1987).
2. P.P. Gaspar, in *Reactive Intermediates*, M. Jones and R.A. Moss, Eds., Vol. 3 (Wiley, New York, 1985).
3. J.M. Jasinski and J.O. Chu, *J. Chem. Phys.*, **88**, 1678 (1988).
4. J.E. Baggott, R.M. Frey, I.D. King, P.D. Lightfoot, R. Walsh and I.M. Watts, *J. Phys. Chem.*, in press.

HIGH-TEMPERATURE REACTOR STUDIES OF ISOLATED ELEMENTARY REACTIONS

Arthur Fontijn

High-Temperature Reaction Kinetics Laboratory
Department of Chemical Engineering
Rensselaer Polytechnic Institute
Troy, NY 12180-3590

Proper understanding of high-temperature reaction environments requires reliable knowledge of the kinetics of the individual reactions involved and their temperature dependence. For measurements on such reactions in the 300-1900 K range we have developed two basic techniques: HTP (high-temperature photochemistry) and HTFR (high-temperature fast-flow reactor) and some variants thereof. In this presentation we discuss the variety of k-dependences on T observed and make comparisons between measurements and theoretical predictions.

The HTP technique is similar in principle to the lower temperature flash-photolysis resonance-fluorescence technique. We have used it extensively for O and H, D atom reactions. The k(T) data for $\text{O} + \text{C}_2\text{H}_2$ and $\text{O} + \text{C}_3\text{H}_6$ have been found to be consistent with simple TST calculations assuming O-atom attack on the unsaturated bond as the rate-controlling step. For $\text{O} + \text{C}_2\text{H}_4$ additional mechanisms need to be considered to explain the sharp upward curvature of the Arrhenius plot above 850 K.³ By contrast, $\text{O} + \text{C}_2\text{H}_6 + \text{OH} + \text{C}_2\text{H}_5$ has significantly larger rate coefficients below 450 K than would be obtained by extrapolation from the higher temperature data.⁴ This result is consistent with calculations based on transition state theory, TST, and tunneling through an Eckart barrier. Such leveling off also is evident at low temperatures in other H-atom transfer reactions, such as $\text{O} + \text{H}_2 + \text{OH} + \text{H} + \text{N}_2\text{O} + \text{N}_2 + \text{OH}$.⁶ For both these reactions the deuterium equivalents show less curvature, in agreement with the postulated contribution of tunneling. It follows, for H-atom transfer reactions, that high-temperature rate coefficients obtained by extrapolation from low (e.g., <700 K) temperature data, whether directly or through the use of semi-empirical TST, can be seriously underestimated. Rather, extrapolations should be made from a part of the Arrhenius plot at which the low-temperature curvature is no longer evident. In general, this of course does not guard against errors introduced by further reaction channels becoming significant at higher temperatures. Measurements at actual temperatures of interest offer the most reliable approach.

HTFR results will be shown for twelve oxidation reactions of Al or B atoms, monoxides and monohalides.⁷⁻¹² These include a variety of k(T) dependences. Missing, however, is the mild upward curvature described by $k(T) = AT^m \exp(-E/T)$, $n < 4$, predicted, e.g., by simple TST,¹³ and found frequently in hydrocarbon oxidation reactions, such as $\text{O} + \text{C}_2\text{H}_2$, C_3H_6 above. In fact, apart from a few reactions, such as $\text{Al} + \text{Cl}_2 + \text{AlCl}$ + Cl, where a harpooning mechanism seems to dominate, little theory is available for reactions of such species to compare with experimental results.¹⁰ In these experiments the Al and B species have been monitored by optical spectrometry. Mass spectrometric studies have commenced to identify some of the products which have no known electronic transition spectra.

This work is supported by AFOSR (Al and B species reactions), DOE/BES (H, D/C/O systems), and ARO (H-D/N/O systems). I thank them and my collaborators, whose names are given in the references.

References

1. K. Mahmud and A. Fontijn, *J. Phys. Chem.*, **91**, 1918 (1987).
2. K. Mahmud and A. Fontijn, 22nd Symp. (Int.) Combust., in press.
3. K. Mahmud, P. Marshall, and A. Fontijn, *J. Phys. Chem.*, **91**, 1568 (1987).
4. K. Mahmud, P. Marshall, and A. Fontijn, *J. Chem. Phys.*, **88**, 2393 (1988).
5. P. Marshall and A. Fontijn, *J. Chem. Phys.*, **87**, 6988 (1987).
6. P. Marshall, A. Fontijn, and C.F. Melius, *J. Chem. Phys.*, **86**, 5540 (1987).
7. A. Fontijn, *Combust. Sci. Tech.*, **50**, 151 (1986).
8. A. Fontijn, *Spectrochim. Acta B*, in press.
9. D.F. Rogowski and A. Fontijn, 21st Symp. (Int.) Combust., p. 943 (1986).
10. D.F. Rogowski, P. Marshall, and A. Fontijn, *J. Phys. Chem.*, submitted.
11. A. Fontijn and R. Zellner, in *Reactions of Small Transient Species, Kinetics and Energetics*, A. Fontijn and M.A.A. Clyne, Eds., Academic Press, London, 1983, Chap. 1.
12. A.G. Slavejko, D.F. Rogowski and A. Fontijn, *Chem. Phys. Lett.*, **143**, 26 (1988).
13. N. Cohen, this symposium.

OSCILLATIONS AND IGNITIONS IN EXOTHERMIC REACTIONS

Peter GRAY

School of Chemistry, University of Leeds, Leeds LS2 9JT

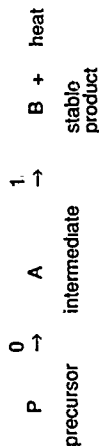
Many years ago, combustion chemistry set out on the road towards the complete characterisation and interpretation of non-isothermal, free-radical-mediated oxidations. The goal was the ability to understand and to predict the detailed course of events in simple or complicated conditions. Thanks to the power to conduct numerical computations on the grand scale it is now in reach. This modern weapon is effective but it can be extravagant of effort and expense, and it may miss its mark. To exploit computation to its maximum extent, the foundations of analytical understanding must be strengthened.

One challenge of long standing is to deal successfully with the oscillatory behaviour shown by hydrocarbon oxidation. First encountered in propane oxidation (in a closed system), oscillations are nowhere more richly displayed¹ than by acetaldehyde oxidation (in an open, flow-through system). Griffiths' landmark experimental and computational studies^{1,2} have brought the latter subject to maturity in a quantitative way. The roles played by free radicals and other intermediates are clarified. The contributions of the Knox-Benson equilibrium $R + O_2 = RO_2$ are incorporated alongside those of chain-branching, and the vital role of self-heating is established quantitatively.

Nevertheless, numerical computation is not the most elegant way to understand how jumps of ignition or extinction occur from one state to another or how oscillations are born and die. For closed systems particularly, the computational effort would be prohibitive. There is a leading role for lucid analysis and a need to recognize the simplest ways in which oscillatory and other instabilities set in. Accordingly we choose

a system³ that can be represented with great simplicity, with behaviour that is subtle and varied, but which nevertheless can be analyzed deeply. We emphasize the transient oscillatory behaviour that can be displayed in a closed system. We end by being able to account for oscillations of considerable size that give no warning of their birth yet which are born, live, grow and die long before reaction is complete.

The model incorporates only a pair of consecutive reactions



Both steps may be exothermic and responsive to temperature; one very simple case⁴ actually sets $E_0 = \Delta H_0 = 0$. The heat released in the second step raises the temperature and accelerates reaction. This intensifies the thermokinetic feedback. Heat is lost to the surroundings, so concentrations and temperatures are decoupled. There is no truly stationary state save that of ultimate chemical equilibrium. Nevertheless, simple quantitative rules can be derived and predictions made of the number and duration of oscillations.

This model has a ready experimental realisation under certain circumstances when the organic peroxide $Me_3COOCMe_3$ (= DTBP) is decomposed or oxidized in a closed vessel. Prediction and reality can be convincingly matched and an important archetypal scheme given its place in the kineticists' armoury.

1. J.F. Griffiths *et al.* Proc. Roy. Soc. **A374** 313 (1981).
2. J.F. Griffiths *et al.* Twentieth Symp. (Int.) Comb. pp. 101-109 Comb. Inst. Pittsburgh (1984).
3. P. Gray, S.R. Kay & S.K. Scott Proc. Roy. Soc. **A416** 321-331 (1988).
4. I.E. Sainikov Zh. Fiz. Khim. **23** 258 (1949).
5. See, e.g. P. Gray Proc. Roy. Soc. **A415** 1-34 (1988).

EXPERIMENTAL STUDY OF THE HIGH TEMPERATURE REACTION SCHEMES ACCOUNTING FOR THE AUTOIGNITION OF ALKANE

F. BARONNET, G. SCACCHI and Y. SIMON

Département de Chimie-Physique des Réactions, U.A. n° 328 CNRS
INPL-ENSIC, 1, rue Grandville, 54042 NANCY, France

The chemical models which have been proposed in the literature can be divided into two categories :

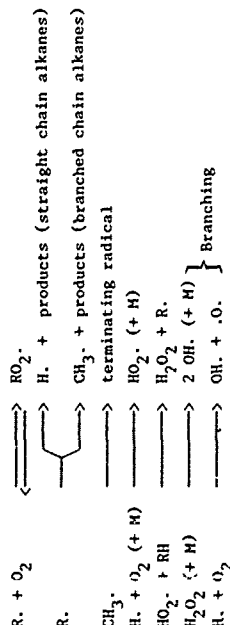
- the low temperature models, especially that proposed by QUINN, HALSTEAD, KIESCH and co-workers, recently refined and extended by COX and COLE, in which the chain cycle of the alkane (RH) oxidation is based on the alkylperoxy radical (RO₂) isomerisation theory. But the addition of oxygen on the alkyl radical (R. derived from RH by hydrogen abstraction) is a reversible step :



and it can be assumed that these models are valid for temperatures up to 800-850 K.

- the high temperature mechanisms developed by WESTBROOK et al. in the United States and by WARNATZ in Federal Republic of Germany. WESTBROOK et al. measured end-gas temperatures up to 1100 K : quite logically, they assumed that the addition of oxygen can be neglected and that R. decomposes by unimolecular steps. The scission of C-C bonds leads to the formation of smaller alkyl radicals whose subsequent decomposition gives in the end either H. atoms or CH₃ radicals.

Their mechanisms can be outlined as follows :

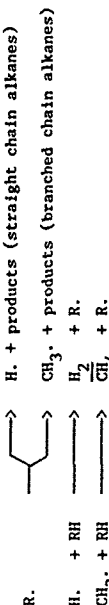


If the dominant reactions lead to the formation of H atoms, the alkane should oxidize rather easily ; the ignition delays are short and the octane number is low.

WESTBROOK and PITZ derived from this scheme an implicit correlation between molecular structure and octane number in several papers published in 1985 and 1986. Straight chain alkanes should have a low octane number since in this case H. is the dominant species (n-heptane, RON = 0) whereas in branched chain alkanes CH₃. is predominant ; their octane number is high (isooctane, RON = 100).

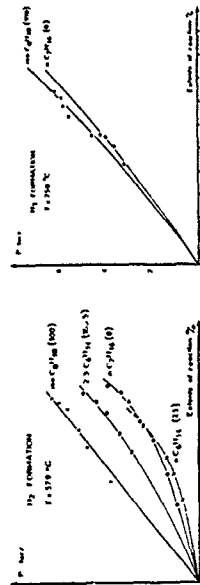
A number of experimental results have suggested that this correlation might be oversimplified and in our recent work we have examined this approach.

If we consider the above-mentioned mechanism in the absence of oxygen (pyrolysis), it becomes quite simple



If the correlation between structure and H. formation is correct, the formation of hydrogen in the absence of oxygen should be linked with the octane number, since molecular hydrogen is a kind of tracer of atomic hydrogen. Alkanes which have a low octane number should produce large amounts of H₂.

At 579°C the correlation does not work ; at 750°C, in a self-stirred reaction vessel isooctane still produces more hydrogen than n-heptane.



The origin of the discrepancies are discussed and further experiments are suggested.

REACTION MECHANISMS FOR PYROLYSIS AND OXIDATION OF HYDROCARBON FUELS OF INTERMEDIATE SIZE OVER EXTENDED TEMPERATURE RANGES

Charles K. Westbrook and William J. Pitz

Lawrence Livermore National Laboratory
Livermore, California U.S.A. 94550

In practical combustion systems, hydrocarbon fuels undergo oxidation over wide ranges of temperature and pressure. Numerical models of the fuel oxidation kinetics in such systems must therefore include all those mechanistic steps which are relevant at any portion of the entire range of operating parameters. In the present work, detailed kinetic reaction mechanisms for the pyrolysis and oxidation of straight- and branched-chain C₅ and C₆ alkane hydrocarbon fuels are developed. This includes n-pentane, 2-methyl butane, and neo-pentane (2,2-dimethyl propane) among the C₅ species, and n-hexane, 2-methyl pentane, 3-methyl pentane, 2,2-dimethyl butane, and 2,3-dimethyl butane for the C₆ species. This family of fuels is of particular interest for applied studies of autoignition in knocking automobile engines; the octane ratings of these fuels range from 25 for n-hexane to more than 100 for 2,3-dimethyl butane. Since all of these molecules are nearly the same size and have approximately the same heat of combustion and laminar burning velocity, the vast range in autoignition rates must be due only to differences in molecular structure. Therefore, particular attention has been given in this study to those factors which relate to structural distinctions.

Mechanisms have been constructed using several simple principles. The H₂-O₂-CO and C₁-C₄ submechanisms, common to all of the C₅ and C₆ mechanisms, have been taken intact from established reaction mechanisms which were shown to be suitable for comparable studies of knocking in engines with C₇ and C₈ fuels. The pyrolysis reactions and many of the corresponding elementary rate expressions were taken from the extensive pyrolysis studies of Marshall, Purnell and co-workers at the University College of Swansea²⁻⁵. Rates of H atom abstraction from these fuels by radicals, particularly OH, O and HO₂, were estimated by assuming that these rates would be equal, on a per-H atom basis, with rates in smaller fuel molecules where site-specific data were available. In other cases in which rate data were not available, estimates were made based on analog reactions. These rate assignments were then tested by means of sensitivity analyses to determine which warrant further attention in experimental and other modeling studies.

The resulting reaction mechanisms were assembled and tested for a variety of conditions which included high temperature ignition such as in shock tubes, lower temperature pyrolysis where the computed results were compared with experimental data²⁻⁵. Finally, the autoignition of each of these fuels was examined numerically under near-knocking conditions found in combustion chamber end gases.

Under high temperature conditions, thermal decomposition reactions dominate. Decomposition of alkyl radicals occurs primarily by means of β -scission. The lower temperature portions of the reaction mechanisms generally follow established principles of alkylperoxy radical isomerization theory. Addition of O₂ to alkyl radicals is followed by internal H atom abstraction within the alkylperoxy radical. Decomposition of the resulting QOOH radical to produce OH and HO₂ radicals and formation of various O-heterocyclic and conjugate alkene species then compete with addition of further molecular oxygen and production of dihydroperoxides.

Computed simulations of autoignition of stoichiometric fuel-air mixtures under internal combustion engine conditions were of particular interest in these studies. Using pressure-time data provided by Leppard⁶, times of autoignition were computed for each of the C₅ and C₆ fuels, and these times were then compared with the octane ratings of these fuels. In general, fuels with higher octane ratings ignite at later times than fuels with lower octane ratings. These trends were reproduced by the numerical kinetic model. In general, it is observed that highly branched chain hydrocarbons are more resistant to autoignition and knock. In the computed models, it was found that the higher fraction of H atoms at primary sites which are a feature of branched fuels is an important factor in the computed times of ignition. Straight chains, with many relatively loosely bound secondary H atoms, lead to large rates of OH radical production through alkylperoxy and dihydroperoxyalkyl radical processes. The extra energy barrier associated with primary C-H bonds is sufficient to retard the rate of OH radical production relative to fuels with predominantly secondary C-H bonds, and this difference correlates well with observed knock tendencies.

1. Westbrook, C. K., Warnatz, J., and Pitz, W. J., Twenty-second Symposium (International) on Combustion, in press (1988).
2. Halstead, H. P., Konar, R. S., Leathard, D. A., Marshall, R. M., and Purnell, J. H., Proc. Roy. Soc. A310, 525 (1969).
3. Konar, R. S., Marshall, R. M., and Purnell, J. H., Int. J. Chem. Kinet. 5, 1007 (1973).
4. Bull, K. R., Marshall, R. M., and Purnell, J. H., Proc. Roy. Soc. A342, 259 (1975).
5. Marshall, R. M., Int. J. Chem. Kinet. 19, 649 (1987).
6. Leppard, W., personal communication, 1988.

THE FORMATION OF FORMALDEHYDE AND ACETYLENE IN A METHANE-OXYGEN FLAME

R. LE BEC, M. P. MARTIN, P. M. MARQUAIRE and G. M. CÔME

D.C.P.R. (CNRS), ENSIC (INPL) and University Nancy I
1, rue Grandville, 54000 NANCY (France)

INTRODUCTION

This study is a part of a research program devoted to the study of some gas phase reactions of methane at "high" temperatures. The present work aims at a better knowledge of a very short duration methane-oxygen-inert gas diffusion flame, and, therefore, a particular emphasis has been put on the quenching process.

EXPERIMENTAL

The burner is made of two coaxial tubes, the output of the inner one being some millimeters at the inside of the outer one. Just at the output of the outer tube, four perpendicular turbulent jets of inert gas could ensure quenching rates up to about 10^6 K.s^{-1} (1). The reaction times thus can be very low, down to some milliseconds. The reaction products are analyzed by GPC and polarography.

EXPERIMENTAL RESULTS

The main carbon containing products are C_2H_2 , C_2H_4 , C_2H_6 , HCHO, CO and CO_2 . When the richness of the flame increases, the C_2 selectivity increases, but the conversion of methane decreases. Diluting the reagents with an inert gas decreases the selectivities in C_2H_2 , C_2H_4 and CO and increases those of C_2H_6 , HCHO and CO_2 . The maximum selectivity in HCHO, of about 0.4 %, has been obtained at the maximum dilution, i.e. at the flame extinction limit. The selectivities in C_2H_6 and HCHO fall down either if the reaction time is increased or if the quenching efficiency is reduced. The maximum selectivity in C_2 (~ 20 %) and the maximum methane conversion (~ 60 %) have been obtained by introducing oxygen by a small diameter central pipe.

The temperature of the gases in various parts of the quenching zone has been measured, and exhibits either one or two maxima.

MODELLING THE REACTOR AND THE QUENCH

Our experimental results were not intended to elucidate the mechanism of methane-oxygen flames, and therefore, as reaction model, we have used the comprehensive scheme proposed by WARNATZ (2). The flame has been modelled by an isothermal plug flow reactor, and the quench by two stirred tank reactors, the first for the mixing of the reacted mixture with the cold quench gas, and the second for the heat transfer through the walls of the casing.

CONCLUSIONS

Despite the crudeness of the reactor and quench models, the adjustable parameters (e.g. the "flame temperature") are reasonable, and the results of the simulations are qualitatively in line with the above experimental results.

From a practical point of view, our results show that much more "exotic" conditions are to be searched for, in view of producing formaldehyde by homogeneous reactions. Concerning the formation of C_2 molecules, our results are similar to those obtained in the BASF and analog processes.

REFERENCES

1. F. LAPICQUE, J. LEDE and J. VILLERMAUX, Can. J. Chem. Eng., **63**, 470 (1985).
2. J. WARNATZ, Ber. Buns. Phys. Chem., **87**, 1008 (1983).

ACKNOWLEDGMENT

This work has been funded in part by the Commission of the European Communities, through the research programme "Optimization of the production and utilisation of hydrocarbons", under contract N° ENSC/0035-F (CD).

ANALYSIS OF THE STRUCTURE OF FLAMES : EXPERIMENTAL AND MODELLING APPROACHES

J.-F. Pauwels, K. Carlier, P. Davolder and L.-R. Sochet
Laboratoire de Chimie et Chimie de la Combustion, UA CIRS 876
Université des Sciences et Techniques de Lille, Flandres Artois
59655 Villeneuve d'Ascq cedex, France

Two ways are generally used for the flame structure analysis. The first is to compare the net reaction rates obtained from experimental data processing with the calculated ones. The second and more recent approach is to compare directly the experimental mole fraction profiles of the species with the calculated ones by a global computer modelling of the flame. These two methods are combined to study a stoichiometric methanol-air flame stabilized, at low pressure (80 Torr), on a flat flame burner.

The gas samples are withdrawn continuously at low pressure (3.10⁻² Torr) through a quartz probe. The same probe is used to analyze both the paramagnetic species as H, O and OH by electron spin resonance spectroscopy and the molecular products by gas chromatography. An extrapolation method to zero pressure is used in order to take into account the possible destruction of the labile species during the residence time in the probe. The cooling effect of the probe and the perturbed temperature profiles are measured with a coated Pt/Rh thermocouple.

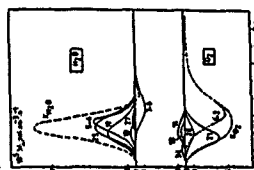
In parallel with the experimental data, two codes using the CHEMKIN formalism (SANDIA) have been developed for the structure analysis of flames : (1) CH-FLA, a home-made code calculating the net reaction rates from experimental data (11) PREMIX, from SANDIA which computes the concentration profiles from a postulated kinetics mechanism. Two kinetic mechanisms for methanol combustion are used to compute the species profiles : a revised version of the Dove-Varnatz mechanism (1984) and our chemical mechanism derived from Veathrook-Pryor scheme (1980) after reduction by sensitivity

analysis to 34 pairs of reactions involving 18 species. In order to validate the experimental procedure for ESR detection of the labile species we reported together with the experimental, three computed values based on different assumptions (1) the partial equilibrium, (2) Dove-Varnatz mechanism and (3) our model.

SPECIES	EXPERIMENTAL	CALCULATED		
		Partial Equilibrium	Dove-Varnatz	Our Model
H	2.2 x 10 ⁻¹⁰	3.5 x 10 ⁻¹⁰	10.4 x 10 ⁻¹⁰	0.4 x 10 ⁻¹⁰
O	11 x 10 ⁻¹⁰	8.8 x 10 ⁻¹⁰	1.8 x 10 ⁻¹⁰	1.8 x 10 ⁻¹⁰
OH	9 x 10 ⁻¹⁰	2.8 x 10 ⁻¹⁰	4.1 x 10 ⁻¹⁰	2.8 x 10 ⁻¹⁰

Experimental investigation and direct modelling of flames present their own drawback. While for experimental study by probe sampling procedure it is difficult to achieve measurements for the whole species concentrations in the flame and to adjust the temperature profile with the concentration ones, the uncertainties in the kinetics have significant effects on the computed species profiles.

In order to specify the role of each reaction in the methanol flame it is necessary to know the total concentration profiles especially for the minor species which are important intermediates. Actually this purpose is only possible in the case of computed flame where mechanism and species are determined as a whole.



The individual contributions of the different elementary reactions V_i to the net reaction rates R_i (plotted for O₂ and H₂O species using Dove-Varnatz mechanism) appears as a powerful means to describe the importance of the reactions along the flame.

This latter investigation may be connected with the classical sensitivity analysis of computed mechanisms.

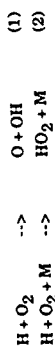
NOVEL THERMOKINETIC OSCILLATIONS IN HYDROGEN OXIDATION

by D.L. Baulch, J.F. Griffiths, Amanda J. Pappin and Anne F. Sykes

Department of Physical Chemistry, University of Leeds, U.K.

This study concerns the combustion of hydrogen-oxygen mixtures under flowing conditions in a non-adiabatic, jet-stirred vessel (continuous stirred tank reactor, CSTR). The conditions used bridge the region between "slow reaction" and ignition at the second (p-Ta) limit at pressures below 100 Torr. An oscillatory mode of ignition is observed at the boundary: it gives way to a stable stationary state corresponding to complete reactant consumption at higher temperatures within the ignition peninsula.

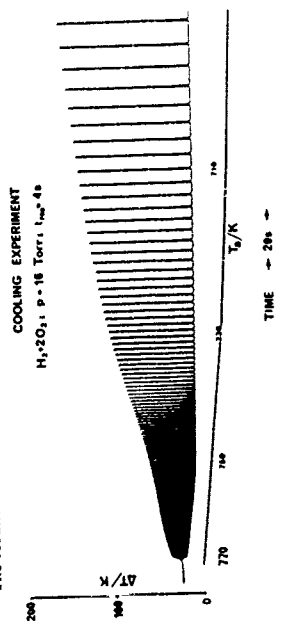
The existence of oscillations is due to the competition between the chain-branching and non-branching reactions.



The period of the oscillations is governed by the composition of the reaction mixture. Addition of different diluents (He, Ar, N₂, CO, CO₂ and C₃F₈) changes the period by virtue of their different efficiencies in promoting reaction (2).

The oscillations were studied by monitoring changes in temperature and light output from the system, and by mass spectrometry. Experiments were performed keeping conditions of composition and pressure constant while varying the temperature upwards or downwards so that the system passes through the oscillatory regime thus state: of the system can be approached from either direction and regions of multiple stability and hysteresis effects can be identified.

The results of one such experiment are shown in the figure.



Such experimental traces can be modelled successfully using an accepted, H₂/O₂ reaction scheme and allow third body efficiencies to be derived for the diluent gases. With some mixtures hysteresis and birhythmicity are observed; these effects too can be modelled.

The interpretation of the oscillations in this system form the basis for understanding the corresponding oscillatory glow phenomena in "wet" CO/O₂ mixtures under similar flowing conditions.

The ignition behaviour in gaseous thermal explosions

Lok Thang, Avygdor Moise and Huw O. Pritchard

Centre for Research in Experimental Space Science, York University,
Downsview, Ontario, Canada M3J 1P3

We have recently completed a modelling calculation of the thermal explosions of gaseous methyl isocyanide over a wide range of (spherical) vessel size (0.3–12.6 litres) and over the temperature range 320–370°C. We found good agreement between the observed¹ and calculated² values of the critical explosion pressure (p_c) and the induction time in all cases, and were able to show the magnitudes of the errors associated with various approximations that are made in the Frank-Kamenetskii theory: most important was the neglect of reactant consumption, followed by the neglect of variation of thermal conductivity with temperature, and the neglect of gas flow away from the centre as the non-uniform temperature profile developed (the two latter, taken together, being about as important as the neglect of reactant consumption). This was the first calculation in which anyone had tried to preserve a uniform pressure across the vessel during the evolution of the non-uniform temperature distribution.

In its original form, the integration algorithm used a fixed time step, for simplicity, and because of the extremely large rates of change at ignition, we were not able to integrate through an ignition; these integrations were extremely time-consuming, approximately 1 day of VAX 11/780 CPU time per 1 second of reaction time, but they run very efficiently on a GRAY computer (typical induction times are of the order of 1.5 seconds). The present work uses variable time-step integrations, and we will show how the temperature distribution and reactant consumption profiles evolve through an ignition. For relatively strong explosions (e.g. pure methyl isocyanide), the temperature remains highest at the centre of the vessel

until ignition occurs, and the reactant consumption is of the order of a few percent: ignition starts at the centre, and propagates rapidly outwards; this is consistent with the Frank-Kamenetskii model, and the critical explosion pressures are characterised by an approximately constant value of the dimensionless heat production rate (δ_c) over the whole range of temperature and vessel size noted above. However, for weak explosions (e.g. 3:1 mixture of $\text{CH}_3\text{CN}:\text{CH}_3\text{NC}$), consumption at the centre of the vessel is so severe that the temperature maximum moves away from the centre some time before ignition occurs; under these conditions, the Frank-Kamenetskii parameter δ_c has little predictive capacity.

An interesting feature of thermal explosions, and one which is shown clearly by these calculations, is the occurrence of an inflection in the spatial temperature profile (i.e. in $T(r)$) for critical and marginally sub-critical reactions, i.e. $p \geq 0.96p_c$. Below about $0.96p_c$, the temperature vs. distance profile is always convex, and ignition does not occur; conversely, above p_c , the inflection forms at the wall and propagates inwards, ignition occurring when the inflection reaches the centre of the vessel. However, in the small range $0.96p_c \leq p \leq p_c$, the inflection forms at the wall and propagates inwards, but cannot proceed to the centre because it encounters a "hole" in the reactant concentration, caused by reactant consumption, whence the incipient ignition fails. The most curious aspect of this behaviour is that the inflection forms at the wall at a time that is about 30% of the induction time: thus, the reaction appears to "know" for a long time before it happens that it is going to explode, or else come very close to exploding!

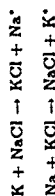
1. A. Moise and H. O. Pritchard, *J. Chem. Soc., Faraday Trans. 2*, 1988, 84, 41.
2. P. Q. E. Clothier, M. T. J. Glienna and H. O. Pritchard, *J. Phys. Chem.*, 1985, 89, 2992.

POTENTIAL ENERGY SURFACES AND DYNAMICS
OF SOME GAS PHASE REACTIONS

Keiji Morokuma, Koichi Yamashita and Satoshi Yabushita
Institute for Molecular Science, Myodaiji, Okazaki 444, Japan

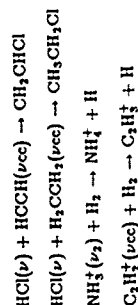
By the use of the ab initio MO method we have been studying potential energy surfaces and dynamics of varieties of chemical reactions. In the present talk, we will present results of a few of such studies.

1. Surface Hopping Trajectory Study on Transition State Spectroscopy. The first topic is the spectroscopy during chemical reactions. This new exciting field of study has recently been reviewed by Brooks.¹ We have studied the transition state spectroscopy of the K+NaCl and its reverse reactions by calculation of potential energy surfaces and surface hopping trajectories.



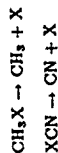
Photoabsorption and photoemission processes are modeled as the non-adiabatic transitions between the dressed ground and excited states, which are constructed from our ab initio potential energy and transition dipole functions. The theoretical emission spectrum from Na-D line as a function of laser wavenumber agrees qualitatively with the experiment by Maguire et al.² We have analyzed the spectrum in terms of the dynamics on the ground and the excited state and the nonadiabatic process between them. The Na^{*} excitation spectrum is found to be very different from the absorption spectrum, because only a small portion of excited trajectories reach the Na^{*} product due to the endoergicity of the excited state reaction. We also predict the absorption and excitation spectra for the reverse reaction.

2. State-Selected Reaction Rate Based on the Intrinsic Reaction Coordinate and Vibrational Adiabaticity. There have been several experiments in which the effects of reactant vibrational excitation on the rate constant have been studied.³⁻⁶ The systems we are interested in are



In order to shed some light on this problem, we have calculated the transition state geometry and energy, the intrinsic reaction coordinate (IRC) from the transition state to the reactant and to the product, and the normal coordinate analysis along the IRC. Using these data, we have obtained the state-selected relative rate constant based on the assumption of the vibrational adiabaticity and using the variational transition state theory. We have furthermore analyzed the curvature of the IRC, in order to examine the coupling of various vibrational modes during the reaction. In the addition of HCl to unsaturated hydrocarbons, the strong coupling between the HCl vibration and the reaction coordinate that takes place before the transition state causes energy redistribution among various vibrational modes.

3. Potential Energy Surfaces of Photodissociation of CH₃X and XCN. Photodissociation of methyl halides CH₃X and cyano halides XCN has been attracting a renewed interest in connection to the vibrational and rotational distribution of the product.



As to the potential energy surfaces of CH₃X, we find that the lowest excited state, both vertically and along the dissociation pathway, is the 1¹Π(x → σ^{*}) state, in contrast to an earlier Xσ theoretical result of the 1¹Σ⁺ state. The 1¹Π state prefers bent geometry with a large bending angle of about 50°, splitting into nearly degenerate 1¹A⁺ and 2¹A⁺ states.

With respect to CH₃I, the CI calculation using the relativistic effective core potential for I gave 1³E(x → σ^{*}) as the lowest excited state, as was predicted by Mulliken. However, the lowest excited state for ICN was found to be 1³Π(x → σ^{*}) in contrast to an earlier prediction. For both molecules the calculated vertical excitation energy agrees well with the experimental absorption peak. The torque that could give rise to the rotational excitation in the product has been found to be important only in the vicinity of the conical intersection between the two spin-orbit levels, ³Q₀ and ¹Q₁ in CH₃I. In ICN the torque is substantial in the wide range of 1³Π and 1¹Π potential surfaces, both of which are unstable with respect to bending due to the Renner-Teller effect.

1. P.R. Brooks, Chem. Rev., in press (1988)
2. T.C. Maguire, R.F. Curl, J.H. Spence and S.J. Ulvick, J. Chem. Phys. 85, 844 (1986)
3. L.P. Herman and J.B. Marling, J. Chem. Phys. 71, 643 (1979)
4. D. Klennerman and R.N. Zare, Chem. Phys. Lett. 130, 190 (1986)
5. R.J.S. Morrison, W.E. Conaway, T. Ebata and R.N. Zare, J. Chem. Phys. 84, 5527 (1986)
6. T. Turner and Y.T. Lee, J. Chem. Phys. 81, 5638 (1984)

EXACT 3D QUANTUM REACTIVITY OF THE Li+HF REACTION

A. Laganà

Dipartimento di Chimica, Università di Perugia,
06100 Perugia (Italy)

R.T. Pack

Theoretical Division, Los Alamos National Laboratory,
Los Alamos, New Mexico 87545 (USA)

G.A. Parker

Department of Physics and Astronomy, University of
Oklahoma, Norman, Oklahoma 73019 (USA)

An approach to the evaluation of the quantum reactive probability of $A + BC$ (atom + diatom) collisions has been worked out using adiabatically adjusting principle axes hyperspherical (APH) coordinates¹. The solution of the Schrödinger equation for the reactive process is performed by dividing the hyperradius (Q) interval into a series of small segments (sectors) and expanding locally the wavefunction of the three reacting nuclei in terms of the eigenfunctions of the hamiltonian of internal coordinates calculated at the center of each sector. The coupled differential equations in Q obtained in this way are then solved by applying standard numerical integrators starting from small Q values. At large distance scattering equations are reformulated in Jacobi coordinates and proper boundary conditions are applied to evaluate reactive S matrix elements.

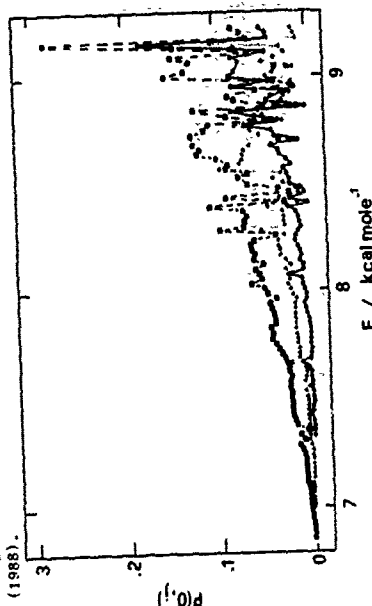
Hyperspherical coordinates are very convenient for the characteristic of singling out the privileged (almost separable) coordinate Q and reducing the remaining calculation to that of a lower dimensionality bound state problem. In this way, it is not only possible to generalize the formalism to any number of colliding atoms but it is also conceptually easy to extend findings of lower dimensionality studies to more complex situations. In our case we have applied the hyperspherical approach to the $Li + HF$ reaction which may well be considered as the prototype of (electronic and nuclear) asymmetric reactive processes. Calculations have been performed on a Bond-order potential energy

surface² fitted to the ab initio points of Chen and Schaefer after some adjustments aimed at taking into account experimental information.

Preliminary results are illustrated in the figure where the three lowest reactive probabilities ($P(v,j)$) computed at zero total angular momentum and including the lowest 80 channels are reported as a function of the total energy. As expected, the energy dependence of the reactive probability is quite structured especially at high value of the collision energy. Tunneling effects at threshold are also apparent from the figure.

References

1. R.T. Pack, G.A. Parker, J. Chem. Phys. 87, 3888 (1987).
2. A. Laganà, O. Gervasi and E. Garcia, Chem. Phys. Letters 143, 174 (1988).



Reactive probabilities calculated at $J=0$, $v=0$ and $j=0$ (circles connected by a dotted line), $j=1$ (triangles connected by a dashed line) reported as a function of the total energy. Connections have been drawn for aim of clarity.

CLASSICAL TRAJECTORY STUDIES OF THE ADDITION AND DISSOCIATION REACTION: $H + CO \rightleftharpoons HCO$

Albert L. Wagner and Rozanne Steckert†

Chemistry Division, Argonne National Laboratory, Argonne, IL 60439

Quasi-classical trajectory studies of the rotational inelasticity, complex formation, and unimolecular dissociation of $H+CO$ are being carried out on the Harding potential energy surface. This surface is known to be accurate for both HCO spectroscopy and CO inelasticity induced by hot H atom collisions. Complex-forming trajectories on this surface can last a long time (many thousands of time steps) yet, with few exceptions, be followed through to termination by unimolecular dissociation. Trajectories are selected at fixed total angular momentum J instead of the more typical fixed impact parameter. Thus, $J=0$ corresponds to trajectories in a space-fixed plane and higher J 's corresponding to increasingly complicated tumbling motion. For total $J=0$, uniform sampling of the only two initial variables (rotational and vibrational phase) leads to full detail in describing the scattering processes.

The results for rotational inelasticity indicate four different mechanisms: direct collisions off the O or the C end and complex-forming collisions that are statistical or non-statistical. The product rotational distribution is predicted to be bimodal with the lower rotational excitations produced by collisions with the O end of CO and the higher rotational excitations produced by collisions with the C end of CO . Collisions that form HCO^* ultimately produce both low and high rotational excitation in the product CO with roughly equal probability.

The results for HCO^* formation show vibrationally adiabatic behavior for the dependence on initial vibrational phase but rotationally sudden behavior for the dependence on initial rotational angle. In contrast to the vibrationally adiabatic behavior of HCO^* formation, HCO^* decay almost always leads to trajectories with less than zero-point energy in the product CO . Thus either the rotational or translational distribution of products (or both) contains excess energy in the trajectory description. This is a generic limitation of classical trajectories.

The results for the HCO^* unimolecular decay rate show the presence of both statistical and non-statistical decay processes. The statistical complex-forming trajectories decay with a single exponential and are characterized by a chaotic

function of final action with respect to initial angle. The non-statistical complex-forming trajectories can persist for over 80 turning points in the well but display a regular function of final action with initial angle. Both types of trajectories are present in approximately equal proportions. Although the non-statistical decay can not be characterized by a single exponential decay, in a coarse sense, its decay rate is considerably larger than the statistical decay rate. The statistical decay rate as a function of energy and total angular momentum shows definite differences from either exact quantum¹ or statistical RRKM² rate constants on the same potential energy surface.

ACKNOWLEDGEMENTS: This work was performed under the auspices of the Office of Basic Energy Sciences, Division of Chemical Sciences, U. S. Department of Energy, under Contract W-31-109-Eng-38.

† Permanent address: San Diego Supercomputer Center, San Diego, CA 92138-5608

References

1. Lee, K.-T.; Bowman, J. M. *J. Chem. Phys.* **1986**, *85*, 6225.
2. Wagner, A.F.; Bowman, J. M. *J. Chem. Phys.* **1987**, *91*, 5314.

NON-EQUILIBRIUM H_3 KINETICS

Carol Boves and Heshel Teitelbaum

University of Ottawa
Department of Chemistry
Ottawa, Ont., Canada K1N 6N5

We have solved the master equation describing the rates of change of the vibrational level populations of hydrogen in the reaction



and its isotopic variants, in the steady-state limit. The reaction itself depletes the vibrational level population, which in turn reduces the reaction rate. Although there have been a handful of efforts to evaluate such non-equilibrium effects in bimolecular reactions, there have been no efforts to assess them for the important reaction (1).

Our study makes use of measured¹ and calculated² microscopic state-to-state rate constants for (1) as well as measured $V \rightarrow V$ and $V \rightarrow V+1$ energy transfer rate constants involving hydrogen, in order to estimate the population depletion. The effect is manifested as a reduction of the rate coefficient. The Arrhenius activation energy is thus affected, and depends on the identity and quantity of the species which can vibrationally relax the hydrogen.

We find that the effect is negligible at low temperatures but becomes more important at higher temperatures. Consequently, we believe that theoretical values of thermal rate coefficients^{3,6} should account for these effects before comparison is made with corresponding experimental data⁷.

1. T. Dreier, J. Wolfrum, *Int. J. Chem. Kinet.* **18**, 1 (1982).
2. J.-M. Rowman, K.-T. Lee, R.B. Walker, *J. Chem. Phys.* **79**, 3742 (1983).
3. J.-E. Dove, H. Teitelbaum, *Chem. Phys.* **6**, 431 (1974).
4. H. Teitelbaum, *Chem. Phys. Lett.* **106**, 69 (1984).
5. B.-C. Garrett, D.G. Truhlar, *J. Chem. Phys.* **72**, 3460 (1980).
6. H.C. Colton, C. Schatz, *Int. J. Chem. Kinet.* **18**, 961 (1986).
7. D.N. Mitchell, L.J. DeRoy, *J. Chem. Phys.* **58**, 3649 (1973).

FEMTOSECOND REAL-TIME DYNAMICS OF REACTIONS

Ahmed H. ZewailArthur Amos Noyes Laboratory of Chemical Physics
California Institute of Technology
Pasadena, California 91125, USA

In this talk, we will discuss current applications of femtosecond spectroscopy and molecular beams to studies of chemical reactions in transition from reagents to products. Since transition states typically live for less than a picosecond, femtosecond techniques enable one to detect them and to view molecules in the process of fragmentation or formation. Hence, knowledge of the potential energy surface at the moment of separation (few Å's) is obtained.

Two types of applications of these techniques will be discussed:

First, the process of bond breaking in elementary chemical reactions involving triatomic and tetraatomic molecules. Second, we will present results for a special class of bimolecular reactions, where the collision complex between two fragments is observed in real-time.

More recent observations of "resonance" wave packet dynamics (oscillation and dephasing) in salt reactions involving two degrees of freedom will also be discussed. Comparison between theory and early cross-beam experiments will be made.

Recent References

1. M. Dantus, M. J. Rosker, and A. H. Zewail, *J. Chem. Phys.* **87**, 2395 (1987).
2. N. F. Scherer, L. R. Khundkar, R. B. Bernstein, and A. H. Zewail, *J. Chem. Phys.* **87**, 1451 (1987).
3. T. S. Rose, M. J. Rosker, and A. H. Zewail, *J. Chem. Phys.* **88**, 66,2 (1988).
4. M. J. Rosker, T. S. Rose, and A. H. Zewail, *Chem. Phys. Lett.* **146**, 175 (1988).

PHOTOFRAGMENT VECTOR CORRELATIONS IN SINGLE PHOTON AND VIBRATIONALLY MEDIATED PHOTODISSOCIATION

M Bruard, M T Martinez, J O'Mahony and J P Simons

Department of Chemistry, The University, Nottingham NG7 2RD, UK

Experimental studies of the stereochemistry of reactive (and inelastic) molecular collisions are rapidly evolving - for a recent survey and celebration see the collection of papers and articles in ref. 1. The evolution has been particularly rapid in the study of photo-initiated half-collisions thanks to the impact of polarised, Doppler resolved laser probe techniques² and a 'user-friendly' theoretical apparatus for analysing the photofragment spectral line shapes³. The new experiments have triggered in at least one case (H_2O), classical scattering calculations on 'ab initio' potential surfaces which reproduce the observed photofragment helicities⁴. The new experiments supplement the inventory of scalar photofragment properties, eg rotational, vibrational, translational and spin-orbit populations, with a new set of vectorial attributes involving the correlations between the product rotational angular momenta and recoil velocities, the E-vector of the incident photon, and the transition dipole in the parent molecule. The new data provide a three dimensional image of the half-collision dynamics, since they reflect the influence of angular, as opposed to radial actions in the dissociating molecule. Since direct photodissociation processes are associated with structureless absorption continua, the photofragment vector correlations provide a unique insight into the structural changes promoted by the electronic transition. For example, in the single photon dissociation of H_2O , from low lying electronically excited states, the preferred parallel alignment of the rotational and photofragment recoil vectors can be directly related to differences in the torsional potentials in the ground and excited states of the parent molecule (2(c), 4). The beauty of the H_2O system lies in its relative simplicity: only one type of fragment is generated and the majority of the available energy is channelled into fragment translation. For a more general application of the technique it is necessary to determine, at least approximately, the distribution of recoil velocities which arises because of the range of initial states populated in the partner fragment. When this can be ascertained, the recoil velocity averaged vector properties still provide valuable insight into the source of photofragment linear and angular momenta: recent illustrative examples include the one

photon dissociations of the X-OH systems (CH_3COOH , $HOMO_2$ and $HOCHO$).

In parallel with these developments, and serendipitously often on the same molecular systems, (eg H_2O , (CH_3COOH , $HOMO_2$), Grim's research group have been developing the art of vibrationally mediated photodissociation⁵ - the electronic continuum is accessed via excitation from an intermediate high overtone level in the ground electronic state, in a single or two-colour double resonance experiment. Unlike the conventional single photon, vertical excitation process, which initiates the half-collision from a Franck-Condon region close to the normal equilibrium geometry, vibrationally mediated excitation can be used to prepare the molecule in geometries already stretched far beyond their equilibrium dimensions. The degree of initial distortion can be tuned by varying the frequency of the second photon.

We have recently combined the strategies described in paragraphs (1) and (2) to gain an insight into the angular anisotropy of the repulsive potentials at ranges intermediate between the equilibrium geometry and the asymptotic, separated atom limit. Preliminary studies with H_2O at (2 x 752 nm) which result in photodissociation mediated via the overtone level $4v(O-H)$ from a configuration in which the initial HO-OH separation has been increased to ca. 2 Å suggest that the angular anisotropies associated with torsion about the O-O axis have all but disappeared.

Recent and new experiments involving both single photon and vibrationally mediated dissociation systems will be presented, including studies in H_2O , (CH_3COOH , $HOMO_2$ and $HOCHO$).

We are grateful for the support of the SERC and of the Laser Support Facility; MTM thanks the Spanish Ministry of Education and Science (M.E.C.) for a Research Fellowship.

1. J. Phys. Chem. 1987, 91, 5365-5515
2. (a) P L Houston, *ibid.*, 5388; (b) J P Simons, *ibid.*, 5378; (c) K H Gericke, S Klee, R J Comes and R M Dixon, J. Chem. Phys., 1986, 85, 4463; (d) M Dubs, U Brühlmann and J R Huber, J. Chem. Phys., 1986, 84, 3106
3. R N Dixon, J. Chem. Phys., 1986, 85, 1866
4. (a) J August, M Bruard, M P Docker, A Hodgson, C J Milne and J P Simons, Ber. Bunsenges., 1988, 92, 264; (b) R Schinke and V Staemmler, Chem. Phys. Lett., 1988, 145, 486
5. (a) A Sinha, R L Vander Wal, L J Bakler and F F Grim, J. Phys. Chem., 1987, 91, 4645; (b) M D Lika, J E Baggott, A Sinha, T H Fitch, R L Vander Wal and F F Grim, J. Chem. Soc. Faraday 2, 1988, in press.

STATE SELECTIVE PHOTODISSOCIATION DYNAMICS OF \bar{A} STATE AMMONIA

M.N.R. Ashfold¹, G. Ahlers², J. Giesner², R.N. Dixon¹,
L. Schneider², K.H. Welge² and X. Xie^{2,3}

¹ School of Chemistry, University of Bristol,
Bristol BS8 1TS, U.K.

² Fakultät für Physik, Universität Bielefeld,
D-4800 Bielefeld 1, F.R.G.

³ Permanent Address: Chinese Academy of Science,
Anhui Institute of Optics and Fine Mechanics,
Hefei, P.R. China

The photofragmentation dynamics of ammonia molecules following pulsed laser excitation to a number of bending vibrational levels of their \bar{A}^1_2 state has been investigated by monitoring the time-of-flight spectra of the nascent H(D)-atom products. These spectra all show well resolved structure (see fig. 1). Analysis of which reveals that the accompanying $\text{NH}_2(\text{ND}_2)$ fragments are formed predominantly in the \bar{X}^2_{2g} ground state, with little vibrational excitation, but with high levels of rotational excitation specifically concentrated about the a-inertial axis (fig. 2). The detailed energy disposal is sensitive, dependent upon the initially excited parent vibronic level. Trajectory calculations employing the recently reported ab initio potential energy surfaces for the \bar{A} and \bar{X} states of ammonia are able to provide a detailed rationale for the experimentally observed energy disposal; these highlight the massive influence on the eventual fragmentation dynamics of the conical intersection between these surfaces along the H-NH₂ dissociation coordinate.

M.I. McCarthy, P. Rosmus, H.-J. Werner, P. Botschwina and
V. Valda, J. Chem. Phys. **86**, 6693, (1987).

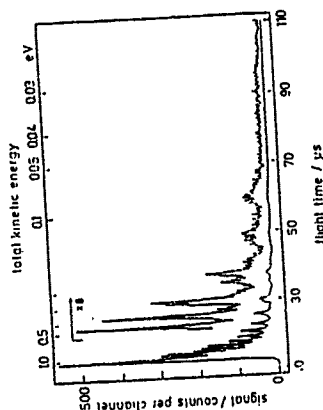


Fig. 1 H^+ ion time-of-flight spectrum resulting from photolysis of jet-cooled NH_3 at 210.2 nm (46200 cm^{-1}), within the $\bar{A}-\bar{X}$ absorption band. For clarity the middle part of the spectrum is also shown on a eight times expanded vertical scale. The top scale indicates the total kinetic energy of the recoiling fragments.

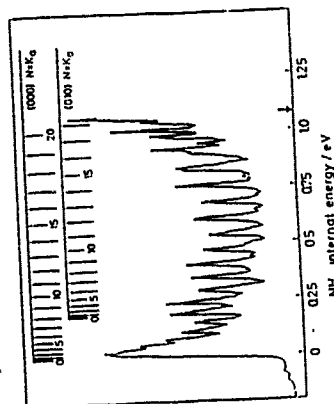


Fig. 2 NH_2 internal energy spectrum resulting from photolysis of NH_3 at 46200 cm^{-1} . Indicated above are the energies of the different vibrational levels of the (000) and (010) vibrational states of $\text{NH}_2(\text{X})$. The vertical arrow indicates the energy corresponding to the maximum available, i.e. $\text{h}\nu - D_0(\text{H}-\text{NH}_2)$.

REACTIONS OF SPIN-ORBITAL-EXCITED
CHLORINE ATOMS ($^2P_{1/2}$)

S.A. Chasovnikov, A.I. Chichinin and L.N. Krasnoperov
Institute of Chemical Kinetics and Combustion,
630090, Novosibirsk, USSR

Collisional quenching of the chlorine atom fine structure upper state- $^2P_{1/2}$ on a number of collisional partners has been studied along with the reactions of $Cl(^2P_{1/2})$ and $Cl(^2P_{3/2})$ with ICl and CINO molecules. The kinetics of these states has been measured using a time-resolved laser magnetic resonance technique (IR LMR) from the chlorine atom fine structure (f_5) transition, $^2P_{1/2} - ^2P_{3/2}$ ($^{13}C^{16}O_2$ -laser, 11P(36), 882.2875 cm^{-1}). Two types of experiments have been performed to study the quenching processes:

- observation of the kinetics of the saturation of the chlorine atom f_5 transition LMR signal by laser radiation field after a fast tuning to the transition by a fast magnetic field jump;
- observation of the chlorine atom f_5 transition LMR signal kinetics after pulse photolysis of ICl and CINO molecules.

Results:

- the quenching of $Cl(^2P_{1/2})$ on a number of collisional partners is 1-3 orders slower than reported earlier.
- The excited $Cl(^2P_{1/2})$ atom reacts with ICl and CINO molecules much slower than the unexcited one ($Cl(^2P_{3/2})$).
- A continuous population inversion between the chlorine atom f_5 structure levels under CW DC and HF-discharge in ICl due to the fast chemical depopulation of low level is observed.
- The laser action of the chlorine atom f_5 transition is obtained with the ICl pulse photolysis. Quantitative data are listed in the table.

Rate data for $Cl(^2P_{1/2})$

- $Cl(^2P_{1/2}) + H \rightarrow Cl(^2P_{3/2}) + H$
- $Cl(^2P_{1/2}) + M \rightarrow$ products
- $Cl(^2P_{3/2}) + M \rightarrow$ products

M	$(k_1 + k_2)/(cm^3/s)$	M	$(k_1 + k_2)/(cm^3/s)$
He	$\leq 7.3 \times 10^{-14}$	CF_4	$(2.8 \pm 1.0) \times 10^{-11}$
Ne	$\leq 4.2 \times 10^{-14}$	CCl_4	$(2.0 \pm 1.0) \times 10^{-16}$
Ar	$\leq 2.7 \times 10^{-15}$	N_2	$\leq 2 \times 10^{-14} *$
Kr	$\leq 5.4 \times 10^{-15}$	H_2	$6 \times 10^{-11} *$
Xe	$\leq 4.5 \times 10^{-14}$	O_2	$2 \times 10^{-11} *$
O_2	$(1.7 \pm 0.4) \times 10^{-13}$	CH_4	$(0.2-2) \times 10^{-11} *$
Cl_2	$(7.4 \pm 2.6) \times 10^{-13}$	NH_3	$(3-6) \times 10^{-12} *$
H_2O	$(7.8 \pm 3.0) \times 10^{-11}$	O_3	$7 \times 10^{-12} *$
CF_2Cl_2	$(1.0 \pm 0.4) \times 10^{-10}$		
M	$(k_1 + k_2)/(cm^3/s)$	$k_3/(cm^3/s)$	
SiH_4	$(4.6 \pm 1.5) \times 10^{-10}$		$(1.6 \pm 0.5) \times 10^{-10}$
ICl	$(3.3 \pm 0.5) \times 10^{-13}$		$(1.0 \pm 0.3) \times 10^{-11}$
CINO	$(1.8 \pm 0.4) \times 10^{-11}$		$(7.7 \pm 1.7) \times 10^{-11}$

* preliminary, believed to be correct within the factor of 3.

¹V. Ch. Bokun, E. B. Gordon, L. N. Krasnoperov, S. A. Sotnichenko, A. I. Chichinin, Sov. Quant. Electron., 13 (1986) 1319.

MOLECULAR BEAM STUDIES OF IONIZATION REACTIONS IN COLLISIONS OF EXCITED RARE GAS ATOMS WITH MOLECULES

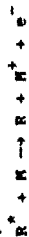
Brunetto Brunetti and Franco Vecchiocattivi

Dipartimento di Chimica, Università di Perugia,
06100 Perugia, Italy.

The ionization reactions occurring in the thermal energy collisions between metastable rare gas atoms and atoms and molecules are studied by a crossed molecular beam experiment. The metastable rare gas atom beam is obtained by electron bombardment of an effusive rare gas beam. The ions and high Rydberg states also produced in the electron bombardment region are removed from beam by an electric field. The target beam is produced by a microcapillary array. All the ions produced in the beam crossing region are extracted, focused and detected after mass analysis by a quadrupole mass filter. The metastable atoms are detected by a channel electron multiplier which can be moved into the scattering volume. The collision energy dependence of the cross sections for the formation of each product ion is obtained by a time-of-flight technique. The metastable rare gas atom beam is pulsed by a slotted rotating disk and the time spectra of metastable atoms and product ion are recorded by an on-line computer.

The ionization of Ar, Kr, Hg, N₂, O₂, CO and NO by metastable Ne atoms has been recently studied¹⁻⁴. For Hg

the ionization by metastable Ar and Kr has been also investigated³. In all cases it has been found that the Penning ionization,



(R = Ne, Ar, Kr and M = Ar, Kr, Hg, N₂, O₂, CO, NO) is the dominant reaction, but associative ionization has been also observed,



The experimental results for the ionization of atoms have been analyzed within a semiclassical treatment with the assumption of an optical potential model. This analysis gives interesting information about the ionization dynamics in these systems.

For the ionization of O₂ and NO it has been found some evidence of the formation of ionic intermediate (Ne⁺-O₂⁻ or Ne⁺-NO⁻) by a "harpooning" mechanism just before the ionization event. In order to study the details of the reaction dynamics in these cases, an analysis of the ionization cross sections together with other scattering results (elastic integral and differential cross sections) has been undertaken.

REFERENCES

- 1 - A. Aguilar, B. Brunetti, S. Rosi, F. Vecchiocattivi, and G.G. Volpi, J.Chem.Phys. 82 (1985) 773.
- 2 - B. Brunetti, F. Vecchiocattivi, and G.G. Volpi, J.Chem.Phys. 84 (1986) 536.
- 3 - L. Appolloni, B. Brunetti, J. Hermannussen, F. Vecchiocattivi, and G.G. Volpi, J.Chem.Phys. 87 (1987) 3804.
- 4 - L. Appolloni, B. Brunetti, F. Vecchiocattivi, and G.G. Volpi, J.Phys.Chem. 92 (1988) 918.

STATE-TO-STATE EXCITATION FUNCTIONS BY TIME PROFILES OF CROSSED BEAM CHEMILUMINESCENCE

by

E. Verdasco, V. Sáez Rábanos, T. Contreras and A. González Ureña

Departamento de Química Física. Facultad de Química. Universidad Complutense de Madrid. 28040-Madrid. Spain.

Experimental

Supersonic pulsed beams of polyatomic molecules were crossed with cw beams of alkaline earth atoms in different electronic states. The metastable Ca^* source¹ consisted of a stainless steel heated oven where ground state Ca atoms are excited to metastable ^1P and ^1D states by a low-voltage dc discharge. By changing the discharge conditions² different metastable concentrations were produced to measure the state-to-state cross section for both the ^1P and ^1D reactions.

Typically time of flight spectra of the supersonic beams were measured by using a quadrupole mass filter. The time profile chemiluminescence of the product reaction was measured at the cross beam volume via a field lens telescope coupled to a photomultiplier and boxcar that is interfaced to an INVES PC for data storage and analysis.

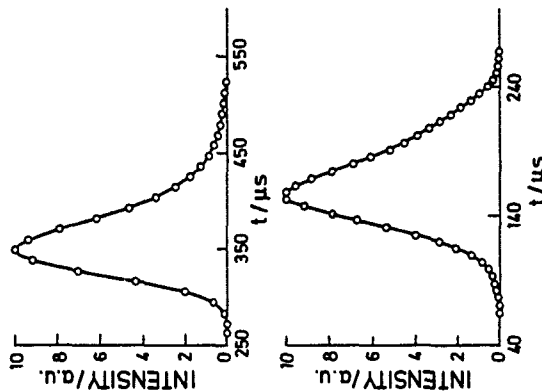
Results

Figure 1 (top) shows a typical time-of-flight spectrum of the N_2O beam as measured by the quadrupole mass spectrometer (54.0 cm beyond the nozzle). The bottom figure displays a time profile of the CaO^* formed, in the cross beam volume, from the Ca^* ($n^1\text{P}/n^1\text{D} \approx 0.30$) + N_2O reaction.

Several examples of excitation functions for different electronic states, obtained by the present cross beam arrangement, will be shown including a comparison of the selectivity of translational versus electronic excitation in these alkaline earth atom reactions.

In addition the capability of the present technique with respect to related experimental methods³ will be discussed.

This work received financial support from the Comisión Interministerial de Ciencia y Tecnología of Spain (Proyecto 85/007)



References

1. E. Verdasco, V. Sáez Rábanos, F.J. Aoiz and A. González Ureña, *J. Phys. Chem.* 91, 2073 (1987).
2. E. Verdasco, V. Sáez Rábanos and A. González Ureña, submitted for publication.
3. See for example A. González Ureña, *Adv. Chem. Phys.* 66, 213 (1987).

SCATTERING OF ORIENTED MOLECULES

S. Stolte

Molecular and Laser Physics, Dept. of Physics
University of Nijmegen, Toernooiveld, 6525 ED Nijmegen
The Netherlands

Experiments studying the influence of molecular orientation (the steric effect) in crossed beam reactive scattering and in beam-surface scattering are discussed. Intensive beams of molecules, with controllable orientation (NO , N_2O , CH_3F , etc.) are produced by cooling these molecules in a supersonic expansion ($T=3-10$ K). By subsequently passing them through an electric hexapole focuser the molecules are state selected in a single rovibrational state (J, K, M). Employing this technique Jalink and coworkers^{1,2} have investigated the orientational dependence for the chemiluminescent reaction $\text{Ba}+\text{N}_2\text{O}(v_2=1) \rightarrow \text{BaO}^+ + \text{N}_2$, state selecting both the $J=1$ and $J=2$ reactant states. This reaction, which is highly exothermic ($\Delta D^0 = -4.11$ eV) for the BaO electronic ground state exit channel, disposes practically all of its excess energy as internal excitation of the BaO product molecule. Evidence has been found that the chemiluminescent yield ($\text{BaO } A^1\Sigma^+ \rightarrow X^1\Sigma^+ + h\nu$) reflects total reactivity. The resulting strong dependence of the reaction cross section upon the initial angle of attack, λ_0 ($\cos \lambda_0 = \langle \cos \theta_{\text{rel}} \rangle$), of the N_2O molecule as a function of the collision energy E_{tr} is displayed in Fig. 1. In agreement with the angular dependent line of center model, proposed by Smith³ and later generalized by Levine and Bernstein⁴, the influence of λ_0 upon the total reaction cross section is found to decrease with E_{tr} . The range of λ_0 -values surrounding an angle dependent (hard sphere) activation barrier $V(\cos \lambda_0)$ surrounding the N_2O molecule in its collision with a Ba atom increases for increasing E_{tr} . A simple barrier, $V(\cos \lambda_0) = (0.063 \pm 0.001 \text{ eV}) \cdot (1 - \cos \lambda_0)$, was essentially found to reproduce the observed dependence of reactivity upon $\cos \lambda_0$. However, in contradiction to our observations, the model predicts the reactive reaction cross section for non-oriented molecules, σ_0 , to increase with E_{tr} . To explain the full dependence of $\sigma_0(\cos \lambda_0)$ upon E_{tr} , the effect of recrossing has to be added to the analysis.

In addition to the influence of $\cos \lambda_0$ upon the total reactivity Jalink¹ discovered also that both the vibrational state distribution and the angular momentum alignment⁵ of the nascent BaO product molecules depend on the angle of attack. By filtering the chemiluminescence a specific electronic exit channel can be probed for electron-jump type reactions as $\text{Ca}(^1\text{D}) +$

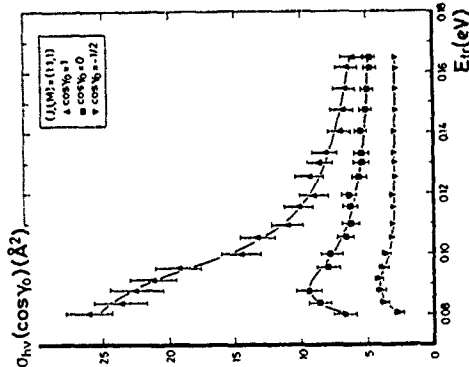


Fig. 1: Deconvoluted steric excitation functions for "heads-on" ($\cos \lambda_0 = 1$), "side-on" ($\cos \lambda_0 = 0$), and "tails-on" ($\cos \lambda_0 = -1$) for the $\text{N}_2=1, J=1$ state of N_2O calculated from the measured Legendre moments, σ_1/σ_0 and σ_2/σ_0 and the chemiluminescent reaction cross section obtained for non-oriented N_2O molecules, σ_0 . Smooth curves are drawn through the plotted points.

$\text{CH}_3\text{F}(J_{\text{rot}}) + \text{Ca}(^1\text{D}) \rightarrow \text{CaF}(^2\Pi) + \text{CH}_3$ and $\text{Ca}(^1\text{D}) + \text{CH}_3\text{Cl} \rightarrow \text{CaBr}(^2\Sigma) + \text{CH}_3$. The steric effect observed for these reactions appears to be strongly influenced by the exit channel.

In an experiment by Kuipers et al. the presence of orientational effects for gas-surface scattering is investigated in Amsterdam⁶. An intense beam of NO molecules selected in the $J=0, M=1/2$ state, resulting from focusing a pulsed supersonic beam ($T_{\text{rot}}=4$ K) with an electric hexapole field, impinges onto an $\text{Ag}(111)$ surface. The nearly specular scattered NO molecules are detected by a quadrupole mass spectrometer. When the O-end is pointing towards the surface the scattering angle is observed to be more preferentially inclined towards the surface than when the N-end is pointing towards the surface. Apparently the anisotropic potential between the surface and the NO molecule induces a larger transfer of incoming E_{tr} into outgoing rotational energy when the O-end is pointing towards the surface.

1. H. Jalink, PhD-thesis, Nijmegen, November 1987
2. D.H. Parker, H. Jalink and S. Stolte, *J. Phys. Chem.* **91** (1987) 5427
3. I.W.M. Smith, *J. Chem. Educ.* **59** (1982) 9
4. R.D. Levine and R.B. Bernstein, *Chem. Phys. Lett.* **105** (1984) 467
5. H. Jalink, S. Stolte and D.H. Parker, *Chem. Phys. Lett.* **140** (1987) 65
6. H. Jalink, D.H. Parker and S. Stolte, *J. Chem. Phys.* **85** (1987) 61
7. M. Janssen, private communication 1988
8. E.W. Kuipers, M.G. Tenner, A.M. Kleyn and S. Stolte, submitted for publication

PLENARY LECTURE

COMPLEX IONS: TRANSITION STATES AND INTERMEDIATES IN GAS PHASE
IONIC IN GAS PHASE IONIC REACTIONS

John I. Brauman

Department of Chemistry, Stanford University,
Stanford, CA 94305-5080 USA

Many ionic reactions in the gas phase involve intermediates and transition states which are more stable than reactants or products. The reaction dynamics can be affected by the existence of these intermediates. Examples from S_N2 , carbonyl addition, and proton transfer reactions will be discussed. Evidence for unsymmetrical intermediates will be presented.

A STUDY OF THE MECHANISM OF PROTON TRANSFER TO C.H.₃F AND CH₃C.H₂F USING TANDEM MASS SPECTROMETRY

Robt Mason

Department of Chemistry, University College of Swansea,
Swansea SA2 8PP, UK.

Tandem mass spectrometry is a relatively new technique in the study of ion molecule reactions. The advantage it offers over conventional mass spectrometry is that it is often able to distinguish between unusual isomeric ion species. In this study, competitive proton transfer to either the ring or the substituent of various halogenated aromatic compounds has been investigated as a function of temperature and pressure. Protonated aromatic compounds have long been of interest (1) because they are often invoked as intermediates in acid catalysed processes.

The reactions were carried out in a "high pressure" and temperature variable chemical ionisation source (2) ions diffusing through the ion exit aperture were accelerated to 6kV and analysed using a reversed geometry mass spectrometer. The magnetic first sector is used to isolate the ionic mass of interest from many others formed in the reaction cell. The protonated species is then caused to fragment by collision-induced decomposition, the products of which are analysed using ion kinetic energy spectroscopy. It has been found (2) that species protonated on the fluorine atom of fluorobenzene and the fluorobenzenes can be readily distinguished from those in which the proton is attached to the ring.

Proton transfer from H₃⁺, CH₃⁺, C₂H₅⁺, H₂O⁺ and CH₃OH⁺ were all studied, but only CH₃⁺ gave rise to protonation on the F atom. Molecular orbital (MO) calculations indicated that the F atom is in fact the least thermodynamically favourable site, having a calculated proton affinity of 590 kJ mol⁻¹ compared to a ring carbon atom value of 780 kJ mol⁻¹. This concurs with the observation that the ions of lower Brønsted acidity than CH₃⁺ fail to protonate the F atom site, but does not explain why the more acidic H₃⁺ also fails.

The degree to which substituent protonation occurred increased significantly as the temperature decreased, becoming almost complete below 273K. This behaviour is seemingly odd in that the higher energy species is most favoured at lower temperatures. On the other hand the F atom provides the negative end of a dipolar molecule, which at lower temperatures would become increasingly "locked" onto

an incoming reactant ion (3). At such temperatures the transferring proton will be caused to approach along the potential energy surface via the F atom keeping all other things equal, experiments with the isomers of fluorotoluene showed the degree of substituent protonation increased significantly with the dipole moment of the molecule, as expected according to our MO theory calculations the F atom proton affinities of these compounds remain constant to within 3 kJ mol⁻¹.

Even so the dramatic temperature dependence is too large to be explained only in terms of the locked ion-dipole effect. This predicts (over the 273-600K temperature range studied) an increase in relative rates for the formation of the fluoro over the ring protonated species, to be in the region of 1.2-1.5 compared with the experimental value of 1.9. Likewise the dipole effect is much bigger than theoretically predicted.

It seems likely therefore that the protonation of the F atom site proceeds via the formation of a weakly bound adduct, presumably CH₃-H₃⁺-FC₆H₅. A strong negative temperature dependence is a feature of such association reactions. A full reaction sequence has been suggested, steady state analysis of which predicts the following dependence for the ratio of ring (R) to fluorine (F) protonated ion concentrations, on the total pressure, M, and fractional concentration, x, of the fluorocompound:

$$[R]/[F] = (a+bx)/M + cM + dNx + eM^2x;$$

where a - e are constants. Experiments as a function of x and M support this scheme.

H₃⁺ must also approach the F atom at low temperatures. It does so however at an energy higher than the barrier for intramolecular proton migration over to the ring and with an exothermicity large enough to break the newly formed HF bond. The ring, when accessible, would always be favoured, even at high energies, an entropic grounds this is supported by the observation of an intense metastable ion decomposition (HF loss) peak when H₃⁺ is the reactant. In a loose sense therefore proton capture by the F atom exhibits a form of "resonance" behaviour.

1 V J Hehre and J A Pople, *J Am Chem Soc.*, 1972, 94, 6901.

2 R S Mason, D Milton and F M Harris, *Chem. Comm.*, 1987.

3 T Su and V J Chesnavich, *J Chem. Phys.*, 1982, 76, 5183.

ENERGY UPTAKE IN THE COLLISION OF MASSIVE IONS WITH INERT GAS ATOMS

Peter J Derrick

Department of Chemistry, University of Warwick,
Coventry CV4 7AL, U.K.

Reliable methods now exist for forming massive gaseous ions from involatile, thermally sensitive materials, including small proteins, industrial polymers and solid-state inorganic materials¹. The characterisation of such ions represents a major challenge, because the mechanisms of production are complex and present understanding does not permit predictability². One approach to characterisation is tandem mass spectrometry, whereby a gaseous ion is excited and fragments to give a mass spectrum. Excitation is normally affected by collision between the ion beam (with keV translational energies) and a target gas. The mechanism of energy uptake in such an encounter between a massive ion ($m/z \geq 1000$) and an inert gas atom has been the subject of some discussion³. It is generally recognised that the energy transfer can be substantial (perhaps as much as 10^3 eV). There is one view that the energy deposition proceeds via electronic excitation⁴, however, experimental results presented here weigh against this mechanism. An alternative view that energy deposition is via direct momentum transfer in impulsive collisions is consistent with available experimental data.

The experimental results presented concern translational spectroscopy of the molecular ion of valinomycin (a cyclic peptide of mass 1110.6u) and ionic clusters of caesium iodide $(Cs(CsI)_n)^+$. The translational energy E_f of a fragment ion m_f^+ is measured, and the translational energy E_p of the parent ion m_p^+ from which it is formed taken to be $(m_p/m_f) E_f$. If the translational energy of the parent ion prior to collision is E_0 , the energy loss ΔE suffered by the parent ion as a result of collision is $E_0 - E_p$, i.e. $\Delta E = E_0 - (m_p/m_f) E_f$. Such energy losses ΔE have been obtained from measurements on various fragment ions from the aforementioned peptide ion and from cluster ions of various sizes, using He, Ar, D₂ and H₂ as target gases and a range of parent ion energies (8keV to 20keV). The energy losses ΔE can be used to obtain the internal energies Q taken up by the

parent ions in collision, if a simplifying assumption is made concerning scattering. The dependences found for energy loss ΔE on parent ion mass, parent ion energy and target gas mass are consistent with energy transfer via direct momentum transfer.

An impulsive collision theory is used to rationalise the trends in the results. An explanation is found for the fact that helium seems to be a more efficient target gas than argon for collisional activation of massive ions, even when with helium the centre-of-mass collision energy is very low as a result of the high-mass of the incident ion.

Acknowledgements

All experiments were performed in the School of Chemistry, University of New South Wales, Australia, under grants provided by the Australian Research Grants Scheme.

References

- 1 P J Derrick, *Z.Fres.Anal.Chem.*, 1986, **324**, 486-491.
- 2 See "Gaseous Ions from Involatile, Thermally-Sensitive Materials: Energetics and Mechanisms", eds. P J Derrick and B U R Sundqvist, *Int.J.Mass.Spectrom. Ion Proc.*, Vol 78 (1987).
- 3 G M Neumann, M M Shell and P J Derrick, *Z.Naturforsch.*, 1986, **39A**, 584-592.
- 4 D L Bricker and D H Russell, *J. Am Chem Soc.*, 1986, **108**, 6174-6179.
- 5 B C Freasier, D L Jolly, N D Hamer and S Nordholm, *Chem Phys.*, 1986, **106**, 413.

CHARGE TRANSFER EXCITATION AND FRAGMENTATION OF MOLECULAR IONS IN ASSOCIATION WITH ARGON CLUSTERS

D. M. Bernard, N. G. Gollig and A. J. Stace

School of Molecular Sciences, University of Sussex, Falmer,
Brighton BN1 9QJ, U.K.

Ion clusters of the type $Ar_n \cdot CH_3OC(H)O^+$, $Ar_n \cdot CH_3OC(D)O^+$ and $Ar_n \cdot CD_3OC(H)O^+$ for $n = 10$ to 130 have been formed by electron impact following the adiabatic expansion of an argon-methyl formate mixture. In each case the methyl formate was observed to undergo unimolecular decomposition to give $Ar_n \cdot CH_3OH^+$, $Ar_n \cdot CH_2OH^+$, $Ar_n \cdot CHOH^+$, $Ar_n \cdot CHO^+$, $Ar_n \cdot CO^+$, $Ar_n \cdot CH_2OC(H)O^+$, and $Ar_n \cdot CHOC(H)O^+$, or its deuterated equivalent. However, other fragments, which are present in the mass spectrum of the isolated molecular ion, do not appear when methyl formate is clustered with argon. These observations can be explained in terms of a model that the molecular ion receives the energy difference $I.P.(argon) - I.P.(methyl\ formate)$ via a charge transfer mechanism. To date we have been unable to assign an exact value for the I.P. of large argon clusters. However, it would appear to lie within the range $13.8\text{ eV} - 15.75\text{ eV}$. The difference depends on whether or not there is self-trapping of the positive charge within the inert gas component prior to its transfer to the molecular ion. Self-trapping of the charge will reduce the energy available to the molecular ion by approximately 2 eV . Therefore, by comparing the energetics of the various unimolecular reaction steps open to the methyl formate ion, either in isolation or clustered with argon, we might achieve a better understanding of the charge transfer process.

In addition, the fragment ions exhibit considerable variations in their relative intensities as a function of cluster size. This we explain in terms of so called 'magic number' configurations for the integral cluster structure, where the oxygen atom in the fragment ions is required to complete the 'magic number'

structure. Any remaining portion of the fragment ion is assumed to protrude from the main body of the cluster. This effect is specifically highlighted with the enhanced intensity of $Ar_n \cdot CH_3OH^+$, $Ar_n \cdot CH_2OH^+$, $Ar_n \cdot CHOH^+$, $Ar_n \cdot CHO^+$ and $Ar_n \cdot CO^+$ compared to the average intensity of the majority of clusters. However, this pattern is not repeated for the $CH_3OC(H)O^+$ and $CHOC(H)O^+$ fragments. Instead, the most intense combinations occur for argon clusters containing one less argon atom, i.e. $Ar_{n-1} \cdot CH_3OC(H)O^+$, and $Ar_{n-1} \cdot CHOC(H)O^+$. This, we suggest, is caused by the rapid dissociation of the methyl formate ion into a methanol ion and neutral carbon monoxide, with both fragments remaining in association with the argon cluster.

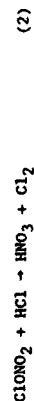
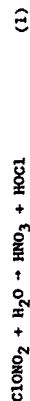
Neutral clusters were produced by an adiabatic expansion of an argon-methyl formate mixture through a pulsed nozzle operating at 20 Hz . The clusters then passed, via a skimmer, into the ion source of a reverse geometry, high resolution VG ZAB-E mass spectrometer, where they were ionized with 70 eV electrons. The ion clusters were monitored using phase sensitive detection with a reference being provided by the unit which drives the nozzle.

1. A.J.Stace, *J. Amer. Chem. Soc.*, **107**, 755 (1985).
2. A.J.Stace, *J. Phys. Chem.*, **91**, 1505 (1987).
3. A.J.Stace and D.M.Bernard, *Chem. Phys. Lett.*, in print.

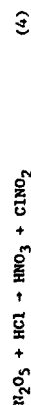
HETEROGENEOUS CHEMISTRY RELATED TO ANTARCTIC OZONE DEPLETION: REACTION OF ClONO_2 AND N_2O_5 ON ICE SURFACES

Margaret A. Tolbert, Michel J. Rossi, and David M. Golden
Department of Chemical Kinetics, Chemical Physics Laboratory
SRI International, Menlo Park CA 94025

Laboratory studies of heterogeneous reactions of possible importance for Antarctic ozone depletion have been performed. In particular, the reactions of chlorine nitrate (ClONO_2) and dinitrogen pentoxide (N_2O_5) have been investigated on ice and HCl/ice surfaces. Reactions 1 and 2, proposed to occur on the surfaces of polar



polar stratospheric clouds (PSCs) over Antarctica, [1] transform the stable chlorine reservoir species (ClONO_2 and HCl) into photochemically active chlorine in the form of HOCl and Cl_2 . Condensation of HNO_3 in the above reactions removes odd nitrogen from the stratosphere, a requirement in nearly all models of Antarctic ozone depletion. [1-4] Reactions 3 and 4 may also be important for Antarctic



ozone depletion. Like the reactions of chlorine nitrate, these reactions deplete odd nitrogen through HNO_3 condensation. In addition, reaction 4 converts a stable chlorine reservoir species (HCl) into photochemically active chlorine (ClONO_2). Reactions 1 - 4 were studied with a modified version of a Knudsen cell flow reactor. [5]

Heterogeneous Reactions of Chlorine Nitrate on Ice. Chlorine nitrate reacted readily with H_2O and HCl on ice surfaces at 185 K. Upon exposure of an ice surface to ClONO_2 , gas phase HOCl was detected (reaction 1). When the surface is slowly warmed, the other product of reaction 1, HNO_3 , is detected in thermal desorption

spectrometry (TDS). Thus reaction 1 on ice produces gas phase HOCl and condensed phase HNO_3 .

The reaction of ClONO_2 with HCl on ice, reaction 2, may be especially important in the Antarctic stratosphere because it converts two chlorine reservoir species into photochemically active Cl_2 . We and others [6-8] have observed this reaction to proceed readily. This reaction was studied on a surface prepared by co-condensing a 7:1 ratio of $\text{H}_2\text{O}:\text{HCl}$ onto a wax-coated copper block at 185 K. When ClONO_2 was introduced into the Knudsen cell containing this surface, gas phase Cl_2 was formed. Cl_2 does not stick to, or react with, ice at 185 K. The reaction of ClONO_2 on HCl/ice proceeded until at least 95% of the total deposited HCl was depleted, indicating rapid diffusion of HCl in ice. [7] As was the case for reaction 1, HNO_3 formed via reaction 2 was observed in TDS after the reaction by slowly warming the sample.

Heterogeneous Reactions of Dinitrogen Pentoxide on Ice. Dinitrogen pentoxide reacted readily with ice and HCl/ice at 185 K. [9] When N_2O_5 was exposed to ice at this temperature, loss of N_2O_5 was indicated by a large decrease in the m/e 46 mass spectrometer signal. The product of reaction 3, HNO_3 , was observed after the reaction in TDS.

The reaction of N_2O_5 with HCl was studied on a cold wax-coated copper surface and on ice. In both cases, gas phase ClONO_2 was observed as the product. ClONO_2 did not stick to, or react with, ice at 185 K. As was the case for the reaction of ClONO_2 with HCl , reaction 4 proceeded until essentially all of the HCl in the ice was depleted. HNO_3 was observed in the ice after reaction using TDS.

References

1. S. Solomon, R. R. Garcia, F. S. Rowland, D. J. Veebles, Nature (London), **321**, 755 (1986).
2. P. J. Crutzen and F. Arnold, Nature (London), **324**, 51 (1986).
3. M. B. McElroy, R. J. Salawitch, S. C. Wofsy, Geophys. Res. Lett., **13**, 1296 (1986).
4. O. B. Toon, P. Hamill, R. P. Turco, and J. Pinto, Geophys. Res. Lett., **13**, 1284 (1986).
5. D. M. Golden, G. N. Spokes, S. W. Benson, Angew. Chem. Int. Ed. Engl., **12**, 534 (1973).
6. M. A. Tolbert, M. J. Rossi, R. Malhotra and D. M. Golden, Science, **238**, 1258 (1987).
7. M. J. Molina, T. L. Tso, L. T. Molina, F. C. Y. Wang, Science, **238**, 1253 (1987).
8. M. T. Lau, Geophys. Res. Lett., **15**, 17 (1988).
9. M. A. Tolbert, M. J. Rossi and D. M. Golden, Science, in press.

INTERACTIONS OF GAS MOLECULES WITH WATER SURFACES

R. Davidovits, J. Gardner, L. Watson, J. Jayne, and J.M. Van Doren
 Boston College, Department of Chemistry, Chestnut Hill, MA 02167 USA
 M.S. Zahniser, D.R. Worsnop and E. Kolb
 Aerodyne Research, Inc., Billerica, MA 01821 USA

In heterogeneous gas-liquid interactions such as those occurring in the atmosphere, the rate of gas uptake by the liquid is a pivotal factor in understanding the process. In this connection a key parameter is the mass accommodation or sticking coefficient (γ) which is the probability that a molecule which hits the surface of the liquid enters the bulk liquid. An experimental technique has been developed to study factors affecting gas uptake and to measure mass accommodation coefficients of gas molecules on liquid surfaces. A controllable stream of monodispersed droplets is produced by a vibrating orifice jet. The droplets enter a flow system containing the trace species. The droplets are turned on and off while the density of the species is monitored spectroscopically. The technique will be discussed and results will be presented for SO_2 , H_2O_2 and O_3 .

Measurement of the mass accommodation process allows one also to study chemical interactions on liquid surfaces. One method for such studies is through Henry's Law saturation effects. The experiments with SO_2 provide an example. The Henry's Law coefficient for the gas/liquid phase equilibrium $[\text{SO}_2(\text{g})] = [\text{SO}_2(\text{l})]$ is small ($H=1.3 \text{ M/atm}$). If the sulfur species were found in the liquid only as $\text{SO}_2(\text{l})$, the surface layer of the droplet would saturate in about $1\mu\text{sec}$. As it is, SO_2 reacts with water to form HSO_3^- . That is $\text{SO}_2 + \text{H}_2\text{O} \rightarrow \text{HSO}_3^- + \text{H}^+$. This pathway increases the capacity for the uptake of SO_2 . The approach to equilibrium (at which point the net uptake of SO_2 is zero) is governed by the reaction rate of SO_2 with H_2O at the liquid surface. The time rate of approach to saturation provides information about the reaction rate at the liquid surface. This reaction (ie $\text{SO}_2 + \text{H}_2\text{O} \rightarrow \text{HSO}_3^- + \text{H}^+$) is relatively slow in the bulk liquid: $k = 3.6 \cdot 10^6 \text{ s}^{-1}$. Our results show that at the surface the reaction is at least an order of magnitude faster. Further related information about surface properties can be obtained by varying the droplet temperature. An example is provided by the results obtained for H_2O_2 and SO_2 . The coefficient for H_2O_2 shows a sharp temperature

dependence. As the temperature decreases from 290K to 260K (supercooled), γ increases exponentially from 0.1 to 0.35. On the other hand, γ for SO_2 is temperature independent. This observation can be interpreted in terms of the difference between the surface chemistry for the two species. The results are consistent with the following process. In the case of SO_2 the molecule lands on the surface and without a barrier reacts to form HSO_3^- . The entry into bulk liquid is therefore in the form of HSO_3^- . The observed independence on temperature is consistent with such a facile process. The mass accommodation process for H_2O_2 is expected to be different. Here one might suppose that the H_2O_2 molecule which lands on the surface will reside there for some time which is proportional to $\exp(\Delta G^\ddagger/\text{RT})$ where ΔG^\ddagger is the surface bond energy. (This is a physisorption process). The molecule will enter the bulk if hydration occurs during this period. One might expect a temperature dependence in such a case.

One can also study surface reactions and the nature of the surface by adding a reactant to the liquid. In one such study we examined the reactivity of I^- (KI solution) with O_3 . The Henry's Law constant for O_3 is so small that in the absence of an additive the uptake of O_3 is too small to observe. As I^- is added, the uptake of O_3 first increases with I^- concentration and then levels off past a concentration of about 10^{-3} M . The results also show saturation with respect to ozone. The net uptake of ozone is limited to about $3 \times 10^{11} \text{ O}_3$ molecules per cm^2 of liquid surface. The results are consistent with the following mechanism: The observed uptake is due to the reaction of O_3 with I^- ; most probably $\text{O}_3 + \text{I}^- \rightarrow \text{IO}_3^- + \text{O}_2$. The reaction occurs at the surface rather than in the bulk liquid. The leveling of uptake with KI concentration indicates that the I^- concentration at the surface saturates. When all the I^- initially at the surface reacts to form IO_3^- the surface is passivated and no further uptake of O_3 is observed. This passivation occurs because the product IO_3^- does not readily hydrate and therefore it is bound to the surface. This blocks the diffusion of the like charged I^- to the surface. Further evidence for this model will be presented.

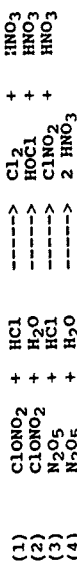
This work sponsored by: The National Science Foundation, Environmental Protection Agency, Electric Power Research Institute, Coordinating Research Council.

LABORATORY STUDIES OF STICKING COEFFICIENTS AND HETEROGENEOUS REACTIONS IMPORTANT IN THE STRATOSPHERE

Ming-Taun Leu and Leon F. Keyser

Jet propulsion Laboratory, California Institute of Technology, 4800 Oak Grove Drive, Pasadena, California 91109

The discovery of ozone depletion during springtime in the Antarctic stratosphere has received wide spread attention. Both meteorological and chemical mechanisms have been used in attempts to explain this observation. The chemical theory focused on the chlorofluoromethanes released into the atmosphere. However, gas-phase, homogeneous reactions alone in the model can not adequately explain such a depletion. Heterogeneous reactions, such as:



on ice surfaces could be important in the Antarctic stratosphere. Reactions (1)-(4) are thought to convert ClONO_2 and N_2O_5 into HNO_3 in the solid phase while Cl_2 , HOCl , and ClNO_2 are released into the stratosphere as gas-phase products. The photolysis of Cl_2 , HOCl , and ClNO_2 then produces active chlorine which subsequently removes ozone through several catalytic cycles, including the Cl_2O_2 mechanism. The polar stratospheric clouds are thought to consist of mixtures of water ice, nitric acid, and sulfuric acid. Condensation of HCl onto the PSC's could provide active surfaces for heterogeneous reactions such as (1) and (3).

A fast flow reactor was used for investigating the sticking coefficients of the trace gases on ice. The diameter of the flow tube was 1.89 cm, and the length was 50 cm. The temperature of the flow tube was measured by a pair of thermocouples and its temperature was maintained at about 190-200 K by circulating cooled dry nitrogen through its outside jacket. The cooling jacket was further insulated by another exterior jacket which was evacuated by a mechanical pump. The pressure was monitored at the downstream end of the flow tube by means of a Baratron pressure meter. The ice surface was prepared by passing water vapor in helium carrier through an injector tube which was slowly moved along the length of the flow tube until a thin uniform ring was formed. Ice was prevented from forming in the injector tube by

flowing dry nitrogen through a jacket which extended beyond its downstream end. The flow rate of water vapor was measured by monitoring the pressure and the temperature at the water reservoir and also monitoring the helium flow rate. The detection of the trace gases was performed by using an EMBA II quadrupole mass spectrometer. We utilized the electron impact ionization method to monitor the parent peak or the fragmentation peaks of the gas molecules. For example, H_2O or HCl were detected by their parent peaks while ClONO_2 or N_2O_5 were measured by NO_2 ions.

Measurements of sticking coefficients for H_2O , HCl , Cl_2 and HNO_3 on ice and of reaction probabilities for reactions (1) and (2) have been summarized in a recent publication. Measured sticking coefficients are: 0.3 (± 0.1) for H_2O , 0.4 (± 0.6 , -0.4) for HCl , $< 1.0 \times 10^{-4}$ for Cl_2 , and 0.3 (± 0.7 , -0.3) for HNO_3 at 200 K. The reaction probability of ClONO_2 on ice was found to be 0.06 (± 0.03) while HOCl was observed as the sole product in the gas phase. In the presence of 0.015-0.071 mole fractions of HCl in ice, the reaction probability of ClONO_2 is greatly enhanced, approaching 0.27 (± 0.73 , -0.13) while molecular chlorine was found to be the major product in the gas phase. Another reaction product was nitric acid which remained in the solid phase.

In a preliminary investigation the reaction probability of N_2O_5 was found to be $2.8 (\pm 1.1) \times 10^{-2}$ on ice at 195 K and $3.4 (\pm 1.4) \times 10^{-2}$ with 0.015-0.040 mole fraction of HCl at 195 K. One of the reaction products, HNO_3 , remained in the condensed phase. It should be noted that the yield of NO_2 , a probable reaction product, was negligible in these N_2O_5 reactions. This work will be continued in the laboratory and the results will be presented at the Symposium.

In addition, similar reactions on sulfuric acid/water ice surfaces will be investigated because of their potential importance for the global stratosphere.

Acknowledgments. The research described in this paper was performed by the Jet Propulsion Laboratory, California Institute of Technology, under a contract with the National Aeronautics and Space Administration.

References:

1. J. C. Farman, B. G. Gardiner, and J. D. Shanklin, *Nature*, **315**, 207 (1985).
2. M.-T. Leu, *Geophys. Res. Lett.*, **15**, 17 (1988).
3. *Geophysical Research Letters*, November Supplement (1986).

PLENARY LECTURE

49

ANTARCTIC OZONE HOLE, ACID RAIN AND ATMOSPHERIC CHEMICAL KINETICS

A. R. Ravishankara

National Oceanic and Atmospheric Administration
Aeronomy Laboratory, 325 Broadway, Boulder CO 80303, U.S.A

Currently, the two areas of intense activity in atmospheric chemistry are the stratospheric ozone loss and enhanced acid precipitation, both due to man's activities. The discovery of the Antarctic "ozone hole" has heightened interest in the stratospheric ozone depletion. The recent field measurements carried out inside the Antarctic ozone hole has shown the importance of unusual species such as the ClO-dimer in destroying ozone. Attempts to understand acid rain formation has made it necessary to carry out detailed investigations of the reactions of peroxides and thereby establish their concentrations in the atmosphere. Peroxides are, in part, responsible for the oxidation of sulfur dioxide to sulfuric acid. Reduced sulfur compounds generate sulfur dioxide in clean marine air and, consequently, reactions of organo-sulfur free radicals, produced during their oxidation process, are of interest.

Gas phase chemical kinetics plays a crucial role in our understanding of the chemistry of the Earth's atmosphere. Gas phase kinetics data is required to quantify the rates and the extent of ozone loss and acid formation. Hence, many laboratory investigations of the kinetics and the photochemistry of the species important in these processes have been carried out. Recent experiments on kinetics of halogen species, peroxides, and sulfur species will be described and the implications of these results to the chemistry of the Earth's atmosphere and gas kinetics will be discussed.

REVERSIBLE ADDUCT FORMATION IN THE REACTIONS OF $\text{Cl}(\text{P}_2)$
WITH CS_2 , COS, AND O_2 : KINETICS AND THERMODYNAMICS

J.M. Nicovich, C.J. Shackelford and P.H. Wine

Molecular Sciences Branch, Georgia Tech Research Institute
Georgia Institute of Technology, Atlanta, Georgia 30332
USA

Time-resolved resonance fluorescence detection has been coupled with pulsed laser photolytic production to study the kinetics of chlorine atom reactions with CS_2 , COS, and O_2 . The 118.9 nm atomic chlorine resonance line, which penetrates through significant optical depths of O_2 , was used as the fluorescence excitation source.

The approach to equilibrium between laser generated chlorine atoms and a CS_2Cl adduct has been observed over the temperature range 190-257K. The $\text{Cl}+\text{CS}_2$ addition rate constant, the adduct decomposition rate constant, and hence, the equilibrium constant are obtained from the data. Analysis of the temperature dependence of the equilibrium constant gives a heat of reaction for the $\text{Cl}+\text{CS}_2$ addition step of -9.8 ± 0.4 kcal/mole and, therefore, a CS_2Cl heat of formation of 47 ± 1 kcal/mole.¹ Some interesting comparisons between the $\text{Cl}+\text{CS}_2$ system and the $\text{OH}+\text{CS}_2$ system are the following: (1) CS_2Cl and CS_2OH have similar binding energies, (2) at a given temperature, pressure, and CS_2 concentration, equilibrium is established more rapidly in the $\text{Cl}+\text{CS}_2$ system, but the equilibrium is shifted more toward adduct in the $\text{OH}+\text{CS}_2$ system, and (3) CS_2OH appears to be much more reactive toward O_2 than does CS_2Cl .

The $\text{Cl}+\text{COS}$ reaction has been investigated at temperatures down to 190K employing COS concentrations as high as 1×10^{16} per cm³ with experimental time resolution of 1 μs . No evidence for a reaction between Cl and COS has been observed. We conclude that the species COSCl , if it exists at all, must be very weakly bound. It does not appear that a reaction between chlorine atoms and COS can be of any importance in atmospheric chemistry.

The $\text{Cl}+\text{O}_2$ reaction has been investigated at temperatures down to 190K employing O_2 concentrations as high as 2.5×10^{16} per cm³ (50 Torr at 190K) and with experimental time resolution of 5 μs . No evidence for decay of Cl into equilibrium with ClOO has

been observed, although, based on recommended values for the $\text{Cl} + \text{O}_2 \rightarrow \text{ClOO}$ equilibrium constant and addition rate constant, the approach to equilibrium should have been readily observable. Further experiments aimed at assessing the potential importance of ClOO in atmospheric chemistry are in progress.

This work was supported by the National Science Foundation and the National Aeronautics and Space Administration.

1. Recommended values for $\Delta H_f^\circ(\text{CS}_2)$, $\Delta H_f^\circ(\text{Cl})$, and the $\text{Cl}+\text{O}_2 \rightarrow \text{ClOO}$ addition rate constant and equilibrium constant were obtained from W.B. DeMore, M.J. Molina, S.P. Sander, D.M. Golden, R.F. Hampson, M.J. Kurylo, C.J. Howard, and A.R. Ravishankara, "Chemical Kinetics and Photochemical Data for Use in Stratospheric Modeling," Evaluation Number 8, IRL publication 87-41, 1987.

2. A.J. Hynes, P.H. Wine and J.M. Nicovich, J. Phys. Chem. **92**, xxxx, 1988, in press.

KINETICS AND UV-SPECTRUM OF THE METHYLPEROXY RADICAL

F. Simon, M. Sunneider, M. Jenkin* and G.K. Moortgat

Max-Planck-Institut für Chemie, Air Chemistry,

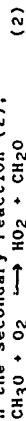
D 5600 Mainz

* AERE-Harwell Laboratory, Didcot, OX11 0RA, G.B.

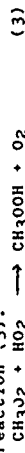
The behaviour of the CH_3O_2 radical, which is an important intermediate in the (photo)oxidation of hydrocarbons, was studied in the near ultra-violet modulated photolysis of flowing Cl_2 , CH_4 , O_2 mixtures. The rate constant k_1 for the self-disproportionation reaction (1)



and the uv-absorption spectrum were measured using uv-absorption techniques combined with diode array detection. Due to the presence of HO_2 radicals, produced in the secondary reaction (2),



the modulated absorption traces cannot be treated as pure second order kinetic behaviour, because of the cross reaction (3).



The observed rate constant obtained in our system is related to k_1 by the equation

$$k_{\text{obs}} = k_1 + k_3/2 (\text{HO}_2)/(\text{CH}_3\text{O}_2).$$

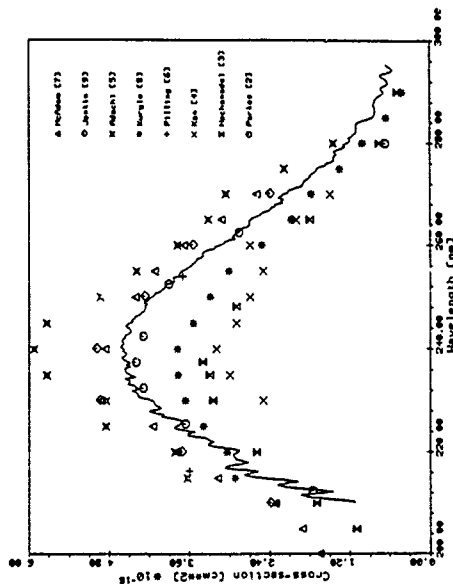
The computer simulation program FACSIMILE was employed to fit the data and retrieve values for k_1 and k_3 in the spectral range 220-270 nm. Using $k_3 = 6.0 \times 10^{-12} \text{ cm}^3 \text{ molecule}^{-1} \text{ s}^{-1}$, a value $k_1 = k_{1a} + k_{1b} + k_{1c} = (3.58 \pm 0.24) \times 10^{-13} \text{ cm}^3 \text{ molecule}^{-1} \text{ s}^{-1}$ was obtained from 14 experiments. (error 2σ) at 240 torr and 298 K. This value is in excellent agreement with the CODATA Evaluation $k_1 = 3.7 \times 10^{-13} \text{ cm}^3 \text{ molecule}^{-1} \text{ s}^{-1}$. At 250 nm $\sigma = 4.14 \times 10^{-18} \text{ cm}^2 \text{ molecule}^{-1}$.

The spectrum of CH_3O_2 was also obtained using a silicon diode array camera. When CH_3O_2 reached steady state concentration during the "light on" phase of the modulated photolysis, the diode array were exposed for 0.25 s providing thus the absorption intensity in the wavelength range 210-292 nm. After correction for

the background absorption and absorption due to other species (mainly HO_2 and CH_3OOH) several scans were averaged, and a final spectrum is shown on Figure 1. Data from other groups are also presented in the figure for comparison. 2-9

References

- 1 Codata, Suppl. II, J. Phys. Chem. Ref. Data, 13, 1259 (1984)
- 2 D.A. Parkes, D.M. Paul, C.P. Quinn and R.C. Robson, Chem. Phys. Lett. 23, 425 (1973)
- 3 C.J. Hochanadel, J.A. Gormley, J.W. Boyle and P. Ogren, J. Phys. Chem. 81, 3 (1977)
- 4 C.S. Kan, R.D. McQuigg, M.R. Whitbeck and J.G. Calvert, Int. J. Chem. Kinet. 11, 921 (1979)
- 5 H. Adachi, N. Basco and D. James, Int. J. Chem. Kinet., 12, 949 (1980)
- 6 R.J. Pilling and M.J.C. Smith, J. Phys. Chem. 89, 4713 (1985)
- 7 K. McAdam, B. Veyret and R. Lesclaux, Chem. Phys. Lett. 133, 39 (1987)
- 8 M.J. Kurylo, T.J. Wallington and P.A. Ouellette, J. Photochem., 39, 201 (1987).
- 9 M.E. Jenkin, R.A. Cox, G.D. Hayman and L.J. Whyte, to be publ.



KINETICS OF THE GAS-PHASE REACTIONS OF NO₃ RADICALS AND N₂O₅ WITH ORGANIC COMPOUNDS

Joger Atkinson, Sara M. Aschmann and James N. Pitts, Jr.
Statewide Air Pollution Research Center, University of
California, Riverside, California 92521, U.S.A.

It is now recognized that the NO₃ radical is an important component of the nighttime atmosphere, and that its reactions with organic compounds can act as a removal process for NO_x and/or the organic compounds. Since the NO₃ radical is in equilibrium with NO₂ and N₂O₅, the observed presence of NO₃ radicals during nighttime implies the concurrent presence of N₂O₅. While rate constants for the gas-phase reactions of NO₃ radicals with a wide variety of organic compounds have been determined using both absolute and relative rate methods, the data for the less reactive alkenes such as ethene and propene, the alkanes and the aromatic hydrocarbons are subject to significant uncertainties. In addition, it has recently been shown that aromatic compounds with two or more six-membered fused rings react with N₂O₅, and not with the NO₃ radical.

In this work we have used a relative rate technique with a "step-ladder" approach to determine the room temperature rate constants for a series of alkenes and alkanes. By choosing pairs of organics whose reactivities towards the NO₃ radical are within a factor of 5 of one another, the experimental uncertainties were minimized, and precise relative rate data were obtained which can be placed on an absolute basis by use of the available absolute rate data. The gas-phase reactions of NO₃ radicals and/or N₂O₅ with a series of aromatics (naphthalene, 1- and 2-methylnaphthalene, 2,3-dimethylnaphthalene, acenaphthene, acenaphthylene, tetralin, styrene, toluene, toluene-*o*,*o*-d₃ and toluene-*o*-d₈) have been studied, also using a relative rate method. Only those aromatics containing multiple fused six-membered ring systems were observed to react with N₂O₅. Acenaphthene reacted with both the NO₃ radical and N₂O₅, while acenaphthylene was observed to react sufficiently rapidly with NO₃ radicals that the expected N₂O₅ reaction was of minor importance. The rate constants obtained are given in Table 1.

*Supported by the National Science Foundation (Grant No. ATM-8617884) and the U.S. Environmental Protection Agency (Grant No. R-81-973).

Table 1. Room Temperature Rate Constants for the Gas-Phase Reactions of a Series of Organic Compounds with the NO₃ Radical and N₂O₅

Organic	K (cm ³ molecule ⁻¹ s ⁻¹) ^a	
	NO ₃	N ₂ O ₅
2,3-Dimethyl-2-butene	(5.69 ± 0.73) × 10 ⁻¹¹	
2-Methyl-2-butene	(9.33 ± 1.18) × 10 ⁻¹²	
8-Pinene	(2.36 ± 0.28) × 10 ⁻¹²	
Propene	(9.40 ± 1.19) × 10 ⁻¹⁵	
2,3-Dimethylbutane	(4.06 ± 0.57) × 10 ⁻¹⁶	
Ethene	(2.14 ± 0.32) × 10 ⁻¹⁶	
n-Heptane	(1.36 ± 0.21) × 10 ⁻¹⁶	
Naphthalene		1.1 × 10 ⁻¹⁷
1-Methylnaphthalene		2.3 × 10 ⁻¹⁷
2-Methylnaphthalene		3.6 × 10 ⁻¹⁷
2,3-Dimethylnaphthalene		5.3 × 10 ⁻¹⁷
Acenaphthene	(4.6 ± 2.6) × 10 ⁻¹³	
Acenaphthylene	(5.4 ± 0.8) × 10 ⁻¹²	
Tetralin	(8.6 ± 1.3) × 10 ⁻¹⁵	
Styrene	(1.51 ± 0.20) × 10 ⁻¹³	
Toluene	(7.8 ± 1.5) × 10 ⁻¹⁷	
Toluene- <i>o</i> , <i>o</i> -d ₃	(3.8 ± 0.9) × 10 ⁻¹⁷	
Toluene- <i>o</i> -d ₈	(3.4 ± 1.9) × 10 ⁻¹⁷	

^aRelative rate constant ratios placed on an absolute basis by use of k(NO₃ + trans-2-butene) = (3.87 ± 0.45) × 10⁻¹³ cm³ molecule⁻¹ s⁻¹,^{1,2} and an equilibrium constant K for the NO₂ + NO₃ ⇌ N₂O₅ reactions of 5.0 × 10⁻¹⁰ cm³ molecule⁻¹ at 298 K.³

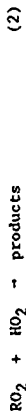
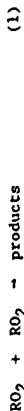
1. A. R. Ravishankara and R. L. Mauldin III, J. Phys. Chem., **89**, 3144 (1985).
2. E. Dlugokencky and C. J. Howard, J. Phys. Chem., in press (1988).
3. W. B. DeMore, M. J. Molina, S. P. Sander, D. M. Golden, R. F. Hampson, M. J. Kurylo, C. J. Howard and A. R. Ravishankara, "Chemical Kinetics and Photochemical Data for Use in Stratospheric Modeling" NASA Panel for Data Evaluation, Evaluation Number 8, JPL Publication 87-41, September 15, 1987.

KINETICS AND MECHANISMS OF REACTIONS OF ORGANIC PEROXY RADICALS AND HO₂

M.E. Jenkin and R.A. Cox

Environmental and Medical Sciences Division, Harwell Laboratory,
Oxfordshire OX11 0RA, U.K.

Work is currently in progress to investigate the kinetics and product channels of a series of reactions involving organic peroxy radicals (RO₂) and HO₂ using infra-red diode laser spectroscopy and ultra-violet absorption spectroscopy. The programme is concentrating on the characterisation of the self and mutual reactions (1) and (2).



The molecular modulation technique is used to study the kinetics of these reactions, with the RO₂ radicals detected in their ultra-violet absorption bands, which are consequently characterised routinely. HO₂ is detected either in the ultra-violet, or in the infra-red using resolved vibration-rotation lines in the ν₂ and ν₃ bands near 1390 cm⁻¹ and 1110 cm⁻¹ respectively.

Organic peroxy radicals and HO₂ are important intermediates in the oxidation mechanisms for hydrocarbons and solvents in the atmosphere, and reactions such as (1) and (2) may act as radical sinks, thereby influencing the tropospheric ozone budget.

Consequently, this work has concentrated on studying peroxy radicals of particular significance in atmospheric photo-oxidation schemes.

- (a) **Methyl Peroxy Radicals:** The behaviour of CH₃O₂ radicals generated during the modulated photolysis of Cl₂/CH₄/O₂/N₂ and CH₃I/O₂/N₂ mixtures has been investigated for a range of temperatures and pressures. This has enabled measurement of the CH₃O₂ absorption spectrum in the range 210-300 nm, and the kinetics of the self reaction (type (1)). Addition of H₂ or H₂O₂ to the Cl₂ photolysis system has allowed simultaneous generation of HO₂ and

measurement of the rate constant for the reaction of CH₃O₂ and HO₂. This reaction has been shown previously to produce CH₃OOH (and O₂). Further experiments have been performed to investigate the products of this reaction, and evidence for the existence of a HCHO + H₂O + O₂ forming channel will be presented. Results suggest that this may account for up to 40% of the reaction.

- (b) **Hydroxy-ethyl peroxy radicals:** HOCH₂CH₂O₂ radicals are generated during the photo-oxidation of ethene and, to a lesser extent, during the photo-oxidation of ethanol. Modulated photolysis of HOCH₂CH₂I/O₂/N₂ mixtures has been used to generate HOCH₂CH₂O₂, and characterisation of its absorption spectrum and self reaction kinetics is currently in progress.

- (c) **Detection of peroxy radicals produced during the photo-oxidation of acetone and acetaldehyde is also being carried out and may be discussed briefly.**

Acknowledgement: This work was supported by the U.K. Department of the Environment as part of a programme of atmospheric pollution chemistry research.

AN EXPERIMENTAL AND COMPUTATIONAL STUDY OF THE REACTIONS OF NO₃ RADICALS WITH Cl AND HO₂

F. Ewig, A. Hoffmann and R. Zellner

Institut für Physikalische Chemie, Universität Göttingen
D-3400 Göttingen, Federal Republic of Germany

The dynamics of bimolecular reactions proceeding via bound intermediates has only recently found increased attention. This type of reaction may be classified to belong to either of the following categories:

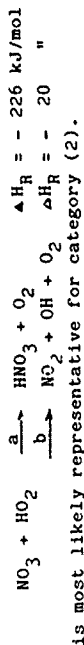
1. Adduct formation followed by fast dissociation via low energy exit channels. The overall rate coefficient represents the fast scavenging process only and is not significantly dependent on either pressure or temperature.
2. Adduct formation followed by competitive dissociation into products and reagents. The overall rate coefficient is low, but may show pressure and negative temperature dependence.

The title reactions have been studied using the flash photolysis of mixtures of HNO₃/HCl (H₂O₂) for the competitive generation of NO₃ and Cl(HO₂) via the corresponding reactions of OH radicals with HCl(H₂O₂). By adjustment of the relative concentrations of HNO₃ and HCl(H₂O₂) the concentrations of Cl(HO₂) can be varied and allowed to exceed [NO₃] such that pseudo-first order kinetics for the decay of NO₃ are maintained. The temporal behaviour of NO₃ was monitored by long-path cw-laser absorption at 629.4 nm. Experiments were performed in the temperature region T = 250 - 400 K at pressures of 20 mbar of He.

The following results were obtained:
 $k(\text{NO}_3 + \text{Cl}) = (4.3 \pm 1.3) \cdot 10^{-11} \text{ cm}^3/\text{s}$ (independent of T)

$$k(\text{NO}_3 + \text{HO}_2) = (7.5 \pm 2.5) \cdot 10^{-13} \exp(550/T) \text{ cm}^3/\text{s}$$

These expressions may be taken as macroscopic indication that the reaction
 $\text{NO}_3 + \text{Cl} \rightarrow \text{NO}_2 + \text{ClO}$, $\Delta H_R = -58 \text{ kJ/mol}$
belongs to category 2(1) whereas the reaction



is most likely representative for category (2).

We have attempted to model the dynamics of both reactions using RRKM theory and available or estimated thermochemical data for both the intermediate adducts (ClONO₂, HO₂NO₃) and the transition state configurations. The results obtained with this approach are found to reproduce the experimental observations of the overall kinetics very satisfactorily. In order to explain the branching ratio of the NO₃ + HO₂ reaction ($k_a/k_b = 0.25/1$) a tight cyclic transition state with a barrier height close to the initial reagent energy is required.

REFERENCE

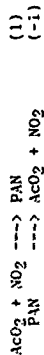
1. A. Mellouki, G. LeBras, G. Foullet: J. Phys. Chem. 1., press 1988

FLASH PHOTOLYSIS KINETIC STUDY OF PEROXYACETYLNITRATE FORMATION

I. Bridier, B. Veyret and R. Lesclaux,

Laboratoire de Chimie Physique A,
Université de Bordeaux I, 33405 Talence Cedex, France.

It is now well established that, in the troposphere, acetylperoxynitrate (PAN) acts as a reservoir of both NO_x and peroxy radicals. The importance of this role of PAN obviously depends on the value of the equilibrium constant, under conditions prevalent in the troposphere, for the reaction of the acetylperoxy radical (AcO_2) with NO_2 :



The kinetics of the dissociation reaction (-1) has been studied by Reiser and Zabel¹, and there are two published papers on the kinetics of reaction (1) at room temperatures^{2,3}. We have recently investigated the kinetics of reactions of the acetylperoxy radical with itself (2) and with CH_3O_2 (3) and their temperature dependence⁴. The cross-sections for the AcO_2 radical were also measured.

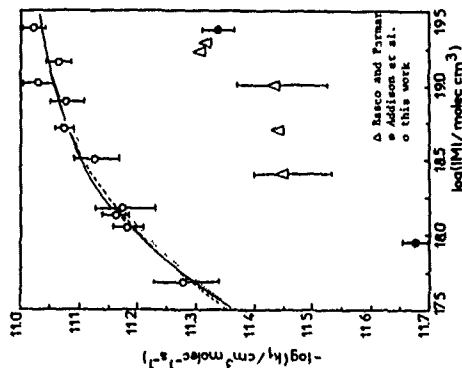
Following these necessary measurements, we have initiated a study of the kinetics of reaction (1) as function of temperature and pressure. The AcO_2 radical was produced by flash photolysis of $\text{Cl}_2/\text{CH}_3\text{CHO}/\text{Air}$ mixtures, and its concentration was monitored by UV absorption at 245 nm. The concentration of NO_2 , in excess relative to the peroxy radical, was measured by absorption at 440 nm. Because of the occurrence of reactions (2), (3) and the subsequent reaction (4): $\text{CH}_3\text{O}_2 + \text{NO}_2 \rightarrow \text{CH}_3\text{O}_2\text{NO}_2$, pseudo-first order conditions could not be obtained easily and exhaustive kinetic simulations, including reactions (1)-(4), were thus performed: $k_1[\text{NO}_2]$ varied linearly with $[\text{NO}_2]$.

The fall-off data for reaction (1) at 298 K, are shown in figure 1 (the error bars are 1 σ), along with the data of Addison et al.² and Basco and Parmar³. Our data were fitted with a nonlinear least-squares method to the expression of Troe with two parameters k_0 and k_∞ , using $\text{Fc} = 0.27$, (full line). The fall-off curve for the decomposition of PAN, obtained by Reiser and Zabel was extrapolated to 298 K (dashed line) and used to calculate an equilibrium constant value at room temperature of $K_1^\circ = 2.2 \times 10^{-8} \text{ cm}^3 \text{ molecule}^{-1}$.

There is clearly a large discrepancy between our k_1 values and those of references 2 and 3. We believe that it is due to the ways the roles of reactions 2 and 3 were taken into account in the earlier studies. RRNM calculations were performed on k_1 and the results are shown in the figure (dotted line). Further experiments are in progress in the temperature range 248-400 K. The temperature dependences of k_0 and k_∞ will thus be determined experimentally and compared to those obtained with the RRNM calculations.

References

- 1 - Reiser A. and Zabel F., Proceedings of the 9th International Symposium on Gas Kinetics, Bordeaux July 1986.
- 2 - Addison M.C., Burrows J.P. and Cox R.A., Chem. Phys. Lett., 73, 283, 1980.
- 3 - Basco N. and Parmar S.S., Int. J. Chem. Kinet., 19, 115, 1987.
- 4 - Moor-gat G.K., Veyret B. and Lesclaux R., (submitted)



A NOVEL APPROACH TO WEAK-COLLISION FACTOR β

Wendell Forst

Département de Chimie Physique des Réactions, UA 328 CNRS
INPL-ENSIC, 1 rue Grandville, 54042 Nancy Cedex, France

The pressure dependence of k_{uni} , the unimolecular rate constant for dissociation in a gas phase thermal system, gives rise to the well-known "fall-off" which generally serves for the comparison of theory with experiment. The standard RRQM formula assumes that collisions are "strong", whereas for small colliders they are actually "weak". While fairly rigorous weak-collision treatments are now available, the usual log-log representation of k_{uni} fall-off does not require many-digit calculational accuracy. This suggests that a simple approximate treatment, consisting of multiplying the usual hard-sphere collision frequency by a properly defined weak-collision correction factor β , should be quite adequate for fall-off purposes.

In the present approach β incorporates a realistic representation of the weak-collision transition probability. We start with the Fokker-Planck approximation to the weak-collision master equation which is transformed into an energy diffusion equation. It can be shown that after some reduction ultimately¹

$$\beta = \langle \langle \Delta E^2 \rangle \rangle_{sc,eq} / \langle \langle \Delta E^2 \rangle \rangle_{sc,eq} \quad (1)$$

where $\langle \langle \Delta E^2 \rangle \rangle_{sc,eq}$ is the equilibrium bulk average of the second moment of the weak collision transition probability, and $\langle \langle \Delta E^2 \rangle \rangle_{sc,eq}$ is the analogous bulk average of the second moment of the strong-collision transition probability.

A matrix approach is used to evaluate eq.(1). Let Q be the matrix of transition probabilities, normalized and satisfying detailed balance exactly; let the threshold to reaction be at energy E_0 . The transition matrix Q can be usefully partitioned at E_0 into sub-matrices Q_1, Q_2, Q_3 and Q_4 :

$$Q = \begin{array}{c|c|c|c} Q_1 & Q_2 & Q_3 & Q_4 \\ \hline \hline \hline \hline \end{array} \quad (2)$$

where Q_1 involves only transitions below threshold. Let R be the vector of the discrete energies of the system ("grains"); then

$$\langle \Delta E^2 \rangle = R^2 (Q_1 + I_1) - 2 (R Q_1) R \quad (3)$$

where I_1 is the sub-matrix of similarly partitioned unit matrix I . The weak- and strong-collision versions of $\langle \Delta E^2 \rangle$ are obtained by

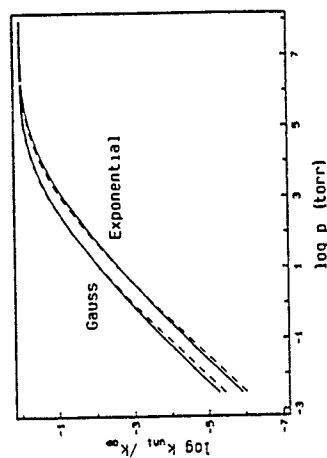
using for Q_1 in eq.(3) the appropriate partition of the weak- and strong-collision matrices Q_{sc} and Q_{sc} , respectively. The equilibrium average (weak- or strong-collision) of $\langle \Delta E^2 \rangle$, follows from

$$\langle \langle \Delta E^2 \rangle \rangle_{eq} = \sum_j \langle \Delta E^2 \rangle_j q_{jj} \quad (4)$$

where q_{jj} are the diagonal elements of the strong-collision matrix partition Q_1 .

For typical model system we have chosen the dissociation of ethane into two methyl radicals at 2000 K. Microcanonical rate constants as elements of rate constant matrix K were based on molecule and transition state parameters as given by Smith and Gilbert². Two weak-collision models were used, the exponential and the offset Gauss,an³. The Figure below shows the results: continuous line is the exact result obtained as eigenvalue of full transport matrix $\omega(Q_{sc} - I) - K$ (ω = collision frequency), dashed line is obtained using eq.(1) for $\beta\omega$ in place of ω in the standard RRQM formula for k_{uni} . The advantage of the present treatment is that it avoids the difficult calculation of eigenvalues and replaces it by the much simpler matrix products in eq.(3), while at the same time preserving all the properties of the weak collision matrix Q_{sc} .

1.W.Forst, J.Phys.Chem.90,455(1986) and unpublished preprint.
2.S.C.Smith and R.G.Gilbert,Int.J.Chem.Kinet.20,307(1988), Table II.
3.R.C.Bhattacharjee and W. Forst, Chem. Phys. Lett. 26, 395 (1974).



KINETIC PATHS FOR ELEMENTARY CHEMICAL REACTIONS: THE HYPERSPHERICAL PERSPECTIVE.

V. Aquilanti, S. Cavalli and G. Grossi

Dipartimento di Chimica dell'Università, 06100 Perugia, Italy.

For the theory of elementary chemical processes, an important alternative to the familiar use of reaction path coordinates, emerges from extensive recent applications of the hyperspherical formalism.

Such a formalism, which has been shown to provide unique advantages for the description of collinear reactions [1], especially for the transfer of light atoms, is now being extended to the full three-dimensional case, where it appears most promising in general and in particular for dealing with reactions that lead to branching and to break-up. Some work on unimolecular dissociations has also been started [2]. For zero total angular momentum the advantages over other approaches are being demonstrated [3].

The change in the perspective from the reaction path coordinate viewpoint, which focusses on potential energy and leads to strong couplings in kinetic energy, is a drastic one: Hamiltonians where the kinetic energy is diagonal can be easily formulated [4] and analysed [5], the hyperradius (a measure of closeness of atoms and a unique invariant of the hyperspace onto which the overall dynamics is mapped) appears to be a variable nearly separable in most of configuration space: there are indications that such a kinetic radius will play a role in chemical kinetics similar to that of internuclear distance in the Born-Oppenheimer separation for molecular-structure studies. As far as accurate dynamical calculation are concerned, it is necessary to refine our computational tools to solve efficiently problems of quantization on hyperspheres.

To fully exploit the insight that this approach may provide for chemical kinetics, the following lines are being pursued:

(i) The evolution as a function of the kinetic radius of minima (valley bottoms) and saddles (ridges) in potential energy surfaces, has to be characterized accurately because adiabatic dynamics and nonadiabatic couplings are localized there. In our nomenclature they provide the kinetic paths for reactivity.

(ii) The role of large angular momenta has to be assessed, specifically for excluding from dynamics regions of configuration space and opening others, and in providing barriers that may support long lived states [6].

(iii) The possibility of extending the formulation to polyatomic reactions has to be explored by proper identification of spheres of lower dimensionalities where the dynamics can be confined.

Some progress on (i) and (ii) will be reported: both quantum and classical formulations appear useful. The role of quantum chemistry (especially the exploit of gradient techniques) for (i) and (ii) is crucial and is being investigated.

References:

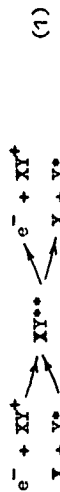
1. See, e.g., V. Aquilanti, in *Theory of Chemical Reaction Dynamics*, ed. D.C. Clary (Reidel, Dordrecht, 1986), p. 383.
2. V. Aquilanti, S. Cavalli and G. Grossi, *Chem. Phys. Lett.*, 1987, 133, 533; V. Aquilanti and S. Cavalli, *Chem. Phys. Lett.*, 1987, 133, 538.
3. J. Linderberg, *Int. J. Quantum Chem.*, 1986, S19, 467; A. Kuppermann and P.G. Hipes, *J. Chem. Phys.*, 1986, 84, 5962; A. Laganà, R.T. Pack and G.A. Parker, *Faraday Discuss. Chem. Soc.*, 1987, 84, remark on the paper by Iruñlar et al.
4. V. Aquilanti, G. Grossi and A. Laganà, *Chem. Phys. Lett.*, 1982, 93, 174.
5. V. Aquilanti, S. Cavalli and G. Grossi, *J. Chem. Phys.*, 1986, 85, 1362.
6. V. Aquilanti and S. Cavalli, *Chem. Phys. Lett.*, 1987, 141, 309.

COLLISION PROCESSES THROUGH RYDBERG STATES OF MOLECULES IN THE FIELD OF STRONG INFRARED RADIATION

G.K. Ivanov, A.S. Vartazaryan, G.V. Golubkov

Institute of Chemical Physics, Academy of Sciences, Kosygin Str. 4, 117977, MOSCOW, USSR.

Basic collision processes occurring through the autodecaying Rydberg complex XY^{**} may be represented schematically as



These are the scattering (elastic and inelastic) of slow electrons on molecular ions, the dissociative recombination (DR) of electrons and ions, the associative ionization of atoms (AI) and some types of elastic and inelastic collisions of atoms in the states which correlate with the dissociative terms passing via the minimum of ionic potential U_i . In the present work we have investigated the processes (1) in the presence of monochromatic field $U = 2V^2 \cos^2 \omega t$ with the frequency ω , and the strength f ($V^2 = Df/2$, where D is the dipole moment operator).

If $f \ll 1$ ($e = \hbar = m_e = 1$) the field affects the processes (1) only during the formation of intermediate complex XY^{**} , rearranging its resonance structure. Moreover the field manifests itself in creating new channels accompanying by absorption and emission of photons.

Following method^{1,2} we have derived general equations describing the processes (1) in the field of monochromatic infrared radiation. These equations are constructed for collision T-matrix on a basis in which quasisenergy states (QES), differing by the number of photons m and coupling together by the field interaction V_f , are included.

In the case of strong mixing of two series of Rydberg resonances λ_n and λ_m with quasisenergy indexes $n = 0$ and $m = -1$ the following amplitudes have

been obtained:

$$T_{n0} = t_{n0} + \frac{t_{n-1} [tg(\pi \lambda_n + \mu_0) + i \delta \lambda_n] t_{n-1}}{d} \quad (2)$$

for the photonless processes, and

$$T_{n0} = \frac{t_{n-1} t_{n-1}^* t_{n-1} p_L}{d} \quad (3)$$

for the processes accompanying with the exchange of energy with the external field. Here

$$d = [tg(\pi \lambda_n + \mu_0) + i \delta \lambda_n] [tg(\pi \lambda_n + \mu_0) + i \delta \lambda_n]^* + (t_{n-1}^*)^2$$

μ_0 is the adiabatic quantum defect at equilibrium internuclear distance of XY^+ , p and λ are respectively the open and closed channel indexes, $t_{n-1}^* = t_{n-1}^*$, $t_{n-1}^* = t_{n-1}^*$ have the straightforward relation with the width of Rydberg level $\Gamma = 2\hbar/\tau$, (t_{n-1}^*) is responsible for the field effect, and

$$\lambda_n = [2(E_n + m\omega_f - E)]^{-1/2}$$

where E_n is the excitation energy of ion core vibrations, E is the total energy. The term t_{n-1}^* is the field-free matrix element which describes direct nonresonant coupling between the channels p and n .

It is clear from the expressions (2) and (3) that in case of the interaction of QES compared with the level width ($f \sim 10^2 - 10^3$ V/cm) the electromagnetic field which is nearly resonant to the vibrational transitions in the XY^+ ion affects substantially the detail spectrum structure and the characteristics of processes averaged on the energy.

1. Ivanov G.K., Golubkov G.V. Z. D. 1, 199, 1986
2. Ivanov G.K., Chem. Phys. Lett. 132, 89, 1987

ON DYNAMICS OF THE ELEMENTARY MULTIPHOTON PROCESSES IN GASES

A.V. Ivanova

Institute of Chemical Physics, USSR Academy of Sciences, Kosygin Street 4, SV-117977 SZD-1, Moscow V-334, USSR

A new approach is proposed to solving the matrix density equation of gas, consistent of interacting multilevel atoms, in a strong resonant light field. The equation is solved by the method of the canonical transformation (variant of Bogolyubov-Mitropolski method of averages). Earlier this method has been worked out in the MMR-theory for interacting two-level spins. In the case of interacting multilevel atoms in a strong electromagnetic field.

This method takes into account the rapidly oscillating interactions arising in all allowed nonresonant atom transitions in that field by means of the time-independent effective interactions. Just these infinitely large number of rapidly oscillating interactions (ignored in the traditionally used resonant approximation, based on the two-level atom model) cause effects typical of nonlinear optics, as the dynamic Stark shifts, multiphoton transitions, etc. The values specific of these processes were found to be described with the effective interactions. Moreover the rapidly oscillating interactions induce trembling of the atomic electron cloud responsible for the excitation of high harmonics. Using the canonical transformations of the type

$$h = \exp[iA(t)]h' \exp[-iA(t)], \quad p = \exp[iA(t)]p' \exp[-iA(t)]$$

(where h, p' - Hamiltonian and density matrix in the usually used interaction representation) and choosing operator $A(t)$ so that h' involving no rapidly oscillating terms, we reduce the matrix density equation to new representation. This result in an equation with an effective Hamiltonian h_A that describes, taking into account the Stark shifts and the real motion of energy level populations, dynamics of slow processes in a gas, setting in a steady regime. The information about rapid motions reintroduced into the density matrix by means of inverse canonical transformations. This enables descriptions of the high harmonics gene-

ration and the relevant nonlinear susceptibility. Thus an important feature of the proposed theoretical method differing it from all those used at present in nonlinear optics is the establishing of analytic dependence between the slow and rapid parts of the density matrix. This provides an unified approach to description of both resonant and nonresonant nonlinear optical processes in gas.

The results obtained are:

1. The matrix density equation has been solved², where only the interaction of multilevel atoms with a strong resonant light field has been explicitly taken into account, while the spontaneous relaxation and collisions were accounted for by means of relaxation constants.
2. A time-dependent expression for cubic gas susceptibility, enabling analysis of the transient processes, has been obtained. This expression valid both for nonresonant and resonant (for any saturation extent) events is a generalization of the Armstrong-Blombergen formula applicable for the nonresonant region only.
3. A theoretical model of resonant third harmonic generation and two-photon induced fluorescence in a gas have been presented³. The effect of an intermediate metastable state on the kinetics and the line shapes of these processes, where the metastable state lifetime is in excess of the pulse duration, has been studied. In this case the metastable state acts as a sink for excited atoms and the processes become nonstationary.
4. The doubly-resonant cubic gas susceptibility in the case when the frequencies of the external light fields are in one- and two-photon resonances with two distinct atomic transitions, has been calculated⁴. One- and two-photon resonant lines were found to have nearly the same intensity. It followed also, that in the case of two-photon resonant saturation the one-photon resonance considerably increases the width of the third-harmonic line. These facts permits to study transitions between the excited atom states from a new point of view.

1. Provotorov B N, Feldman B B 1980 Zh. Eksp. Teor. Fiz. (USSR)

29 2206

2. Ivanova A V, Melikyan G G 1983 Khim. Fiz. (USSR) 2 297

3. Ivanova A V, Melikyan G G 1985 J. Phys. B: At. Mol. Phys.

18 557

4. Ivanova A V, Melikyan G G 1984 Opt. Commun. 40 189.

COMPETING REACTIONS OF THE ACETONE CATION-RADICAL,
RRKM-QET CALCULATIONS ON AN
AB INITIO POTENTIAL ENERGY SURFACE

Chava Lifshitz and Frank Louage

The Hebrew University of Jerusalem, Israel

and

Nikolaus Heinrich and Helmut Schwarz

Technical University, Berlin, W. Germany

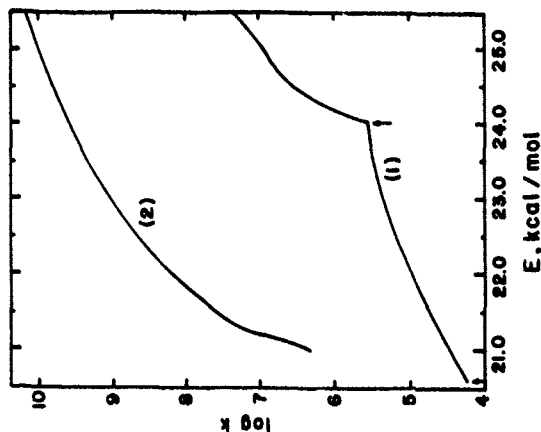
We have employed, for the first time in RRKM-QET calculations, sets of reactant and transition state frequencies as well as energetics based on *ab initio* calculations of a reaction potential energy profile. The reaction system involves two parallel dissociations of the acetone cation radical



Ab initio calculations demonstrate the intermediate existence of a hydrogen-bridged $[\text{CH}_3\text{CO}^+\text{CH}_3]$ complex for both reactions. Assumptions made and data used in the RRKM calculations are as follows: 1) Dissociation takes place from the acetone cation radical potential well, i.e., the reactant, even if going through the H-bridged complex, has available to it the high density of states of the acetone well. 2) The energetics of the dissociations conform to those of the highest level *ab initio* calculations, MP3/6-31G(d,p)/6-31G(d) + ZPVE. 3) Reaction (1) can take place at its endothermic threshold by quantum-mechanical tunneling through the barrier. An unsymmetrical Eckart barrier has been assumed with tunneling taking place between the H-bridged complex and a ketene ion/methane complex. By invoking tunneling in the second unimolecular reaction channel (CH_4 elimination) we were able to reproduce several experimental observations: (a) Reaction channel (1) is the major channel for so-called "metastable ion" fragmentations in the microsecond lifetime range; (b) Channel (2) becomes the major reaction channel at high internal energies of the reactant ion. Photoionization efficiency (PIE) curves for the two competing channels calculated on the basis of RRKM-QET

microcanonical rate coefficients $k(E)$ reproduce experimental results¹ rather well. The microcanonical rate coefficients are reproduced in the Figure. Reaction channel (1) takes place in the internal energy range between the arrows by tunneling through a genuine barrier whose height is 240 kcal/mol above the acetone well.

The reaction system is a quite general example in mass spectrometry for two parallel reaction paths with slightly different critical energies and different activation entropies. The special interest in this system is two-fold: The formation of a single intermediate through which both reaction paths proceed, and the possibility of tunneling through a barrier other than a centrifugal one.



1 J.C. Traeger, C. E. Husson and D.J. McAdoo, J. Phys. Chem. **92**, 1519 (1988).

PROPERTIES OF ACTIVATION BARRIERS FROM FORWARD AND
REVERSE RATES OF HYDROGEN ATOM TRANSFERS

Hiroshi Furue and Philip D. Pacey
Department of Chemistry
Dalhousie University
Halifax, NS B3H 4J3

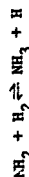
Experimental data on the temperature dependence of forward and reverse transfers of hydrogen atoms have been reviewed.

The following transition state theory (TST) expressions, incorporating a factor, κ , for tunneling through a one-dimensional Eckart barrier of effective height E_e and thickness $\Delta S_1/2$ at half height, were fitted by least squares methods to the data for each reaction.

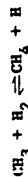
$$k_f = \kappa B_f(T) Q_v(T, \bar{V}_0) \exp(-E_e/RT)$$

$$k_r = \kappa B_r(T) Q_v(T, \bar{V}_0) \exp(-E_e + \Delta H^\ddagger)/RT$$

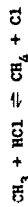
Here E_e , $\Delta S_1/2$, \bar{V}_0 and ΔH^\ddagger were adjustable parameters; \bar{V}_0 is the geometric mean of five low frequency bending vibrations of the transition species and ΔH^\ddagger is the enthalpy of reaction at OK. $Q_v(T, \bar{V}_0)$ is the partition function for the five low frequency bends and $B_f(T)$ and $B_r(T)$ incorporate other TST factors, calculated from spectroscopic properties of reactants and semi-empirical internuclear distances of the transition species. For the reactions,



the standard deviations are from 4 to 10% of the parameter values and all parameters agree well with independent quantum chemical or thermochemical estimates. For the reactions,



ΔH^\ddagger disagrees with the values from thermochemical tables, suggesting that there are errors in these tables or errors of an order of magnitude in the low temperature rate constants. The latter possibility seems more likely, as we do find agreement between the established thermochemistry and the kinetic data for the reactions,



DYNAMICAL STUDIES ON EXOERGIC INDIRECT EXCHANGE REACTIONS $A + BCD \rightarrow AB + CD$

M.T. Ravez, J.C. Ravez, P. Halvick, B. Duguay

Laboratoire de Physicochimie Théorique associé au CNRS (UA 503)
 Université de Bordeaux I - 33405 TALENCE Cedex - FRANCE

An analysis of the role of the topological factors of potential energy hypersurfaces containing an intermediate ABCD well on the nascent distribution of the energy among the products of indirect reactive exoergic four-atom processes is presented. Analytical 1D models of four-atom potential energy surfaces have been built which satisfy several requirements. Firstly, the surface presents an adequate asymptotic shape for the diatomics AB and CD and for the triatomic BCD and displays an intermediate well along the route $A + BCD \rightarrow AB + CD$ corresponding to the ABCD species. Secondly, the model must be sufficiently flexible to allow changes of several parameters almost independently. A systematic study of different anisotropies and depths of the ABCD intermediate well were investigated through the quasi classical trajectory (Q.C.T.) approach. Since the reaction $C + H_2O$ is at the origin of this work, the masses have been taken 12, 14, 14, 16 amu respectively for A, B, C and D atoms. The relative translational energy between A and BCD of 0.15 eV and the vibrational energy of BCD corresponding to the zero point level have been taken as initial conditions in these Q.C.T. studies.

Our main results are the following :

- i) The partition of the energy disposal between the vibration and the relative translational motion of the two diatomics is neither really sensitive to the variation of the depth of the intermediate well nor to the anisotropy of the well. The recoil energy represents roughly 30% of the energy of the reaction for this model.
- ii) For surfaces having near isotropic wells related to the linear ABCD structure, we show that the complexes have short lifetimes and that the mean vibrational excitations of AB are smaller than those of CD.
- iii) When the well becomes largely anisotropic a transfer of the vibrational excitation from CD towards the newly formed bond, AB, is observed. Moreover, the percentage of non reactive collisions, which is very small for near isotropic wells, increases.

iv) The percentages of vibrational energy $\langle E_{AB} \rangle$ and $\langle E_{CD} \rangle$ on the bonds AB and CD with respect to the two vibrational phases ζ_1 and ζ_2 corresponding to the normal modes of the reactant BCD vary smoothly in the case of a direct surface (without any well on the route from the reactants to the products). As the ABCD well depth grows, the domain of chaotic behaviour grows at the expense of the domain of continuous variation of $\langle E_{AB} \rangle$ and $\langle E_{CD} \rangle$ with ζ_1 and ζ_2 .

This work represents an attempt to go beyond specific studies of particular reactions by linking important features of the potential energy surfaces to the energy disposal on the products. A similar study for $A + BC$ three atom indirect reactions has already been published¹.

Reference

- 1 - J.C. Ravez, P. Halvick, M.T. Ravez and B. Duguay
 Chem. Phys. 101 (1986) 401
 - P. Halvick, J.C. Ravez, M.T. Ravez and B. Duguay
 Chem. Phys. 114 (1987) 375.

MOLECULAR FORMATION BY RADIATIVE ASSOCIATION IN RADICAL-RADICAL AND ION-MOLECULE COLLISIONS

Ian W.M. Smith

Department of Chemistry
University of Birmingham
P.O. Box 363, Birmingham, B15 2TT, England.

It is now generally accepted that radiative association plays an important role in molecular synthesis in the rarefied, super-cold environment of interstellar clouds. Unfortunately, calculations of the rates of such processes in ion-molecule collisions are prone to considerable uncertainty because of the scarcity of the necessary information (e.g. dissociation energies, vibrational frequencies and transition moments) for molecular ions. This paper will report the first extensive calculations of the rates of radiative association in a range of neutral radical-neutral radical systems where more of the required fundamental data are available

The method of calculation is based on Troe's formulation of unimolecular reaction rate theory as applied to radical-radical association in the low pressure limit [1], with *collisional stabilisation replaced by radiative stabilisation*. It is generally assumed that in calculating the 'equilibrium constant' (k_i/k_{-i}) , for formation of energised complexes



one should count only those states in $(R_1 R_2)^{\ddagger}$ that have total energies E which exceed any 'centrifugal maximum' on the effective potential energy curve for a state of defined adiabatic, total angular momentum J . The calculations reported here compare the results obtained on this basis with those derived after allowing approximately for quantum mechanical tunnelling through the centrifugal barriers.

The averaged rate constant for radiative emission from the collision complexes is estimated by a method similar to that described by Herbst [2]. According to this approach for molecules of vibrational energy E_{vib} ,

$$k_{\text{rad}}(E_{\text{vib}}) = \sum_i \sum_j \frac{P_{n_i}^{(j)}}{n_i} (E_{\text{vib}}) n_i A_{1,0}^{(j)}$$

where $P_{n_i}^{(j)}$ is the probability that a molecule with energy E_{vib} contains n_i quanta in mode i for which the Einstein coefficient for emission is the

lowest fundamental band is $A_{1,0}^{(j)}$.

Results will be reported for radical-radical association reactions in the temperature range 10 - 300 K producing the molecules: HCN, DCN, H_2O , NO_2 , SO_2 , CH_3F , CF_3H and HNO_2 . In all cases, the rate constant for spontaneous emission falls within the range $10^2 - 10^3 \text{ s}^{-1}$, which has usually been assumed for ion-molecule systems. The overall rates of radiative association therefore reflect the magnitude of (k_i/k_{-i}) . This quantity increases as the temperature is lowered and the molecular complexity of the system increases. The calculations indicate that tunnelling can be important at low temperatures; for example, the rate of radiative association of H with OH is increased by a factor of 5 at 20 K when tunnelling corrections are included. Results will also be reported for the astrophysically important reactions: $\text{C}^+ + \text{H}_2 \rightarrow \text{CH}_2^+ + \text{h}\nu$ and $\text{CH}_3^+ + \text{H}_2 \rightarrow \text{CH}_5^+ + \text{h}\nu$. One advantage of the ion-molecule systems is that the long range potential can be more accurately defined.

[1] J. Troe, J. Chem. Phys., **66**, 4758 (1977).

[2] E. Herbst, Chem. Phys., **65**, 185 (1985).

KINETIC MEASUREMENTS BY PULSED PHOTOLYSIS AND TIME-RESOLVED INFRARED LASER ABSORPTION

John Brunning, Michael J. Frost and Ian W.M. Smith

Department of Chemistry
University of Birmingham
P. O. Box 363, Birmingham, B15 2TT, England

Recent papers [1] from our laboratory report rate measurements on association-dissociation in the weakly bound system:



The method combined: (i) pulsed photolysis of N_2O_3 to perturb the low temperature equilibrium, with (ii) measurement of the N_2O_3 concentration changes by observing the transmittance of a selected line from a cw CO infrared laser.

This experimental method has now been significantly improved in two ways. First, our home-built, low power, CO laser has been replaced by a commercial laser of greater power and stability. Second, the simple, single pass, reaction cell of the original experiments has been replaced by a large reactor incorporating White cell mirrors which allow us to obtain much larger optical paths (ca 20 m) for our monitoring laser, thereby considerably improving the sensitivity of the technique for measuring small transient changes in concentration. Moreover, the design of the cell allows us to examine kinetics over a wide range of temperature and total pressure.

In this paper, we shall report measurements on two reaction systems. First, we have examined the kinetics in the system:



which is a close analogue to reaction (1). The results will be compared with those for reaction (1) and with the results of theoretical calculations. Secondly, we shall report data on the reaction of methoxy radicals with NO. In these experiments, CH_3 radicals are produced by photolysis of CH_3ONO which is reformed by the association of the radicals with the excess NO present. The kinetics are followed by observing absorption in the NO bond-stretching fundamental band of the parent compound

[1] I.W.M. Smith and G. Yarwood, Chem. Phys. Letters, **130**, 24 (1986) and Faraday Discuss. Chem. Soc., **84**, in press (1987).

REARRANGEMENT OF CHANNELS IN REACTION OF O(³P) ATOMS WITH ETHYLENE

E.N. Aleksandrov, V.S. Arutyunov, V.I. Vedenev,
V.D. Anjazev, S.N. Kozlov.

Institute of Chemical Physics, Acad. Sci., USSR,
117334, Moscow.

The reaction of O atoms with ethylene has received a good deal of attention. There are two main channels
 $O + C_2H_4 = CH_2 + CH_2O$ (a)
 $O + C_2H_4 = H_2 + C_2H_3O$ (b)

but experimental data about their relative contribution are very contradictory. In this work the appearance of H atoms in reaction was followed by resonance fluorescence technique under discharge-flow conditions at 298K. It was found that although O atoms disappearing reaction rate constant remained unchanged and equal to $(8.0 \pm 0.5) \cdot 10^{-12}$ cm³/molecule s, in good agreement with previous works, the relative yield of H atoms drops with increase of total pressure. At 9.5 Torr the ratio of H atoms yield to O atoms consumption was only 0.62 ± 0.06 of that at 1.0 Torr. The found rearrangement of channels with pressure enables to explain almost all experimental data presented at Fig. 6. On the base of theoretical calculations of this system we have presented a tentative qualitative explanation of this rearrangement. In collisionless conditions one of two possible states of triplet biradical CH₂CH₂O decays into channel (b) at a time of approximately 10⁻¹² s. And the second one due to high energy barrier can decay only into initial products. With pressure rise emerges a possibility of stabilization of this biradical in second state. Collisions induce transmittance from the second state into the first state with subsequent decay into channel (b). At higher pressures arises possibility of collision induced transmittance from triplet into singlet state of stabilized CH₂CH₂O biradical with possibility of subsequent decay into other channels, mainly to channel (a). Predicted by this explanation the fall of total reaction rate constant

by approximately 3 times must take place at pressures below 0.3 Torr.

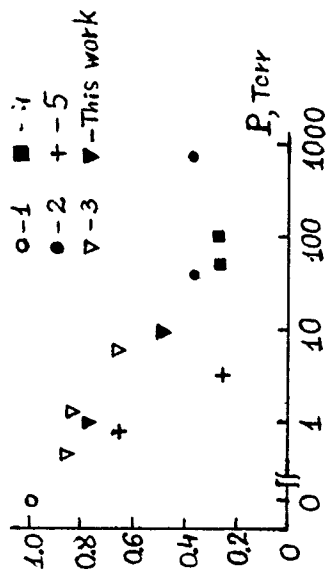


Fig. The yield of H atoms per O atom as a function of total pressure.

References

1. R.J. Buss, R.J. Baseman, G. He et al., J. Photochem., 17, 339, (1981).
2. H.P. Hunziker, H. Knepe, H.R. Wendt, J. Photochem., 17, 377 (1981).
3. U.S. Shridharen, P. Kaufman, Chem. Phys. Lett., 102, 45 (1983).
4. J.F. Smalley, P.L. Nesbitt, R.B. Klemm, J. Phys. Chem., 90, 491 (1986).
5. F. Temps, H. Og. Wagner, Max-Planck - Institut für Stömungsforschung, Bericht 18/1982.
6. M. Dupuis, J.J. Wendoloski, T. Tokada et al., J. Chem. Phys., 72, 481 (1982).
7. E.N. Aleksandrov, V.S. Arutyunov, V.I. Vedenev, V.D. Anjazev, S.N. Kozlov, Khimicheskaya Fizika (Rus.), 5, 1413, (1987).

THE FIRST STEP OF N ATOMS INTERACTION WITH METHANE,
AMMONIA AND HYDROGEN.

Basevich V. Ya., Vedenev V. I.

Institute of Chemical Physics, USSR Academy of Sciences
USSR, 117334, Moscow, 4ul. Kosighin'a

Reactions of N atoms with methane, ammonia and hydrogen are of great interest since it is clear now, that they can not be the usual abstraction type. They are of importance for ecology as well, since all reagents mentioned including N are chemical participants in combustion on zone practically any real hydrocarbon fuel.

There are few quantitative data on the elementary reactions of N atoms while the literature on the chemistry of N atoms is vast¹.

The reactions under survey have been investigated under flow conditions in quartz reactors. Total pressures are 2-8 torr. The temperatures used 550-1020 K were slightly higher than in previous experiments. N (⁴S) atoms were generated in discharge. In special experiments small quantities of CO were added after discharge to the flow to deactivate electronically and vibrationally excited species $N_2(A^3\Sigma_u^+, N_2(B^3\Pi_g))$ were deactivated by molecular nitrogen in ground state.

Reaction products were analysed by gas chromatography and colorimetrically. N and H atoms being detected by ESR.

Some special experiments have been carried out to

elucidate the role of heterogeneous factors and proof, that in all cases the first steps of interaction were homogeneous. The following rate constant parameters have been found:

Reagent	lgA cm/sec	E cal/mol
CH ₄	-10,79±0,07	9348±217
NH ₃	-11,13±0,24	9600±900
H ₂	-10,82±0,09	1038±302

In all cases activation energies E are much less, then corresponding H-abstraction endothermicity (18,21 and 20 kcal/mol). On this ground it has been suggested, that the first step of interaction in all cases is N atoms insertion. However, the dependence of rate constants from total pressure has not been observed (total pressure change was 3-4 times).

Using well-known simple formula of statistical theory of monomolecular reactions the life times of vibrationally excited species H₂GMH, H₂NMH and HNH have been estimated. The estimations have shown, that both decompositions and stabilizations could take place.

The mechanism describing kinetical behaviour of the systems have been suggested. The calculations are compared with the experimental data.

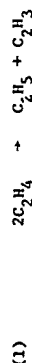
REFERENCE

1. Wright A. N., Winkler C. A. "Active Nitrogen". N.-Y., London, Acad. Press, 1968.

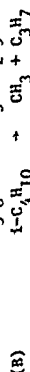
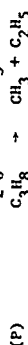
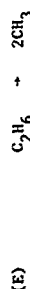
RATE CONSTANTS FOR ABSTRACTION OF HYDROGEN FROM ETHYLENE BY METHYL AND ETHYL RADICALS RELATIVE TO ABSTRACTION FROM PROPANE AND ISOBUTANE.

S.I. Ahonzhai, X-H. Lin and M.H. Back
Ottawa-Carleton Chemistry Institute, University of Ottawa campus,
Ottawa, Canada K1N 6N5.

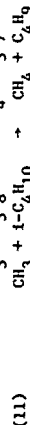
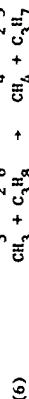
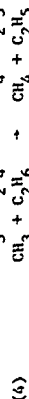
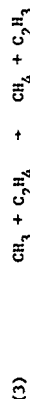
Small quantities of ethane, propane and isobutane were added separately to thermally-reacting ethylene at temperatures in the neighbourhood of 750 K. The additives affect the rate of reaction of ethylene in two ways [1]. At high temperatures and low concentration of additive, in addition to the initiation process in pure ethylene,



dissociation of the additive may contribute to the initiation of radicals by the following reactions:



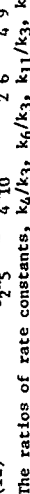
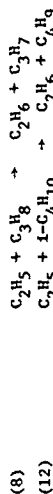
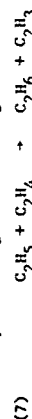
At lower temperatures where the rate of initiation by the additive becomes negligible compared to the rate of reaction (1), the additive may contribute to the propagation reactions by providing an easily-abstractable hydrogen atom, as for example, for the formation of methane:



Taking into account both effects, the ratio of the initial rate of formation of methane in the presence and absence of, for example, ethane, may be expressed as follows:

$$(5) \quad \frac{(v_0)_{CH_4}^a}{(v_0)_{CH_4}^b} = \left[\frac{k_E[C_2H_6]}{k_1[C_2H_4]^2} \right]^{1/2} \left[\frac{k_4[C_2H_6]}{k_3[C_2H_4]} \right]$$

Similar equations describe the ratio of rates of formation of methane or of ethane in the presence and absence of propane or isobutane, including the following additional reactions:



The ratios of rate constants, k_4/k_3 , k_6/k_3 , k_{11}/k_3 , k_8/k_7 , k_{12}/k_7 were obtained from the ratios of rates of formation of methane and of ethane through equations similar to (5), in each case making appropriate correction for the additional initiation process as illustrated by the first term in equation (5). From the results with the three additives, ethane, propane and isobutane, three independent measurements of k_3 were obtained, shown in Figure 1, using the values for the reference reactions from the literature.

The average value for k_3 may be expressed as
 $\log k_3 (\text{Lmol}^{-1}\text{s}^{-1}) = 8.8 \pm 0.4 - (16400 \pm 700/2.3RT) (R = 1.987 \text{ calmol}^{-1}\text{deg}^{-1})$
 Using values for k_{12} the following expression was obtained for k_7 :
 $\log k_7 (\text{Lmol}^{-1}\text{s}^{-1}) = 9.6 - (21500 \pm 2.3RT) (R = 1.987 \text{ calmol}^{-1}\text{deg}^{-1})$

Figure 2 shows these results (curve d) together with previous measurement: curve a: ref.[2]; curve b: ref.[1]; curve c: ref.[4]; vertical bars: ref.[1]; O: ref.[3]; Δ: ref.[5].

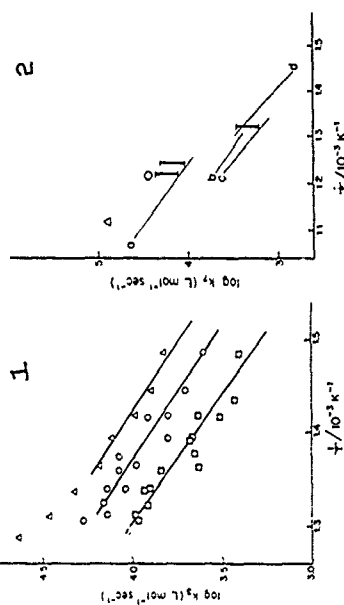
1. G. Ayranci and M.H. Back, Int. J. Chem. Kin. **15**, 83 (1983).

2. M.P. Halstead and C.P. Quinn, Trans. Far. Soc. **64**, 103 (1968).

3. M.P. Halstead and C.P. Quinn, Trans. Far. Soc. **64**, 1560 (1968).

4. D. Delliste, C. Richard and R. Martin, J.Chim.Phys. **78**, 655 (1981).

5. A.L. Mackenzie, P.D. Pacey and J.H. Wimalasena, Can. J. Chem. **61**, 2033 (1983).



STUDY OF THE SELF-REACTIONS OF PROPYLPEROXY RADICALS IN THE GAS PHASE

S. Forgyeteg, B. László and I. Bérces
Central Research Institute for Chemistry,
Hungarian Academy of Sciences,
Budapest, Hungary

Reactions of alkylperoxy radicals play major roles in atmospheric and combustion chemistry. The main routes of the mutual interactions lead both to terminating and to non-terminating products. Significant changes occur in the overall rate coefficients and the Arrhenius parameters of the second-order removal processes with the structure of the alkylperoxy radicals.

We investigated the self-reactions of ethylperoxy, n-propylperoxy radicals over the temperature range of 300-374 K. The overall rates of self-reactions were determined by monitoring the decay of peroxy radicals at 258 nm in the laser flash photolysis of the appropriate azoalkanes in the presence of O_2 . In the case of ethylperoxy radicals, a second order rate constant of $4.1 \times 10^7 \text{ dm}^3 \text{ mol}^{-1} \text{ s}^{-1}$ was obtained in reasonable agreement with the latest literature value¹. In addition, a first order reaction was found to contribute to the ethylperoxy radical consumption, which was shown to depend on the experimental conditions (azoethane concentration, overall pressure etc.) further experiments are in progress in order to reveal the nature of the first order component.

The overall second order rate constant of n-propylperoxy radical decay at 300 K was found to be smaller than the reported literature value². Again, a first order contribution to the propylperoxy radical consumption was observed.

Three channels are known to contribute to the self-reactions of alkylperoxy radicals. These lead to the production of (a) two alkoxy radicals, (b) a carbonyl and an alcohol molecule, (c) a dialkylperoxide molecule. The rate constant ratio k_a/k_b is known to be 0.53 in case of methylperoxy radicals³, and 1.5 in the case of ethylperoxy radicals^{4,5}. Product analyses made in our laboratory gave about 5 for k_a/k_b in the photooxidation of of azo-n-propane. Further studies are carried out in order to determine the temperature dependence of the overall second order rate constants for propylperoxy self-reactions and for the branching ratios.

1. I.J. Wallington, Ph. Dagaut and M.J. Kurylo, J.Photochem.Photobiol. A, **42**, 173 (1988)
2. H. Adachi and N. Basco, Int.J.Chem.Kinet., **14**, 1125(1982)
3. H. Niki, P.D. Maker, C.M. Savage and L.P. Breitenbach, J.Phys.Chem. **85**, 877(1981)
4. H. Niki, P.D. Maker, C.M. Savage and L.P. Breitenbach, J.Phys.Chem. **86**, 3825(1982)
5. C. Anastasi, D.J. Maddington and A. Wooley, J.Chem.Soc.Faraday Trans. 1, **79**, 555(1983)

STUDY OF OXETANE DECOMPOSITION BY THE VARIABLE ENCOUNTER METHOD

L. Zalotai, T. Bérces and F. Márta

Central Research Institute for Chemistry
Hungarian Academy of Sciences
Budapest, Hungary

Oxetane is known to decompose thermally into ethylene and formaldehyde in a homogeneous reaction¹. This reaction has been studied by the variable encounter method^{2,3}. Four cylindrical quartz reactors were used; the size of the reactors determined the mean number of wall collisions as $m = 2.1, 3.5, 10.5$ and 21.7 , respectively. Reaction temperature varied from 745 to 1131 K, while reactant pressure in the reactor was in the range of $1 \times 10^{-4} - 3 \times 10^{-4}$ Torr.

Apparent first order rate coefficients for decomposition were measured and these were used to calculate the average reaction probabilities per collision with the hot wall, $\bar{P}_C(m)$.

The experimental plots of the average reaction probabilities per collision are shown as a function of temperature in Fig. 1. The experimental data are compared with stochastic calculations based on various models for energy transfer probability, $P_{\Delta E}$. The best fit to the data is obtained using a Gaussian model with $P_{\Delta E} = A \exp[-(\Delta E - \Delta E_{mp})^2 / 2\sigma^2]$ for $\sigma \Delta E \leq 9500 \text{ cm}^{-1}$ and $P_{\Delta E} = 0$ for $\Delta E > 9500 \text{ cm}^{-1}$. Here A is a normalization constant, ΔE_{mp} and σ are parameters of the model. ΔE_{mp}

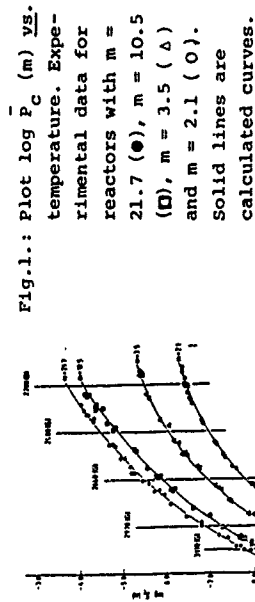


Fig. 1.: Plot $\log \bar{P}_C(m)$ vs. temperature. Experimental data for reactors with $m = 21.7$ (\bullet), $m = 10.5$ (Δ), $m = 3.5$ (Δ) and $m = 2.1$ (\circ). Solid lines are calculated curves.

was taken a constant, independent of the initial energy level. (Because of the truncation and limited matrix size, ΔE_{mp} is not necessarily equal to the average down transition size $\langle \Delta E' \rangle$).

The calculations enabled us to determine the average amount of energy transferred in a collision between the oxetane molecule and the hot surface of reaction wall. Values of $\langle \Delta E' \rangle$ (in cm^{-1}) that fit the data for the reactors at particular temperatures are shown in Fig. 1. and a trend of decreasing $\langle \Delta E' \rangle$ with increasing temperature is apparent.

The results will be compared with similar investigations of cyclobutane.

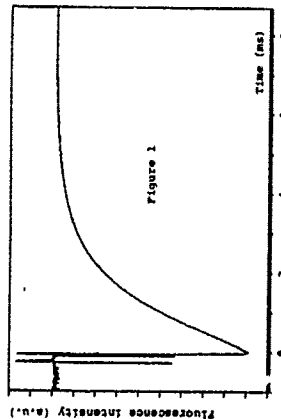
1. L. Zalotai, Zs. Hunyadi-Zoltán, T. Bérces and F. Márta, Int. J. Chem. Kinet., 15, 505 (1983).
2. D.F. Kelley, B.D. Barton, L. Zalotai and B.S. Rabinovitch, J. Chem. Phys., 71, 358 (1979).
3. D.F. Kelley, L. Zalotai and B. S. Rabinovitch, Chem. Phys., 46, 379 (1980)

Reaction kinetics of Mg (3p₂) with hydrocarbons

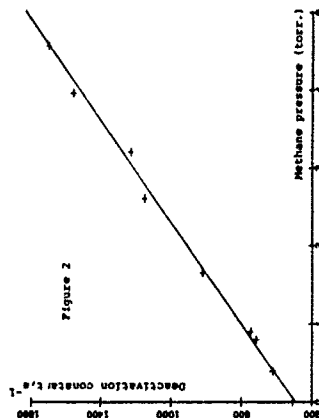
F. Beitia, F. Castaño* and E. Martinez

Depart. Química Física. Univ. País Vasco. Apart. 644. 48080 Bilbao. SPAIN.

Excited states of Mg (3p₂) were prepared by pumping Mg vapor in a calibrated heater able to reach 1000 K with a narrow band dye laser at 457.1 nm (Quintel YG 581-10 / Quantel Datachrom with Coumarin 460). Energies greater than 5 eV are required in order to get a sizable signal. The kinetics of the reactions between excited Mg atoms and hydrocarbon are studied by following the emission from Mg (3p₂) state with a gated photomultiplier, a digital scope (Tektronix mod 2430A) and a personal computer. Noble gases and hydrocarbons were introduced into the sample space with the aid of a flow vacuum manifold. Reported measurements are under static conditions (1).



Shown in Figure 1 is an example of the scope trace of the decay of Mg(3p₂) state at 800 K and a helium pressure of 10 Torr. The Stern-Volmer plot yields a lifetime for the mentioned state of 1.8 ns. Figure 2 shows the plot of the pseudo-second order deactivation constant of Mg by methane at 810 K, that yields a value of $k_q = 4.1 \cdot 10^{-4} \text{ cm}^3 \text{ molecule}^{-1} \text{ s}^{-1}$.



Further studies at temperatures between 650 and 900 K gives the following kinetic constant:

$$k_{\text{Mg/CH}_4} = 2.1 (\pm 0.8) 10^8 \cdot \exp(21.3/RT) \text{ cm}^3 \text{ molecule}^{-1} \text{ s}^{-1}$$

where the activation constant, 21.3 (± 1.6), is given in Kcal/mol. The Arrhenius behaviour indicates a single energy transfer mechanism. This, the kinetics constants with other saturated hydrocarbons and their mechanisms will be discussed (2).

References

1. D. Husain and J. Schifano. J. Chem. Soc., Faraday Trans. 2, 79, 919 (1983).
2. W.H. Beckenridge in Reactions of small transient species. A Fontijn and M.A.A. Clyne, eds. Academic Press (1983).

Reaction Kinetics and Spectroscopy of CHF radical with some hydrocarbons.

by F. Castaños*, A. Ortiz de Zárate and E. Martínez

Depart. Química Física. Univ. Pais Vasco. Apart. 644. 48980 Bilbao. SPAIN

Infrared multiphoton dissociation (IRMPD) has been used to prepare carbene and other radicals in order to perform spectroscopic and kinetic studies (1). Shown in figure 1 is a versatile experimental set up in our laboratory to study high resolution spectroscopy and kinetics of ground and excited states of radicals.

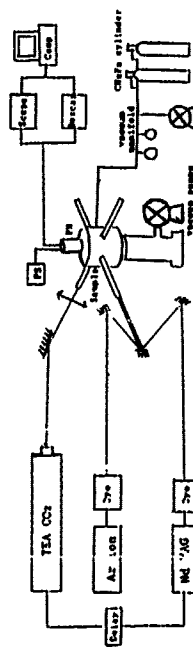


Figure 1

The high power TEA CO₂ Lumonics K 103 laser beam dissociate selected precursor molecules under collisionless conditions, in a noble gas buffer. Radicals produced are probed either by a C.W. Argon ion/dye laser (for ground states) or a Pulsed Nd-Yag/dye laser system variably delayed respect to the CO₂ laser pulse. Perpendicular, collinear and anti-collinear geometries between the pump and probe lasers are used in order to improve the signal-to-noise ratio. Emission from excited states of the radicals are detected by an RCA C31034A02 photomultiplier, followed by either a 150 MHz scope (Tektronix, mod. 2430A), a boxcar averager (Stanford Research SR250/Sr200) or a time correlated photon counting system. The detected signal is stored, averaged and processed by a personal computer.

In this work CH₂F₂ has been selected as the precursor to be pumped at 9.27 μ m and to produce CHF radical, that were conveniently detected and identified by its optical transition A₁ - X₁A₁ near 580 nm (measured lifetime 2.5 ns). Calibration of the system has been performed with the reaction of the radical with NO, yielding values in close agreement with those obtained in other laboratories (2) (9.2.10⁻¹² cm³mole⁻¹s⁻¹). Kinetic constants of the reactions between the CHF radical and halogenated hydrocarbons will be presented and discussed.

References

- 1.- M.N.K. Ashfold and G. Hancock. Chem. Soc. Specialist Periodical Reports. Gas kinetics and Energy Transfer. Vol 4, 73 (1980).
- 2.- K. Mackendrick. D. Phil. Thesis. Oxford University (1985).

J. CHABOUX, F. JORAND, V. VIOSAT, K. SMETCHIAN
Laboratoire de Chimie Générale, C.N.R.S. UA 40870
Université P. et M. Curie, Tour 55 (4^e Etage)
4 Place Jussieu, 75252 Paris Cedex 05

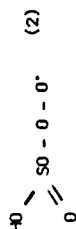
and
C. CHACHATY

IRDI/DESIP Département de Physico Chimie,
C. E. N. SACLAY - 91181 GIF SUR YVETTE CEDEX

The influence of SO_2 (0 to 20 %) on the hydrogen slow oxidation (793K -400 torrs) can allow the study of some reactions between SO_2 and the slow oxidation intermediates. We observed both an accelerating and an inhibiting effect which depends on the extent of the reaction and on the H_2/O_2 ratio. The accelerating effect is detected in the earliest stages of the oxidation ; it is explained by the reaction $\text{HO}_2 + \text{SO}_2 = \text{SO}_3 + \text{OH}^{\cdot(1)}$. The interpretation of the inhibiting effect, detected after the maximum rate, needs further studies of the reactions between SO_2 and the oxidation products.

The $\text{SO}_2 + \text{H}_2\text{O}_2$ reaction was studied at lower temperatures (below -100°C). The H_2O_2 radicals are extracted from the reaction mixture by means of a microprobe, and SO_2 is added to the gaseous flow after the reactor. A new radical was detected by E.S.R. analysis. We attempted to precise the nature of this compound and the conditions of its formation. The E.S.R. spectrum identification was confirmed by the substitution of H_2 by $^2\text{H}_2$ and substitution of SO_2^{16} by labelled SO_2^{17} ; in both cases we observed no change in the E.S.R. spectra. These results and the simulation

of the spectrum showed that a peroxidic structure can be attributed for the radical formed by addition of HO_2 on SO_2 :



This radical can be formed :

a) either in the gaseous phase, at ambient temperature, after the microprobe ($T = 298\text{ K}$, $P = 0,3\text{ torr}$).

b) or at the temperature of liquid nitrogen (77 K). If the contact time between SO_2 and H_2O_2 was varied, no modification was observed on the spectrum. This result can be in favour of the HSO_4 radical formation at low temperature (77 K), on the solid (cold finger).

- (1) J. CHAMBOUX, V. VIOSSAT, F. JORAND, K. SAWETCHIAN.
J. Chim. Phys. 1985, 82 (5), 499.
- (2) J. CHAMBOUX, F. JORAND, V. VIOSSAT, K. SAWETCHIAN, C. CHACHATY
J. Chim. Phys. 1985, 82 (9), 835.

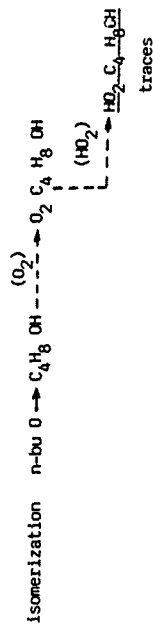
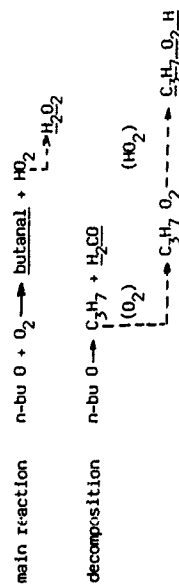
STUDY OF SOME REACTIONS OF N-ALKOXY RADICALS.

K.A. SMETCHIAN, A. HEISS, R. RIGNY.

Laboratoire de Chimie Générale, Université P. et M. Curie,
C.N.R.S. UA 40870, 4 Place Jussieu, T. 55,
75252 PARIS CEDEX 05

Alkoxy radicals are key intermediates in hydrocarbon degradation, in combustion and in atmospheric pollution. We have studied the reaction of n-butoxy radicals with oxygen at ambient temperature and at temperatures ranging from 150 to 200°C, under atmospheric pressure. In order to do this, these radicals were generated by photochemical or thermal decomposition of di-n-butylperoxide in oxygen. In this system and from the products obtained, we try to go back to the initial reactions : with oxygen, decomposition, isomerization.

Analyses are made by TLC and HPLC for peroxides and by HPLC for carbonyl compounds, after their transformation into characteristic derivatives, 2-4 D⁺ phenylhydrazones which are very sensitive to UV detection about 340 nm. The main results are the following :



Thus, we have shown the formation of butanal, formaldehyde, hydrogen peroxide, propyl hydroperoxide and traces of an oxyhydroperoxide. Formation of these products and knowledge of their concentration ratios will allow to determine the relative importance of different pathways : reaction with O_2 , decomposition and isomerization.

In conclusion, from results obtained with n-bu O radicals, it seems that the study of reactions of n-alkoxy radicals with oxygen is suited to atmospheric and combustion chemistry.

OH VIBRATIONAL ENERGY DISTRIBUTION IN REACTIONS OF O(¹D) ATOMS.

S.G.Cheskis, A.A.Iogansen, P.V.Kulakov, I.Yu.Razuvaev,
O.M.Sarkisov and A.A.Titov.

Institute of Chemical Physics, USSR Academy of Sciences,
Moscow, USSR.

1. Direct time-resolved measurements of OH(v) vibrational relaxation kinetics are demonstrated to be a powerful means of determining nascent vibrational energy distribution (VED) of OH radicals in reactions of O(¹D) atoms with H-containing molecules.

For a number of interesting systems this "kinetic approach" enables to obtain almost total OH VED by monitoring only three states of OH in relative units (one rovibronic state for each vibrational level v=0,1,2). The experimental procedure¹ is much more easier than those used in analogous studies.

2. OH VED in O(¹D)+H₂, CH₄, NH₃ reactions were obtained (see Table 1). The surprisal plots for all three are reasonably linear. For O(¹D)+H₂ reaction the measured OH VED is in good agreement with the results of trajectory calculations².

Using kinetic approach for O₃/CH₄ system, we have determined the role of chain reactions, in which the vibrationally excited OH radicals do participate³. Comparison with VED data reported in literature shows that the results, obtained by various fixed-time-delay methods, are probably somewhat distorted either by fast relaxation processes⁴ (in case of NH₃) or by subsequent chain reactions with OH(v) participation^{5,6}.

3. Alongside with distributions, the rate constants of vibrational relaxation of OH(v=1,2,3) in collisions with ammonia and methanol were measured (see Table 2). The reactive channel in deactivation of OH(v) by H₂ molecules seems to be dominating, though the reaction rate doesn't accelerate noticeably with vibrational excitation of OH radicals.

Table 1. OH(v) disposal
in O(¹D)+RH reactions.

v	Population (%)		
	NH ₃	CH ₄	H ₂
0	20	18	28
1	32	35	30
2	34	36	24
3	14	11	13
4	0	0	5

Table 2. OH(v) quenching
rate constants (cm³/s).

v	Quencher	
	NH ₃	CH ₄
1	2.1 10 ⁻¹¹	3.5 10 ⁻¹³
2	1.0 10 ⁻¹⁰	2.1 10 ⁻¹²
3	3.0 10 ⁻¹⁰	1.0 10 ⁻¹¹

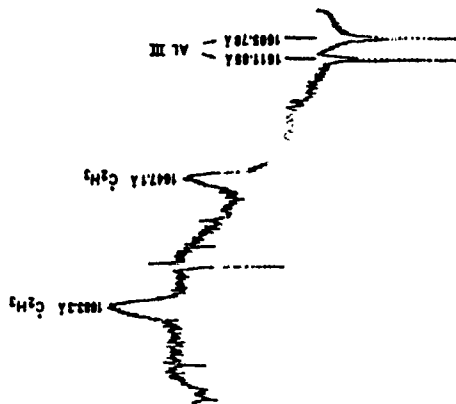
1. S.G.Cheskis, A.A.Iogansen, P.V.Kulakov, O.M.Sarkisov, A.A.Titov // Chem.Phys.Lett, 1988, v.143, 348.
2. N.S.Fitscharles, G.C.Schatz // J.Phys.Chem.1986, v.90, 36.
3. S.G.Cheskis, A.A.Iogansen, P.V.Kulakov, O.M.Sarkisov, A.A.Titov // Khim.Fizika (in Russian) 1988, (in press).
4. P.M.Aker, J.A.O'Brien, J.M.Parsons, J.J.Sloan // Can.J.Chem., 1986, v.64, p.2315
5. P.M.Aker, J.J.Sloan // J.Chem.Phys., 1986, v.85, p.1412
6. P.M.Aker, J.J.Sloan // J.Chem.Phys., 1986, v.84, p.745

OBSERVATIONS OF NEW ABSORPTIONS OF THE C_2H_3 (VINYL)
RADICAL AND SOME OF ITS CHEMISTRY

Askar Fahr and Allan H. Laufer*

Center for Chemical Physics
National Bureau of Standards
Gaithersburg, Md. 20899

Aside from the interest inherent in the chemistry of unsaturated hydrocarbon radicals the vinyl radical, in particular, has been recognized for its important role in a variety of areas of great interest to gas kinetics. They range from the broad temperature regimes associated with planetary atmospheres to the high temperatures of combustion systems. While the chemistry of small, unsaturated hydrocarbon radicals have been the subject of several investigations relatively little is known about C_2H_3 . This is probably due to difficulty in its direct observation which to the present has been done by mass spectrometric detection¹. The relatively weak electronic transition observed in the near ultraviolet² has not been used for kinetic studies. We report here the observation of an intense absorption of the C_2H_3 in the vacuum ultraviolet, useful for the study of kinetics. Using the venerable technique of flash photolysis in conjunction with absorption kinetic "spectroscopy", both in the vacuum ultraviolet region and with microsecond time resolution, we have observed two strong features that we can assign to the C_2H_3 radical. Photolysis of either $Sn(C_2H_3)_4$ or $ig(C_2H_3)_2$ produced a pair of well resolved, but diffuse, transient features at 1647.1 Å and 1683.3 Å. The maximum intensity appeared at the shortest delay times, 4-5 microseconds, and decayed monotonically with time. The spacing between the bands, 1306 cm^{-1} , agrees with calculated values for vibrational frequencies of the C_2H_3 radical. In addition to the precursor species that are "expected" to produce C_2H_3 radicals, we compared the well-characterized rate constant for reaction of C_2H_3 radicals with O_2 obtained by mass spectroscopy¹ with that measured spectroscopically by monitoring the feature at 1683.3 Å. The values are in good agreement and support the assignment to the vinyl radical. A densitometer trace of the absorption bands is shown on the next page.



Frequently an absolute measure of the radical concentration is needed that requires a value of the extinction coefficient. The initial concentration of vinyl radicals was obtained by gas chromatographic analysis of the photolysis products. Assuming that the disproportionation process is small relative to that for combination, the yield of 1,3-butadiene was used as a measure of the initial vinyl concentration. The extinction coefficient, ϵ , derived from the kinetic data and fitted to the Lambert-Beer expression $I/I_0 = \exp(-\epsilon c l)$ was determined to be $1120 \text{ cm}^2 \text{ atm}^{-1}$ for the band at 1683 Å and $1650 \text{ cm}^2 \text{ atm}^{-1}$ for the band at 1647 Å.

1. I. R. Slagle, J.-Y. Park, M. C. Heaven, and D. Gutman, *J. Am. Chem. Soc.*, (1986) **108**, 4356.
2. H. E. Hunziker, H. Knepp, A. D. McLean, P. Siegbahn, and H. R. Wendt, *Can. J. Chem.*, (1983) **61**, 993.

*. Guest Worker, Present Address: U.S. Department of Energy, ER-14, Washington, D.C. 20545

REACTIONS OF VINYL AND PHENYL RADICALS WITH ETHYLENE, ETHENE AND BENZENE

Asker Fahr and Stephen E. Stein
Chemical Kinetics Division
National Bureau of Standards
Gaithersburg, MD 20899

Vinyl and phenyl radicals and related species are commonly proposed as intermediates in the pyrolysis and combustion of hydrocarbons. Their addition reactions provide a plausible high temperature path for carbon growth.

We report here, rate constants for vinylation and phenylation of ethylene, ethene and benzene. These rates have been determined relative to vinyl recombination in a temperature range of 900-1300°K.

Kinetic studies employed a very low pressure pyrolysis (VLPP) reactor connected to a differentially pumped, quadrupole mass spectrometer. Divinylmercury and phenylvinylsulfone were used as radical precursors. The lower temperature limit was set by the onset of appreciable decomposition of the radical initiator and the upper limit by the softening point of the fused silica reactor.

Assuming a recombination rate constant of $10^{10.3} \text{ M}^{-1} \text{ s}^{-1}$ for vinyl and $10^{9.5}$ for phenyl, we obtain the following rate constants ($\text{M}^{-1} \text{ s}^{-1}$)

	$k(\text{R} = \text{vinyl})$	$k(\text{R} = \text{phenyl})$
$\text{R}^{\cdot} + \text{C}_2\text{H}_2 \rightarrow$	$\text{R} \cdot \text{C}_2\text{H} + \text{H}^{\cdot}$	$2.0 \pm 0.4 \times 10^8$ $2.6 \pm 0.6 \times 10^8$
$\text{R}^{\cdot} + \text{C}_2\text{H}_4 \rightarrow$	$\text{R} \cdot \text{C}_2\text{H}_3 + \text{H}^{\cdot}$	$1.4 \pm 0.2 \times 10^8$ $1.5 \pm 0.4 \times 10^8$
$\text{R}^{\cdot} + \text{C}_6\text{H}_6 \rightarrow$	$\text{R} \cdot \text{C}_6\text{H}_5 + \text{H}^{\cdot}$	$4.5 \pm 1.2 \times 10^7$ $6.0 \pm 2.0 \times 10^7$

These are the only available data for vinylation reactions, at high temperatures. Phenylation rates are in good agreement with our earlier VLPP values, using nitrosobenzene as initiator(1).

For two of the reactions studied, vinyl + ethyne and phenyl + benzene low temperature addition rates are available(2,3). By combining these values with the present data we can derive the following Arrhenius expressions:

$$k(\text{vinyl} + \text{ethyne} \rightarrow \text{vinylacetylene} + \text{H}) = 10^{9.3} \exp(-5.0 \text{ kcal/RT})$$

$$k(\text{phenyl} + \text{benzene} \rightarrow \text{biphenyl} + \text{H}) = 10^{8.6} \exp(-4.0 \text{ kcal/RT})$$

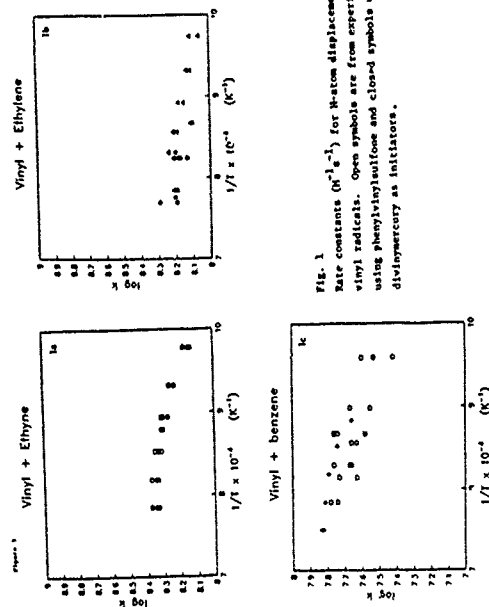


Fig. 1
Rate constants ($\text{M}^{-1} \text{ s}^{-1}$) for H-atom displacement by vinyl radicals. Open symbols are from experiments using phenylvinylsulfone and closed symbols using divinylmercury as initiators.

- 1) Fahr, A.; Mallard, G. and Stein, S.E., 21st Symp. on Combustion (1986), in press.
- 2) Sciano, J. and Stewart, L., J. Am. Chem. Soc. 105, 3609, (1983).
- 3) Callear, A. and Smith, G.B., J. Phys. Chem. 20, 3229, (1986).

RATE CONSTANTS FOR THE REACTIONS
 $t\text{-C}_4\text{H}_9 + \text{DX} \rightarrow t\text{-C}_4\text{H}_9\text{D} + \text{X}$, (X = Br, I) 29557/K5384:
 THE HEAT OF FORMATION OF *t*-BUTYL RADICAL

Wolfgang Muller-Markgraf, Michel V. Rossi, and David M. Golden
 Department of Chemical Kinetics, Chemical Physics Laboratory SRI
 International, Menlo Park, CA 94025

Absolute rate constants for the metathesis reactions of DBr and DI with *t*-butyl radicals have been measured using the Very Low Pressure Photolysis (VLPP) technique. The *t*-butyl radical was prepared by means of 351 nm laser photolysis of 2,2'-azobiscyclohexane and allowed to react with DBr/DI.

In order to facilitate a separation of possible contributions from heterogeneous (wall catalyzed) reactions to the overall observable, the Knudsen cell reactor was equipped with interchangeable apertures. Thus the reactor allowed us to titrate *t*-butyl radicals with DBr/DI using four different escape rate constants.

Comparing the results of independent measurements with different escape rate constants, it was possible to assess the relative importance of heterogeneous reactions and to find a suitable range of experimental conditions where undisputed values for the rate constants of interest can be obtained.

The first order heterogeneous loss rate of *t*-butyl radicals on the teflon coated reactor surface employed was found to be small ($< 2 \text{ sec}^{-1}$). The multiple aperture data set yielded the following values for the rate constants of the metathesis reaction:

$10^{-8} \text{ s} \cdot \text{K} / \text{M}^{-1} \cdot \text{s}^{-1}$	T/K	DX (X = Br, I)
0.9 ± 0.4	295	DBr
2.3 ± 0.3	384	DBr
2.1 ± 0.9	295	DI
3.1 ± 1.0	384	DI

The DI - values are in good agreement with earlier measurements from this laboratory,^{1,2} whereas the rate constants for the analogous DBr

- reaction are a factor of 50 (at 295 K) and 11 (at 384 K) smaller than those recently reported³ (after correction for the primary isotope effect). They also do not show the negative activation energy found in Reference 3.

The results of the present work, if combined with the rate constants for the reverse reaction,⁴ lead to

$$\Delta H_f^{\circ} 298 / \text{kcal mol}^{-1} = 9.2 \pm 0.5$$

in contrast to the results of Reference 3 ($11.6 \text{ kcal mol}^{-1}$).

References

- 1) Rossi, M. J.; Golden, D. M., Int. J. Chem. Kinet. 1983, 15, 1283.
- 2) Rossi, M. J.; Golden, D. M., Int. J. Chem. Kinet. 1979, 11, 969.
- 3) Russell, J. J.; Seetula, J. A.; Timonen, R. S.; Gutman, D.; Nava, D. F., J. Am. Chem. Soc., in press.

KINETIC STUDIES OF THE REACTIONS OF CH_3 , C_2H_5 , $i\text{-C}_3\text{H}_7$, AND $t\text{-C}_4\text{H}_9$ WITH HBr AND HI AND THE HEATS OF FORMATION OF THE ALKYL RADICAL

J. J. Russell, J. A. Seetula, and D. Gutman

Department of Chemistry, Illinois Institute of Technology
Chicago, Illinois 60616, U. S. A.

The kinetics of the reactions between CH_3 , C_2H_5 , $i\text{-C}_3\text{H}_7$, and $t\text{-C}_4\text{H}_9$ with both HBr and HI have been studied using a heatable tubular reactor coupled to a photoionization mass spectrometer. Rate constants were determined as a function of temperature to determine Arrhenius parameters.

Second and Third law calculations (using these measured values for the $\text{R} + \text{HX}$ rate constants and Arrhenius parameters and rate constants for the reverse reactions determined by others) have been done to obtain the heats of formation and entropies of these alkyl radicals. The heats of formation obtained are in good agreement with those derived from prior studies of dissociation-recombination equilibria¹ but not with those obtained in earlier investigations of $\text{R} + \text{HX} \rightleftharpoons \text{R-H} + \text{X}$ equilibria².

The source of the disparity between alkyl-radical heats of formation which have been derived from studies of dissociation-recombination equilibria and those which have been obtained from prior investigations of the kinetics of $\text{R} + \text{HX}$ reactions has been identified. It is the difference between the actual activation energies of the $\text{R} + \text{HX}$ reactions and those which have had to be assumed in the latter group of studies to calculate free radical heats of formation. The assumed activation energies for $\text{R} + \text{HBr}$ and $\text{R} + \text{HI}$ reactions were 2 and 1 kcal mol⁻¹ respectively.³ The measured activation energies are all negative, varying from -0.3 kcal mol⁻¹ for the $\text{CH}_3 + \text{HX}$ reactions to -1.5 kcal mol⁻¹ for the $t\text{-C}_4\text{H}_9 + \text{HX}$ reactions. The measured Arrhenius parameters for the reactions which have been studied in the current investigation are presented in Table I.

It is suggested that the cause of the negative activation energies is a complex mechanism for $\text{R} + \text{HX}$ reactions, one which proceeds via a quasi-bound intermediate:



Evidence for related bound intermediates has been reported by Grace ($\text{CH}_3 + \text{ICl}$ and IBr)⁴ and by Lee ($\text{CH}_3 + \text{IF}$)⁵.

1. Tsang, W.; J. Am. Chem. Soc. 1985, 107, 2872.
2. McMillen, D.; Golden, D. M. Ann Rev. Phys. Chem. 1982, 33, 493.
3. O'Me l, H. E.; Benson, S. W. In "Free Radicals"; Kochi, J. K., Ed; Wiley: New York, 1973; Vol. 2, Chapter 17.
4. Hoffmann, S. H. A.; Smith, D. J.; Bradshaw, M.; Grace, R. Mol. Phys., 1986, 57, 1219.
5. Farrar, J. M.; Lee, Y. T. J. Chem. Phys. 1975, 63, 3639.

TABLE I

R	ARRHENIUS PARAMETERS OF THE $\text{R} + \text{HX}$ RATE CONSTANTS	
	$A/\text{cm}^3\text{molecule}^{-1}\text{s}^{-1}$	$E/\text{kcal mol}^{-1}$
R + HBr Reactions		
CH_3	8.7×10^{13}	-0.31
C_2H_5	1.0×10^{12}	-0.81
$i\text{-C}_3\text{H}_7$	1.1×10^{12}	-1.1
$t\text{-C}_4\text{H}_9$	9.9×10^{12}	-1.4
R + HI Reactions		
CH_3	4.0×10^{12}	-0.36
C_2H_5	4.5×10^{12}	-0.77
$i\text{-C}_3\text{H}_7$	3.9×10^{12}	-1.2
$t\text{-C}_4\text{H}_9$	3.1×10^{12}	-1.5

The NBS Chemical Kinetics Data Center
Databases and Computational Programs for Use on
Personal Computers

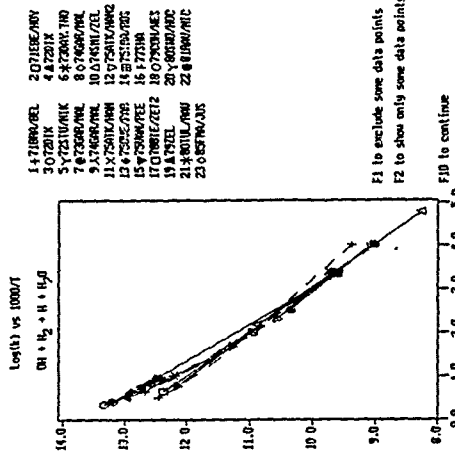
J. T. Herron and W. G. Mallard
Chemical Kinetics Division, National Bureau of
Standards, Gaithersburg, MD 20899.

The Chemical Kinetics Data Center of the National Bureau of Standards is developing a series of databases and a library of computational programs for use on personal computers. The goal is to provide numerical databases of chemical kinetic and thermochemical data, and the means to manipulate these data as an adjunct to data evaluation, or for application in modeling complex phenomena. The Chemical Kinetics Data Center has built up an extensive text-based file of numerical data on the kinetics of gas-phase chemical reactions covering the literature from about 1971 to the present^{1,2}. These data files now have been converted to a database format and programs written to permit rapid searching of the database. There are over 6000 data entries in the system corresponding to about 2500 elementary reactions. Searching can be done by reactants, reaction, reactant classes, or by authors. The result of a search can be graphically displayed - shown in the figure. This is an exact representation of the screen image seen on plotting data for the reaction $H_2 + HO \rightarrow H + H_2O$.

A companion database contains thermochemical data on over 5000 compounds based on published reviews and tabulating the thermochemical properties of ions (an activity of the related NBS Ion Energetics Data Center).

The development of computational programs in support of data compilation or evaluation activities is aimed at providing a chemical kineticists "toolbox" for the analysis, fitting, and extrapolation of chemical kinetic data. The first one available is "AcuChem", which is a program for solving the system of differential equations describing the temporal behavior of spatially homogeneous, isothermal, multi-component chemical reaction systems. It provides an easy to use program for modeling complex chemical reactions, and for presenting the results in tabular or graphical form. Other support programs under

development include RRRM and BEBO.
The databases and computational programs will be distributed for use on IBM PC or compatible personal computer.



1. F. Westley, J. T. Herron, and R. J. Cvetanovic, "Compilation of Chemical Kinetic Data for Combustion Chemistry. Part 1. Non-aromatic C, H, O, N, and S Containing Compounds (1971-1982)", NSRDS-NBS 73, Part 1 (1987).
2. F. Westley, J. T. Herron, and R. J. Cvetanovic, "Compilation of Chemical Kinetic Data for Combustion Chemistry. Part 2. Non-aromatic C, H, O, N, and S Containing Compounds (1983)", NSRDS-NBS 73, Part 2 (1987).
3. W. Braun, D. Kahaner, and J. T. Herron, "AcuChem: A Computer Code for Modeling Complex Chemical Reaction Systems", Int. J. Chem. Kinetics, 20, 51 (1988).

Design and Implementation of a Chemical Kinetics Database

M.G. Mallard and J.T. Herron
Chemical Kinetics Data Center
National Bureau of Standards
Gaithersburg, MD 20899 U.S.A.

Given a large set of kinetic data, what kind of information will be most widely sought after, what supplementary information will be needed, what kind of search options will be desired. The modeling community will have very different needs from the measurement community and both of these groups will have different needs from those of the ab initio calculation community. The approach used in designing this database attempts to address the needs of the modeling and the measurement community. Both groups need to have a quickly available summary of the available data on a given reactant pair. This summary should include the measured rate parameters for all studied pathways as well as information on mechanism. Modelers need review papers that select the best rate parameters for a given reaction or pathway. Experimentalists need more information on experimental techniques, temperature or pressure ranges of other determinations or rates of comparable reactions.

To insure that this kind of information is properly entered the abstracting process required that data on experimental procedure such as apparatus, analysis technique, excitation method, pressure and temperature be entered. The very act of demanding this information in the abstract pointed up the surprising number of cases where some of this information was missing in the original papers or could be found only by a certain amount of reading between the lines.

The core of this kind of database is the reactions and the rate parameters determined experimentally. The organization of the database was chosen to facilitate the search for reactions in terms of the reactants, without regard to the products. In order to implement this system a database of chemical compounds was built-up. This database consisted of

the molecular formula, compound name, Chemical Abstracts registry number, and if available the enthalpy of formation, entropy and heat capacity at 298 K. To conserve space the molecular name is kept in a separate variable record length file and only a reference to it is contained in the primary chemical database. The name is viewed as the unique identifier for each compound, thus while CH_4 is the valid name for methane, C_6H_6 is not the valid name for benzene since the data base contains 14 isomers with that molecular formula. All numeric data is stored in integer format. In the case of the enthalpy $H/R \times 10$ is stored. The resulting data stored to a precision of 12 J/mol. For entropy and heat capacity a different approach was adopted since both of these values typically scale with molecular weight, the value stored was $X \times 1000 / (R \times MW)$ where X is S or Cp. The molecular weight is calculated from the molecular formula. For output all of the data is reconstructed into its standard form. The thermodynamic data allows the calculation of ΔG and ΔH of the reaction. In addition the compound record will have structural information in the future so that searching for the reaction of H with all compounds having an -OH will be a simple addition to the current search techniques.

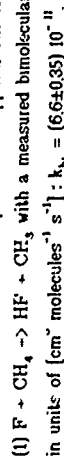
In order to make the search rapid, the data is fully indexed by reactants and by reference. Thus one may access the data by asking for all of the data on $\text{H} + \text{O}_2$, or by asking for all of the data abstracted from a given reference. In addition it is possible to ask for all reactions of a single species (e.g. OH), or the reactions of a single species with a restricted set (e.g. molecules with C and N atoms). The retrieval for all examples of a single reactant pair - $\text{H} + \text{CH}_4$ - is very fast, typically less than 2-5 seconds (on a 8088 class machine with a hard disk). The system will keep a set of summary pages of the results of the last inquiry directly available. The program will detect the presence of a graphic board and utilize them to plot Arrhenius graphs of the data for all direct determinations of the rate constant. Once a particular data item is found the program will display all of the data as well as the full reference.

BIMOLECULAR REACTIONS OF FLUORINE ATOMS WITH HALOGENATED METHANE IN THE GAS PHASE

Udo Wörzförer and Horst Heydtmann

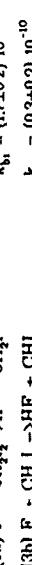
Inst. f. Physikalische und Theoretische Chemie
University of Frankfurt/Main, FRG

The reactions of F atoms with CH_4 , CH_3I , CH_2I_2 , CF_3I and CHCl_3 were studied in a flow system at pressures of about 3 mbar and flow velocities in the range of 10 m s^{-1} – 20 m s^{-1} at room temperature. Helium was used as carrier gas and also gas mixtures of reactants in He, F atoms were generated by microwave discharge of 0.5 % F_2/He mixture and a quadrupole mass spectrometer was used for analysis. Excess of F atoms as well as of the molecular species were applied. The test reaction was



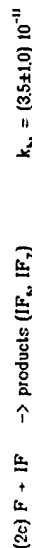
in units of $[\text{cm}^3 \text{ molecules}^{-1} \text{ s}^{-1}]$: $k_{\text{b1}} = (6.6 \pm 0.35) 10^{-10}$

For the reactions (2) $\text{F} + \text{CH}_3\text{I}$ and (3) $\text{F} + \text{CH}_2\text{I}_2$ the branching ratios between the HF and IF forming channels could be studied. The reaction (4) $\text{F} + \text{CF}_3\text{I}$, which only forms IF and $\text{CF}_3^{1,2}$, allowed the calibration of the IF signal.



Two different methods were used to arrive at the branching ratio. With the kinetic simulation program LARKIN³ calculation and a fit to the

experimental IF intensities using k_{b1} values (2a, 2b) was possible. k_{b1} of the occurring secondary reaction could be determined:



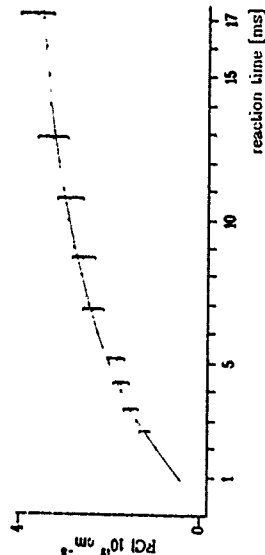
In the reaction system $\text{F} + \text{CHCl}_3$, in a primary reaction step only H abstraction was observed.



A fast formation of FCI was detected. Using the reaction $\text{F} + \text{Cl}_2 \rightarrow \text{FCI} + \text{Cl}$ a calibration of the FCI signal was possible⁴. Rate constants for the following secondary reactions could be fitted to the experimental FCI data:



With an additional F-Cl atom substitution (5c), already postulated by², the best fit to experimental FCI concentrations was obtained. Fig. 1 shows calculated and measured FCI concentrations.



References: 1) T. Venkitchalam, P. Das, R. Bersohn, J. Am. Chem. Soc. 105 (1983) 7452. 2) J. W. Bozelli, M. Kaufman, J. Phys. Chem. 77 (1973) 1748. 3) F. Douillard, U. Novak, Ber. Bunsenges. Phys. Chem. 90 (1986) 940. 4) M. A. Clyne, D. J. Mc Kenney, Can. J. Chem. 51 (1973) 3596.

DIRECT MEASUREMENTS OF ELEMENTARY RADICAL REACTIONS AT VARIOUS ENERGIES STUDIED BY UV-LIF

A. Jacobs, M. Wahl, R. Weller, J. Wolfrum

Physikalisches Institut der Universität Heidelberg
Im Neuenheimer Feld 253, D-6900 Heidelberg 1

Conventionally, the energy dependence of a chemical reaction is studied under conditions in which the rate of reaction is slow compared to that of collisional energy transfer. Under these conditions, the energy of the reactants is characterized by a temperature. In the temperature region of 300 K to 1000 K some very new data¹ for the rate constants and the pathways in the reaction systems



measured by UV-LIF were measured. We observed the time history of the CN and OH radicals by laser induced fluorescence. The temperature dependent rate coefficients for reactions (1), (2), (3), and (5) could be fit by Arrhenius expressions and are

$$\begin{aligned}
 k_1 (518 - 1027 \text{ K}) &= (8.0 \pm 0.8) \times 10^{12} \exp \{-(31.2 \pm 0.6) \text{ kJ/RT}\} \text{ cm}^3 \text{ mol}^{-1} \text{ s}^{-1} \\
 k_2 (295 - 1000 \text{ K}) &= (2.1 \pm 0.2) \times 10^{13} \exp \{-(19.7 \pm 0.5) \text{ kJ/RT}\} \text{ cm}^3 \text{ mol}^{-1} \text{ s}^{-1} \\
 k_3 (295 - 1000 \text{ K}) &= (8.7 \pm 0.8) \times 10^{12} \exp \{-(1.8 \pm 0.1) \text{ kJ/RT}\} \text{ cm}^3 \text{ mol}^{-1} \text{ s}^{-1} \\
 k_5 (295 - 1025 \text{ K}) &= (9.7 \pm 1.0) \times 10^{11} \exp \{-(5.7 \pm 0.2) \text{ kJ/RT}\} \text{ cm}^3 \text{ mol}^{-1} \text{ s}^{-1}
 \end{aligned}$$

From thermodynamical properties of reaction (1) we evaluated the temperature dependent rate coefficient for the reverse reaction:

$$k_{-1} = (7.7 \pm 1) \times 10^{12} \exp \{-(34.6 \pm 1) \text{ kJ/RT}\} \text{ cm}^3 \text{ mol}^{-1} \text{ s}^{-1}$$

In the CN + CO₂ system we did not observe CN(1st) order rate constants attributable to chemical reaction at temperatures up to 1000 K. We estimated an upper limit for k_4 of $2.5 \times 10^9 \text{ cm}^3 \text{ mol}^{-1} \text{ s}^{-1}$. The experimental results are compared with literature data. In the case of reactions (1), (2), (3) and (5) the agreement with previous experimental and theoretical studies is good, whereas our results for k_4 strongly differ from former measurements. Concerning the reaction (1) vibrational relaxation of the CN(v=1) species by collisions with water is fast compared with the reaction rate. Therefore we could only estimate the specific

rate constant of the vibrationally excited CN radicals to be $k_4 [\text{CN}(v=1)] \leq 1.5 k_1 [\text{CN}(v=0)]$. In contrast, for the reaction systems (2) and (3) vibrational relaxation cannot compete with reaction and we determined $k_2 [\text{CN}(v=1)]$ to be $(1.4 \pm 0.2) \times k_2 [\text{CN}(v=0)]$; $k_3 [\text{CN}(v=1)]$ seems to be slightly lower than $k_3 [\text{CN}(v=0)]$. The observed CN(v=1) decays through reactions (4) delivered a coefficient $k_4 [\text{CN}(v=1)] = 9 \times 10^9 \text{ cm}^3 \text{ mol}^{-1} \text{ s}^{-1}$ at 300 K. We believe that this value describes the vibrational relaxation by CO₂. Using a hard sphere model yields a quenching probability $P = 4 \times 10^{-5}$ which is close to the predictions of the SSH theory.

The Arrhenius parameters obtained in this way, however, contain no direct information on how the various degrees of freedom of the reacting molecules contribute to overcoming the potential barriers of product formation in the chemical reaction. Investigations on the chemical reactivity under a range of conditions such as specific excitation of the reactants therefore give an important insight into the microscopic dynamics of the chemical reaction. Various laser sources with definite polarisation, tunability and short pulse duration allow the preparation and detection of chemically reacting molecules and radicals with an unprecedented degree of selectivity. Photolysis of HCl with an ArF excimer laser at a wavelength of 193 nm produces high translationally excited H atoms with a velocity of 18900 m/s corresponding to a collision energy of 1.84 eV (= 43 kcal/mol). The reaction of these H atoms with CO₂



was investigated by time-resolved LIF of the OH radicals. At typical conditions of 7 mTorr HCl and 70 mTorr CO₂ the very first OH radicals produced by reaction (6) 30-40 ns after photolysis of HCl were observed.

Within the detection limit we could not observe any vibrationally excited OH. The rotational distribution in OH(v=0) shows a broad maximum between $J = 4-8$ and falls off to $J = 12$. The lambda components were found to be equally populated ($I(J)/I(1) = 0.98 \pm 0.17$) while there was a slight performance for the upper spin state $\Pi_{3/2}$ versus the $\Pi_{1/2}$ state ($I(\Pi_{3/2})/I(\Pi_{1/2}) = 1.36 \pm 0.19$). Using a narrow-bandwidth dye laser we determined the OH-velocity from Doppler-profile measurements to be ca. 2300 m/s. By comparison of the OH-LIF signal with the well known LIF-signals from OH produced by photolysis of H₂O₂ at 193 nm we were able to measure the absolute reactive cross section for the reaction (6).

$$\sigma_6 = (0.48 \pm 0.15) \text{ \AA}^2$$

Previous experiments² with a collision energy of 2.6 eV reported a cross section of $(0.35 \pm 0.1) \text{ \AA}^2$. OCT calculations³ at a collision energy of 1.9 eV predict a value of 0.22 \AA^2 . In order to investigate the reverse reaction (6) we are now detecting H atoms via Lyman- α -LIF.

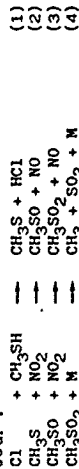
1. A. Jacobs, M. Wahl, R. Weller, J. Wolfrum, Chem. Phys. Lett. 144, 203-207 (1988)
2. A. Jacobs, M. Wahl, R. Weller, J. Wolfrum, Appl. Phys. B 42, 173-179 (1987)
3. K. Kleinermanns, J. Wolfrum, Laser Chem. 2, 339-359 (1983)
4. G. C. Schatz, M. S. Fitzcharles, Far. Disc. Chem. Soc. (1987)

DISCHARGE-FLOW KINETIC STUDY OF THE REACTION $\text{CH}_3\text{S} + \text{NO}_2$

J.L. JOURDAIN, A. MELLOUKI and G. LE BRAS

(Centre de Recherches sur la Chimie de la Combustion et des Hautes Températures - C.N.R.S. - 45071 Orléans-Cedex 2 FRANCE)

The title reaction is potentially important in the atmospheric oxidation of CH_3S which is an intermediate species in the oxidation of organic sulfur compounds such as CH_3SCH_3 . This reaction has been studied at room temperature using the discharge-flow mass spectrometric technique using flows of Cl atoms and CH_3SH in excess NO_2 . The total pressure was 0.3 Torr and the flow rate 44 m/s with helium as the diluent. The 22 mm id quartz reactor was coated with halocarbon wax in order to prevent wall effects. The kinetics of CH_3SH , NO and SO_2 were monitored as a function of reaction time and Cl atoms were titrated by $\text{C}_2\text{H}_5\text{Br}$ before and after each kinetic run. The following main reactions were considered to occur:



Rate constant for reaction (1) was measured from the CH_3SH decay in the presence of excess NO_2 in order to prevent any secondary reactions. Without NO_2 , the reaction of CH_3S with Cl_2 undissociated in the discharge was likely to occur, leading to the formation of CH_3SCl and Cl . The following value was obtained $k_1 = (1.1 \pm 0.4) \times 10^{-10} \text{ cm}^3 \text{ molecule}^{-1} \text{ s}^{-1}$.

Reaction (1) appeared to be a convenient non photolytic source of CH_3S in discharge - flow systems.

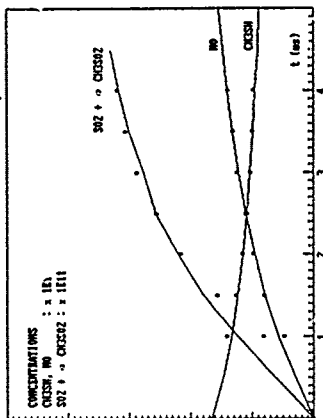
Evidence for the occurrence of fast reactions (2) and (3) was supported by the measurement of a stoichiometry ratio $[\text{NO}]_{\text{prod}} / [\text{CH}_3\text{SH}]_{\text{react}}$ which was around two, in agreement with the results of TYNDALL and RAVISHANKARA¹ and BARNES et al.². k_3 was determined by fitting the NO kinetic curves using a computer simulation of a reacting system including reactions (1-3). k_3 was determined as:

$$k_3 = (3 \pm 2) \times 10^{-11} \text{ cm}^3 \text{ molecule}^{-1} \text{ s}^{-1}$$

using our value for k_1 and for reaction (2), the value reported by TYNDALL and RAVISHANKARA¹: $k_2 = 6.1 \times 10^{-11}$. The value $k_2 = 1.05 \times 10^{-10}$ reported by BALLA et al.³ was also entered in the calculations and led to similar results.

A computer simulation was also carried out to fit the kinetics of the SO_2 peak, taking into account the contribution of CH_3SO_2 and SO_2 to this peak. It was assumed that the SO_2 peak intensity calibrated for SO_2 alone should be taken as $\text{SO}_2^+ = [\text{SO}_2] + \alpha x$

$[\text{CH}_3\text{SO}_2]$ were α is the sensitivity of the mass spectrometer for CH_3SO_2 at the SO_2^+ peak relative to SO_2 . We obtained $k_4 \leq 10 \text{ s}^{-1}$ at 0.3 Torr of Helium. This result is consistent with the activation energy of 18 Kcal / mole for k_4 reported by BENSON⁴ from thermochemical calculations. At higher pressure (760 Torr of N_2 or synthetic air) and higher reaction times (100 to 800 s instead of less than 10 ms in our work), BARNES et al.² found SO_2 yields around 40% of CH_3S reacted. This result may be consistent with our measurements as we can expect that k_4 is pressure dependent. A typical result of a computer fitting of the experimental profiles of reactant CH_3SH and products NO and SO_2 is reported in figure 1 (initial concentrations were: $[\text{CH}_3\text{SH}]_0 = 3.27 \times 10^{-12}$, $[\text{Cl}]_0 = 2.09 \times 10^{-12}$ and $[\text{NO}]_0 = 2.16 \times 10^{-10} \text{ cm}^{-3}$. Solid lines are the calculated curves and the dots the experimental data).



For atmospheric implications, the present results confirm that the reaction $\text{CH}_3\text{S} + \text{NO}_2$ can be an important oxidation route of CH_3S with NO_2 concentrations at ppb levels or even lower. The actual importance of this reaction will depend on the importance of the rate constant value for the reaction $\text{CH}_3\text{S} + \text{O}_2$ for which an upper limit of 3×10^{-18} at 298 K is presently the best estimate⁵. Reaction $\text{CH}_3\text{SO} + \text{NO}_2$ is also of potential atmospheric importance, depending on the rates of the alternate oxidation routes of CH_3SO by O_2 and O_3 .

References

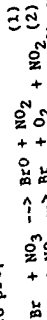
- 1 G.S. TYNDALL, A.R. RAVISHANKARA - 194th ACS meeting - Div. Envir. Chemistry, New Orleans 30 Aug.- 4 Sept. 1987.
- 2 I. BARNES, V. BASTIAN, K. H. BECKER and H. NIKI : Int. J. Chem. Kinet. : in press.
- 3 R.J. BALLA, R.H. NELSON and J.R. Mc DONALD : Chem. Physics, 109, 101, (1986).
- 4 S. W. BENSON : Chem. Rev., 78, 23, (1978).

KINETIC STUDY OF THE REACTIONS OF NO₃ RADICALS WITH Br₂, BrO AND HBr

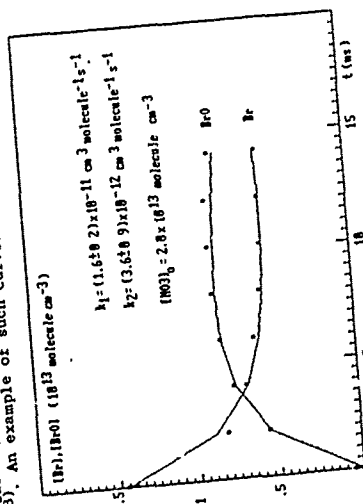
G. POULET*, A. MELLOUKI*, G. LE BRAS*
2. SINGER†, G. MOORTGAT† and J. BURROWS†

*Centre de Recherches sur la Chimie de la Combustion et des Hautes Températures - CNRS 45071 ORLÈANS Cedex 2 - FRANCE.
†Hautes Températures - Institut für Chemie/Hochschule Max Planck D - 6500 MAINZ - FRG

The kinetics of the above reactions have been studied at 298 K using the complementary techniques of discharge flow - EPR and modulated photolysis - absorption spectroscopy, both of which have previously been used to study the reaction of NO₃ to an EPR spectrometer was used to flow the concentration of atoms in excess NO₃ at various reaction times. NO₃ was titrated by the reaction F + HNO₃ → HF + NO₃ and it was titrated by excess NO₃ which was monitored by EPR. NO₃ concentrations ranged from 0.9 to 8.4 × 10¹³ cm⁻³. Br and BrO radicals were directly detected by EPR and the bromine budget could be established ([Br]₀ + [BrO]₀ = [Br]_t). This led to propose the following mechanism for reactions (1) and (2):



The rate constants for reactions (1) and (2) were extracted from the experimental BrO and Br curves by computer simulation, in a similar way to a recent study of the reaction of NO₃ with OH and H₂O³. An example of such curves is given below:



The following values of the rate constants were obtained at 298 K:

$$k_1 = (1.5 \pm 0.5) \times 10^{-11} \text{ cm}^3 \text{ molecule}^{-1} \text{ s}^{-1} \text{ (preliminary value)}$$

$$k_2 = (3.0 \pm 2.0) \times 10^{-12} \text{ cm}^3 \text{ molecule}^{-1} \text{ s}^{-1}$$

During the modulated photolysis experiments, slowly flowing mixtures of HNO₃ and Br₂ in N₂ were photolysed at 254 nm to produce NO₃ via the reactions HNO₃ + hν → OH + NO₂ and HNO₃ + Br₂ → HOBr + Br₂. The absorption of NO₃ at 623 nm was monitored during the flash cycles, and subsequent simulation of data was performed to extract the values of k₁ and k₂.

A typical data set, with simulation, is reproduced below.

COMPARISON OF EXPERIMENTAL (•) AND SIMULATED (—) ABSORPTION OF NO₃ AT 623 nm

Optical Density x10³

Time / sec

MTT CONSTANTS USED
k₁ = 1.58E-11
k₂ = 3.6E-12

lamps on

lamps off

EXP

EXP

EXP

EXP

EXP

EXP

EXP

EXP

EXP

EXP

EXP

EXP

EXP

EXP

EXP

EXP

EXP

EXP

EXP

EXP

EXP

EXP

EXP

EXP

EXP

EXP

EXP

EXP

EXP

EXP

EXP

EXP

EXP

EXP

EXP

EXP

EXP

EXP

EXP

EXP

EXP

EXP

EXP

EXP

EXP

EXP

EXP

EXP

EXP

EXP

EXP

EXP

EXP

EXP

EXP

EXP

EXP

EXP

EXP

EXP

EXP

EXP

EXP

EXP

EXP

EXP

EXP

EXP

EXP

Using the 30 reactions steps of the simulation mechanism, an additional loss of NO₂ was required in order to fit the experimental data. The values of k₁ and k₂ subsequently obtained were in good agreement with the values found in the discharge flow experiments.

The reaction of NO₃ with HBr was also investigated using both methods. A negligible reactivity was observed, leading to the upper limit for the rate constant, at 298 K: k < 1 × 10⁻¹⁰ cm³ molecule⁻¹ s⁻¹.

References

1. A. MELLOUKI, G. LE BRAS and G. POULET.
J. Phys. Chem. 91, 5760 (1987)
2. J.P. BURROWS, G.S. TYNDALL and G.K. MOORTGAT.
J. Phys. Chem. 89, 4848 (1985)
3. A. MELLOUKI, G. LE BRAS and G. POULET.
J. Phys. Chem. 92, 2229 (1988)

KINETICS OF THE COMBINATION REACTIONS OF CHLOROFLUOROMETHYL-
PEROXY RADICALS WITH NO₂ IN THE TEMPERATURE RANGE 233-373 K.

F. CARALP, R. LESCLAUX, M.T. RAYEZ, J.C. RAYEZ,
Université de Bordeaux I, 33405 TALENCE Cedex, France.

and W. FORST,
INPL, 1 Rue Grandville, 54042 NANCY Cedex, France.

The rate parameters for the combination reactions of CCl₃O₂, CCl₂FO₂ and CF₃O₂ radicals with NO₂ were measured in the pressure range 1 to 10 Torr and from 233 to 373 K. Experiments were performed by pulsed laser photolysis and time-resolved mass spectrometry. All reactions are in the fall-off region and are significantly faster than the equivalent reaction of CH₃O₂. They exhibit strong negative temperature coefficients and the rate constants increase in the series from CF₃O₂ to CCl₃O₂.

The experimental equilibrium constant was obtained for the reaction of CCl₂FO₂ at 273 K, by using previously determined rate constants for the reverse reaction (1). This determination allowed us to obtain ΔH_0° of the reaction by calculating the structural and spectroscopic parameters by the semi-empirical MINDO method. Assuming that ΔH_0° value is the same for all reactions of the series it was possible to calculate the temperature dependence of all equilibrium constants and the bond dissociation energies $D^{*298}(\text{CX}_3\text{O}_2\text{-NO}_2) = 105 \pm 5 \text{ kJ.mol}^{-1}$ (X = F or Cl).

A RRKM model was set up for these reactions and calibrated for the reaction of CCl₂FO₂. The model is shown to reproduce quite adequately the fall-off curves and the variations of the association rate constants with temperature, and with the

substitution of chlorine for fluorine in the series of radicals investigated. This model was used to extrapolate the low pressure data to high pressure, where no experimental data were available, and to calculate the kinetic parameters for the CCl₂FO₂ reaction which could not be investigated experimentally in the present study. Kinetic parameters are reported for the association reaction of the entire series of chlorofluoromethyl-peroxy radicals with NO₂.

(1) F. ZABEL, XIth International Conference on Photochemistry, Budapest, Hungary, 1987.

PRODUCT DISTRIBUTION OF THE ELEMENTARY C_2H_4+O
REACTION IN THE $p=0.7-5$ TORR RANGE AT
 $T=300$ AND 600 K

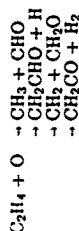
J. Peeters and D. Maes

Department of Chemistry, K.U. Leuven
3030 Leuven, Belgium

The primary product distribution of the C_2H_4+O reaction was measured at $p=0.7-5$ torr at $T=287$ and 607 K using the Discharge Flow technique in combination with Molecular Beam Mass Spectrometry.

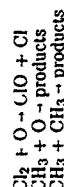
Small amounts of O-atoms, at concentrations of about 10^{-12} mol cm^{-3} , were generated by dissociating O_2 in a microv. av. discharge through a O_2/He gas mixture. Calibration of the MBMS instrument for $[O]$ was based on the $N+NO \rightarrow N_2+O$ titration reaction.

The known O-atom flow was mixed with a large excess of ethylene: $[C_2H_4] \approx 4 \cdot 10^{-9}$ mol cm^{-3} , resulting in a fast conversion of the reactant atoms into primary products:



The product radicals R_1 (CH_3, H, CH_2) were then reacted with Cl_2 , added in large amounts ($\sim 2 \cdot 10^{-9}$ mol cm^{-3}) to the mixture either together with C_2H_4 or a few ms later, thus resulting in a near quantitative conversion into stable R_1Cl molecules (CH_3Cl, HCl, CH_2Cl_2). The absolute concentration of these and of the stable primary product CH_2CO was measured by MIMS, using calibration mixtures.

The branching fractions α to γ of the first three channels are extracted from the ratio $[R_1Cl]/[O]_0$, whereas the ketene yield δ is of course found from $[CH_2CO]/[O]_0$. Small corrections were made for minor competing reactions such as



which remove O, R_1 or both. These corrections usually amounted to only a few percent, on an absolute basis.

At 600 K, the H-yield β could not be determined from the amount of HCl produced with Cl_2 as H-scavenger, because there is significant additional HCl production then by the reaction $Cl + C_2H_4 \rightarrow HCl + C_2H_3$. The H-yield at 600 K was determined instead from the $[HCl]$ formed using NOCl as scavenger: $NOCl + H \rightarrow NO + HCl$; here, there can be no Cl-atom formation and hence no additional HCl production.

The results are listed in the table below

Branching fraction ^a	T = 287 K		T = 607 K		
	0.7 torr	2 torr	5 torr	0.7 torr	2 torr
$\alpha(CH_3)$	0.40	0.46	0.50	0.33	0.44
$\beta(H)$	0.45	0.35	0.30	—	0.38 ^c
$\gamma(CH_2)$	—	(0.1) ^b	—	—	0.15
$\delta(CH_2CO)$	—	0.05	—	—	0.05

^a statistical standard error: ± 0.03

^b indirect value

^c obtained with NOCl as scavenger

Our product distribution results show only a slight pressure dependence, the influence of temperature is also small. Our 287 K data for α and β agree well with those of Hunziker et al. (1) at $40-760$ torr and with those of Koda et al. (2) at $0.03-0.3$ torr; all these results can be represented as $\alpha=0.48 \pm 0.10$ and $\beta=0.38 \pm 0.10$ for the entire 0.03 to 760 torr range.

References

1. H.E. Hunziker, H. Knepe and H.R. Wrendt, J. Photochem. 17, 337 (1981)
2. S. Koda, S. Tsuchiya, Y. Endo, C. Yamada and E. Hirota, 9th Symposium (Internat.) on Gas Kinetics, Bordeaux (1986).

KINETICS AND COMPUTER MODELLING OF REACTIONS OF N(⁴S) WITH HYDROCARBONS

C. S. Blatt, S. G. Roscoe, and J. M. Roscoe
Acadia University, Department of Chemistry,
Wolfville, Nova Scotia, Canada, B0P 1X0

The reactions of N(⁴S) with propane and isobutane have been studied in a fast flow high vacuum system with N(⁴S) produced by a microwave discharge through nitrogen. The well known NO titration method with photometric end point detection was used to measure the concentration of N(⁴S). The reactions of N(⁴S) atoms with aliphatics were found to be very sensitive to the presence of both H atoms and olefin impurities which react rapidly with N(⁴S) atoms to produce radicals. Rigorous purification procedures and analyses were required to ensure the purity of reactants.

The reaction of propane with active nitrogen was found to proceed very slowly, and even with a ten-fold excess of propane to N atoms, the yield of HCN at 300 K and 270 ms was only 1% of the initial N(⁴S) concentration. When H₂ was added in trace amounts to the N₂ gas stream before the discharge, the HCN production increased by a factor of ca. 100 for the same concentrations of N(⁴S).

The reaction of N(⁴S) with isobutane was second order in N(⁴S) and first order in isobutane at short reaction times. At longer reaction times the consumption of N(⁴S) became autocatalytic and the autocatalysis was temperature dependent with a substantial activation energy. A mechanism is proposed in which N atoms recombine on isobutane resulting in decomposition to methyl and propyl radicals:



This mechanism is supported by computer modelling which quantitatively fits the experimentally observed HCN production and N(⁴S) consumption as a function of temperature and time. The rate parameters for this reaction which gave satisfactory agreement with experiment in the temperature range 300 to 550 K fit an Arrhenius function with a preexponential factor of $1.38 \times 10^{16} \text{ L}^2 \text{ mol}^{-2} \text{ s}^{-1}$ and an activation energy of 22 kJ mol⁻¹.

An alternative mechanism involves energy transfer to isobutane by an excited nitrogen molecule, N₂, formed by recombination of N(⁴S). Rate constants are available in the literature for quenching of these excited molecules by organic compounds. However, reasonable estimates of the rate constant for quenching excited nitrogen molecules with isobutane did not give a quantitative fit to the experimental data for the reaction of N(⁴S) with isobutane. These results are also consistent with recent work in the literature on the kinetics of generation of the CN violet system in reactions of N(⁴S) with organic compounds which is also second order in N(⁴S) and first order in the organic compound.

EFFECTS OF PRESSURE IN OH-ALKENE REACTIONS*

Frank P. Tully

Combustion Research Facility
Sandia National Laboratories
Livermore, CA 94550

Hydroxyl-radical reactions with unsaturated hydrocarbons are critically important in combustion and atmospheric chemistry. In previous work on the reactions $\text{OH} + \text{ethene}$,^{1,2} and $\text{OH} + \text{propene}$,³ we showed that the reaction mechanisms change markedly with temperature. At $T \leq 500$ K, electrophilic addition of OH to the alkene double bond dominates the reaction mechanism. Both OH + ethene and OH + propene are pressure-dependent reactions at these temperatures because energized $\text{F}(\text{O})\text{C}_n\text{H}_{2n}$ is stabilized by collisions with buffer gas. Recent results for the reactions of OH with C_2H_4 and C_2D_4 are shown in Figs. 1 and 2. At temperatures between 500 and 650 K, the recombination/dissociation reactions $\text{OH} + \text{C}_n\text{H}_{2n} \rightleftharpoons \text{HO-C}_n\text{H}_{2n}$ approach chemical equilibrium on the millisecond time scale of the laser photolysis/laser-induced fluorescence experiments, and the phenomenological OH disappearance rate decreases by a factor of 3-15 as the temperature is raised. Buffer-gas pressure is found to affect the kinetics of approach to chemical equilibrium. Above 700 K, rate coefficients increase with temperature and are independent of pressure, indicating dominance of hydrogen-abstraction reaction channels at high temperatures. The current status of these studies is discussed.

* This research is supported by the Division of Chemical Sciences, the Office of Basic Energy Sciences, the U. S. Department of Energy.

1 F. P. Tully, *Chem. Phys. Lett.* **96**, 148 (1983).

2 F. P. Tully and J. E. M. Goldsmith, *Chem. Phys. Lett.* **116**, 345 (1985).

3 F. P. Tully, *Chem. Phys. Lett.* **143**, 510 (1988).

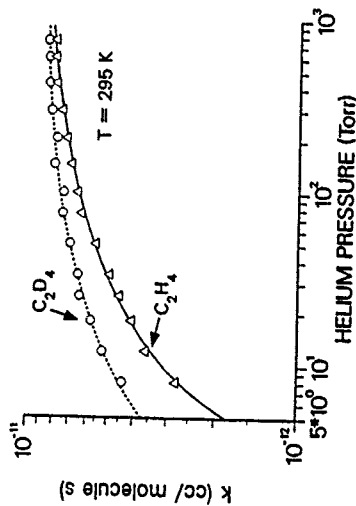


Figure 1. Absolute rate coefficients for the reactions of OH with C_2H_4 and C_2D_4 in helium buffer gas.

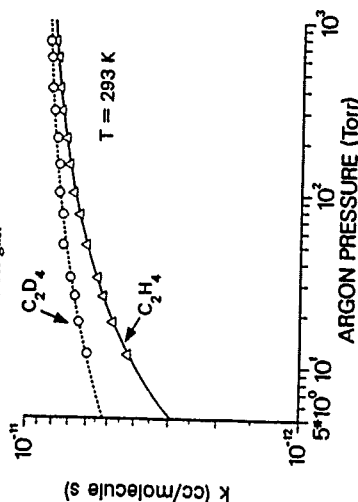


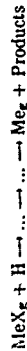
Figure 2. Absolute rate coefficients for the reactions of OH with C_2H_4 and C_2D_4 in argon buffer gas.

A NEW LOW TEMPERATURE SOURCE OF NON-VOLATILE METAL ATOMS

C. Vinckier, J. Corthouts and S. De Jaegere

Department of Chemistry, K.U. Leuven, Celestijnenlaan 200F, 3030 Leuven (Belgium)

In the past studies of the gas phase processes involving non-volatile metal atoms have been carried out in flame systems ^{1,2}. The kinetic interpretation of concentration profiles in flames however is complex due to steep concentration and temperature gradients, and in many cases an unknown flame composition. The introduction of the high temperature controlled fast flow reactor ³ simplified to a large extent the kinetic analysis but required the construction of a rather complex oven system to reach temperatures up to 2000K. Recently we have developed an alternative flow reactor technique ⁴ in which non-volatile metal atoms Me_g can be generated in the gas phase in the temperature range from 300 to 800K. A volatile compound of the solid MeX_g is evaporated and the gas phase compound MeX_g is mixed with the afterglow products of a microwave induced plasma (MIP) of H₂/He or H₂/Ar mixtures. When [H]²>>[MeX_g] a fast gas phase reaction can convert MeX_g to metal atoms Me_g according to the overall scheme



Downstream of this region Me_g is detected by atomic absorption spectroscopy and the nature of the products by mass spectrometric analysis. The capabilities of this technique were tested extensively for the non-volatile metal copper.

Gas phase copper atoms are generated by reactions of hydrogen atoms with the gas phase compounds of CuCl, CuCl₂ and Cu(CH₃COO)₂ heated to temperatures from 418 to 550K and a pressure range from 5 to 12 Torr. In this way [Cu_g] concentrations between 2x10⁹ and 2x10¹¹ at.cm⁻³ could be generated. In view of a thousand fold excess of hydrogen atoms over CuX_g, the latter compounds are rapidly transformed in Cu_g + products. The measured copper absorbance A_{Cu} primarily depends on the temperature T_s of MeX_g and of the residence time of Cu_g downstream of the MIP inlet. On the other hand the MIP characteristics such as composition and microwave power P_w have no influence on A_{Cu} in the downstream region at 300K the A_{Cu} drops due to the loss process of copper atoms on the reactor wall. Apparently under these experimental conditions γ_{Cu} ≈ 1 so that the slope of ln A_{Cu} versus time yields a first order loss constant k_{obs} equal to ⁵

$$k_{\text{obs}} = \frac{7.34 \times D_{\text{Cu},i}}{2 \times \bar{a}^2 \times p} + 0.63k_r \quad \text{Eq. I}$$

where D_{Cu,i} is the binary diffusion coefficient of Cu_g in the carrier gas i at 1 Torr, a the reactor radius, p the total pressure in Torr and k_r the pseudo first order reaction rate constant. The magnitude of k_{obs} has been determined at 300 K at various experimental conditions such as the total pressure, mixture composition and microwave power. The results as a function of the pressure in argon are shown in Table I.

Table I : k_{obs} as a function of the reactor pressure p

p (Torr)	12	12	11	10	10	10	10	9	8	7	5.5
k _{obs} (s ⁻¹)	7.7	6.1	11.7	12.1	10.0	13.8	9.8	10.0	9.0	9.3	14.7

From the graph of k_{obs} versus 1/T, the value of D_{Cu,Ar} at 300 K was calculated to be equal to 212.9±9.2 cm²/Torr s⁻¹. This result yields a diffusion coefficient D_{Cu,Ar} at 10 Torr of 21.3±0.9 cm²s⁻¹ which is within the error limits of our earlier value of 23.6±7.1 cm²s⁻¹ derived on the basis of our 10 Torr data only ⁴.

When now molecular oxygen is added to the system, the rate constant of the 3rd order reaction R.II could be derived :



From the observed first order decay at 10 Torr argon and 300K and after correction for the wall loss by diffusion, the rate constant k_{III} was found to be equal to 3.7±0.7 x 10⁻³ cm³/mole.s⁻¹.

References

1. R. Mavrodineanu and H. Boiteux, *Flame Spectroscopy*, J. Wiley, NY 1965.
2. J.W. Hastie, *High Temperature Vapors - Science and Technology*, Acad. Press, NY, 1975.
3. A. Fontijn and W. Felder, *Reactive Intermediates in the Gas Phase*, Acad. Press, NY, 1979.
4. C. Vinckier, A. Dumoulin, J. Corthouts and S. De Jaegere : paper submitted to the J. of Chem. Soc., Farad. Trans.
5. R.W. Huggins and J.H. Cahn, *J. Appl. Phys.* 38, 180, 1967.

TIME-RESOLVED STUDIES OF THE KINETICS OF THE REACTIONS OF DIMETHYLSILYLENE

J.E. Baggett, M.A. Blitz, H.M. Frey, P.D. Lightfoot* and R. Walsh.

Department of Chemistry, University of Reading, Whiteknights,
P.O. Box 224, Reading RG6 2AD, U.K.

1. Introduction.

Singlet dimethylcarbene cannot be studied in the gas-phase due to its rapid isomerisation to give propene. However, dimethylsilylene, SiMe_2 , can be generated by both thermal and photochemical means and the kinetics of its reactions can be studied by direct time-resolved and end product analysis techniques. Many similarities between the reactions of SiMe_2 and singlet carbenes may be discerned,¹ and so the study of SiMe_2 kinetics provides us with an opportunity to explore facets of the behavior and reactivity of intermediates which possess this characteristic electronic structure which is denied us in hydrocarbon chemistry. In this paper, we will present the results of our latest investigations into the tendency for SiMe_2 to form loose association complexes with 0-atom containing electron donors.

2. Experimental.

High concentrations of SiMe_2 were generated by the 193 nm (ArF exciplex) laser flash photolysis of pentamethyldisilane or octamethyltrisilane. The radical concentrations were monitored in real time using a multipass c.w. laser absorption technique. The monitoring light source was provided by the 457.9 nm single line output of an Ar⁺ laser, which is close to the maximum of the blue SiMe_2 absorption feature identified in matrix-isolation studies.^{2,3} Concentration-time profiles were determined from the transient attenuation of the monitoring light intensity incident on a fast photodiode. Differential amplification and signal averaging methods were used to improve the signal/noise ratios and the resulting profiles were transferred to a mainframe computer for analysis.

3. Results and Discussion.

In the presence of dimethylether the SiMe_2 decay profiles show bi-exponential decay behaviour, as illustrated in Fig. 1. Although the loss of single exponential behaviour automatically renders any discussion of the reaction mechanism speculative, we will present evidence based on a careful study of the kinetics of this system which indicates that a simple mechanism, based on reversible silylene-ether complex formation and reaction between SiMe_2 and its precursor, is sufficient to account for much of the

observed behaviour. Estimates of the rate coefficients for the complex formation and decomposition processes will be presented. Our studies have been extended to a wide variety of 0-containing compounds, including O_2 , H_2O , D_2O , MeOH , MeOD , ethylene oxide, oxetane, dimethyloxetane, and tetrahydrofuran (THF). Experimental evidence for silylene-THF complex formation exists in the literature,⁴ and we will examine the role of complex formation in all of these reactions.

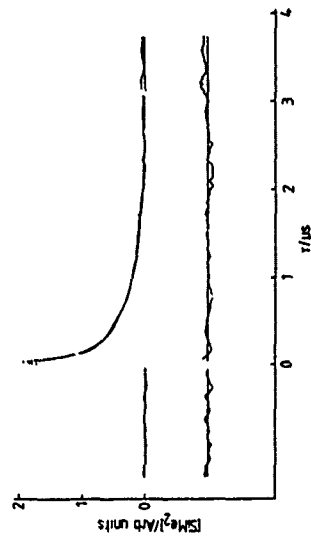


Fig. 1. SiMe_2 concentration-time profile in the presence of 4.04 Torr of dimethylether. The radicals were generated by 193 nm photolysis of 39 mTorr pentamethyldisilane. A total of 15 laser shots were averaged.

4. References and Notes.

- * Present address: Laboratoire de Chimie Physique A, Université de Bordeaux 1, 33405 Talence Cedex, France.
1. T.Y. Gu and W.P. Weber, *J. Organomet. Chem.*, **184**, 7 (1980); **195**, 29 (1980); V.J. Tortorelli, M. Jones, S. Wu and Z. Li, *Organometallics*, **2**, 759 (1983).
2. J.E. Baggett, M.A. Blitz, H.M. Frey, P.D. Lightfoot and R. Walsh, *Chem. Phys. Lett.*, **135**, 39 (1987).
3. G. Raabe, H. Vancik, R. West and J. Michl, *J. Am. Chem. Soc.*, **108**, 671 (1986).
4. G.R. Gillette, G.H. Noren and R. West, *Organometallics*, **6**, 2617 (1987).

248nm LASER PHOTOLYSIS OF GASEOUS FLUORINE / ALKYL IODIDE MIXTURES

D. Raybone, I.M. Watkinson, J.C. Whitehead and E. Winterbottom

Department of Chemistry, University of Manchester, Manchester M13 9PL, U.K.

We have studied the emission (200 - 900 nm) resulting from the 248 nm laser photolysis of a gaseous mixture of an alkyl iodide ($\text{C}_2\text{H}_5\text{I}$, $\text{C}_3\text{H}_7\text{I}$, CF_3I , $\text{C}_2\text{F}_5\text{I}$ or $n\text{-C}_4\text{F}_9\text{I}$) and 5% F_2 in He. The flow cell and detection system have been described previously.¹ The relative contributions of the species to the total cell pressure were approximately 0.02 mbar of F_2 , 0.14 mbar of the iodide and 0.30 mbar of He. The emission produced by the different photolyses was clearly visible by eye and the colour varied between purple and yellow-green depending on the iodide. The resulting spectra were found to result from two major emitters. In the ultraviolet region of the spectrum, from 248 - 480 nm, we observe the dispersed fluorescence of CF_2 ($\tilde{\text{A}}^1\text{B}_1 \rightarrow \tilde{\text{X}}^1\text{A}_1$) and in the visible, from 450 - 900 nm, we see emission from the $\text{B} \rightarrow \text{X}$ system of IF. In addition to the analysis of the spectra, we have studied the time dependence of the IF(B) emission and also the $\text{I}^*(^2\text{P}_{1/2})$ concentration using atomic fluorescence.

CF₂ Production

The CF_2 $\tilde{\text{A}} \rightarrow \tilde{\text{X}}$ emission takes the form of dispersed fluorescence following 248.4 nm excitation by the KrF laser. The emission is dominated by the 26 progression and no emission is seen to the blue of the laser line. The fluorescence is synchronous with the laser pulse indicating that the $\text{CF}_2(\tilde{\text{X}})$ radicals are either formed prior to the laser pulse or are produced and excited by the same laser pulse. In previous experiments^{2,4} CF_2 was produced by KrF laser photolysis of CF_2Br_2 followed by $\text{A} + \text{X}$ excitation by the same laser pulse. We find that there is no CF_2 emission in the absence of F_2 indicating that CF_2 is not produced by direct 248 nm photolysis of the alkyl iodide but by some prior reaction. (The only report of emission following 248 nm photolysis of alkyl iodides alone is of emission from $\text{I}_2(\text{B})$ resulting from recombination of iodine atoms produced by the photolysis.⁵) The total intensities of the CF_2 emission are a strong function of the identity of the iodide and are in the ratio 100:50.4:1:1.5:0.5:0.02 for CH_3I , $\text{C}_2\text{H}_5\text{I}$, CF_3I , $\text{C}_2\text{F}_5\text{I}$, $\text{C}_3\text{H}_7\text{I}$ and $\text{C}_4\text{F}_9\text{I}$. This would suggest that the methyl group plays a key role in the production of the ground state CF_2 that is pumped by the laser. Fluorine atoms (either generated by the slow reaction $\text{F}_2 + \text{RI} \rightarrow \text{RIF} + \text{F}$ or resulting from the small amount of 248 nm photolysis of the F_2) may displace the CH_3 group from the iodide. The CH_3 group is then further reduced to CH_2 and converted to CF_2 by the highly exothermic reactions $\text{F}_2 + \text{CH}_2 \rightarrow \text{HCF} + \text{HF}$



Production of IF(B)

The IF(B) spectra from all the photolyses are essentially identical and show population of v' levels up to 7. The IF(B) vibrational and rotational distributions are Boltzmann in form, characterised by temperatures of 750 ± 50 K and 525 ± 50 K, respectively. The relative integrated intensities of the IF(B) emissions vary over five orders of magnitude and increase in the sequence $\text{C}_2\text{H}_5\text{I} < \text{C}_3\text{H}_7\text{I} < \text{CH}_3\text{I} < \text{CF}_3\text{I} < \text{C}_2\text{F}_5\text{I} < \text{C}_4\text{F}_9\text{I}$. The most interesting feature of the IF(B) emission in these systems is the time over which it extends following the laser pulse. The half-lives for the IF(B) decays range from 5 μs for $\text{C}_2\text{H}_5\text{I}$ to 770 μs for $\text{C}_4\text{F}_9\text{I}$, increasing in the same sequence as the intensities above. This sequence can be correlated with the 248 nm photon yields for the production of I^* from the alkyl iodides. In all cases the decay of I^* has a much longer half-life than for IF(B) indicating that it is always in excess. We suggest that IF(B) is created either by the recombination of I^* and F atoms or by multistep collisional excitation of ground state IF(X) by I^* , where the IF(X) can result either from a dark reaction between molecular fluorine and the alkyl iodide or from the fast reaction $\text{F} + \text{RI} \rightarrow \text{IF} + \text{R}$. Thus, in addition to I^* , the other key reagent in the production of IF(B) is likely to be a F atom. This can be created by the sequence



Reaction (2) is likely to possess activation energy but this will be overcome by the internal and translational energy of the radical produced in the photolysis (1). By analogy with the corresponding rates for reaction (2) with Cl_2 and Br_2 , the rates for reaction (2) are likely to be in the sequence $\text{R} = \text{C}_2\text{H}_5 > \text{C}_3\text{H}_7 > \text{CH}_3 > \text{CF}_3 > \text{C}_2\text{F}_5 > \text{C}_4\text{F}_9$, giving the fastest supply of F atoms and hence the fastest production of IF(B) in that sequence in accord with the IF(B) decay times.

References

- 1 H.S. Braynis, D. Raybone and J.C. Whitehead, *J. Chem. Soc. Faraday Trans. 2*, 1987, **83**, 627.
- 2 C.L. Sam and J.T. Yandley, *Chem. Phys. Lett.*, 1979, **61**, 509.
- 3 F.B. Wampler, J.J. Tsee, W.W. Rice and R.C. Oldenborg, *J. Chem. Phys.*, 1979, **71**, 3926.
- 4 W. Hack and W. Langel, *J. Photochem.*, 1983, **21**, 105.
- 5 R.J. Donovan, *Specialist Periodical Reports Chem. Soc., Gas Kinetics and Energy Transfer*, 1981, **4**, 117.

KINETICS OF THE REACTIONS OF C_2H_5S WITH NO_2 , NO , AND O_2 AT 296 K

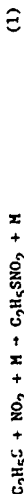
Graham Black, Leonard E. Jusinski,† and Roger Patrick*

†Chemical Physics Dept., SRI International Menlo Park, CA 94025
*LSI Logic, Santa Clara, CA 95050 USA

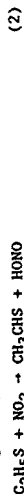
Alkylthio radicals (RS) are important intermediates in the reaction of reduced sulfur compounds (RSH, RSR', RSSR) with OH and NO_3 radicals in the atmosphere. Until recently, the only reported absolute rate coefficient measurements involved the HS^{18} and CH_3S^{10} radicals. Very recently rate coefficients for reactions of i - C_3H_7S were reported.¹¹ This paper reports the first direct measurements of the rate coefficients for the reactions of C_2H_5S with NO_2 , NO , and O_2 at 296 K.

C_2H_5S radicals were generated by 248 nm photodissociation of C_2H_5SH [ethyl mercaptan (EM)] and $(C_2H_5S)_2$ [diethyl disulfide (DEDS)], and monitored by LIF on the A-X transition¹² using the 34 transition at 410.3 nm. Both EM and DEDS were used as sources of C_2H_5S radicals in these studies, and the EM concentration was varied by ~20, to be sure that the results obtained were the same, and presumably, therefore, not affected by the secondary chemistry that can occur in these systems.

When measuring the $C_2H_5S + NO_2$ reaction, it was necessary to work at a high buffer-gas concentration ($Ar \sim 1.3 \times 10^{19}$ molecule/cm³) to quench the NO_2 fluorescence excited by the probing dye laser [it does not quench¹² the $C_2H_5S(A_1)$ emission]. This prevented measurements of the rate coefficients as a function of buffer-gas pressure. A rate coefficient of $(9.2 \pm 0.9) \times 10^{-11}$ cm³ molecule⁻¹ s⁻¹ was found for the removal of C_2H_5S by NO_2 . Previous work on $HS^{2,4,8}$ and $CH_3S^{9,10}$ found no evidence that the reaction with NO_2 proceeds by addition. If this holds true for C_2H_5S , then reaction (1) is not an important channel



The remaining two possibilities are



and the analogue of (2) does occur¹³ with C_2H_5O (producing acetaldehyde) and a similar reaction to (3) has been found for $HS^{2,4-8}$

with NO_2 . Further work is planned to determine the details of the reaction pathway.

The reaction of C_2H_5S with NO , like the reactions of $HS^{2,3}$ and CH_3S^9 with NO , is an addition reaction involving a third body and has been shown to be in the transition region between the low- and high-pressure limits. Using an expression developed by Troe^{14,15} to fit the results, the following values were obtained.

$$F = 0.49 + 0.04$$

$$k_{\infty} = (5.2 \pm 0.5) \times 10^{-11} \text{ cm}^3 \text{ molecule}^{-1} \text{ s}^{-1}$$

$$k_0 (\text{He, Ar}) = (7.5 \pm 3.5) \times 10^{-28} \text{ cm}^6 \text{ molecule}^{-2} \text{ s}^{-1}$$

$$k_0 (\text{SF}_6) = (2.2 \pm 1.2) \times 10^{-27} \text{ cm}^6 \text{ molecule}^{-2} \text{ s}^{-1}$$

No reaction could be found with O_2 , for which an upper limit on the rate coefficient of 2×10^{-17} cm³ molecule⁻¹ s⁻¹ was estimated. This reaction is worthy of further study since a rate coefficient as low as 10^{-18} cm³ molecule⁻¹ s⁻¹ could still suffice to make $C_2H_5S + O_2$ the dominant tropospheric removal reaction for C_2H_5S radicals.

Supported by Grant No. ATM-8411581, Nat'l Science Foundation.

1. J. J. Ties, F. B. Wampler, R. C. Oldenborg, and W. W. Rice, *Chem. Phys. Lett.* **82**, 80, 1981.
2. G. Black, J. Chem. Phys. **80**, 1103 (1984).
3. G. Black, R. Patrick, L. E. Jusinski, and T. G. Slanger, *J. Chem. Phys.* **80**, 4065 (1984).
4. V. P. Bulatov, M. Z. Kozliner, O. M. Sarkisov, *Khim. Fiz.* **3**, 1300 (1984).
5. R. R. Friedl, W. H. Brune, and J. G. Anderson, *J. Phys. Chem.* **89**, 5505 (1985).
6. G. Schönlke, M. M. Rahman, R. N. Schindler, *Ber. Bunsenges. Phys. Chem.* **91**, 66 (1987).
7. R. A. Strachnik and M. J. Molina, *J. Phys. Chem.* **91**, 4603 (1987).
8. N. S. Wang, E. R. Lovejoy, and C. J. Howard, *J. Phys. Chem.* **91**, 5743 (1987).
9. R. J. Balla, H. H. Nelson, and J. R. McDonald, *Chem. Phys.* **109**, 101 (1986).
10. G. Black and L. E. Jusinski, *J. Chem. Soc. Faraday Trans II*, **82**, 2143 (1986).
11. G. Black, L. E. Jusinski, and R. Patrick, *J. Phys. Chem.* **92**, 1134 (1988).
12. G. Black and L. Jusinski, *Chem. Phys. Lett.* **136**, 241 (1987).
13. L. Batt and R. J. Milne, *Int. J. Chem. Kinet.* **9**, 549 (1977).
14. J. Troe, *Ber. Bunsenges. Phys. Chem.* **87**, 161 (1983).
15. R. S. Gilbert, K. Luther, and J. Troe, *Ber. Bunsenges. Phys. Chem.* **87**, 169 (1983).

TRANSFORMIC OXIDATION OF AROMATIC HYDROCARBONS :
RATE CONSTANTS OF THE REACTIONS OF OH WITH BENZENE
AND TOLUENE BY THE DISCHARGE FLOW METHOD.

Thierry Bourassa, Pascal Devolder, Jean-François Pauwels
and Jean-Pierre Sawersyn

Laboratoire de Chimie et Chimie de la Combustion
Unité Associée au CERS n°76
Université des Sciences et Techniques de Lille, Flandres Artois
59655 Villeneuve d'Ascq cedex, France

The rate constants of the reactions of OH with benzene (k_1) and toluene (k_2) have been investigated in the temperature range 297 K to 353 K and in a pressure range of helium from 0.5 torr to ≈ 10 torr. The experimental technique is the discharge flow-resonance fluorescence on OH in halocarbon wax coated tubes. The experimental range of pressures cover the fall-off range for both reactions. For toluene at ~ 297 K, the following Troe parameters have been derived : $k_{\infty} = (4.0 \pm 0.5) 10^{-20} \text{ cm}^3 \text{ molecule}^{-1} \text{ s}^{-1}$; $k_0 = (6.0 \pm 0.7) 10^{-12} \text{ cm}^3 \text{ molecule}^{-1} \text{ s}^{-1}$.

At 353 K, the reverse reaction k_{-2} : adduct \rightarrow OH + toluene is shown to occur thanks to a very fast reaction of this adduct with NO_2 .

KINETICS AND MECHANISM FOR THE REACTION OF HYDROXYL RADICALS WITH NITROGEN CONTAINING COMPOUNDS

Michael Donlon, Denis O'Farrell and Jack Ivin

Department of Chemistry, Dublin Institute of Technology, Ireland

Howard Sidebottom

Department of Chemistry, University College Dublin, Ireland

Ole John Nielsen

Department of Chemistry, Riso National Laboratory, Denmark

The interaction of peroxy organic radicals with NO and NO₂ to form nitrates and peroxynitrates is an important factor in the distribution of NO_x in the troposphere. These species provide temporary reservoirs and are expected to be involved in long range transport of NO_x. The reaction of these organonitrogen compounds with hydroxyl radicals has been suggested as an important factor in their atmospheric residence time; however, to date no mechanistic information concerning the formation and release of NO_x from these reservoirs is available. Further, there appears to be a major inconsistency between the direct measurements and relative rate techniques in the reported rate constants for OH + NO₂-containing organic compounds. It would appear that at the higher pressures pertaining in relative rate studies the measured rate constants are about an order of magnitude higher than those found in the low pressure direct determinations leading to the suggestion that as well as hydrogen atom abstraction OH radical addition also occurs to a significant extent at high pressures.

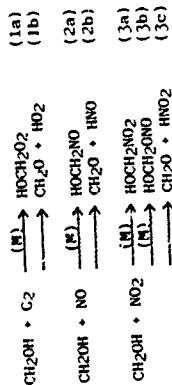
The purpose of this work was to determine relative and absolute rate data for OH radical reactions with nitroalkanes as a model for nitro compounds that may be present in the troposphere. Absolute rate data were obtained at atmospheric pressure using pulse radiolysis combined with kinetic absorption spectroscopy. Relative rate studies were carried out using a smog chamber facility having FTIR and GLC detection systems. This facility was also used to determine rate data for the reaction of chlorine atoms with the nitroalkanes.

The results of the present study indicate that at atmospheric pressure rate data for the reaction of hydroxyl radicals with nitroalkanes from both direct and relative rate experiments are in reasonable agreement. The NO₂ group substantially decreases the rate constants for H atom abstraction from groups bonded to the NO₂ group and decreases those from the groups in the β position. Similar results were found for the reaction of chlorine atoms with some deactivation occurring even at groups in the γ position. Evidence is also provided for an addition reaction of HO radicals with the nitroalkanes.

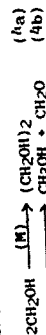
THE REACTION OF CH₂OH WITH O₂, NO AND NO₂C Anastasi^(*), J Munk^(*), P Pagsberg^(*) and V J Simpson^(*)

^(*) Department of Chemistry, Risø National Laboratory, DK-4000 Roskilde, Denmark.
^(*) Department of Chemistry, University of York, Heslington, York YO1 5DD, England.

CH₂OH radicals are important intermediates in combustion chemistry and to a lesser extent atmospheric chemistry. The only kinetic studies involving this species, other than the mutual reaction, have addressed its reaction with oxygen and even here the results differ by almost an order of magnitude.¹⁻⁵ Recently we have observed the ultra-violet absorption spectrum for CH₂OH for the first time using a pulse radiolysis / kinetic absorption technique⁶, making kinetic studies involving this species possible. We have conducted a study of gas phase reactions of CH₂OH with O₂, NO and NO₂ and derived overall rate constants for reactions 1-3 at 298K:



At low concentrations of reactant the fast self-reaction of CH₂OH⁶ also contributes to the overall removal of CH₂OH.



A simple analytical expression that describes the half-life(t) of the experimental CH₂OH decays is used to extract the kinetic information:

$$1/t = 1/t_0 + k[R]/\ln 2$$

where R is O₂, NO or NO₂ and t₀ is the half-life of CH₂OH in the

absence of a reactant. A plot of 1/t versus [R] is a straight line whose gradient is the desired rate constant, k/ln2. Table 1 summarises the rate constants derived in this way and compares our results with previously reported values.

Table 1. Summary of the rate constants for the reactions of CH₂OH with O₂, NO and NO₂. (a)

O ₂	(b)	ref	NO	NO ₂
2.0 x 10 ⁻¹²	LMR	1		
1.4 x 10 ⁻¹²	PFE	2		
9.5 x 10 ⁻¹²	MS	3		
10.5 x 10 ⁻¹²	LMR	4		
8.6 x 10 ⁻¹²	MS	5		
8.8 x 10 ⁻¹²	this (c) work	(c)	2.5 x 10 ⁻¹¹ this (c) work	2.3 x 10 ⁻¹¹ this (c) work

(a) units of cm³ molecule⁻¹ s⁻¹; (b) LMR - laser magnetic resonance, PFE - photofragment emission, MS - mass spectrometry; (c) errors of ± 8%.

A study of the kinetic decay traces at different wavelengths and in particular the residual absorption observed at long times has yielded valuable information on the nature of the products in these reactions. Reaction (1b) dominates the oxygen system, but there is also evidence to suggest the formation of the adduct HOCH₂O₂ via reaction (1a). In contrast to the oxygen reaction, adduct formation is a major pathway in the reaction of CH₂OH with NO and NO₂. Studies are currently underway to quantify the various pathways involved in these systems.

1. H E Radford, Chem Phys Letts, 71, 195 (1980)
2. W C Wang, M Suto, L C Lee, J Phys Chem, 81, 3122 (1984)
3. H H Grotheer, G Reikert, U Meier, T Just, Ber Bunsenges Phys Chem, 89, 187 (1985)
4. S Dobe, F Temps, T Bohland, H Gg Wagner, Z Naturforsch, 40, 1289 (1985)
5. M A Payne, J Brunning, M B Mitchell, L J Slief, Int J Chem Kinet, 20, 63 (1988)
6. C Anastasi, J Munk, P Pagsberg, A Sillesen, Chem Phys Letts, 146, 371 (1988)
7. E Bjarnov, J Munk, O J Nielsen, P Pagsberg, A Sillesen, Riso-M-2366, Risø National Laboratory, Denmark, April 1983

NO_x CHEMISTRY OF ELECTRICAL DISCHARGES

C. Anastasi, J. T. H. Harrison and M. S. Stark

Department of Chemistry, University of York, York, YO1 5DD, UK

All combustion processes lead to significant inputs of nitrogen oxides (NO and NO₂) into the atmosphere, pollutants which are very important contributors to the "Acid Rain" problem and photochemical air pollution. However to assess the full impact of anthropogenic emissions of these pollutants, an understanding of the natural sources of NO_x (NO plus NO₂) is also needed. One important source of nitrogen oxides is lightning¹. There are many factors that must be considered in estimating the atmospheric loading of NO_x by this phenomenon² and there is considerable uncertainty in the theoretical models^{3,4,5,6} used for this purpose; also the results of laboratory studies^{7,8,9} which are scaled for atmospheric applications, have not been extensive enough.

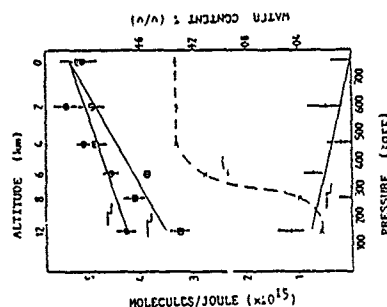
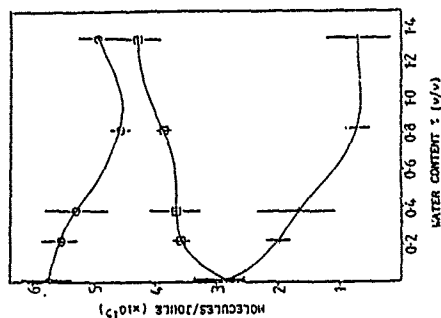
Concentrations of NO and NO₂ produced by an electric discharge in a simple reactor, have been measured using a chemiluminescent detector. To minimise laboratory effects, the electrode ends were small (1mm) and made of tungsten while the reactor size was large enough to ensure wall effects did not play a role. We have investigated the effect of spark gap, total pressure and the addition of minor species such as water, nitrous oxide, carbon dioxide and methane on the NO and NO₂ concentrations. Figure 1 shows that NO and NO₂ production falls as the pressure is decreased from 760 torr to 146 torr, equivalent to increasing altitude (a water content similar to that present in the atmosphere was added to the gas mixture). The effect of water content on NO_x production at constant pressure (350 torr) is shown in figure 2. These results suggest that both these variables should be included in calculating atmospheric loading of NO_x and allowance should be made for the sizeable NO₂ concentration that is formed, particularly at lower pressure.

The addition of atmospheric values of N₂O, CH₄ and CO₂ had no measurable effect on NO_x production by the discharge (accuracy 5%). However, the effect of larger additions is useful in testing the robustness and uniqueness of chemical models that describe the lightning phenomenon.

The spark gap was also varied in these experiments from 4 to 20mm, causing a factor of 3 increase in NO_x molecules produced per joule¹⁰. This is unusual because this quantity has been assumed constant when laboratory measurements have been scaled up to atmospheric dimensions. This variation may be a real effect or an

artefact of our experimental apparatus and others like it; for example it may be that different quantities of energy are discharged into the gap as it is changed.

1. A. F. Tuck, Quart. J. R. Met. Soc., 102, 749-755 (1976)
2. G. A. Dawson, J. Atmos. Sci., 37, 174-178 (1980)
3. R. D. Hill and R. G. Rinker, J. Geophys. Res., 86, 3203-3209 (1981)
4. W. L. Chameides, D. H. Stedman, R. R. Dickerson, D. W. Rusc and R. J. Ciccerone, J. Atmos. Sci., 34, 143-149 (1977)
5. J. S. Levine, R. S. Rogowski, G. L. Gregory, W. E. Howell and J. Fishman, J. Geophys. Res. Letts., 8, 357-360 (1981)
6. R. Peyroux and R. M. Lapeyre, Atmos. Environ., 16, 959-968 (1982)

KEY: NO_x (○), NO₂ (□), NO₂ (+), H₂O (x)FIGURE 1:
THE VARIATION OF NO_x AND NO₂ WITH PRESSUREFIGURE 2:
THE VARIATION OF NO_x AND NO₂ WITH WATER CONTENT

RATE OF THE REACTION OF THE HYDROXYMETHYL
RADICAL WITH NITRIC OXIDE FROM 230 - 373 K

Louis J. Stief, Fred L. Nesbitt and Walter A. Payne

Astrochemistry Branch, Code 691
NASA/Goddard Space Flight Center, Greenbelt, MD 20771 USA

Reactions of the hydroxymethyl radical (CH_2OH) are of interest in atmospheric chemistry and combustion chemistry. The most important reaction of CH_2OH in either case is that with O_2 . We have recently reported¹ the rate constant for the reaction $\text{CH}_2\text{OH} + \text{O}_2 \rightarrow \text{HO}_2 + \text{H}_2\text{CO}$ from 215 to 300 K. Reaction of this radical with NO would also be of atmospheric interest, and we have now completed a study of this reaction over the temperature range 230 - 373 K using the discharge flow-mass spectrometry technique. Observation of HNO and H_2CO as reaction products is consistent with the process $\text{CH}_2\text{OH} + \text{NO} \rightarrow \text{HNO} + \text{H}_2\text{CO}$. It was necessary to use CD_2OH ($m/e = 33$) in the rate constant measurements to avoid contribution of HNO to the hydroxymethyl signal. The rate constants were determined from the decay of CD_2OH in the presence of excess NO. At 298 K, $k = 2.2 \times 10^{-12} \text{ cm}^3 \text{ s}^{-1}$, independent of pressure from 0.5 to 1.5 Torr (Table I). This is about $1/4$ the rate constant for the O_2 reaction. Experiments over the temperature range 230 - 373 K (Table II) yield the Arrhenius expression $k = 7.6 \times 10^{-12} \exp(-815/\text{RT}) \text{ cm}^3 \text{ s}^{-1}$. Experiments at 423 K yielded non-exponential decays of CD_2OH , whereas linear decays were observed at all other temperatures. The reaction mechanism probably involves formation of an adduct followed by rearrangement and decomposition to products.

1. F. L. Nesbitt, W. A. Payne and L. J. Stief, J. Phys. Chem. (in press), 1988.

Table I. Rate Constant for the Reaction
 $\text{CH}_2\text{OH} + \text{NO} \rightarrow \text{HNO} + \text{H}_2\text{CO}$ at 298 K from 0.5 to 1.5 Torr Pressure

Pressure/Torr	No. of Expts.	$k/\text{cm}^3 \text{ s}^{-1}$ ($\pm 2\sigma$)
0.5	6	$(2.1 \pm 1.4) \times 10^{-12}$
1.0	11	$(2.2 \pm 0.4) \times 10^{-12}$
1.5	3	$(2.0 \pm 0.6) \times 10^{-12}$

Table II. Temperature Dependence of the Rate Constant
for the Reaction $\text{CH}_2\text{OH} + \text{NO} \rightarrow \text{HNO} + \text{H}_2\text{CO}$

T/K	No. of Expts.	$k/\text{cm}^3 \text{ s}^{-1}$ ($\pm 2\sigma$)
230	9	$(1.3 \pm 0.2) \times 10^{-12}$
260	6	$(1.5 \pm 0.2) \times 10^{-12}$
298	20	$(2.2 \pm 0.4) \times 10^{-12}$
373	7	$(2.4 \pm 0.7) \times 10^{-12}$

PRE-EXPONENTIAL TEMPERATURE DEPENDENCES OF BIMOLECULAR REACTION
RATE COEFFICIENTS PREDICTED BY TRANSITION STATE THEORY

N. Cohen
The Aerospace Corporation
El Segundo, California, USA

The thermochemical kinetics formulation of conventional transition state theory for bimolecular reactions allows for a separate contribution from each degree of freedom (translation, rotation, vibration, etc.) in the activated complex to the ΔS^\ddagger and ΔH^\ddagger capacity of activation, and thus to the pre-exponential terms in the Arrhenius rate expression, $k = A \exp(-E_a/RT)$. The number of vibrations and (possibly hindered) internal rotations varies depending on the nature of the reaction: atom + diatom, diatom + linear polyatom, etc. The temperature exponent n can be evaluated explicitly for each type of reaction if the harmonic oscillator-rigid free rotor approximation is valid for the reagents and activated complex and if the contribution from tunneling is small.

The fundamental equation of transition-state theory is

$$k(T) = \frac{(RT)^2}{101.725 N_A h} \exp(\Delta S^\ddagger/R) \exp(-[\Delta H_0^\ddagger/RT]) \exp(-C/RT) \quad (1)$$

where: $C = \Delta H_0^\ddagger - RT \ln \kappa$ and κ is the transmission coefficient. N_A and h are Avogadro's and Planck's constants, with the relation $hT = 2RT$, Eq. (1) becomes, in liter, mole, second units,

$$k(T) = 10^{9.2} \exp(\Delta S_{298}^\ddagger/R) T^2 \exp(I_1 + I_2) \exp(-E_{298}/RT) \exp(596/T) \quad (2)$$

where:

$$I_1 = \frac{1}{R} \int_0^T \Delta C_p^\ddagger \, d \ln T = \frac{\Delta S^\ddagger(T) - \Delta S^\ddagger(298)}{R} \quad (3)$$

$$I_2 = -\frac{1}{RT} \int_0^T \Delta C_p^\ddagger \, dT = \frac{\Delta H^\ddagger(T) - \Delta H^\ddagger(298)}{RT} \quad (4)$$

In terms of an experimental rate coefficient at 298 K,

$$k(T) = \{10^{9.2} \Delta S_{298}^\ddagger/R\} (T-298)/T [k(298)/(298)^2]^{298/T} T^2 \exp(I_1 + I_2)$$

According to Eqs. (2) - (4), the pre-exponential temperature dependence of $k(T)$ results from $T^2 \exp(I_1 + I_2)$. The contributions to the integrals can be broken down according to the individual terms of Eq. (5):

$$C_p^\ddagger = C_{p\text{trans}} + C_{p\text{vib}} + C_{p\text{rot}} + C_{p\text{int rot}} + C_{p\text{el}} \quad (5)$$

For a rigid rotor harmonic oscillator $C_{p\text{trans}} + C_{p\text{rot}} = (1/2)nR$ where n is an integer between 6 and 8. Retaining only the temperature-dependent terms of Eq. (2), we obtain

$$k(T) = T^2 \exp(I_1 + I_2) \quad (6)$$

$$= T^{(2+n')} \exp(I_1' + I_2') \quad (7)$$

where the integrals I_1' and I_2' now include only the contributions from vibrations and internal rotations.

For a harmonic oscillator,

$$C_{p\text{vib}}/R = u^2 e^{-u}/(1 - e^{-u})^2 \quad (8)$$

where $u = 1.44 e_v/T$ for vibrational energy e_v in cm^{-1} . For $e_v/T \ll 1$,

$$\exp(I_1' + I_2')_{\text{vib}} = (T/298) \exp[(298-T)/T] \quad (9)$$

$$= 10^{-2.91} T^{1.1} \exp(-298/T) \quad (10)$$

For $e_v/T \gg 1$, $\exp(I_1' + I_2')_{\text{vib}} = 1$. For cases between the two extremes of very large or very small e_v/T , we can perform a numerical integration and then express the results in a three-parameter expression.

Each free internal rotation contributes $R/2$ to C_p . The contribution to $k(T)$ is, accordingly,

$$k_{\text{int rot}}(T) = (T/298)^{0.5} \exp[(298-T)/2T] \quad (11)$$

$$= 10^{-1.46} T^{0.5} \exp(149/T) \quad (12)$$

If the internal rotation is hindered, its effect on the temperature dependence of $k(T)$ is more complicated. For the limiting case of a high barrier, the hindered rotation can be approximated by a vibration with frequency (in cm^{-1})

$$v = 360 (T/298) (1/Q_r) (V/RT)^{1/2} \quad (13)$$

$$= 58 s^{-1/2} (V/298R)^{1/2} \quad (14)$$

where s is the symmetry of the rotation, I , the moment of inertia, is in atomic mass units, and V and R are both in cal/mol . The contribution to $k(T)$ for a hindered rotor for various values of Q_r , the partition function, and V , the barrier to rotation, can be approximated by a three-parameter expression, which is never off by more than 50% and is usually considerably more accurate.

THE REACTION OF O(3P) WITH NO₂

C.E. Cargoes-Mas, P. J. Carpenter, S. J. Smith and R. P. Wayne.

Physical Chemistry Laboratory, University of Oxford, South Parks Road, Oxford, OX1 3QZ.

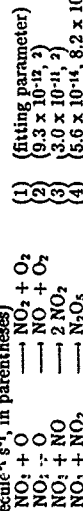
A discharge flow system was used for the first direct determination of the rate constant of the reaction of O atoms with the nitrate radical

$$\text{NO}_3 + \text{O} \longrightarrow \text{NO}_2 + \text{O}_2 \quad (1)$$

The details of the apparatus have been given elsewhere¹. Oxygen atoms were injected into a coated (Halocarbon wax) flow tube. The NO₂ was produced by the reaction of anhydrous nitric acid with P atoms inside a sliding injector. Typical flow velocities were around 14 m s⁻¹, giving contact times of up to 0.03 s. The concentration of O atoms was monitored by resonance fluorescence in the transitions O 3S₁ ← 3P_{2,1,0} corresponding to λ = 130.2, 130.5 and 130.6 nm. The collimated resonance emission was monitored using a solar blind photomultiplier. The reaction of O with NO₂ was employed to calibrate the resonance fluorescence system. Values for [O] were obtained from kinetic modelling and are shown in the table, column c. A dual-beam spectrometer fitted with a multipath (156 cm) White-type absorption cell was used to monitor the [NO₂] at λ = 662 nm. Absolute sensitivities for [O] and [NO₂] were around 10¹¹ molecule cm⁻³ at a signal to noise ratio of 1:1. Wall losses of either O or NO₂ were found to be negligible. The treatment of the experimental data was performed in two ways:

(i) As the plots of $\ln[\text{O}]$ vs. time are good straight lines, first order rate constants, $k' = k_1[\text{NO}_2]_0$, were calculated from their slopes (see table, column d). The plot of k' vs. [NO₂] is a straight line through the origin. The slope yields a value for $k_1 = 1.65 \times 10^{-11}$ cm³ molecule⁻¹ s⁻¹.

(ii) The excess of NO₂ over O is not large enough to ensure first order kinetics. Therefore, it is necessary to check the results of method (i) by numerical modelling of a more detailed mechanism: (rate constants in cm³ molecule⁻¹ s⁻¹, in parentheses)



The fit of the model curves to the experimental data is very good, and derived values of k_1 are listed in the table, column e. The mean value is 1.7×10^{-11} . We estimate the random and systematic errors to be approximately 30%. Hence,

$k_1 = (1.7 \pm 0.5) \times 10^{-11}$ cm³ molecule⁻¹ s⁻¹. This value is larger than that of $(1.0 \pm 0.4) \times 10^{-11}$ proposed by Graham and Johnston² from a study of the photolysis and kinetics of the N₂O₅-O₃-NO₂ system. The apparent first order kinetic behaviour is a consequence of the participation of reaction (2), which has a rate constant similar to that of (1), and is the most important secondary step. As such, there is a constant concentration of co-reactant (NO₂ + NO₂) with which the O atoms react.

Table: Experimental conditions and rate constants

P	a	b	[NO ₂] ₀	c	[O] ₀	k'	d	k ₁	e
2.1	5.71	1.7	60.9	1.8	60.9	1.8			
	3.78	0.81	62.5	1.8	62.5	1.8			
	4.18	0.45	70.0	1.9	70.0	1.9			
	2.34	0.39	33.3	1.5	33.3	1.5			
3.7	3.56	0.85	63.2	1.9	63.2	1.9			
	4.07	0.98	53.3	1.4	53.3	1.4			
	5.43	1.47	87.1	1.6	87.1	1.6			
	5.08	0.69	73.8	1.5	73.8	1.5			
	4.76	0.93	87.9	1.8	87.9	1.8			
	2.08	0.80	36.8	2.0	36.8	2.0			
	3.44	0.77	57.1	1.7	57.1	1.7			

Units: a, torr; b, c, 10¹² molecule cm⁻³; d, s⁻¹; e, 10⁻¹¹ cm³ molecule⁻¹ s⁻¹.

1. R.B. Boodaghians, C.E. Canosa-Mas, P.J. Carpenter and R.P. Wayne, *J. Chem. Soc., Faraday Trans. 2*, **84** (1988), in the press.
2. NASA Panel for data evaluation, "Chemical Kinetics and Photochemical data for use in Stratospheric Modeling. Evaluation No. 7", JPL Publication 85-37 (1985).
3. C.A. Smith, A.R. Ravishankara and P.H. Wine, *J. Phys. Chem.*, **89**, 1423 (1985).
4. R.A. Graham and H.S. Johnston, *J. Chem. Phys.*, **82**, 254 (1978).

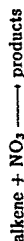
TEMPERATURE STUDY OF THE REACTIONS OF NO₂ WITH ALKANES AND ALKENES

C.E. Canosa-Mas, S.J. Smith, S.J. Waygood and R.P. Wayne.

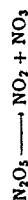
Physical Chemistry Laboratory, University of Oxford, South Parks Road, Oxford, OX1 3QZ.

A discharge flow system was used to study the reactions of the nitrate radical with *n*-butane, isobutane and propene over the temperature range 298–523 K.

The nitrate radical was formed by the reaction $F + HNO_3 \longrightarrow HF + NO_3$. The concentration of NO₃ was measured by absorption at $\lambda = 662\text{ nm}$ in a four pass White cell, the system being calibrated by titration with NO. Except at the highest temperatures for propene, the reactions were studied under pseudo-first order conditions. The experimental results were then analysed using computer integration methods which allowed reaction schemes with secondary reactions to be considered. In the case of the alkanes, the reaction sequence were of the type



R was assumed to be *s*-C₄H₉ for *n*-butane and *i*-C₄H₉ for isobutane. In the case of propene, we have no evidence for a fast reaction of an organic radical with NO₃, and the scheme used was



Using literature values for rate constants and their temperature dependences for the secondary reactions where possible, rate constants were obtained for the primary process over a range of temperatures. When these data were plotted in Arrhenius form ($\ln k$ vs. $1/T$), curvature was seen in all three cases. The data were fitted to the three parameter expression $k = A' \exp(-E'/RT)$ using a non-linear least squares method. The parameters A' , E' and n have no physical significance and so using the equations

$$A = A' (eT)^n \\ E = E' + nRT$$

the parameters A and E were calculated at the mean experimental temperature of 400 K.

Table: Calculated fitting parameters for the experimental temperature range Arrhenius parameters at 400 K

	<i>n</i> -butane	isobutane	propene
k_{298} (a)	(8.25 ± 0.63)	(20.6 ± 2.6)	(1040 ± 120)
T range (K)	298 – 523	298 – 523	298 – 523
$\ln A'$	-105.7 ± 11.5	-116.9 ± 9.15	-112.4 ± 14.6
E' (b)	-9.43 ± 5.34	-15.19 ± 6.59	-28.34 ± 4.17
n	11.4 ± 1.65	12.31 ± 2.10	12.87 ± 1.31
A_{400} (c)	4.80	3.60	9.55
E_{400} (b)	28.47	25.75	14.45

Units: (a) 10⁻¹⁷ cm³molecule⁻¹s⁻¹ (b) kJ mol⁻¹ (c) 10⁻¹² cm³molecule⁻¹s⁻¹

1. C.E. Canosa-Mas, M. Powles, P.J. Houghton and R.P. Wayne, J. Chem. Soc., Faraday Trans. 2, 83, 1465–1474 (1987)

SOME RECENT GAS KINETIC STUDIES INVOLVING SILYLENES

by Michael P. Clarke, Iain M. T. Davidson, Michael Dillon and Graham Eaton

Department of Chemistry, The University, Leicester, LE1 7RH

The kinetics, mechanism and energetics of reactions involving silylenes are of topical interest.¹⁻⁴ We describe some recent gas kinetic studies in a stirred-flow apparatus⁵ with analysis by gc or gc/mass spectrometry.

The mechanism of formation of cyclic adducts of silylenes to 1,3-dienes is believed to proceed by 1,2-addition followed by rearrangement.² We obtained new information on the mechanism by studying the addition to buta-1,3-diene of the range of silylenes, :SiMe₂R (R = Me, Cl, H, D), generated from hydrosilanes. Information on the reverse of dimethylsilene addition to butadiene was obtained from product analysis and kinetic measurements on the pyrolysis of 1,1-dimethyl-1-silacyclo-pent-3-ene, leading to a quantitative overall mechanistic scheme. We also studied the relative rates of silylene addition to a 1,3-diene and insertion into the silicon-hydrogen bond in the disilane precursor. Preliminary kinetic results were obtained for the formation of :SiMe₂ in the pyrolysis of the trisilane Me₂SiH₂.

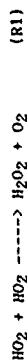
1. R. Wulsh, *Organometallics*, 1988, **7**, 75.
2. D. Lal and P. P. Gaspar, *J. Chem. Soc., Chem. Commun.*, 1985, 1149.
3. M. P. Clarke and I. M. T. Davidson, *J. Chem. Soc., Chem. Commun.*, 1986, 241.
4. I. M. T. Davidson, K. J. Hughes and S. Ijadi-Maghsoodi, *Organometallics*, 1987, **6**, 639.
5. A. C. Baldwin, I. M. T. Davidson and A. V. Howard, *J. Chem. Soc., Faraday Trans. 1*, 1975, **71**, 972.

THE HO₂ + HO₂ REACTION AT ELEVATED TEMPERATURES

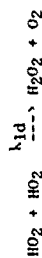
R. Lesclaux, P.D. Lightfoot and B. Veyret

UA 348 CNRS, Université de Bordeaux I
33405 TALENCE Cedex France.

Although reaction (R1) has been much studied under conditions pertaining to atmospheric hydrocarbon oxidation¹, very little is known of its behaviour at combustion temperatures.



The reaction is thought to proceed via an association complex: k₁ displays a negative temperature dependence up to 510K and a linear dependence on pressure. Only the single value of Iro_2 at around 1100K exists above 510K and is about a factor of five greater than the value obtained by extrapolation of the low temperature data. In a recent paper, Walker et al.³ suggested that an additional, direct bimolecular pathway with a positive activation energy becomes accessible at high temperatures:



The reaction was studied by time-resolved u.v. absorption, following the flash lamp photolysis of Cl₂O₂/H₂/CH₃OH and O₂/Cl₂OH mixtures at atmospheric pressure. Experiments were performed between 298 and 777K. A relative spectrum for HO₂ was obtained between 200 and 250 nm at each temperature. The shape of the spectrum was, within experimental error, independent of temperature between 200 and 227.5 nm. The values of $\sigma(\text{HO}_2)$ were normalised to 3.0x10⁻¹⁸ cm² at 227.5 nm, in line with the NASA recommendation¹. The rate constants obtained in this study are shown in Arrhenius form in Figure 1. At temperatures below 500K, our results lie close to those obtained by previous workers. At higher temperatures, an upward curvature in the Arrhenius plot is apparent.

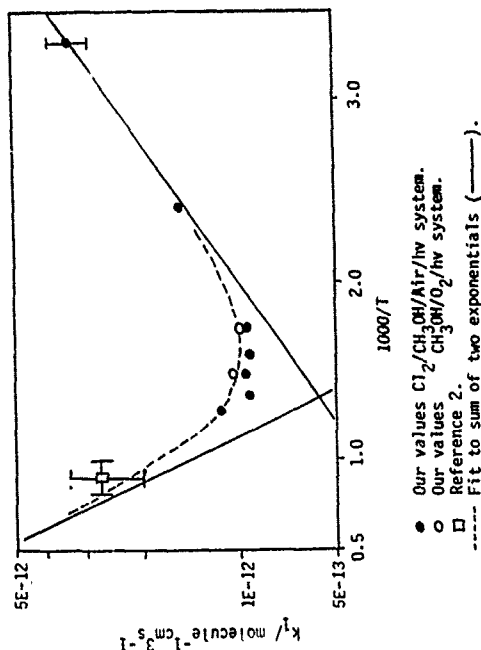
The present results lend strong support to the suggestion of a further reaction channel with a positive activation energy. Our own data, with and without that of Troe, were fitted to the sum of two exponentials, with the low temperature negative activation energy derived from the substantial body of published low temperature work. Best fit values are: $A_{1d}/\text{cm}^3 \text{ molecule}^{-1} \text{ s}^{-1} = (2.2 \pm 1.8) \times 10^{-11}$ and $E_{1d}/\text{kJ mol}^{-1} = 23 \pm 5$.

Further experiments are in progress to determine the effect of temperature on the HO₂ absorption cross section. It is hoped to better define A_{1d} by the use of semi-empirical quantum methods.

References

1. W.B. DeMore, M.J. Molina, S.P. Sander, D.M. Golden, R.F. Hampson, M.J. Hurrylo, C.J. Howard and A.R. Ravishankara "Chemical Kinetics and Photochemical Data for Use in Stratospheric Modelling. Evaluation Number 8." NASA JPL Publication 87-41, (1987).
2. J. Troe Ber. Bunsen. Phys. Chem. 73, 946, (1969).
3. R.R. Baldwin, C.E. Dean, M.R. Honeyman and R.W. Walker J. Chem. Soc. Farad. Trans. 1 82, 89, (1986).

Figure 1



KINETICS OF THE REACTION OF CH_3S WITH O_3 .

Geoffrey S. Tyndall and A.R. Ravishankara

Aeronomy Lab, National Oceanic and Atmospheric Administration,
Boulder, Colorado 80303 and Cooperative Institute for Research in
Environmental Sciences (CIRES), University of Colorado, Boulder,
Colorado

Biogenic activity leads to the release of large amounts of reduced sulfur compounds (CH_3SCH_3 , CH_3SH , CH_3SSCH_3) into the atmosphere. These emissions are most important in the remote marine troposphere. An understanding of the subsequent oxidation pathways is important to describe both the pure gas-phase chemistry and heterogeneous process such as cloud nucleation.

It is currently believed that the tropospheric oxidation of these naturally-produced sulfides proceeds via the methyl thiol radical, CH_3S . Balla et al. were the first to study CH_3S kinetics directly, and measured rate coefficients for the reactions of CH_3S with NO , NO_2 and O_2 .¹

We are studying the reactions of CH_3S radicals with an emphasis on understanding the elementary mechanistic steps. We have recently completed a study of the reactions of CH_3S with O_2 and NO_2 , including an investigation of the reaction products.² Although the reaction with NO_2 is more than 10^7 times faster than with O_2 , the very low background NO_2 concentrations mean that this reaction may

not be important. We report here an investigation of the reaction of CH_3S with O_3 , another potential tropospheric oxidant. This reaction has been studied by Black and Jusinski who set an upper limit of $8 \times 10^{-14} \text{ cm}^3 \text{ molecule}^{-1} \text{ s}^{-1}$ on the rate coefficient.³ If the rate coefficient is larger than $10^{-12} \text{ cm}^3 \text{ molecule}^{-1} \text{ s}^{-1}$, the reaction will be an important loss mechanism for CH_3S in the atmosphere.

CH_3S radicals were detected by pulsed laser induced fluorescence and produced either by pulsed laser photolysis or by discharge flow. These complementary methods allow a wide variation of the experimental conditions, which reduces potential systematic errors in the measurements. In the photolysis experiments, O-atoms were produced in the 248 nm photolysis of O_3 , and these reacted with CH_3SSCH_3 to give CH_3S and CH_3SO . The reaction $\text{CH}_3\text{S} + \text{O}_3$ appears to be faster than the experiments of Black and Jusinski would suggest, and the reaction may be important in the atmosphere. Experiments are currently in progress using discharge-flow production of CH_3S .

References

1. R.J. Balla, H.M. Nelson and J.R. McDonald, *Chem. Phys.* 102 (1986) 101.
2. G.S. Tyndall and A.R. Ravishankara, submitted to *J. Phys. Chem.*
3. G. Black and L.E. Jusinski, *J. Chem. Soc. Fara. 2* 26 (1986) 2143.

Theoretical Study of the Recombination Reaction $\text{CH}_3 + \text{CH}_3 + \text{C}_2\text{H}_6$

Albert F. Wagner

Chemistry Division, Argonne National Laboratory, Argonne IL 60439 USA

David M. Wardlaw†

Department of Chemistry, Queen's University, Kingston, Ont K7L 3N6 CANADA

Abstract

A microcanonical variational RRKM rate constant calculation, based on the flexible transition state theory of Wardlaw and Marcus and an adjustable empirical potential energy surface, is compared to recent measurements of the methyl radical self-recombination rate constant in Ar buffer gas. The calculations contain two adjustable parameters: a potential parameter α , which influences the tightness of the transition state and $\langle \Delta E \rangle_{\text{tot}}$, the total average energy change in metastable C_2H_6^* per collision with the buffer gas. When the parameters are optimized, the resulting calculated rate constants have a 9.9% rms error with respect to the measurements in Ar buffer gas. The rate calculations have been extended to 2000K and then fit over the full temperature and pressure range to a relatively simple functional form suitable for modeling studies; this function is expected to reproduce measured rates within about 10-20% below 1000K and within about 40-50% by 2000K.

† author making the presentation.

KINETICS OF THE REACTION OF CF_2ClO_2 WITH NO_2

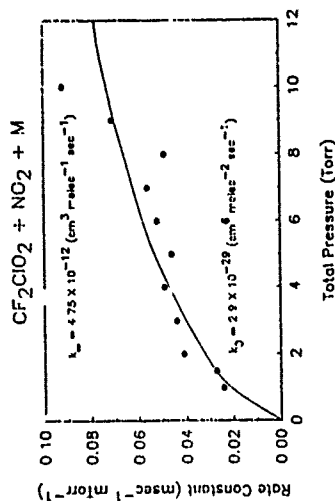
Steven B. Moore and Robert W. Carr

Department of Chemical Engineering and Materials Science
University of Minnesota
Minneapolis, MN 55455

The kinetics of the reaction of CF_2ClO_2 with NO_2 have been studied by broadband flash photolysis with time-resolved mass spectrometry at 298K and pressures between 1 and 10 torr. Mixtures of CF_2ClBr , O_2 and NO_2 slowly flowing in a square tubular reactor were photolysed through suprasil by an Xe-filled flashlamp operated at 10 Hz. CF_2Cl radicals, produced by photolysis of CF_2ClBr , reacted rapidly with O_2 to form CF_2ClO_2 radicals. The radicals effused into the ion source of an Extrel quadrupole mass spectrometer, through a pinhole located midway along a reactor wall and were monitored at $m/e = 82$, corresponding to the CF_2O_2^+ ion fragment resulting from electron bombardment of CF_2ClO_2 . Data was gathered by pulse counting techniques via a Daly detector and multichannel scaling. CF_2ClO_2 decayed by pseudo first order kinetics with a few mtorr of NO_2 (up to 10 mtorr) present. Half lives were typically a few msec. Plots of the pseudo-first order rate coefficients vs $[\text{NO}_2]$ were linear, and the slopes depended upon total pressure, increasing with increasing total pressure, indicating that the reaction observed is



In these experiments M was primarily CF_2ClBr . A plot of the observed pseudo-second order rate coefficients versus total pressure is shown in the Figure. The filled circles are experimental data points, and the curve drawn through them is a calculation using the method for termolecular reactions developed by Trice¹



Limiting second order and third order rate coefficients estimated by this model are given in the Table. Excellent agreement was found with literature values of rate coefficients for other halomethylperoxy radical reactions with NO_2 . Estimates were made of the stratospheric formation of $\text{CF}_2\text{ClO}_2\text{NO}_2$.

Low- and high-pressure limiting rate constants for $\text{RO}_2 + \text{NO}_2 + \text{M} \rightarrow \text{RO}_2\text{NO}_2 + \text{M}$ at

Species	k_0 ($\text{cm}^3 \text{ molecule}^{-1} \text{ s}^{-1}$)	k_∞ ($\text{cm}^6 \text{ molecule}^{-2} \text{ s}^{-1}$)	Reference
CH_3O_2	2.3×10^{-10}	8.0×10^{-13}	Buech, D.L. et al. 1982
$\text{C}_2\text{H}_5\text{O}_2$	4.0×10^{-10}	8.0×10^{-13}	Dugones 1983*
CF_3O_2	3.3×10^{-10}	6.0×10^{-13}	Leclerc and Caralp 1984
CF_2ClO_2	3.5×10^{-10}	5.2×10^{-13}	This work
CF_3O_2	2.3×10^{-10}	5.0×10^{-13}	Dugones 1983*

It was found that $\text{CF}_2\text{ClO}_2\text{NO}_2$ may be present in significant amounts if the photolysis lifetime is long. However, the photolysis lifetime is highly uncertain since absorption cross-sections have not been reported at wavelengths longer than 285 nm, and quantum yields have not yet been determined at any wavelength.

1 J. Trice, Ber. Bunsenges. Phys. Chem. 87, 161 (1983).

THE ENERGY TRANSFER PROCESSES IN R-MX MIXTURES (R-Ar, Kr, Xe).

A. JóŹko, E. Bartkiewicz, M. Symanowicz, K. Wojciechowski, M. Rosa and M. Forys

Agricultural and Teachers University, Department of Chemistry, 08-110 Siedlce, POLAND

The interaction mechanism of the excited rare gas species (R^*) and halogen donors (MX) was investigated by Vuv photolysis and pulse radiolysis methods.

The (RX^*) excimers as well as the stable products of the photolysis/radiolysis were monitored. The results point to the reactions (1) and/or (2) as the very important channels of the energy transfer.

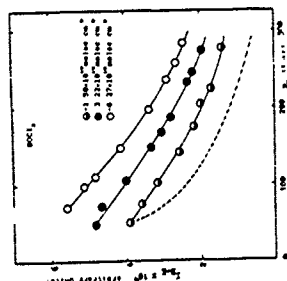
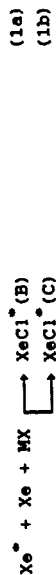


Fig.1. $XeCl^*$ fluorescence ($B \rightarrow X$) intensity vs Xe pressure. Points from the experiments. Solid lines from best fitting procedure. Dashed line - calculated when reaction (2) were omitted.

For the fluorescence measurements the computer fittings gave k_{10} and k_{1b} of the range $(1-4) \times 10^{-20} \text{ cm}^3 \text{ s}^{-1}$



for $MX = SOCl_2, S_2Cl_2, PCl_3, CCl_4, SnCl_4$.

The same procedure for the radiolysis data has given $k_2 = 5 \pm 3 \times 10^{-28} \text{ cm}^3 \text{ s}^{-1}$



Additionally the pulse radiolysis experiments have allowed us to evaluate the effectiveness of the subexcited electrons (e_s) interactions (3,4) in R-HX mixtures i.e. $G_3 = 1 \pm 0.2$ and $G_4 = 1.5 \pm 0.5$ (products/100 eV)



A LASER PHOTOLYSIS/CW LASER ABSORPTION STUDY OF THE REACTIONS OF PHENYL RADICALS WITH NO, NO₂, O₂, CCl₄ AND SELECTED HYDROCARBONS

Markus Preidel and Reinhard Zellner

Institut für Physikalische Chemie, Universität Göttingen
D-3400 Göttingen, Federal Republic of Germany

Phenyl is the smallest of the aryl radicals. Its reactions are therefore expected to provide valuable insight into the reactivity of this radical type and therefore to characterize potential differences to reactions of alkyl radicals. Moreover, in reactions with hydrocarbons (notably benzene, acetylene) phenyl is expected to provide the rate limiting step of the formation of polycyclic aromatics in combustion environments.

Except for the liquid phase there have been surprisingly few studies of reactions of the phenyl radical. This is most likely a reflection of the experimental difficulties associated with the generation and detection of phenyl in the gas phase. By use of a combined laser photolysis-cw laser absorption technique we have recently succeeded to generate and detect the phenyl radical at concentrations suitable for kinetic studies. The phenyl precursors used in this study were substituted benzenes such as chloro-, bromo-, and nitrobenzene which were photolyzed at 248 nm. The detection of phenyl is achieved by using the 488 nm output of an argon ion laser in combination with a white mirror multiple path absorption cell. According to the work of Porter and Ward ^{1/1} phenyl has a strongly structured visible absorption corresponding to the A²P₁ ← X²A₁ transition. From the present work the absorption coefficient at 488 nm is estimated to be (9-3) · 10⁴ cm².

The reactions of phenyl with NO and NO₂ have been studied in the temperature range from 298° to 404 K. The reactions are found to be relatively fast and most likely to correspond to simple recombination reactions. For the reaction with NO₂, however, an oxygen atom transfer is energetically also possible. Arrhenius graphs of the results are shown in figure 1.

The corresponding Arrhenius expressions are:

$$k(\text{NO}_2) = 10^{-11.9} \exp(540/T) \text{ cm}^3/\text{mole} \cdot \text{s}$$

$$k(\text{NO}) = 10^{-11.4} \exp(300/T) \text{ cm}^3/\text{mole} \cdot \text{s}$$

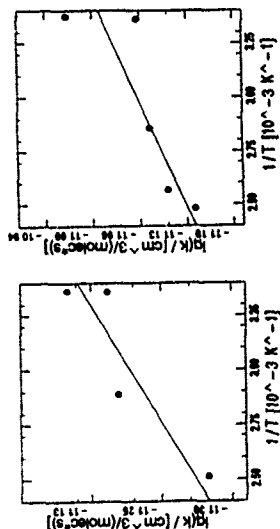


Fig.1: Arrhenius representations for the reactions of phenyl with NO₂ (left) and NO (right)

The reactions of phenyl with O₂, CCl₄, ethene, 2-butene, benzene, and toluene were studied at 298 and 410 K. In each case only upper limits of the rate coefficients could be determined. The following limits were derived: k(O₂) < 2 · 10⁻¹², k(CCl₄) < 3 · 10⁻¹⁵, k(ethene) < 8 · 10⁻¹⁷, k(2-butene) < 9 · 10⁻¹⁴, k(benzene) < 3 · 10⁻¹⁴, k(toluene) < 2 · 10⁻¹⁴.

Whereas the low reactivity of phenyl with respect to either addition (unsaturated hydrocarbons) or abstraction (CCl₄) is relatively consistent with the low reactivity of this radical at lower temperatures ^{2,3/}, we are at present unable to explain the low reactivity towards O₂. Possible reasons include: a) a rapid equilibration caused by a low (< 10 kcal/mol) bond strength of phenyl-O₂ and b) an interfering absorption of phenyl-O₂ at 488 nm.

REFERENCES

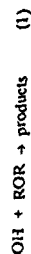
1. G. Porter, B. Ward: Proc. Roy. Soc. London **287**, 457 (1965)
2. J.C. Scaiano, L.C. Stewart: J. Am. Chem. Soc. **105**, 3609 (1983)
3. A. Fahr, W.G. Mallard, S.E. Stein: 21st Int. Symp. on Combustion, The Combustion Institute, p. 825 (1988)

KINETIC AND MECHANISTIC STUDIES OF THE PHOTO-OXIDATIONS OF ALIPHATIC ETHERS STUDIED UNDER TROPOSPHERIC CONDITIONS

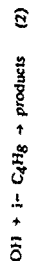
Paul J. Benning and J. Alistair Kerr

Department of Chemistry, University of Birmingham,
Birmingham. B15 2TT England

Relative rate coefficients for OH reactions with aliphatic ethers,



have been measured at room temperature. Experiments have been performed in a Teflon bag smog chamber (220 litres) with HONO as a photolytic source of OH, in the presence of synthetic air containing NO_x , together with an ether plus isobutene as the reference compound:



The rates of consumption of the ether and of the isobutene have been monitored by g.c. analyses and the relative rate coefficients calculated from the equation:

$$\ln(\text{ROR}_0/\text{ROR}_t) = (k_1/k_2) \ln\{[i\text{-C}_4\text{H}_{10}]_0/[i\text{-C}_4\text{H}_{10}]_t\}$$

Absolute values of k_1 have been determined for the ethers listed below from the relative rate data on the bases of the value:

$$k_2 = 9.51 \times 10^{-12} \exp(-503/T) \text{ cm}^3 \text{ molecule}^{-1} \text{ s}^{-1}$$

Ether	$10^{12} k_1/\text{cm}^3 \text{ molecule}^{-1} \text{ s}^{-1}$ at 294±2K
Diethyl ether	12.0
Di-n-propyl ether	15.3
Di-n-butyl ether	17.1
Ethyl n-butyl ether	13.5
Ethyl t-butyl ether	5.6
Di-isobutyl	26.1

These data have been incorporated into the structure-activity relationship developed by Atkinson, for calculating the rate coefficients of OH radicals with organic molecules, and the nearest-neighbour interaction factor for the O atom in ethers has been revised to $F(\text{-O-}) = 6.1 \pm 1.0$.

Experiments are now being carried out in an atmospheric flow reactor which will enable the temperature coefficients of these k_1 values to be measured over the range -30 to +50°C.

Additional experiments are in hand in the static smog chamber to investigate the products of the OH radical initiated photo-oxidations of these ethers in the presence of air containing NO_x . This will enable a detailed mechanism to be constructed.

Reference

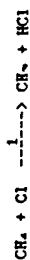
1 R. Atkinson, Chem Rev. 66, 69 (1986).

KINETIC STUDY OF THE REACTIONS OF ATOMIC CHLORINE WITH METHANE AT 294 ± 1 K BY MASS SPECTROMETRY

J.-P. Sawersyn, P. Devolder, B. Mériaux and A. Tighezza

Laboratoire de Cinétique et Chimie de la Combustion, UA CNRS 876
Université des Sciences et Techniques de Lille, Flandres Artois
59655 Villeneuve d'Ascq cedex, France

In order to test the experimental method used to investigate the reaction of atomic chlorine with ethanol as a potential source of α -hydroxyradicals, we have previously undertaken the kinetic study of atomic chlorine with methane



This reaction has been selected because of its importance in the stratospheric chemistry of ozone and because the value of the rate constant preferred at room temperature by the CODATA Task Group (1) was exclusively based on the values determined by fluorescence spectroscopy.

Experimental and results

The experiments were carried out by means of a conventional-flow tube coupled to modulated molecular beam mass spectrometric sampling technique previously described (2). The absolute rate constant of the reaction was determined at 294 ± 1 K under pseudo-first order conditions with a large excess of chlorine atoms with respect to methane and vice-versa. Chlorine atoms were generated in a microwave discharge of Cl_2 highly diluted in helium in order to minimize the heterogeneous removal of Cl atoms, all surfaces exposed to these species were coated with orthophosphoric acid. The Cl concentration

was determined by chemical titration. The flow rates of all gases feeding the reactor were measured by mass flowmeters. Experiments were performed over a range of low pressure ($0.7 - 2.9$ torr) at moderate flow velocities ($11 - 23$ m/s).

The least squares treatment of the experimental data yields a value of k_1 of $(9.17 \pm 0.75) \cdot 10^{-14}$ cc/mole.s in very good agreement with the recent values from the literature.

References

- (1) D.L. Baulsch, R.A. Cox, P.J. Cutzen, R.F. Hampson, I.A. Kerr, J. Troe and R.T. Watson : J. Phys. and Chem. Ref. Data, 11(2), 459
- (2) J.P. Sawersyn, C. Lafage, B. Mériaux et A. Tighezza : J. Chim. Phys. 1987, 10, 127.

HIGH PRECISION DETERMINATION OF RATE CONSTANTS FOR THE REACTIONS OF ALKANES WITH OH AT 300 K, USING A SMOG CHAMBER TECHNIQUE

M. Behnke, F. Nolting and C. Zetzsch

Fraunhofer-Institut für Toxikologie und Aerosolforschung
Nikolai-Fuchs-Straße 1, D 3000 Hannover 61

In many cases during smog chamber experiments the compounds under investigation are consumed by more than one species. Alkanes may be consumed simultaneously by OH and Cl, alkenes by OH and O₃, alkenes and aromatics by OH and NO₂; with substituted compounds photolysis may occur as well, and in the presence of aerosols gases and vapours may be consumed by heterogeneous reactions to a considerable portion. Besides such contributions of interfering active species, dilution by the gas sampling has to be considered in constant volume smog chambers.

The present study describes a method for the detection and correction for interfering species in smog chamber experiments, employing several reference compounds simultaneously. Supposed that the reference compounds R_i are consumed by reaction with OH alone and that the gas consumption of analyzing equipment contributes to a corresponding (in many cases exponential) dilution d_i of the chamber content between the data points, the corresponding differential equation, describing the decay, is given by

$$d[R_i]/dt = -k_{OH}[OH][R_i] - d_i R_i \quad (1)$$

or in integrated form:

$$\ln[R_i]_t/[R_i]_0 = -k_{OH} \int_0^t [OH] dt - d_i \cdot t \quad (2)$$

According to equation 2, a plot of $\ln[R_i]_t/[R_i]_0$ versus known k_{OH} of the reference compounds yields the relative dilution, d_i, as intercept at each time interval, and the integrated concentration of OH as slope. The recommended rate constants (corrected for 300 K in units of 10⁻¹² cm³ s⁻¹) for the compounds n-butane (2.55), n-hexane (5.63), n-octane (8.79), 2,2,3,3-tetramethylbutane (1.08) and 2,2,4-trimethylpentane (3.70) and for hexafluorobenzene (0.219) are employed as initial references.

A systematic deviation may be interpreted in several ways:

- 1) An additional degradation process by other active species besides OH may contribute to the consumption

- 2) A reaction product may interfere malitically with one of the reference compounds

- 3) An impurity of one of the reactants may interfere analytically with one of the reference compounds

- 4) One ore more reference rate constants are incorrect

Rate constants for the hydrocarbons under investigation are then obtained from a plot of $\ln[R_i]_t/[R_i]_0 + d_i$ versus $\int[OH] dt$. The obtained rate constants are summarized in table I. They are compared with literature data ² and with estimates using the parameters recommended by Atkinson.

Table I: Rate constants, $k_{OH}/10^{-12} \text{ cm}^3 \text{ s}^{-1}$ and 95% confidence intervals obtained at 300₂ K in comparison with literature from a recent review² (data corrected for 300 K)

Compound	n	k _{OH} ± s	k _{OH} lit	k _{OH} est
propane	130	1.27 ± 0.09	1.20	1.22
n-pentane	121	4.09 ± 0.08	4.08	3.97
n-heptane	115	7.28 ± 0.08	7.3	6.78
n-nonane	150	10.3 ± 0.2	10.5	9.59
n-decane	49	12.4 ± 0.3	11.2	11.0
2,2-dimethylpropane	140	0.67 ± 0.15	0.87	0.76
2,2-dimethylbutane	156	2.32 ± 0.06	2.63	1.85
2,2-dimethylpentane	159	3.37 ± 0.03	-	3.25
2,2-dimethylhexane	162	4.83 ± 0.04	-	4.66
1,1,3-trimethylcyclohexane	158	8.73 ± 0.09	-	9.22
cycloheptane	111	11.8 ± 0.2	13.2	9.84
cyclooctane	105	13.7 ± 0.3	-	11.3
tricyclo(3,3,1,3,7)decane	72	22.1 ± 0.3	22.7	24.1
2-methyloctane	148	10.1 ± 0.12	-	9.63
4-methyloctane	153	9.72 ± 0.12	-	10.0
2,3,5-trimethylhexane	160	7.88 ± 0.09	-	10.1

References

- 1) C. Zetzsch in: Formation, Distribution and Chemical Transformation of Air Pollutants (ed. R. Zellner), Dechema-Monograph 104, pp. 187-212, VCH-Verlagsgesellschaft, Weinheim 1987
- 2) R. Atkinson, Chem. Rev. 86 (1986) 69-201; Internat. J. Chem. Kinet. 18 (1986) 555-568

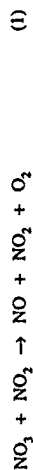
LATE ENTRY

Determination of the $\text{NO}_3 + \text{NO}_2 \rightarrow \text{NO} + \text{O}_2 + \text{NO}_2$ Rate Constant
by Infrared Diode Laser and FT Spectroscopy

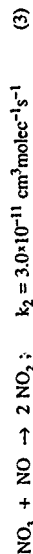
J. Hjorth, F. Cappellani, C. J. Nielsen † and G. Restelli

*Commission of the European Communities,
Joint Research Centre - Ispra Establishment,
I-21020 Ispra (VA), Italy.*

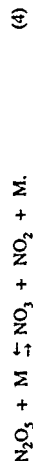
One of the reactions that destroy NO_3 in the troposphere at night is:



Although this reaction is not the most important sink for NO_3 it is far from negligible. The determination of k_1 is complicated by the occurrence of several other reactions leading to interconversion of nitrogen oxides, e. g.



and



In the present study k_1 was evaluated from a simultaneous determination of $[\text{NO}]$ and $[\text{NO}_2]$ in a steady state situation after mixing NO_2 and N_2O_5 in a large reaction chamber. The steady state condition for NO is given by:

$$k_2 [\text{NO}_3] + k_1 [\text{NO}_2] [\text{NO}_3] = k_3 [\text{NO}] [\text{NO}_3] \quad (a)$$

A comparison between k_2 as evaluated in Ref.(1) and the product $k_1 [\text{NO}_2]$ under our experimental conditions shows that with k_1 approximately $5 \times 10^{-16} \text{ cm}^3 \text{molec}^{-1} \text{s}^{-1}$ reaction (2) has negligible (<1%) influence on the concentration of NO . The rate constant k_1 can then be derived from

† On leave from Department of Chemistry, University of Oslo, P.O. Box 1033 Blindern, N-0315 Oslo 3, Norway.

$$k_1 = k_2 \frac{[\text{NO}]}{[\text{NO}_2]} \quad (b)$$

and its determination will depend upon the knowledge of k_2 and the accuracy with which $[\text{NO}]$ and $[\text{NO}_2]$ in the system can be measured. The $[\text{NO}_2]$ can easily be determined accurately by IR spectroscopy using an FT spectrometer. The obviously low NO concentration can conveniently be measured by a tunable infrared diode laser absorption spectrometer operating in second harmonic mode.

We consider it an advantage of the method outlined that k_1 has been determined by procedures that do not require the equilibrium constant K for reaction (4). The value of K is in fact still an unsettled question as determinations in literature vary within a factor two.

The rate constant k_1 was calculated from the results of 18 experimental runs by use of eqn (b) as $k_1 = (5.12 \pm 1.62) \times 10^{-16} \text{ cm}^3 \text{molec}^{-1} \text{s}^{-1}$ at 296 K. This value is somewhat higher than the value obtained for the temperature of 296 K from the expression given in Ref.(2) but the uncertainty limits of the two results overlap.

Acknowledgement

The authors gratefully acknowledge the help of G. Melandrone and G. Ottobriani in the experimental measurements. This work was carried out within the framework of the Lactoz Project jointly organized by Eurotrac and by the European Commission Coordinated Action Cost 611.

REFERENCES

1. Johnston, H.S.; Cantrell, C.A. and Calvert, J.G. *J. Geophys. Res.* **1986**, *91*, 5159.
2. Graham, R.A. and Johnston, H.S. *J. Phys. Chem.* **1978**, *82*, 254.

OPEN SHELL ATOMIC BEAM SCATTERING AND THE SPIN ORBIT DEPENDENCE OF POTENTIAL ENERGY SURFACES

V. Aquilanti, R. Candori, F. Pirani

Dipartimento di Chimica dell'Università,
06100 Perugia, Italy

G. Liuti

Dipartimento di Chimica dell'Università,
53100 Siena, Italy

The extension of molecular beam scattering measurements beyond the closed shell atom-atom systems is an important step forward to obtain intermolecular potentials for more complicated interactions, such as the chemically interesting ones of open shell atoms with rare gases, diatomic and polyatomic molecules. 1-3

The useful theoretical framework recently proposed together with the experimental data obtained from scattering experiments where the open shell atom is in well defined states allow an accurate characterization of the weak interactions involved. 4,5

Scattering data involving nitrogen, oxygen and fluorine atoms have been reported previously. 6-8 The results shown here on the scattering of fluorine and oxygen atoms by rare gases, obtained under much improved experimental conditions, supersede the old ones: they confirm previous qualitative conclusions but permit a much more refined analysis. In addition the scattering data obtained on the interaction of oxygen atoms with molecular hydrogen and methane are also presented and discussed within the same theoretical scheme developed for the open shell-closed shell atom-atom interaction.

The experimental technique exploits magnetic analysis of atomic sub-levels and provides insight on the influence of spin-orbit and electronic angular momenta on the long range part of potential energy surfaces.

The results are analyzed in terms of an adiabatic decoupling scheme to derive the interaction as a spherical part and an anisotropic component, from which detailed information is obtained on the adiabatic potential energy surfaces and on nonadiabatic coupling terms. The surfaces so obtained are of interest not only for all kinetic processes where intramultiplet mixing and polarization phenomena are explicitly observed, but also for understanding orientation and alignment effects in reactive collisions when dominated by anisotropy at long range. Also these surfaces can be profitably used in dealing with important processes such as combustion, flames, lasers and atmospheric chemistry.

References

1. F. Vecchiocattivi, Comments At. Mol. Phys. 1986, 17, 163
2. V. Aquilanti, F. Pirani, F. Vecchiocattivi, Structure and Dynamics of Weakly Bound Molecular Complexes, A. Weber Ed. (Plenum, New York, 1987) pg. 423
3. G. Liuti, F. Pirani, J. Chem. Phys. 1987, 87, 5266
4. V. Aquilanti, G. Grossi, J. Chem. Phys. 1980, 73, 1165
5. V. Aquilanti, P. Casavecchia, G. Grossi and A. Laganà, J. Chem. Phys. 1980, 73, 1173
6. V. Aquilanti, G. Liuti, F. Pirani, F. Vecchiocattivi, and G. G. Volpi, J. Chem. Phys. 1976, 65, 4751; V. Aquilanti, E. Luzzatti, F. Pirani and G. G. Volpi, J. Chem. Phys. 1980, 73, 1181.
7. B. Brunetti, G. Liuti, E. Luzzatti, F. Pirani and G. G. Volpi, J. Chem. Phys. 1983, 79, 273; G. Liuti, E. Luzzatti, F. Pirani and G. G. Volpi, Chem. Phys. Lett. 1985, 121, 559
8. V. Aquilanti, E. Luzzatti, F. Pirani and G. G. Volpi, Chem. Phys. Lett. 1982, 90, 382

ACCURATE ATOM-DIATOM INTERMOLECULAR POTENTIALS FROM
HIGH RESOLUTION CROSSED MOLECULAR BEAM SCATTERING
EXPERIMENTS

L. Beneventi, P. Casavecchia and G.G. Volpi
Dipartimento di Chimica, Università di Perugia
06100 Perugia, Italy

Molecular beam scattering experiments have successfully contributed to our precise knowledge of the interaction potentials between the colliding atoms and molecules.¹ The rainbow scattering angle is probably the most direct and unique measure of the potential well depth, ϵ , while the diffraction oscillations give a direct measure of the diameter, σ , of the repulsive wall (and then of the minimum position, R_0).

We have recently extended to some simple atom-diatom systems² the same approach used successfully for the rare gas-rare gas systems,⁴ and found that precise diffraction scattering measurements, coupled to other available experimental properties, also lead for systems as He interacting with N₂, O₂ and NO to rather precise determinations of the intermolecular potentials. It was found that an accurate evaluation, within the framework of the infinite-order-sudden (IOS) approximation,⁵ of the diffraction oscillations in total differential cross section (DCS) measurements carried out under high resolution conditions not only give the absolute scale of the potential, but also provide quantitative reliable information on the anisotropy of the interaction.

In the present study we have extended the same approach used for the He-diatom systems³ to heavier cases, namely Ne-N₂, Ne-O₂ and Ne-NO. The experiments were performed in a high-resolution crossed molecular beam apparatus which has been described in detail previously.³ The total DCS data in the thermal energy range show well resolved closely spaced diffraction oscillations superimposed on the main rainbow oscillation. The scattering data are analyzed simultaneously with second virial coefficient and transport (diffusion and viscosity) data available in

the literature. The validity of the IOS approximation for the analysis of total DCS in our experimental conditions and for obtaining reliable estimates of the anisotropy from the quenching of the diffraction oscillations has been successfully tested by comparison with exact close-coupling calculations for Ne-N₂. An accuracy (about 1% in R_0 and 3% in ϵ) comparable to that attained for many isotropic systems has been obtained for the spherical part of the potential energy surfaces (PES).

The derived PES for the Ne-N₂, O₂ and NO systems are compared with previously proposed theoretical and/or empirical potential surfaces, none of them comparing satisfactorily with our results.^{6,7} Very recently, total DCS measurements with well resolved rainbow and diffraction oscillations have also been carried out for the Ne-Cl₂ and Ne-Cl systems. An analysis along the lines followed for the other rare gas-diatom systems should allow us to derive reliable potential surfaces, which can contribute to the understanding of the vibrational predissociation process occurring in these interesting van der Waals molecules when the halogen stretch is excited by a quantum of vibration.

References

1. U. Buck, Comments At. Mol. Phys. 17, 143 (1986).
2. U. Buck, in Atomic and Molecular Beams Methods, edited by G. Scoles (Oxford, New York, 1987), Vol. 1.
3. L. Beneventi, P. Casavecchia and G.G. Volpi, J. Chem. Phys. 85, 7011 (1986).
4. L. Beneventi, P. Casavecchia and G.G. Volpi, J. Chem. Phys. 84, 4828 (1986); and in Structure and Dynamics of Weakly Bound Molecular Complexes, NATO ASI Series C 212 441 (1987).
5. R.T. Pack, J. Chem. Phys. 60, 633 (1974).
6. L. Beneventi, P. Casavecchia, F. Vecchiocattivi, G.G. Volpi, D. Lemoine and M.H. Alexander, J. Chem. Phys. (1988), in press.
7. L. Beneventi, P. Casavecchia and G.G. Volpi, to be published.
8. N. Halberstadt, J.A. Beswick and K.C. Janda, J. Chem. Phys. (1988), in press.

C + NO → CN + O REACTION DYNAMICS STUDIED WITH PULSED CROSSED
SUPERSONIC MOLECULAR BEAMS

Michel Costes, Christian Naulin and Gérard Dorthé

Laboratoire de Photophysique Photochimie Moléculaire, UA 348
Université de Bordeaux I, 33405 Talence, France

Although ground state atomic carbon 3P_2 is a very reactive element, little is known about its reaction dynamics and the majority of experimental studies reported so far have been made under bulk conditions. The C + NO → CN + O reaction has been the most extensively studied system¹⁻⁴ but the results lack of coherence.

In recent years we have developed a pulsed crossed supersonic molecular beam apparatus suitable for reaction dynamics studies of metal or solid metalloidal atoms⁵. The heart of the instrument is the use of a pulsed metal beam, generated by laser ablation of the solid (graphite in the present case) and seeding in the supersonic expansion of a carrier gas. The performances of this pulsed atom beam exceed those of metal-oven effusive sources. A large range of continuously adjustable velocities: 800 to 3400 m.s⁻¹ is obtained with velocity spread between 20 and 11 % FWHM. Atoms are cooled in the ground state sublevels and cluster production remains marginal.

The reaction is studied between 0.064 and 0.24 eV relative translational energy. A translational energy threshold for CN(X²) production near 0.05 eV is extrapolated from the excitation function and this behaviour is in excellent agreement with a value of the rate constant determined in a companion kinetics study at 300 K using a fast flow reactor⁶.

LIF spectra of the CN(X²) product taken for different translational energies of reactants are always consistent with ground state energetics. A value D₀(CN) = 7.78 eV is deduced from the excitation limit. It is emphasised that excited states of atomic carbon do not contribute to the LIF signal in our conditions.

C₂ radicals are detected in the carbon beam. Nonetheless we can easily conclude that the scattered CN product comes from the C + NO reaction and not from C₂ + NO reactive collisions.

Results on energy partitioning are $\langle E_{\text{tr}} \rangle \approx 16 \%$ and $\langle E_{\text{vib}} \rangle \approx 28 \%$ in fair agreement with theoretical results obtained by quasi classical trajectory calculations⁷ on a potential energy surface derived from ab initio points⁸. The vibrational populations are

near the statistical case (Levine-Bernstein theory) for vibrational levels $v'' = 0-3$ but well above the prior for $v'' = 4-5$. Rotational distributions, characterized by a reduced surprisal parameter $B_r = 3.5$ differ significantly from statistical. These results are in complete disagreement with the flash photolysis and beam-gas⁹ experiments where relaxed rather than nascent populations were certainly observed. The vibrational distribution is also significantly different to the one obtained by extrapolation to zero pressure in fast flow work³. A direct mode mechanism can be invoked in spite of the deep well in the potential energy surface: the CNO lifetime is short because the complex dissociates into products after two bounces in the well. Electronically excited CN(A²) radicals are also produced. They are detected by LIF using B-A (0-0) excitation near 600nm and collecting the B-X (0-0) fluorescence near 388 nm. The translational energy threshold for CN(A²) production is the same as that for the ground state. This supports energy profile calculations in the bent configuration which show that the first excited surface is without a significant barrier in the entrance valley⁷.

1 W.M. Jackson, C.N. Beugre and J.B. K. Halpern, *J. Photochem.* 13 (1980) 319

2 H.F. Krause, *Chem. Phys. Letters* 78 (1981) 78

3 H. Sekiya, M. Tsuji and Y. Nishimura, *J. Chem. Phys.* 84 (1986) 739

4 M. Costes, B. Dugay, G. Dorthé, P. Halvick, J. Jousset-Dubien, C. Naulin, G. Mouchi, J.C. Rayez, M.T. Rayez and C. Vaucamps, Recent Advances in Molecular Reaction Dynamics, ed. R. Vetter and J. Vigué, CNRS, Paris (1986) p. 97

5 M. Costes, C. Naulin, G. Dorthé, C. Vaucamps and G. Nouchi, Faraday Discuss. Chem. Soc., 84 (1987) paper 6

6 B. Barrère, P. Caubet, G. Dorthé and J. Marchais, presented at this symposium

7 P. Halvick, J. C. Rayez and E.M. Evleth, *J. Chem. Phys.* 81 (1984) 728

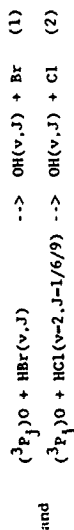
8 J.C. Rayez, P. Halvick, M.T. Rayez and B. Dugay, *Chem. Phys.* 101 (1986) 401

COMPUTER SIMULATION OF THE STATE-RESOLVED REACTIONS
OF (³P)OXYGEN ATOMS WITH HCl AND HBr.

Per-Anders Elofson and Løif Holmlid

Dept. Physical Chemistry G.U. and Chalmers Univ. of Technology,
S - 412 96 Göteborg, Sweden

The reactions of Oxygen atoms with Hydrogen halides have been investigated using a statistical simulation procedure. This means simulating the O + HX collision complex formation, the distribution of energy in an RRK-like way at the Transition States and the decomposition into products, including channel interaction. The reactions



were studied and the results compared with the experimental results of McKendrick et al.² and Rakestraw et al.³ Great care was taken to correctly account for the experimental details: The velocity distribution of the Oxygen atom, being produced in photolysis of NO₂ at 355nm, turned out to be crucial since most initial energy is supplied in the form of translational energy. Reaction (1) is rather strongly exothermic, while (2) is slightly endothermic. Both reactions have barriers towards reaction, to match the experimental results for (2), an entrance channel potential energy barrier of 4.3 kcal/mole was used.⁴ This is in the lower range region of the values commonly recognized,⁴ but gives the best fits for all three sets of J_{HCl}(J=1,6 or 9).

The conclusion is that both reactions may well, in spite of the apparently 'non-statistical' OH product distributions, proceed by entirely statistical mechanisms. This is certainly the case for the factors governing the rotational energy release; including the assumption that the vibrational levels of the diatomic at transition state have a width of 1 - 2 per cent around the level value of the undisturbed diatomic molecule also explains the vibrational distribution from O + HBr where >90% of the OH formed are in v = 1, the remainder being found in v = 2. No ground state OH is found from this reaction.

The inverted rotational distributions of product OH from both reactions is shown to be the result of strict TOTAL angular momentum conservation.

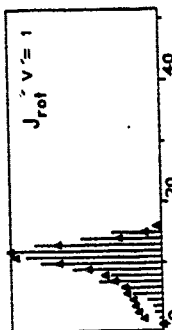


Fig 1. Distribution of OH rotational quantum number from reaction (1). Triangles are the experimental results of McKendrick et al. The high experimental intensity at low J is thought to be due to the formation of Br.

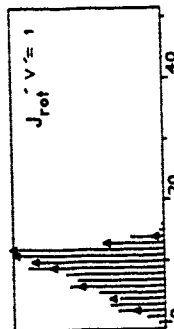


Fig 2. Distribution of OH rotational quantum number from reaction (2). Initial state of HCl was v=2, J=1/6/9. Triangles are the experimental results of Rakestraw et al.

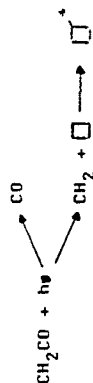
References:

1. K. Rynefors, *Computer Phys. Commun.*, 27(1982), 201.
2. K.C. McKendrick, D.J. Rakestraw and R.M. Zare, *Paper No. 2, Faraday Discuss. Chem. Soc.* 84(1987).
3. D.J. Rakestraw, K.C. McKendrick and R.M. Zare, *Journal of Chemical Physics* 87(1988), No.12, 7341.
4. R.D.H. Brown and I.V.M. Smith, *Int. J. Chem. Kinet.* 10(1978), 1.
5. J.E. Spencer and G.P. Glass, *ibid.*, 9(1977), 97.

ENERGY DISTRIBUTION BY DIRECT DECONVOLUTION: EXPERIMENTAL TEST. ENERGY TRANSFERRED BY COLLISION IN METHYLCYCLOBUTANE*/CYCLOBUTANE, AND THE CH₂(¹A₁) HEAT OF FORMATION

J.M. Figueroa, M. Fuentes and J.C. Rodríguez
Instituto de Química Física "Rocasolano", CSIC,
Serrano 119, 28006 Madrid, Spain.

The photoactivation scheme:



produces at 337 nm methylcyclobutane (MCB)* with an energy distribution thermochemically well defined if we assume, as generally accepted, that both photofragments are formed "cold". The calculated value for this distribution is 107 Kcal/mol.¹

The singlet methylene heat of formation deduced from this data is $\Delta H_0^\circ \approx 100$ Kcal/mol. However this is an upper value, that is based on the assumption that methylene is initially formed with no excess of energy; any rotational or translational energy initially present in CH₂ would had to be subtracted from the above figure.

Very good data for the unimolecular MCB* decomposition can be found in the literature². Therefore, direct deconvolution³ can be attempted and the energy distribution obtained compared with the thermochemical value. Results, depending on the energy transferred per collision (step ladder model) and kinetic model used, provide distributions with maxima between 114 Kcal/mol (h-rd collisions) and 100 Kcal/mol (average energy transferred per collision 1 Kcal/mol).

Of the three Arrhenius based models used⁴, model I could have been discarded "a priori" on kinetic grounds and model III is probably the more reliable. A resume of the results obtained are in the table.

Resume of the deconvolution results: f(E) maxima and areas

Model	1	2	3	4	5	6	7	8	9	10	11
f (Max)	104	108	110	113							
f (Area)	1.02	1.03	1.05	1.07							
II (Max)	104	106	108	110							
II (Area)	1.03	1.03	1.04	1.05							
III (Max)	100	105	106	107							
III (Area)	1.02	1.04	1.05	1.06							

Uncertainties in the Arrhenius parameters seem to be the more prominent error source in the obtention of the energy distribution by direct deconvolution of the experimental O/D+S results, followed by the errors introduced by the average energy transferred per collision (ΔE) if this is not precisely known.

However, even with rate constants differing by a factor of 2 and ΔE with errors of ± 2 Kcal/mol the position of the deconvoluted f(E) maximum is within 14% of the experimental value. This error value could be reduced considerably if good input kinetic data are available (model III in this case). It should be noticed that these results could depend on the energy of the distribution width and energy. At lower energies the extremely strong dependence of k(E) on energy makes that errors in k(E) values would introduce relatively small errors in the corresponding energy. On the other hand at very high energy the variation of k with energy is reduced, so small errors in k(E) induce more important variations into the corresponding energy.

1. J.W. Simons, W.L. Hase, R.J. Phillips, E.J. Porter and F.B. Growcock, *Inter. J. Chem. Kinetics* **7**, 879 (1975).
2. W.C. Mahone, W. Kolln and J.W. Simons, *J. Phys. Chem.* **89**, 3902 (1985) and references therein.
3. M.J. Avila, J.M. Figueroa and J.C. Rodríguez, *Chem. Phys.* **113**, 231 (1987) and references therein.

ENERGY TRANSFER REACTIONS OF $N_2(A^1\Sigma_u^+)$

by Michael F. Golde, Grace Ho, Robert F. Sperlein and Wen Tao
Department of Chemistry, University of Pittsburgh, Pittsburgh,
PA 15260, USA

The rate constants and products of selected gas-phase energy transfer reactions of $N_2(A^1\Sigma_u^+)$, the lowest electronically-excited state of N_2 , have been measured by the discharge flow technique. $N_2(A, v'')$ was detected by $N_2(S, v''-A, v')$ laser-induced fluorescence and the reaction products by LIF, atomic resonance fluorescence and emission spectroscopy. For each of the reagents selected, which included H_2 , H_2O , D_2O , CF_3Cl , CF_2HCl and HCl , the lowest electronically-excited state is known to lie at a vertical excitation energy above the ground state of somewhat more than 6.2 eV, the excitation energy of $N_2(A, v=0)$; however, the bond energy of each molecule is considerably smaller than 6.2 eV.

For each reagent, the rate constant for collisional deactivation of $N_2(A, v)$ increases markedly with v as follows (data in $cm^3 s^{-1}$; literature data in parentheses): for H_2 : $(2.4 \times 10^{-15}$ for $v=0$) to 1.0×10^{-12} for $v=6$; for D_2O : 1.1×10^{-13} ($v=0$) to 6×10^{-11} ($v=6$); for CF_3Cl : 6×10^{-14} ($v=0$) to 1.7×10^{-11} ($v=6$); for CF_2HCl : 1.0×10^{-13} ($v=0$) to 3.0×10^{-11} ($v=6$); for HCl : 1.2×10^{-12} ($v=0$) to 2.1×10^{-11} ($v=3$). Evidence for both electronic quenching and vibrational relaxation of $N_2(A, v)$ was obtained: the former is more important and appears to occur principally via dissociation of the reagent molecule; the latter is, curiously, very important in the deactivation of $N_2(A, v=1)$ by D_2O and CF_2HCl , and contributes also in the reactions of H_2 .

These data and others suggest that electronic energy transfer proceeds by near-vertical transitions in the N_2 and reagent molecules. In support, an empirical correlation was found between the deactivation rate constant of level $N_2(A, v')$ by reagent Q and the effective absorption coefficient of the reagent, σ_{eff} :

$$\sigma_{eff} = \sum \sigma(Ev', v'') \cdot qv', v''$$

where q is the Franck-Condon factor of the $N_2(A, v'-X, v'')$ transition and σ is the absorption coefficient of Q at the energy of this transition.

Additional insight into these reactions has been provided by ab initio potential surface calculations for $N_2(A) + H_2$ and for $CH_3I + H_2$, which involves similar energetics to the $N_2(A)$ reaction but proceeds at close to the collision rate. Both multi-configuration

SCF and extensive CI calculations were employed. In both cases, energy transfer was found to proceed via access to the repulsive $N_2(b^1\Sigma_u)$ state, which subsequently dissociates. In both reactions in selected geometries, the reagents and products correlate along a single adiabatic surface, because of a strongly avoided crossing between diabatic states as the H-H bond stretches. The difference between the rate constants of the two reactions can be understood in terms of the different barrier heights in the respective surfaces. The features of the surface serve also to explain, currently in qualitative terms, the dependence of the rate constants on vibrational energy in $N_2(A)$ and the competition between vibrational relaxation and electronic quenching.

Time resolved infrared emission in the $O + CF_2$ reaction

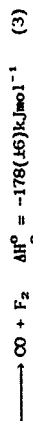
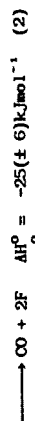
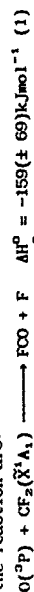
G. Hancock and D.E. Heard

Physical Chemistry Laboratory, South Parks Road,
Oxford, OX1 3QZ

Time resolved infrared emission from the products of bimolecular chemical reactions gives direct information on the nascent distribution of internal energy released by the reactive collision, and its subsequent relaxation. Infrared multiple-photon dissociation (IRMPD) offers an excellent method for producing ground electronic state radicals with low vibrational excitation for use in kinetic studies. IRMPD of CF_2HCl was used in this study to generate $CF_2(\tilde{X}^1A_1)$ and its reaction with $O(^3P)$ was followed by the IR chemiluminescence from the products.

A low cost, teaching Michelson interferometer has been used to time and wavelength resolve the weak IR emission. Each discrete value of path difference in the interferometer, the dissociating CO_2 -laser pulse triggered the recording of the temporal behaviour of the emission. Accurate sampling of the interferogram was ensured by using a Helium Neon Laser reference which passed through the centre of the main optics. In this way one scan of the interferometer gives, after Fourier transform, a complete time evolution of the IR emission spectrum.

Three thermodynamically acceptable product channels for the reaction are:



The overall rate constant for CF_2 removal, previously measured in this laboratory by time resolved laser induced fluorescence, is $(1.75 \pm 0.35) \times 10^{-11} \text{ cm}^3 \text{ molecule}^{-1} \text{ s}^{-1}$, a value consistent with the IR emission risetimes. Wavelength and time resolution of the emission (see Fig.1) indicates two main features:

(i) A fast component between 1900 cm^{-1} and 2400 cm^{-1} . The low frequency end corresponds to $CO(X,v)$, formed initially in high vibrational levels, with energy reaching the thermodynamic limit of reaction (3), relaxing to lower levels at longer times. The high frequency part cannot be explained by CO emission (R branch $1 \rightarrow 0$ stops at $\sim 2200 \text{ cm}^{-1}$) and the $(001-000)$ band of CO_2 formed in the reaction $O + FCO \rightarrow CO_2 + F$ is tentatively ascribed as the source.

(ii) A slow component at frequencies $> 3000 \text{ cm}^{-1}$, due to vibrationally excited HF, formed at longer times from the $F + HCl$ reaction, HCl being the co-product of the IRMPD of the CF_2HCl precursor.

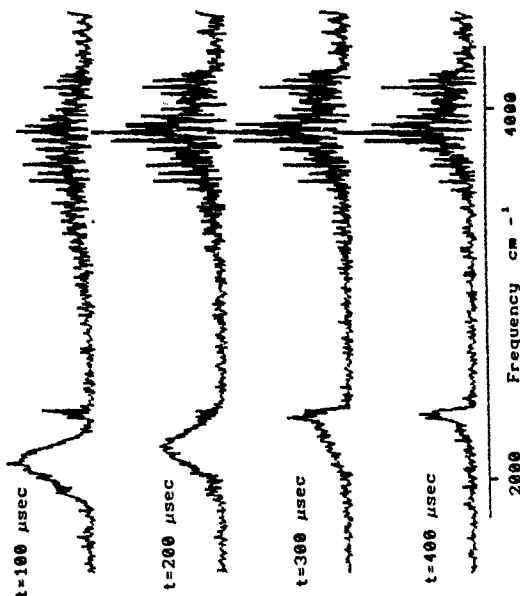


Fig 1. Time resolved IR chemiluminescence from the $O+CF_2$ reaction.

RESONANCE-ENHANCED TWO-PHOTON IONIZATION SPECTRA OF BENZENE IN THE THIRD CHANNEL REGION

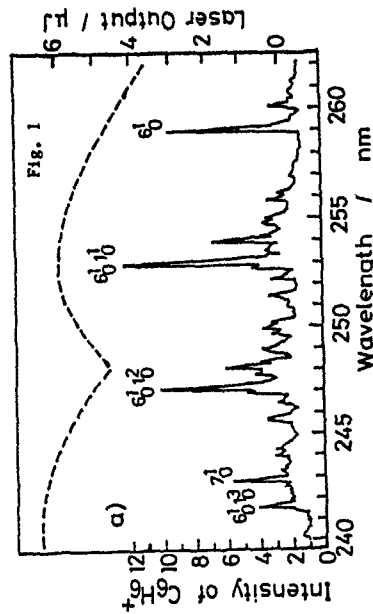
Teihiro Ichimura, Hisanori Shinohara* and Nobuyuki Nishi*

Department of Chemistry, Tokyo Institute of Technology,
Ohokayama, Meguro, Tokyo, 152, Japan

*Institute for Molecular Science, Myodaiji, Okazaki, 444, Japan

Resonance-enhanced two-photon ionization(RE2PI) spectrum of S_1 benzene in the molecular beam was for the first time studied in the third channel region. The benzene molecular beam was formed by expanding benzene seeded in He(500 Torr-1 atm) or Ar generated through a modified pulsed nozzle of 120 μ s pulse duration. The pulsed beam was skimmed and introduced to the ionization region where it was crossed perpendicularly by a focused ionizing laser beam of a pulsed dye laser pumped by a XeCl excimer laser and the pulse width was 8 ns. The dye laser output was frequency doubled by an auto-tracker which contains a BaB₂O₄ angle-tuned crystal and Pellin-Broca prisms. The benzene molecule was excited to S_1 in the wavelength region(262-233 nm). Detection of the benzene fragments was performed by a linear reflectron TOF mass spectrometer with the short drift length(53.6 cm).

RE2PI-TOF spectra of benzene were measured for various intensities of excitation laser outputs, and the parent ion $C_6H_6^+$ and fragment ions also were observed. It should be noted here that the multiphoton-absorption-fragmentation of $C_6H_6^+$ is very efficient, but it can be negligibly small with the excitation laser intensity less than 20 uJ/pulse. The mass-tuned($m/e = 78$) excitation spectrum(Fig. 1-a) has been observed under different laser outputs. The spectra were normalized at appropriate band peaks since two or three dye solutions were necessary to cover these wavelengths. Above the channel three threshold the intensity of the ion is substantially reduced. The peaks observed in the figure correspond to the various vibrational modes of benzene in the S_1 state. This observation confirms the occurrence of RE2PI which overwhelms non-resonant 2PI. The ion intensities obtained in the RE2PI of these vibrational modes shown in Fig. 1 give information about the nonradiative process occurring in the resonant state. The ion yield for the excitation in the channel three region was determined from the observed spectrum and compared with that below the channel three threshold. The value of $C_6H_6^+$ intensity should first be divided by the laser intensity(Fig. 1-a) and the absorption coefficient. And then the



ratios of the intensities for each vibrational band are normalized to that for 6^1_1 band which is believed to be below the channel three threshold. The values of the derived amount is inversely proportional to the nonradiative decay rate. General trends of the values are that the value is fairly constant for the 6^1_1 progression($n=0,1,\dots$) below the channel three threshold, but becomes smaller above the channel. The values for the 6^1_1 progression band showed the relatively smaller values than those for other vibrational bands including the 7^1_1 band regardless the excitation wavelengths. The reason of the large value for the section of the ionization from the 7^1_1 vibronic state compared to that from the 6^1_1 state. The normalized RE2PI intensity for the 6^1_1 band is substantially smaller than that for 6^1_1 . As it is well known, this 6^1_1 band is the onset of the third channel of benzene. In order to make sure this result the relative value of the ion intensity has been carefully measured with the various ion intensities of the laser output for the two vibrational bands, 6^1_1 and 6^1_2 . The result indicated the ionization intensity of the 6^1_1 band in the channel three is getting smaller than that of the 6^1_2 band with decreasing the laser intensity. The intramolecular vibrational redistribution process in the channel three is responsible for the decrease of the ionization intensity.

Reference

1. T. Ichimura, H. Shinohara and N. Nishi, Chem. Phys. Lett. in press.

CHEMILUMINESCENCE AND ROTATIONAL POLARISATION IN THE REACTIONS $\text{Mn} + \text{O}_2, \text{NO}_2, \text{SO}_2, \text{CO}_2, \text{N}_2\text{O}$

Martin R Levy

Department of Chemical and Life Sciences
 Newcastle upon Tyne Polytechnic
 Newcastle upon Tyne NE1 8ST

As a result of the highly refractory nature of the elements, there have been very few dynamical investigations of transition metal atom reactions. However, such studies have the potential to be particularly rewarding, since a large number of potential surfaces may interact. A novel means to study such reactions is laser ablation of a solid metal target¹, which generates a pulsed atomic beam of wide velocity range and containing a number of metastable states. The technique is particularly appropriate for determining translational excitation functions and product rotational polarisations of chemiluminescent reactions. The title reactions represent a suitable place to start since the complexity is at a minimum: the Mn electronic structure is relatively simple² and the $\text{MnO}(\text{A}^2\text{T}^+ - \text{X}^2\text{T}^+)$ spectrum from ~450 to ~750 nm is well-known³. In addition, the long-lived $\text{Mn}(\text{z}^2\text{P}_j - \text{s}^2\text{S})$ emission at ~540 nm allows monitoring of the atomic beam intensity.

In the present work, a beam-gas configuration has been employed, the atomic beam being generated by a focused Nd:YAG laser at 1064 nm. Both the beam, and any chemiluminescence, are detected at the same distance from the Mn target, so that a given delay time corresponds to a specific collision velocity and beam flux. The measured time-dependent product emission intensities are inverted to yield the translational excitation functions; while the polarisation of the molecular emission, parallel and perpendicular to the beam axis, yields the rotational polarisation with respect to the collision velocity vector directly.

Despite the complex composition of the beam, the results indicate that only a few Mn states contribute significantly to MnO^+ production. Except for $\text{Mn} + \text{N}_2\text{O}$, the process is endothermic from ground state atoms - in some cases very substantially so. The excitation functions, when analysed according to the simple "line-of-centres" model, show thresholds corresponding to reaction only of ground state atoms, a $^6\text{S}_{5/2}$, and the first metastable state, $^2\text{D}_j$. These results are largely in accordance with simple state

correlation diagrams, taking into consideration the known vibronic interaction between the A^2T^+ and X^2T^+ states of MnO . The various chemiluminescence thresholds in these reactions also allow determination of a lower limit for the MnO bond energy, $D_0 \sim 395 \text{ kJ mol}^{-1}$, and an upper limit for the $\text{SO}(\text{s}^1\text{A})$ excitation energy, $I_0 \sim 100 \text{ kJ mol}^{-1}$. The former is ~40 kJ mol^{-1} higher than the mass spectrometric value preferred by Huber and Herzberg⁴, but is in broad agreement with spectroscopic observations^{5,6}. The exothermic $\text{Mn} + \text{N}_2\text{O}$ system in particular shows significant excess barriers to chemiluminescent reaction, a feature which appears to be due to the lack of appropriate orbital rather than state correlations.

Collision-induced emission from $\text{Mn}^*(\text{z}^2\text{P}_j)$ has also been observed in these systems: the excitation functions suggest that, in a number of cases, at least, its origin is chemical rather than physical, and that the reaction proceeds through a long-lived complex which may decompose via competing paths.

In all these reactions the MnO^+ rotation is essentially unpolarised, even at very high collision energies. This contrasts sharply with most previous studies⁷, which have found increasing polarisation parallel to the collision velocity vector, as reagent translational energy increases. A number of factors may be responsible for this: (i) all but one of the reactant molecules is triatomic, so that the remaining fragment can carry away significant rotational angular momentum; (ii) the reactions all have very high barriers, suggesting a preference for a specific configuration - probably linear for N_2O and CO_2 ; and (iii) for those which do proceed through a long-lived complex, kinematic factors are such as to favour orbital angular momentum, \hat{L} , rather than rotation, \hat{J} .

ACKNOWLEDGEMENTS

I thank the SERC Laser Support Facility, I R Beattie, R Hill and E Lewis for equipment loans, and J L Beauchamp for helpful correspondence.

REFERENCES

1. H Kang & J L Beauchamp, *J Phys Chem* **89** 3364 (1985)
2. J Sugar & C Corliss, *J Phys Chem Ref Data* **14**, Suppl 2, p 338 ff (1985)
3. J M Das Sarma, *Z Physik* **165** 98 (1959); K C Joshi, *Spectrochim Acta* **18** 625 (1962); R M Gordon & A J Merer, *Can J Phys* **58** 642 (1980)
4. K Huber & G Herzberg, *Constants of Diatomic Molecules* (Van Nostrand, New York, 1979)
5. J P Simons, *J Phys Chem* **91** 5378 (1987)
6. D A Case & D R Herschbach, *J Chem Phys* **64** 4212 (1976)

"A LASER INDUCED FLUORESCENCE STUDY OF THE $B(O_u^+)$ AND $A(O_u^+)$ STATES OF TELLURIUM DIMERS".

E. Martínez, F. Castaño, M.T. Martínez, P. Puyuelo and F.J. Basterrechea.

Departamento de Química Física. Universidad del País Vasco. Apartado 644. Bilbao. SPAIN.

Time resolved fluorescence decay studies of different vibrational levels of $A(O_u^+)$ and $B(O_u^+)$ states of Te_2 in natural abundance, have been carried out. Tellurium dimers were prepared by heating natural tellurium in a pyrex cell, between 600-740 K. Laser excitation spectra involving the vibrational levels $5v' \leq 10$ of the $A(O_u^+)$ state, and $1v' \leq 6$ of the $B(O_u^+)$ state have been obtained using excitation wavelength varying from 468 to 520 nm, from a Nd-YAG pumped narrow band dye laser. The radiative lifetime for the above mentioned vibrational levels of the A state appears to be 1080 ± 60 ns, at least a third higher than previously reported^{1,2}. The collision free lifetime for the low lying levels of the B state is much shorter, and was determined to be 80 ± 5 ns. Electronic quenching of the $Te_2 A(O_u^+)$ state is quite efficient, characterized by a collision cross section of $\sigma = 130 \pm 5 \text{ \AA}^2$, that when compared with previous values^{2,3}, seems to suggest that rotational and vibrational transfer mechanisms must be quite inefficient. Suggestion of perturbations for vibrational levels of the $A(O_u^+)$ above $v' = 15$ is presented, in agreement with Carion's lifetimes for $v' = 16, 17$ of the $A(O_u^+)$ state³.

References

1. W.G. Thorpe, R.W. Carper and S.J. Davis, Chem. Phys. Lett. **123**, 493 (1986).
2. R.S. Ferber, O.A. Shmit and M.Y. Tamamis, Chem. Phys. Lett. **92**, 393 (1982).
3. J. Carion, Y. Guern, J. Lotrian and P. Luc, J. Phys. B, **15**, 1841 (1982).

MEASUREMENTS OF STATE-TO-STATE ENERGY TRANSFER RATE COEFFICIENTS FOR OH ($A^2\Sigma^+$, $v'=0$)

A. Jöres, U. Meier, K. Kohse-Hölinghaus, Th. Just
DFVLR-Institut für Physikalische Chemie der Verbrennung
D-7000 Stuttgart, W. Germany

The application of some laser fluorescence techniques for quantitative detection of molecular radicals requires information on non-radiative energy transfer processes between excited states. We determine state-to-state rate coefficients for rotational and/or spin parity inelastic collisions within the $A^2\Sigma^+$, $v'=0$ state of OH. Single rotational states in the range $K'=0-6$ were populated by laser excitation of ground state OH produced in a discharge flow

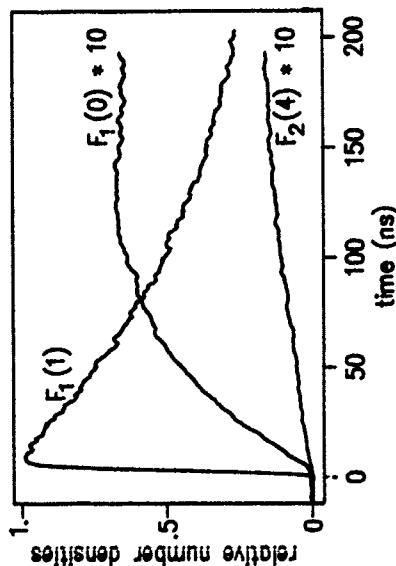


Fig. 1. Relative number densities for OH ($A^2\Sigma^+$, $v'=0$) at $p=2$ mbar: $F_1(1)$ laser excited state; $F_1(0)$, $F_2(4)$ collisionally populated states

reactor at pressures between 0.5 and 5 mbar. The temporal evolutions of relative number densities in the initially pumped and collisionally populated states were observed by monitoring the fluorescence of OH ($A-X$, $0-0$) (Fig. 1).

The temporal resolution in our experimental arrangement at low pressures allows direct determination of state-to-state rate coefficients in the "single collision approximation". Therefore, no fitting laws for the rate coefficients are required. Corrections for multiple collisions can be considered if necessary.

To demonstrate the feasibility of this method, we determined energy transfer rates for OH ($A^2\Sigma^+$, $v'=0$) in thermal collisions with helium. The ratios of measured rates agreed with the assumption of detailed balancing.

Since the A state of OH has a doublet structure, it is necessary to distinguish between the two possible spin components corresponding to $J'=K\pm 1/2$. Measurements with He and N_2 as collision partners were performed. For collisions with He at room temperature, we found that the most probable processes are transitions with $|J'J|=|K'K|=1$ for a given $|K'K|$, transitions that conserve the spin component are faster than those changing the spin component. The measured rate coefficients for $|K'K|=1$ are of the same order of magnitude as those for $|K'K|>1$. These results are in agreement with those found earlier for the energy transfer of OH (A , $v'=0$) in thermal collisions with N_2 . The absolute values of the rate coefficients for collisions with He are approximately 6 times lower than for N_2 .

Since our results are intended to be applied to combustion diagnostics, we shall perform similar investigations for flame-relevant collision partners, like H_2O , CO , CO_2 etc., and to extend these experiments to higher temperatures.

The measured rate coefficients will be used to check the validity of fitting laws for the description of energy transfer processes; also, they can be compared to the results of ab-initio calculations on the dynamics of rotationally inelastic collisions.

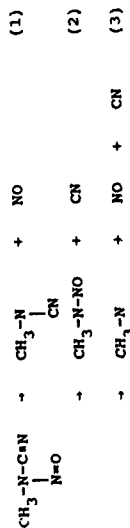
1 R.K. Lengel and D.R. Crosley, J. Chem. Phys. 67, 2085 (1977)

PHOTODISSOCIATION OF JET-COOLED N-NITROSOMETHYLCYANAMIDE
(NMCA) IN THE NEAR-UV

P.A. Giovannacci, M.R.S. McCounstra and J. Pfab

Department of Chemistry, Heriot-Watt University,
Riccarton, Edinburgh, EH14 4AS, Scotland.

The photodissociation of 300K gaseous methyl nitrite and N-nitrosodimethylamine in the near-UV is impact dominated and yields aligned nascent $\text{NO}(\text{N}_1)$ with considerable rotational and vibrational excitation via a single energetically accessible pathway. In contrast the photofragmentation of the title compound NMCA can proceed by the separate pathways 1 - 3 and provides a rare opportunity to examine the effects of wavelength on branching into energetically different channels.



Both CN and NO ground state fragments can be probed readily and with good sensitivity by laser-induced fluorescence (LIF). The CH_3N fragment has been observed recently in emission. Crude estimates of bond dissociation energies in NMCA indicate that the triple fragmentation may become energetically feasible at dissociation wavelengths shorter than 300 nm, and that channel 1 requires significantly less energy than either 2 or 3.

We have examined the pulsed laser photodissociation of NMCA at 396 nm close to the presumed electronic origin of the $\text{S}_1 \leftarrow \text{S}_0$ (n, π) transition of the jet-cooled parent molecule and at 308 nm where absorption takes place into the long wavelength tail of the much more intense $\text{S}_2 \leftarrow \text{S}_0$ transition. $\text{NO}(\text{N}_1)$ fragments were probed by two-

photon LIF near 450 nm, and CN was interrogated by single-photon LIF on the B - X transition near 380 nm. Supersonic expansion with He was employed to narrow the internal energy and angular momentum distribution of the parent molecule under conditions where completion was negligible. NO from the 396 nm photodissociation was found to carry no vibrational excitation but a large amount of rotational energy (16% of the available excess energy). The rotational population distributions for both spin-orbit states are Gaussian shaped peaking near $J = 30.5$ and clearly reflect impact dominated dissociation dynamics known from CH_3ONO and N-nitrosodimethylamine.^{1,2} Nascent NO with high angular momentum is aligned weakly in the plane of the dissociating parent, and the $\text{N}-(\text{A}')$ lambda doublet components are preferred indicating that the plane of the parent framework is preserved during the dissociation process. Doppler profile measurements of several NO two-photon LIF lines were used to estimate the translational energy released in this dissociation. $\text{CH}(\text{X})$ could not be detected in the 396 nm photolysis.

Photolysis of NMCA with unpolarised 308 nm excimer laser light in contrast produced vibrationally excited CN with a Boltzmann like rotational population distribution peaking near $N = 12$. The contrasting energy disposal into CN and NO and the photodissociation mechanisms involving both single and multiphoton absorption processes will be discussed.

References

1. O. Benoist d'Azy, F. Lahaani, C. Lardeux, and D. Solgadi, *Chem. Phys.*, **1985**, 94, 247.
2. M. Dubs, U. Brühlmann, and J.R. Huber, *J. Chem. Phys.*, **1986**, 84, 3106.

TRACE ANALYSIS OF NO_x BY HIGH RESOLUTION JET SPECTROSCOPY

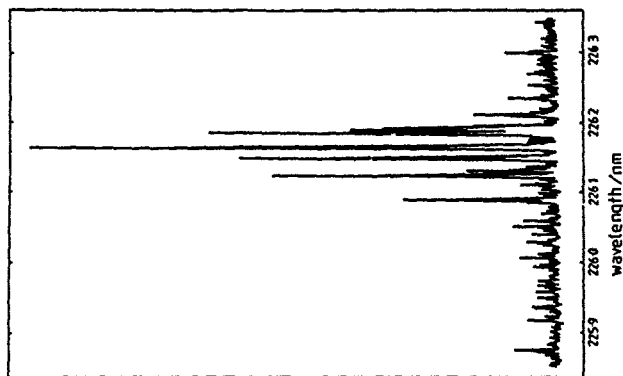
V.M. Young, A.H. Yates, M.R.S. McCoustra and J. Prab
Department of Chemistry, Heriot-Watt University,
Riccarton, Edinburgh EH14 4AS, Scotland

The control and abatement of air pollution by nitrogen oxides (NO_x) and their derivatives requires reliable analytical techniques capable of sub-ppb sensitivity and very high selectivity. A major goal remains the comparison and harmonisation of different measurement techniques using in general very diverse physical and chemical principles. A high resolution spectroscopic technique capable of directly analysing NO_x, HNO₃ (X = 1-4) and their derivatives using the same principle and equipment is highly desirable.

We report first results from a demonstration project that aims to develop and use laser techniques with very high sensitivity and selectivity for the laboratory based analysis of atmospheric NO_x pollutants and their gaseous chemical derivatives. Our approach is based on the detection and analysis of NO and OH by laser-induced fluorescence (LIF) in supersonic jet expansions of air or Ar-air mixtures. This technique minimises loss of sensitivity by collisional relaxation and fluorescence quenching. The low temperature of supersonic jets in combination with a narrow bandwidth tunable laser source provides the spectral selectivity of a high resolution spectroscopic technique in the UV and visible spectral regions.

Both two- and single-photon LIF have been used to analyse NO in Ar and air on the A²Σ⁺ ← X²Π_{1/2} transition. Initial detection limits in the ppb range, limited mainly by background effects and the outgassing of NO from rubber and plastic components are reported. The relative merits of continuous and pulsed supersonic jets and the effects of seed gas and nozzle distance on the rotational cooling of NO have been studied. The detection limits for NO analysis using continuous nozzle expansions are significantly poorer than for pulsed expansions and are influenced by pumping speed of the apparatus and the spatial collection of the fluorescence light.

The example shown in the figure presents an LIF spectrum of 50 ppb NO in a c.w. expansion of 300 torr Ar with a 50 μm glass nozzle.



Results of the analysis of NO_x by photofragmentation/LIF in supersonic jets using two-photon and single-photon photolysis with detection of the NO or O fragments by LIF will also be reported.

We thank the Commission of the European Communities and the Royal Society of Edinburgh for the support of this work.

THE 355nm PHOTODISSOCIATION OF JET-COOLED ALKYL THIONITRITES

P.A. Giovanacci, M.R.S. McCoustra* and J. Pfab

Department of Chemistry, Heriot-Watt University, Edinburgh, EH14 4AS, U.K.

The photodissociation dynamics of molecules containing NO has recently attracted considerable interest in laser photochemistry and spectroscopy¹. The ground state NO molecule (${}^2\Pi$) is an ideal fragment for probing by the powerful laser-induced fluorescence (LIF) technique. Much microscopic detail of the dynamics and stereochemistry of dissociation processes can be inferred from rovibronic and fine-structure populations obtained from LIF spectra of nascent NO.

Our previous single-colour dissociation plus probe experiments showed that the 450 nm photodissociation of gaseous methyl and t-butyl thionitrite at 300 K proceeds from S_2 . The electronic absorption spectra of alkyl thionitrites reveal a weak S_1-S_0 (n, π^*) transition near 550 nm and a more intense S_2-S_0 band peaking near 350 nm. Here we report a more detailed study of the 355 nm photodissociation of jet-cooled CH_3NO and $(CH_3)_3CSNO$.

Mixtures of the thionitrites in helium (500-600 torr) were expanded through a commercial pulsed molecular beam valve. Helium was employed as the carrier gas as earlier studies using argon had exhibited a marked stagnation pressure dependence of the nascent NO rotational state distributions. Similar helium-based expansions containing ca 1% of NO yielded rotational temperatures of between 30 and 50 K. Thus the parent angular momentum and internal energy were appreciably reduced. The free jet expansion was crossed 8-10 mm downstream of the orifice by the collinearly counter-propagating dissociation and probe lasers. The dissociation light was provided by the third harmonic of a Q-switched Nd:YAG laser (JK HyperVAG) while the probe laser was an excimer-pumped dye laser (Lambda Physik EMG101M5C/FL3002).

Nascent NO $X^2\Pi$ state distributions were obtained from two-photon LIF excitation spectra of the nascent NO via the $A^2\Pi - X^2\Pi$ transition. The distributions were highly inverted, typically peaking at around $J''=30.5$. Spin-orbit and Λ -doublet distributions were also extracted from these spectra. The complication of alignment was avoided by saturating the

photodissociation process. Using a sub-Doppler resolution probe laser, rotational line contours for several lines of the nascent NO $A^2\Pi - X^2\Pi$ $O_{1/2}$ branch were recorded. Doppler widths and hence nascent NO translational energies were extracted.

The energy disposal based on an S-N bond dissociation energy of 120 kJ mol⁻¹ is summarised for both molecules in the table. The NO fragment is vibrationally cold but rotationally hot with a strongly inverted, gaussian shaped rotational population distribution. The Λ -doublets show a preference for the $\pi(A'')$ component indicating a planar dissociation process, and there is some spin-orbit selectivity favouring the ${}^2\Pi_{1/2}$ component.

TABLE

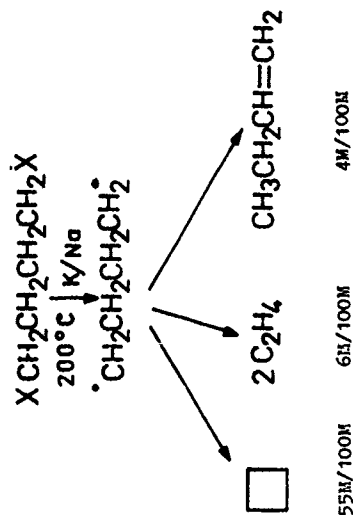
Energy Disposal in the 355nm Photodissociation of Jet-Cooled RSMO

	R=Me/cm ⁻¹	R=t-Bu/cm ⁻¹
NO		
translation	3650 (22.6%)	5022 (30.8%)
rotation	2375 (14.7%)	2096 (12.8%)
vibration	<202 (<1.25%)	<200 (1.2%)
electronic	57 (0.35%)	55 (0.34%)
F_1/F_2	1.2	1.3
R		
translation	2325 (14.4%)	1522 (9.3%)
internal	>7531 (>46.6%)	>7423 (>45.5%)

*Permanent address: School of Chemical Sciences, University of East Anglia, Norwich NR4 7TJ, U.K.

References:

1. H. Reisler, M. Noble and C. Wittig, "Molecular Photodissociation Dynamics", edited by M.N.R. Ashfold and J.E. Baggott (Royal Society of Chemistry, London, 1987), p. 139.
2. M.P.S. McCoustra and J. Pfab, Chem. Phys. Lett., 1987, 137(4), 355.



In the dihalogenide series $\text{C}_5 - \text{C}_{12}$ the ratio of contributions of cyclisation to isomerisation reactions was maximal in C_5 . Then it was sharply falling (for $\text{C}_6 - \text{C}_8$) to become negligible for C_9 and grow again (for $\text{C}_{10} - \text{C}_{12}$). In dihalogen $\text{C}_5 - \text{C}_{12}$ decomposition is practically 100% existent. As the number of hydrogen atoms in the diradical grows, the cyclisation and isomerisation reactions selectivity falls due to competition of bimolecular reactions resulting in alkanes and nonvolatile products.

References

1. L.E. Guselnikov, V.V. Volkova, U. Ziegler, H. Zimmermann, B. Ondruschka, and P.E. Ivanov. *Isv. Akad. Nauk SSSR, Ser. Khim.*, 1986, 2151
2. L.E. Guselnikov, E.A. Volnina, A. Al-Yahya, V.V. Volkova, *Isv. Akad. Nauk SSSR, Ser. Khim.* 1986, 2640
3. C.E.H. Bawn, J. Milsted, *Trans. Faraday Soc.* **35**, 889, 1939.
4. D. Otteson, J. Michl, *J. Org. Chem.* **49**, 886, 1984.

DEHALOGENATION OF α, ω -DIHALOGENOPOLYMETHYLENES USING ALKALI METAL VAPOURS. GAS PHASE GENERATION AND REACTIONS OF DIRADICALS.

A. Al-Yahya, E.A. Volnina and L.E. Guselnikov

A.V. Topchiev Institute of Petrochemical Synthesis, USSR Academy of Sciences, 117912, Moscow, USSR.

Polymethylene diradicals are reaction intermediates in the cycloalkane pyrolysis, in photochemical conversions of cyclic azo compounds and ketones, synthesis of small ring systems, and other organic compounds [1]. We studied gas phase reactions of dehalogenation of α, ω -dihalogeneopolymethylenes $\text{C}_5 - \text{C}_{12}$ by vapours of K/Na (180-300°C, 0.1-1.0 Torr) generating polymethylene diradicals. We pursued the aim of defining the changing contribution of the characteristic reactions of α, ω -diradicals (cyclisation, isomerisation, decomposition) as the length of the polymethylene chain grows and the nature of halogen in the dihalogenide molecule changes. While the high selectivity of cyclopropane formation in the dehalogenation of the 1,3-dichloro- and 1,3-dibromopropane seemed evident, the formation of cyclobutane with a selectivity of 55/100M of converted 1,4-dichlorobutane (35% conversion) was unexpected [2], for it had been reported that analogous reactions do not entail the formation of cyclobutane [3], or its yield does not exceed 3% [4]. After passing over to 1,4-dibromo- and 1-chloro-4-bromobutane, the selectivity of formation of cyclobutane was falling to 34.3 and 32M/100M, correspondingly. Products of decomposition and isomerisation of tetramethylene diradical were formed along with cyclobutane. In the table are given Arrhenius parameters of dehalogenation:

X	log A		E ₁
	s ⁻¹		
Cl	1.24 ± 0.6		kcal/mol 9.1 ± 0.9
Br	3.4 ± 0.3		3.9 ± 0.3

DIRECT INFRARED SPECTROSCOPIC
EVIDENCE FOR ALLYL RADICAL AND
DEFINITION OF THE INITIATION
STEP IN THERMAL DECOMPOSITION
OF CYCLOALKANES

L. E. Gusel'nikov, V. V. Volkova, and L. V. Shevelkova
A. V. Topchiev Institute of Petrochemical Synthesis,
URSS Academy of Sciences, 117912, Moscow, USSR.

G. Zimmermann and U. Ziegler

Central Institute of Organic Chemistry, GDR, Academy
of Sciences, 705 Leipzig, GDR

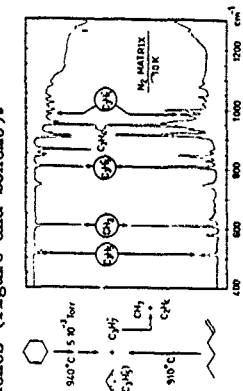
One of the problems of the hydrocarbon pyrolysis mechanism is identifying free radicals responsible for the initiation step of the radical chain reaction and, in particular, detecting and studying the elementary reactions of the low-coordination hydrocarbon compounds making up the active gaseous phase of the cycloalkane pyrolysis. To detect the primary products of monomolecular thermal conversions of cycloalkanes, we used pyrolysis at very low pressures ($750\text{--}970^\circ\text{C}$, $10^{-5}\text{--}10^{-10}$ Torr) along with low-temperature matrix isolation and IR spectroscopy. Following comparative study of pyrolysis of isomeric cycloalkanes and 1-alkenes $\text{C}_4\text{--C}_7$, we obtained direct IR-spectroscopy evidence for the same radicals and stable products produced for each pair of hydrocarbons $\text{C}_5\text{--C}_7$, the allyl radical (517 , 808 , 985 cm^{-1}), ethylene (948 cm^{-1}) and allen (847 , 1940 cm^{-1}) being found in all cases. Moreover, in IR-spectra of cyclohexane pyrolysis products absorption bands of methyl radical (613 cm^{-1}) were observed, whereas in the spectra of cyclopentane and cycloheptane pyrolysis products we have found absorption bands of ethyl radical (535 cm^{-1}).

Among other cycloalkanes pyrolysis products, we also identified isomeric alkenes, and cyclopropane in the case of cyclopentane, and cyclopentane in the case of cycloheptane. The latter seem to be attributable to the loss of ethylene by penta- and heptamethylene radicals.

On the whole the products composition of vacuum pyrolysis of cycloalkanes and of isomeric alkenes is identical, though the decomposition temperature of the for-

mer is about 50K higher than that of the latter. The only exception is cyclobutane. The matrix IR-spectrum of its pyrolysis products reveals only ethylene, while the IR-spectrum of 1-butene pyrolysis reveals absorption bands of methyl and allyl radicals.

Thus, this is a novel identification of radicals formed upon pyrolysis of cycloalkanes, and a direct evidence for isomerisation of the latter into 1-alkenes (Figure and Scheme).



The absence of radicals in the IR-spectrum of the cyclobutane pyrolysis products is due to the nature of the tetramethylene diradical which is favourable for the rupture of the C-C bond in β -position towards the two radical centres. In the conventional pyrolysis the contribution of the cycloalkane isomerisation reaction (initiation step) is negligible. Thus, in the cyclohexane pyrolysis, the yield of methane, produced at the initiation step, is only 5-8% at $750\text{--}880^\circ\text{C}$. Indeed, in the n-hexane, hexene, cyclohexane series the lowest current concentration of methyl radicals is realised in the pyrolysis of the latter. Meanwhile, the concentration of H-atoms, produced at the propagation step of cyclohexane pyrolysis, is nearly a hundred times higher than that of methyl radicals.

At the same time, of the mentioned row of isomeric hydrocarbons C_6 , the cyclohexane pyrolysis is characterised by the lowest concentration of hydrogen atoms, its sharp dependence on the temperature being determined by the activation energy of the initiation stage of the overall decomposition process.

The obtained data reveals that the higher thermal stability of cycloalkanes as against isomeric alkenes and alkanes is determined by the difficulty of the isomerisation of cycloalkane into alkenes.

SELF-IGNITION OF COMBUSTIBLE GASES PROMOTED BY DIFLUOROAMINE RADICALS

A.A. Borisov, V.M. Zamanskii, V.V. Lisiyanski, S.A. Rusakov, and G.I. Skachkov

Institute of Chemical Physics, USSR Acad. Sci.,
USSR, 117977 Moscow

N_2F_4 additives to hydrocarbon/oxygen mixtures (in amounts of one percent of the fuel concentration) shorten substantially the ignition delays τ , it turned out that the promoting effect of NF_2 radicals formed upon thermal decomposition of N_2F_4 is comparable with that of the most efficient promoters, organic nitrates and nitrites, and sometimes even exceeds it. In the present work the effect of NF_2 radicals on self-ignition of a wide variety of fuels, CH_4 , C_2H_6 , C_2H_4 , C_3H_8 , $n-C_4H_{10}$, $n-C_7H_{16}$, CH_3OH , C_2H_5OH and NH_3 was investigated with the purpose of elucidating the mechanism of promoted reactions. The experiments were carried out in a static apparatus and behind reflected shock waves in a shock tube. The ignition delay values were measured from pressure profiles and light absorption signals at 260.0 and 306.4 nm corresponding to absorption bands of NF_2 and OH. Initial temperature, pressure and N_2F_4 concentration were varied in the range 700-1870 K, 1-6 atm, and 1-15% (with respect to the fuel), and τ were measured in the range 20 μ s - 2 s.

The experiments show that NF_2 radicals are efficient promoters of self-ignition of most of the fuels studied. The strongest influence of N_2F_4 additives on ignition was observed for CH_4 . The promoter efficiency is dropping as the number of atoms in a molecule (see Table 1) and initial temperature increase.

Measurements of the rate of NF_2 radical consumption in N_2F_4 mixtures with Ar, CH_4 or O_2 showed that to within a factor of 2-3 the rate constant of the reaction $NF_2 + H \rightarrow NF + F + H$ was not affected by the presence

of CH_4 or O_2 . This implies that the fast disappearance of NF_2 radicals in combustible mixtures observed in the experiments is due to the presence of both CH_4 and O_2 . To elucidate the mechanism of the promoted reaction we performed a mathematical modelling of the self-ignition reaction taking as an example the kinetic CH_4 oxidation scheme consisting of 54 steps supplemented with various hypothetical elementary reactions involving NF_2 and accounting for its promoting effect. Agreement of the calculated and measured τ is attained when the reaction $CH_3O_2 + NF_2 \rightarrow CH_2O + F + FNO$ with a rate constant of $5 \cdot 10^{-12}$ cm³ mol⁻¹ s⁻¹ is taken into account. The promoting effect is chiefly due to the additional formation of CH_3O radicals, that decompose easily to give CH_2O and H atoms, and to the homogeneous catalysis: $NO + HO \rightarrow NO_2 + OH$, $NO_2 + CH_3 \rightarrow CH_3O + NO$. Qualitatively the mechanism of the promoting process is similar for other hydrocarbons and also for alcohols, the rate controlling step in it is the reaction $RO_2 + NF_2 \rightarrow RO + FNO + F$ (with R - hydrocarbon radical). The presence of NF_2 in cool-flame oxidation of hydrocarbons will develop cool-flame into hot ignition, the yield of alcohols in selective hydrocarbon oxidation process is enhanced. A high promoting efficiency of NF_2 radicals allows one for each particular system to select as a promoter an organic or inorganic difluoroamine suitable by its physical and chemical properties. The only condition for such a selection is a fast decomposition of a RNF_2 molecule. The difluoroamine derivatives are a new class of efficient promoters of high-temperature oxidation.

Table 1. An effect of N_2F_4 additives on τ for various mixtures.

% of N_2F_4	T, K	Mixture composition	τ/τ_0 , %
0.06	1000	$6CH_4-12O_2-Ar$	50
0.19	800-1000	$1,5C_2H_6-2O_2-Ar$	3-2
0.2	800-1000	$1C_2H_6-5O_2-Ar$	100-10

1. A.A. Borisov, B.E. Gel'fand, S.V. Dragalova, V.M. Zamanskii, V.V. Lisiyanski, G.I. Skachkov, S.A. Tsyganov. *Khim. Fizika* 1983, 6, p. 838.
2. V.M. Zamanskii, V.V. Lisiyanski, Y.M. Gershenzon, V.B. Rozentshtein. *Khim. Fizika*, to be published.

MATRIX DESIGNED STUDIES IN CHEMICAL KINETICS

C Anastasi and J Alvarez-Alvarez

Department of Chemistry, University of York, Heslington, York YO1 5DD, England.

There are many problems in chemical kinetics in which the key observation is function of many variables. For example, in laboratory studies on the production of NO_x by electrical discharges, the important variables are thought to be pressure, energy, spark gap and the type and magnitude of trace gases in the N_2/O_2 mixtures. To fully establish the NO_x response to each of these variables would require a very large number of experiments. In the early stages of a study of this kind it is often much more important to "map" out the area and identify and quantify the dominant variables. To this end, matrix designed experiments offer a most effective use of experimental time.

Table (1) shows the design of the matrix that has been used to investigate the effect of energy, spark gap and pressure on the NO_x produced in a laboratory study; each of these variables has three values giving a matrix consisting of 3^3 or 27 experiments. This table also shows the NO_x produced for each set of conditions.

Analysis of Variance and Multiple Linear Regression¹ are used to analyse the results from this matrix. Table (2) shows the response factors for each of the three variables considered; if these factors are multiplied by typical experimental values for each variable, their magnitudes are of a similar size. No interaction between variables was evident. Table (2) also shows these response factors to be in very good agreement with those determined in the traditional manner.

It is possible to go a step further to fully exploit the matrix approach to experimental design; the same quantitative results can be extracted from a matrix size considerably smaller than that used above. Table (3) shows three matrices each of just nine experiments derived from the main set in Table (1). Analysis of these matrices using the approach indicated above yields the values shown in Table (2). Clearly the response factors derived are in good agreement with those obtained from the full matrix although the standard errors are larger.

1. C Anastasi, J T H Harrison and M Stark, Tenth International Symposium on Gas Kinetics, Swansea, UK, July 1988 and unpublished results
2. H D Gesser, N R Hunter, C B Prakash, Chem Rev, 85, 235 (1985)
3. "Design and Analysis of Industrial Experiments", Ed. O L Davies, Oliver and Boyd, Edinburgh 1971
4. O Kempthorne, "Design and Analysis of Experiments", Wiley, New York, 1962

Table 1. Full Matrix Design

Exp	Variable ^a			NO_x ^b
	A	B	C	
1	0	0	0	468
2	0	0	1	854
3	0	0	2	1210
4	0	1	0	971
5	0	1	1	1420
6	0	1	2	1800
7	0	2	0	1280
8	0	2	1	1930
9	0	2	2	2780
10	1	0	0	840
11	1	0	1	1180
12	1	0	2	1590
13	1	1	0	1340
14	1	1	1	2020
15	1	1	2	2530
16	1	2	0	2170
17	1	2	1	2690
18	1	2	2	3380
19	2	0	0	1070
20	2	0	1	1410
21	2	0	2	1840
22	2	1	0	2030
23	2	1	1	2400
24	2	1	2	2700
25	2	2	0	2660
26	2	2	1	3190
27	2	2	2	3860

Table 2. NO_x Response Factors^{b,c}

	Variable ^a		
	Spark gap	Energy	Pressure
Full Matrix	235 ± 20	19.0 ± 1.6	3.7 ± 0.2
Partial Matrix I	191 ± 27	17.9 ± 2.2	3.8 ± 0.3
Partial Matrix II	254 ± 31	22.0 ± 2.4	3.4 ± 0.3
Partial Matrix III	259 ± 47	17.2 ± 3.7	3.7 ± 0.5
Reference 1	245	19.0	3.8

Table 3. Partial Matrix Designs

Exp	I Variable ^a A B C			II Variable ^a A B C			III Variable ^a A B C		
	A	B	C	A	B	C	A	B	C
1	0	0	0	0	0	2	0	0	0
2	0	1	1	0	1	1	0	1	2
3	0	2	2	0	2	0	0	2	1
4	1	0	0	1	0	1	1	0	2
5	1	1	1	1	1	0	1	1	1
6	1	2	2	1	2	2	1	2	0
7	2	0	0	2	0	0	2	0	1
8	2	1	1	2	1	2	2	1	0
9	2	2	2	2	2	1	2	2	2

notes:

- (a) A = Spark Gap / mm : 0=4; 1=6; 2=8
 B = Pressure / torr : 0=100; 1=300; 2=500
 C = Energy / J : 0=50; 1=75; 2=100
 (b) Response factor / 10^{14} molecules
 (c) ± standard error

THE SELF-REACTIONS OF METHYLPEROXY RADICALS IN THE GAS-PHASE

C. Anastasi, P.J. Couzens, D.J. Waddington

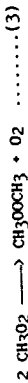
Department of Chemistry, University of York, Heslington,
York, YO1 5DD United Kingdom.

M.J. Brown, D.B. Smith

British Gas plc, London Research Station, Michael Road,
London, SM6 2AD United Kingdom.

A key species involved in both atmospheric and combustion chemistry is the alkylperoxy radical which can undergo both propagation and termination reactions

The self-reactions of methylperoxy radicals have been studied using techniques developed during work on the reactions of ethylperoxy^{1,2} and isopropylperoxy³ radicals in which three individual reaction routes have been proposed. The analogous reaction channels for methylperoxy are:



Methylperoxy radicals were produced by the photo-oxidation of azomethane and their self-reactions have been examined over a temperature range of 250 - 420 K, at a total pressure of 550 torr. Molecular Modulation Spectroscopy (MMS) was used to observe radical absorption changes and hence the overall rate of self-reaction. UV absorption was monitored in the spectrometer by phase-sensitive detection during periodically interrupted photolysis. A second-order decay model was used to fit mathematically the time dependent absorption changes and produce an observed rate constant. Methylperoxy radical absorptions were measured to obtain a spectrum, figure 1.

Stable products from the photo-oxidation of azomethane were analysed using gas chromatography, spectrophotometry and titrimetry.

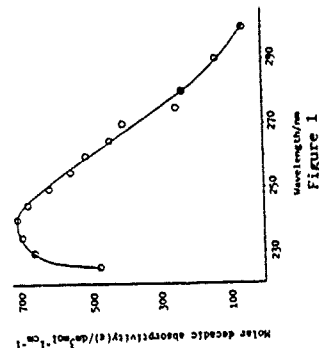
The end product analyses (combined with computer simulation of the kinetics) were linked with the results from the MMS experiments to assign values to the individual self-reaction rate constants.

The overall system was modelled with an 18 step reaction mechanism. The individual rate constants for the three self-reactions of methylperoxy radicals (reactions 1 - 3) at different temperatures were determined by combining the observed second-order decay rate constant, $k_{\text{obs}} = 2k_1 + k_2 + k_3$. Hence the temperature product distribution ($k_{\text{obs}} = 2k_1 + k_2 + k_3$). Hence the temperature dependence of each of the reactions 1 - 3 was obtained.

Reaction	A-factor/ $\text{dm}^3\text{mol}^{-1}\text{s}^{-1}$	Eact/ kJmol^{-1}
1	$(2.4 \pm 0.7) \times 10^8$	(4.8 ± 1.6)
2	$(7.6 \pm 1.3) \times 10^7$	(-2.1 ± 1.1)
3	$(1.1 \pm 0.8) \times 10^6$	(-7.0 ± 2.9)

References

1. C. Anastasi, D.J. Waddington, A. Woolley, J. Chem. Soc. Faraday Trans 1, 79, 505 (1983).
2. M.J. Brown, D.Phil Thesis, University of York, 1988.
3. L.J. Kirsch, D.A. Parkes, D.J. Waddington, A. Woolley, J. Chem. Soc. Faraday Trans 1, 74, 2293 (1978).



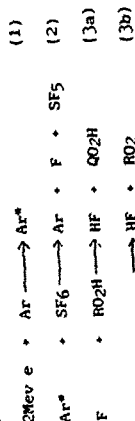
SPECTRUM AND KINETICS OF A QO₂H SPECIES.

C Anastasi(*), P Genske(*), P Pagsberg(*) and M Foxon(*)

(*) Department of Chemistry, Riso National Laboratory, DK-4000, Roskilde, Denmark.
 (*) Department of Chemistry, University of York, Heslington, York, YO1 5DD, England.

The QO₂H radical is a key intermediate in the autoignition chemistry of fuels ^{1,2}. The competition between the decomposition of this species and its addition to oxygen to form a peroxy radical, is thought to provide the thermokinetic "switch" central to the autoignition phenomenon. This intermediate has proved difficult to isolate and study; this paper presents the first direct study of a QO₂H radical, including its ultra violet absorption spectrum and mutual kinetics.

We have generated a QO₂H radical (where Q = CH₂(CH₃)₂COOH) by the pulse radiolysis of mixtures containing Argon, SF₆ and t-butyl hydroperoxide (RO₂H).



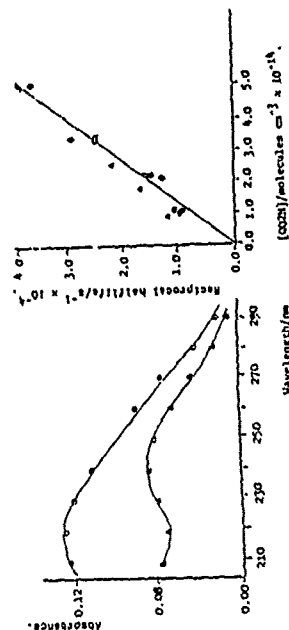
The concentration of F atoms is known ³ and it is assumed that their fast indiscriminate reaction with RO₂H yields a [QO₂H]/[RO₂] ratio of 9:1 in this system. Figure (1) shows the absorption spectra for both QO₂H and RO₂ in the 200-300 nm spectral region. The QO₂H spectrum (corrected for the small concentration of RO₂ using the known absorption cross section for this radical) is given by the "prompt" signal observed, while RO₂, which is essentially unreactive on the time scale of our experiments (.0005 sec), is the stable absorption signal measured at the end of the decay curves. The broad featureless QO₂H spectrum peaks at

220nm with an absorption cross section of $2.6 \times 10^{-18} \text{ cm}^2 \text{ molecule}^{-1}$.

The QO₂H absorption spectrum makes direct kinetic studies involving this species possible for the first time. Figure (2) shows a second order plot of reciprocal half life of QO₂H as a function of its concentration, varied by altering the dose, over the temperature range 298-398K. The gradient of the straight line given in Figure (2) is 2k₄, where $k_4 = 3.8 \times 10^{-11} \text{ cm}^3 \text{ molecule}^{-1} \text{ s}^{-1}$ and is the temperature independent rate constant for the mutual reaction (4).



1. M P Halstead, L J Kirsch, A Prothero and C P Quinn. Proc. R. Soc. Lond. A. 346, 515, 1975.
2. S L Hirst and L J Kirsch. Combustion Modelling in Reciprocating Engines. Ed. C Amano and J Mattavi, 193, Plenum 1980. Chem. Phys. 3. C Anastasi, J Munk, P Pagsberg and A Sillesen. Chem. Phys. Letts. 146, 371, 1988.
4. D A Parkes. Proc. of the Fifteenth Symposium (International) on Combustion, Tokyo, Japan, 1975.

Fig. (1). Spectra of QO₂H (a) and RO₂ (b).Fig. (2). Reciprocal half-life versus [QO₂H]. (a) 298K, (b) 335K, (c) 358K, (d) 398K.

THE DECOMPOSITION OF METHANE

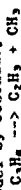
R.W. Barnes and G.L. Pratt

School of Chemistry and Molecular Sciences, University of
Sussex, Brighton, Sussex.
BN1 9QJ.

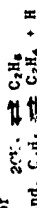
The early stages (0.003 - 0.05% reaction) of the pyrolysis of methane have been studied using a quartz lined incalcoy 800 flow reactor, as a function of temperature and pressure over the ranges 500-1073 K and 10⁻³-10⁻¹ bar. In pure methane and in the diluents helium, argon and hydrogen. The products ethane, ethylene, acetylene and propylene have been analysed by gas chromatography. The reaction profile has been modelled using the 36 step reaction scheme of Roscoe and Thompson¹. The reaction rate is initially constant, determined by the rate constant (k_1) of the dissociation step



Shortly after the appearance of the tertiary product propylene the reaction rate noticeably increases. This autocatalysis is accounted for in the model by secondary initiation, chiefly via,



Using literature rate constants and taking account of the pressure dependencies of



and $\text{C}_2\text{H}_6 \rightleftharpoons \text{C}_2\text{H}_5 + \text{H}$ the model satisfactorily simulates the reaction profiles up to the early stages of autocatalysis over the ranges of temperature and pressure used. Values of k_1 have been extracted directly from the data using measurements of reaction rate up to the point of onset of autocatalysis at lower temperatures and by using the autocatalytic model at 1123 and 1148K. The variation of k_1 with pressure shows the reaction to be in the fall-off region at all pressures studied, but approaching the high-pressure limit at 50 bar. The temperature range is similar to that used by Chen, Back and Back² who measured k_1 at sub-atmospheric pressure in a static system. High-pressure limit values have been obtained from fits of the RRKM curves of Tsang and Hampson³ to the high and low pressure data. These k_1 values are a factor of two higher than those obtained by Chen, Back and Back². Values of k_2 obtained via the equilibrium constant are consistent with an activation energy close to zero for the reverse reaction by comparison with the data of Cheng and Yeh⁴, Patrick et al⁵ and Brouard et al⁶. Taking this value

together with the thermodynamic data gives a value for E_1 which leads to the Arrhenius expression

$$(k_1/\text{s}^{-1}) = (1.75 \times 10^{-25}) \exp(-440.7 \text{ kJ mol}^{-1}/RT)$$

which gives the best fit to the data.

Pyrolysis of mixtures of 10% methane in helium and argon enabled fall-off curves for k_1 in these buffer gases to be obtained. Comparison with strong collision RRKM curves gave ρ values of 0.12, 0.099, 0.092 for CH₄, He, Ar respectively.

Methane pyrolysis has also been studied in 50% and 90% H₂ over the conditions 500-1073 K and 10⁻³-10⁻¹ bar. Ethane and ethylene are the only detectable products under all conditions. The reaction rate is constant initially but at longer residence times is seen to decrease. This is due to the recombination reaction



becoming important when the hydrogen atom concentration rises to a steady value about 1/20 of the methyl radical concentration. In the absence of H₂, hydrogen atoms react via,



to reach a steady concentration four powers of ten below that of the methyl radical. k_1 values have been extracted directly at 5 and 10 bar where the reaction rate is steady and by modelling at 30 and 50 bar using a 9 step mechanism. Comparison with the RRKM curves suggests ρ for hydrogen is small compared with that of methane and probably in the region of 0.01.

The results clearly demonstrate the need to take into account the pressure dependence of reaction (1) when high temperature shock tube studies of methane pyrolysis are interpreted. We thank British Gas for help with all aspects of this work.

References.

1. J.M. Roscoe and M.J. Thompson, *Int. J. Chem. Kinetics*, **17**, 967 (1985).
2. C.J. Chen, M.H. Back and R.A. Back, *Can. J. Chem.*, **53**, 3580 (1975).
3. W. Tsang and R.F. Hampson, *J. Phys. Chem. Ref. Data*, **15**, 1087 (1986).
4. J. Cheng and C. Yeh, *J. Phys. Chem.*, **81**, 1982 (1977).
5. R. Patrick, M.J. Pilling and G.J. Rogers, *Chem. Phys.*, **53**, 279 (1980).
6. M. Brouard, M.T. MacPherson, M.J. Pilling, J.M. Tullock and A.P. Williamson, *Chem. Phys. Lett.*, **113**, 413 (1985).

MODELLING OF THE GAS-PHASE OXIDATION OF CYCLOHEXANE

S.E. KLAÏ and F. BARRINET

Département de Chimie-Physique des Réactions, U.A. n° 328 CNRS
INPL-ENSIC, 1, rue Grandville 54042 NANCY, France

An experimental investigation of the gas-phase oxidation of equimolar mixtures cyclohexane-oxygen at subatmospheric pressure has been performed in a conventional static apparatus; a fine thermocouple in the centre of the reaction vessel allows to record the variations of the instantaneous temperature of the gas phase as a function of time.

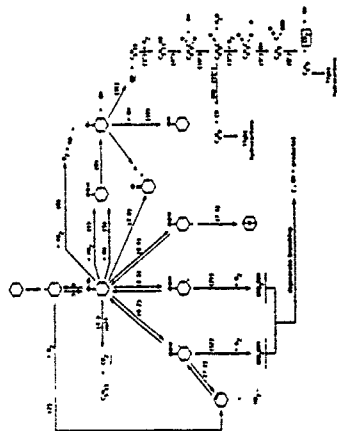
We have plotted a pressure-temperature diagram which is rather close to those already determined by other authors (1). We have used a device for the injection of liquid cyclohexane through a septum, similar to those already proposed by LUCQUIN et al. (2) and by CULLIS (3) since the vapour pressure of cyclohexane is relatively low (≈ 100 torr at 25°C). It is also worth noting that the experiments are not completely reproducible. To improve the reproducibility of our experiments we have used the technique proposed by MARSHALL et al. (4) which aims at reducing the wall effects.

After these preliminary experiments, we have developed a detailed investigation of the slow reaction at 362°C and around 45 torr of equimolar mixture, in order to determine the primary products of the reaction. The product formation has been compared to the reactant consumption (cyclohexane, O_2) and a reasonable mass balance has been obtained.

Taking into account today's background on hydrocarbon oxidation reactions and the experimental distribution of the primary reaction products, we have built a reaction mechanism. Because of the dearth of rate constants in the literature, we have estimated all the rate constants of the elementary steps by the methods of Thermochemical Kinetics proposed by BENSON (5). These calculations make possible a simplification of the reaction mechanism since the minor reaction pathways can be neglected.

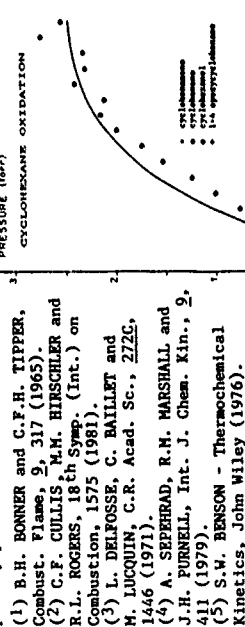
Our mechanism is outlined in the figure.

To simulate the product formation vs time, various integration techniques have been used since the corresponding differential equations are stiff. We have adjusted the kinetic parameters to the experimental results and a rather satisfactory agreement between simulations and experimental results has been obtained.



The initial set of rate parameters obtained by Thermochemical Kinetics has been modified within a limited range (maximum 70 for only one rate constant) which is quite compatible with the accuracy of these calculations.

We give an example of the satisfactory adjustment between computed curves and experimental points for the major primary product formation.



The financial support of Rhône-Poulenc and the assistance of the Computer Department of the Research Centre at Décines are gratefully acknowledged.

- (1) B.H. BONNER and C.F.H. TIPPER, Combust. Flame, 9, 317 (1965).
- (2) C.F. CULLIS, M.M. HIRSCHLER and R.L. ROGERS, 18th Symp. (Int.) on Combustion, 1575 (1981).
- (3) L. DELFOSSE, C. BAILLET and M. LUCQUIN, C.R. Acad. Sc., 272C, 1446 (1971).
- (4) A. SEPPERAD, R.M. MARSHALL and J.H. PURNELL, Int. J. Chem. Kin., 9, 411 (1979).
- (5) S.W. BENSON - Thermochemical Kinetics, John Wiley (1976).

KINETIC MODELING OF N-BUTANE OXIDATION

A. CHAKIR, M. CATHONNET, J. C. BOETTNER and F. GAILLARD.

Centre de Recherches sur la Chimie de la Combustion
et des Hautes Températures - C.N.R.S.
1 C. Avenue de la Recherche Scientifique
45071 ORLÉANS Cedex 2 - FRANCE

The oxidation of n-butane was studied in a jet-stirred flow reactor in the temperature range 900-1200 K at pressures extending from 1 to 10 atm for a wide range of fuel-oxygen equivalence ratio (0.15 to 4.0).

The concentration of the molecular species were measured at different extents of reaction by gas chromatography. The major products were carbon monoxide, carbon dioxide, ethylene, propene and methane. Several other species were also detected as minor products: hydrogen, ethane, butadiene, acetylene, 1-butene, cis and trans 2-butene and acetaldehyde. In addition, some C₃ and C₅ olefins and diolefins were also found at trace level.

A detailed reaction mechanism developed previously for the modeling of C₁ to C₃ hydrocarbon oxidation^{1,2,3} was extended to reproduce the experimental data. The resulting mechanism includes 360 reactions and 56 chemical species.

A sensitivity analysis was used to determine the influence of uncertainties in the rates of reactions on the computation. Extensive comparison between experimental and computed results shows good agreement for most of the measured species.

The validation of the mechanism was extended to higher temperatures. In order to describe the oxidation of n-butane in shock tubes. The experimental ignition delays obtained behind reflected shock waves by Burcat et al.⁴ were compared with the predictions of the model. A good agreement was found with the available experimental data in the temperature range 1200-1700 K.

The results of the sensitivity studies were used to identify the rate determining processes and systematic comparison of the rate of each elementary reaction was made to determine the major reaction paths.

This analysis was performed to select the main reaction steps in various experimental conditions in the well stirred reactor or in the reflected shock wave. It can be used to build reduced mechanisms which can reproduce with sufficient accuracy some of the experimental data.

REFERENCES

1. Dagaut P., Cathonnet, M., Boettner, J.C., and Gaillard, F.: Combust. Flame, 71, 295 (1988).
2. Dagaut P., Cathonnet, M., and Boettner, J.C.: J. Phys. Chem., 92, 661 (1988).
3. Dagaut P., Cathonnet, M., Boettner, J.C., and Gaillard, F.: Combust. Sci. Technol. 56, 23 (1987).
4. Burcat A., Scheller K., and Lifshitz, A.: Combust. Flame, 16, 29 (1971).

AN EXPERT SYSTEM FOR THE DESIGN OF SIMPLIFIED REACTION MECHANISMS

J.-C. GINISTY, V. BUCCI, E. DEMANGE,
C. MULLER, G. SCACCHI and G.M. COME

DCPR (CNRS), ENSIC (INPL) and University NANCY I
1, rue Grandville, 54000 NANCY (France)

A prototype of expert system has been built in order to create gas-phase free radical reaction mechanisms. Its application is now limited to the pyrolyses and chlorinations of hydrocarbons. The required inputs are the molecular formulae of the reagents and a level of temperature, "low" or "high", which correspond respectively to the two limiting cases: long and short chain reactions. If necessary, experimental results, such as an incomplete list of important or negligible free radicals and molecules, can be introduced. Then, the system detects the main free radicals and products, and produces a simplified mechanism. A dialogue is set up between the expert-system and the chemist.

From the first input data, the system suggests a mechanism.

If the chemist does not agree with this mechanism, he can add other experimental results.

The system answers by indicating its deducts and possible contradictions and produces a new mechanism. The user can go until he agrees with a mechanism. The obtained results are the produced mechanism and the list of important products and main free radicals.

The prototype has been built with an expert-system tool using knowledge representation by facts and forward chaining as rule search method. This tool can also include LISP written procedures. Rules may be grouped in packages, which allows the introduction of a hierarchy in the knowledge base. The fact base contains chemical components, generated reactions and experimental information.

The knowledge base contains the rules of mechanism generation and simplification and the rules of base modification and printing. This base is divided into packages of rules, the two most important of which solve "high" and "low" temperature cases.

At "low" temperature, initiation is done by the breaking of C-C and C-Cl bonds. Chains are detected and thus, the system gives the list of the main products and of the chain carrier radicals. Termination processes involve only chain carriers, reactions involving products which are not experimentally observed are suppressed.

At "high" temperature, initiation is achieved by the breaking of simple bonds. Main radicals are only β type (like CH_3 , H, Cl, ...). They occur in metathesis, addition and termination processes.

β radicals disappear by monomolecular decompositions. Main radicals are deduced by logical rules from experimental results.

Until now, constituents are input by means of empirical formulae and only C, H and Cl atoms are treated. The suppression of these restrictions and the use of quantitative data will be the next step of software development.

VERY LOW CONVERSION PYROLYSIS
OF 1,2-DICHLOROETHANE

M. SALOUHI, P.M. MARQUAIRE and G.M. COME

DCPR (CNRS), ENSIC (INPL) and University NANCY I
1, rue Grandville, 54000 NANCY (France)

EXPERIMENTAL

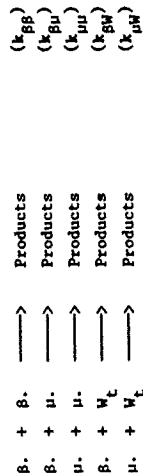
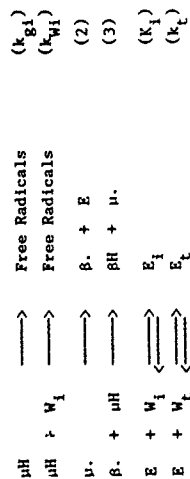
The pyrolysis of DCE has been studied by means of a continuous flow stirred tank reactor, between 360 and 520°C, 6 and 17 Torr, at very low conversions down to 0.001 %. The reaction rate has been deduced from the measured concentration of vinyl chloride, which is the main carbon containing reaction product.

EXPERIMENTAL RESULTS

We find that the kinetic laws (both qualitative and quantitative) are not the same in "fresh" or "seasoned" Pyrex, or walls treated by CCl_4 , C_2H_6 , H_2 . They strongly depend on the temperature. At 520°C, an induction period is observed in fresh Pyrex, while the rate is constant and lower than in the preceding case, in seasoned Pyrex. In seasoned Pyrex, an induction period is observed at 490°C, the rate is constant at 435°C and the reaction is self-inhibited at 410°C.

REACTION MECHANISM

In order to be able to interpret our results, as well as others from the literature, we suggest the following general hetero-homogeneous mechanism :



In this mechanism, μH is the reagent, E one main reaction product or an added unsaturated molecule, W_i and W_t are heterogeneous initiation and termination sites ; E_i and E_t are W_i and W_t sites "inactivated" by a molecule E.

From this mechanism, it is possible to deduce the expressions of the reaction rate and of the induction period.

CONCLUSIONS

By comparing the experimental results and the theoretical kinetic laws, we can deduce the following conclusions. At "high" temperatures, seasoned Pyrex is more efficient for terminating the chains than fresh Pyrex. At "low" temperatures and in seasoned Pyrex, k_i is greater than k_t , which means an inhibiting effect of small quantities of E, because of the inhibition of the heterogeneous initiation.

Generally speaking, wall effects in the reactions of halogenated hydrocarbons are well reconciled by adding to the classical homogeneous free-radical mechanism, heterogeneous initiation and termination processes inhibited by unsaturated molecules.

HIGH TEMPERATURE REACTION BETWEEN METHANE AND CHLORINE

M. CHAMON, P.M. MARQUAIRE and G.M. GOME

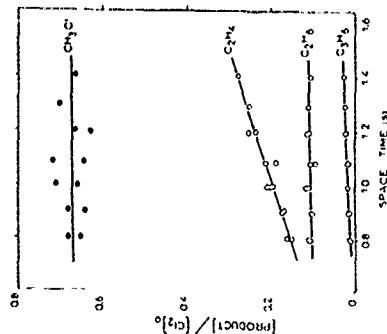
DCPR (CNRS), ENSIC (INPL) and University NANCY I
1, rue Grandville, 54000 NANCY (France)

The so-called BENSON process¹ consists in producing C_2H_4 by the reaction of CH_4 and Cl_2 in a flame. Due to its interest, a fundamental study of this reaction has been carried out using an isothermal continuous flow stirred tank reactor operated at temperatures varying from 1000 to 1300 K and at low concentrations of chlorine (about 1 % in volume).

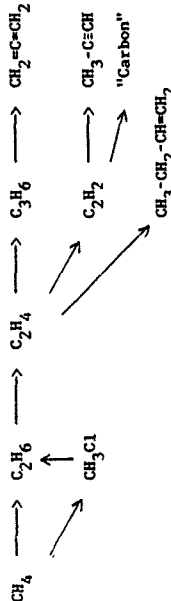
Under these conditions, the reaction leads mainly to the formation of the following carbon containing compounds : CH_3Cl , C_2H_4 , C_2H_6 , C_2H_2 , C_3H_6 .

The figure shows the ratios of the output product concentrations to the input chlorine concentration as a function of space time for the following operating conditions : $T = 1181$ K, $p = 577$ Torr, $[Cl_2]/[CH_4] = 0.0042$. In these conditions, C_2H_4 represents about 3 to 5 % of C_2H_4 and propyne is formed in negligible trace amounts.

For the sake of comparison, the pyrolysis of methane has been studied in the same conditions. Adding 0.41 % chlorine to methane increases the quantity of methane transformed in higher non chlorinated hydrocarbons by a factor equal to 25. If we take into account the increased formation of methylchloride, the total methane converted is multiplied by around 50.



These results agree with the classical radical primary mechanism of CH_4/Cl_2 reaction. At "low" temperatures, the reaction is a long chain one and it produces CH_3Cl , while, at "high" temperatures, the formation of C_2H_6 becomes preponderant when the chain length decreases. The secondary, tertiary ... reactions converts C_2H_6 into C_2H_4 , and further into C_3H_6 or C_2H_2 , according to the following scheme :



Moreover, at high temperatures, the decomposition of CH_3Cl also produced non chlorinated hydrocarbons : C_2H_6 , etc.

A comprehensive discussion of the reaction mechanism is presented. The essential fact in the thermal reaction of chlorine/methane mixtures is the shortening of the chain length of the primary mechanism with an increasing temperature, which results in a growing primary production of C_2H_6 as compared to that of CH_3Cl . In further reactions, C_2H_6 gives rise to C_2H_4 , C_2H_2 , C_3H_6 , etc., and non chlorinated hydrocarbons, at least in our experimental conditions. This is due to the predominant "u character" of alkyl free radicals at high temperatures.

References

1. S.W. BENSON, US Patent No 4 199 533, 1980.
2. M. CHAMON, P.M. MARQUAIRE and G.M. GOME, *C. Mol. Chem.*, **2**, 47, 1987.
3. M. WEISSMAN and S.W. BENSON, *Int. J. Chem. Kin.*, **16**, 307, 1984.
4. M. CHAMON, P.M. MARQUAIRE and G.M. GOME, *Can. J. Chem.*, **65**, 1491, 1987.

COMPUTER MODELLING OF THE THERMAL DECOMPOSITION
OF 3-METHYLPENTANE AT 420°C AND 133 MBAR

F. BILLAUD, K. ELYAHYAOUI, P. MALACARNE and F. BARONNET

Département de Chimie-Physique des Réactions, U.A. n° 328 CNRS,
INPL-ENSIC, 1, rue Grandville, 54042 NANCY, France

The thermal decomposition of 3-methylpentane has been the subject of a previous experimental study [P. MALACARNE, F. BILLAUD and F. BARONNET, J. Anal. Appl. Pyrolysis, 12, 243 (1987)]; the experimental results at low extents of reaction are interpreted by a long-chain radical mechanism of the Rice-Herzfeld type.

We propose now a more comprehensive mechanism which also accounts for the self-inhibited character of the reaction. This simulation has been performed by using a computer programme developed in our Department by the research team of Pr. G.M. CORNE. In this programme, a sensitivity analysis of the kinetic parameters of the reaction mechanism allows to detect among the bulk of the elementary steps those which are negligible, not determining and determining.

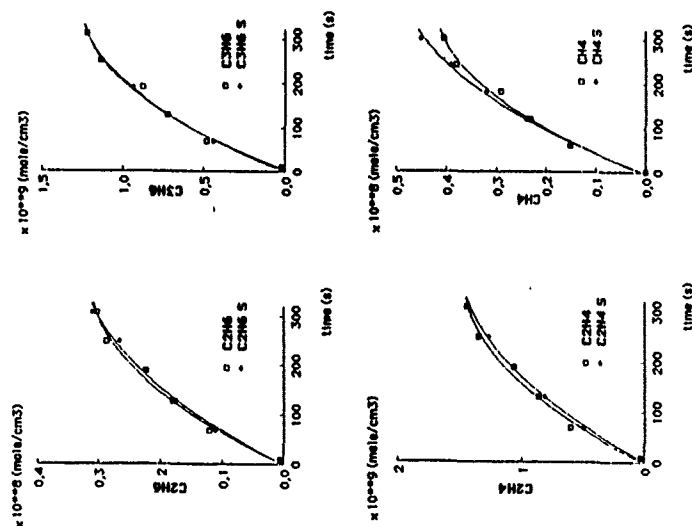
The calculation of the sensitivity coefficients

$$o_{ij} = \frac{\Delta C_i}{C_j} / \frac{\Delta k_i}{k_i} \text{ corresponding to the formation of a product } j (C_j)$$

concentration of j) from an elementary step i allows to know the list of the determining elementary steps which can have an influence on the value of C_j and therefore submitted to the optimisation procedure.

By using the compilation of kinetic parameters (preexponential factors and activation energies) published by ALLARA and SHAW for the pyrolysis of alkanes [J. Phys. Chem., Ref. Data, 9, 523 (1980)] we performed a first simulation. A fitting of the kinetic parameters was done in order to obtain a satisfactory modelling compared with our experimental results.

We present 4 figures describing the formation of the major reaction products (CH_4 , C_2H_6 , C_3H_8 and C_4H_{10}) in which we compare the experimental results and the optimised curves (obtained with a set of Arrhenius parameters) as a function of time.



(S corresponds to the simulated points)

There is a good agreement between our experimental results and the computed curves obtained from our model (49 elementary steps) at 420°C and 133 mbar. This suggests that this model gives a good description of the reaction, including its self-inhibition in our experimental range of residence times (1 to 5 minutes).

The Interaction of Carbon monoxide and Carbon dioxide with the homogeneous Reduction of Nitric Oxide by Ammonia.

H. E. Hemberger, J. Wollum

Physikalisches Chemisches Institut der Universität Heidelberg; Im Neuenheimer Feld 253, D-6900 Heidelberg 1

Control of emissions of oxides of nitrogen from combustion sources continues to be an environmental problem. One method for controlling NO_x emissions is based on the homogeneous noncatalytic reduction of NO by NH_3 in the presence of O_2 in the temperature range around 1250 K. In the present work a mechanistic study of the effects of CO and CO_2 on this system will be presented.

In all proposed chemical kinetics mechanisms nitric oxide is actually removed by the key reaction $\text{NH}_2 + \text{NO} \rightarrow \text{products}$. The amidogen radical is formed through oxidation of ammonia, principally by OH . The amount of OH produced controls the balance of reduction of NO and oxidation of NH_3 .

The reactions of other flue gas compounds besides NO , NH_3 and O_2 which influence the production of OH will also affect the reduction reaction. CO_2 is a main constituent of the flue gas and CO is a model substance for the combustion of hydrocarbons. So all effects of CO will be shown, if a hydrocarbon is added to the flue gas. The amount of OH production introduced by adding a combustible substance will determine the temperature range in which the reduction is practicable.

The reduction reaction does not reduce CO_2 and therefore does not generate CO . However, the reaction can inhibit the oxidation of CO to CO_2 , so if there is any CO left unburned when the NO is reduced, it may be possible that CO will be present in the flue gas, when it is discharged into the atmosphere, although there is enough oxygen at moderate temperatures to oxidise it. In the same way the removal of the rest of the ammonia may be shifted behind the minimum of the NO concentration.

Although the main reaction of the CO oxidation is $\text{CO} + \text{OH} \rightarrow \text{CO}_2 + \text{H}$ and, therefore, the NH_3 production is strongly affected, CO reduces the required temperature for the reduction of NO . In this context, hydrogen atoms, produced by the reaction of CO and OH , result in high concentrations of OH and O via the reaction $\text{H} + \text{O}_2 \rightarrow \text{OH} + \text{O}$, followed by the reaction $\text{O} + \text{NH}_3 \rightarrow \text{NH}_2 + \text{OH}$ and introduce additional chain branching to the system. This means that at low temperatures more NH_2 is produced

and the reduction reaction is started. The concentration profile of ammonia is also be moved to lower temperatures.

The application of the reduction process will be influenced by the results of this study, namely at low and high oxygen concentrations. At high concentrations of oxygen this could be used if the temperature in the flue gas is too low for practicable application of the noncatalytic reduction. Besides the effect of moving the "temperature window" to lower temperatures, the combination of this method with the method of modification of the combustion process, which produces CO in the flue gas, will become important in application. High CO concentrations means very low oxygen concentrations. ($\text{O}_2 < 0.5\%$) In this case the oxidation of the rest of the ammonia to NO is inhibited. Even at high temperatures ($T > 1000^\circ\text{C}$) the reduction is effective.

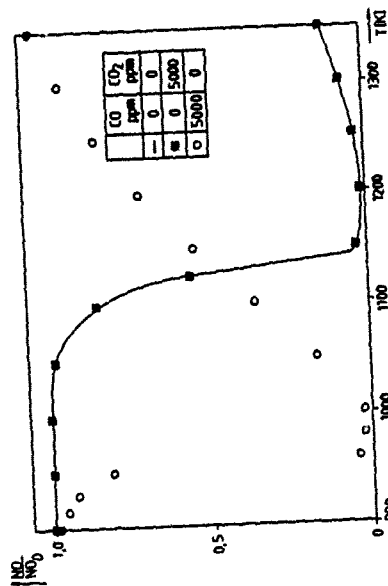


Fig. 1 Temperature dependence of the NO -concentration; shift of the "temperature window", if CO is present in the flue gas

High Temperature Oxidation of Methyl Chloride and Vinyl Chloride

G. Achhammer, M. Schnsieder, and J. Wolfrum
Physikalisch-Chemisches Institut Universitaet Heidelberg
Im Neuenheimer Feld 253, D-6900 Heidelberg, FRG

There are many publications concerning the oxidation of chlorinated hydrocarbons in the low temperature regime /1,2/, which is important for atmospheric chemistry. Only few experiments are reported for higher temperatures /3/ although there is an increasing interest in the understanding of waste incineration. Especially for molecules with low Cl/H ratio the existing studies have been restricted to overall kinetic measurement neglecting detailed mechanistic considerations /4/.

We have investigated the reaction of methyl chloride and vinyl chloride with oxygen at temperatures between 700 and 1200 K. The product distribution was analyzed by capillary gas chromatography and a gc/ms coupling, starting with a static system which facilitated the development of proper analytic conditions. For detailed investigations we used a flow system at total pressures from 100 to 1000 mbar, a residence time from 0.3 to 6 sec., varying the ratios of reactants over a wide range.

For both compounds a similar qualitative composition of the product mixtures was found. With increasing oxygen concentration the reaction changes from a typical pyrolysis (leading to acetylene, 2-chlorobutadiene and aromatics) to oxidation (yielding CO, CO₂ and chloroacetaldehyde). The less reactive methyl chloride showed an inhibiting effect when mixed to vinyl chloride.

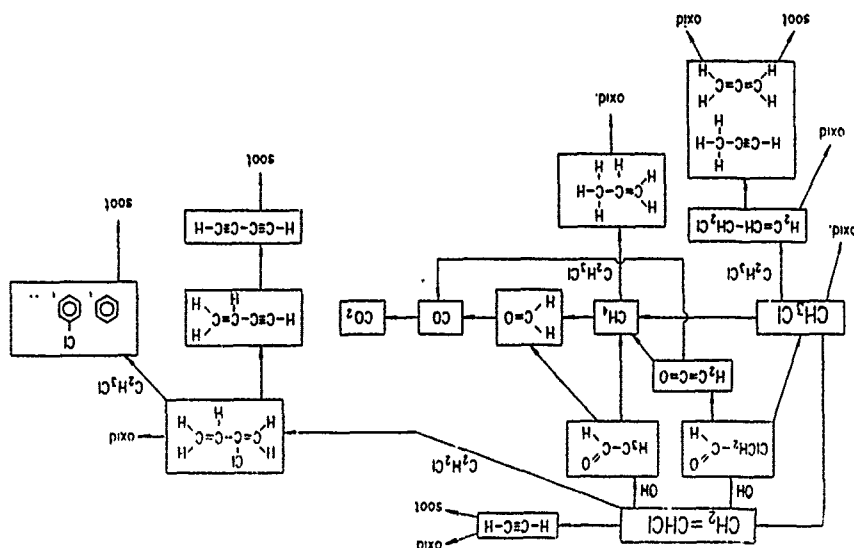
The main products and reaction paths are shown in fig. 1. In addition, we studied the influence of adding molecular chlorine to the reaction system. We found an acceleration in the consumption of vinyl chloride but an extensive rise in the number of products, especially higher chlorinated compounds and aromatics.

The experimental results were used for developing a kinetic model which improves the knowledge of chlorinated hydrocarbon combustion and is useful for the planning of further investigations.

Literature:

- /1/ E. Sanhueza, J. Heicklen; J. Phys. Chem., Vol. 79, No. 1, 1975, 7ff.
- /2/ H. Niki, P.D. Maker, C.M. Savage, L.P. Breitenbach, Int. J. Chem. Kinet. 12, 1980, 915-920
- /3/ W.D. Chang, S.B. Karra, S.M. Senkan; Combust. Sci. and Tech., 1986, Vol. 107, 107-121
- /4/ K.-C. Lee, H.J. Janes, D.C. Macauley, J. Air Pollut. Control Assoc. 25, 1975(7), 749-751

Fig. 1: Reaction Paths in the Oxidation of Vinyl and Methyl Chloride



PERSISTENT LUMINESCENCE AS AN INDICATOR OF THE ENDPOINT OF CHEMILUMINESCENT TITRATIONS

Myron Kaufman

Department of Chemistry, Emory University, Atlanta, GA
30322 USA

We have found that a powerful method of exploring bimolecular chemical reactions is to study their long time behavior. At the stoichiometric ratio of reactants, the decay of reagents in such systems is second order and thus inversely proportional to time. At any other concentration ratio of reactants, the reaction eventually becomes pseudo-first order, with the limiting reagent decaying exponentially. Since exponential decay is much faster than $1/t$ decay, at the stoichiometric ratio reaction persists for a longer time than at any other ratio of concentrations. Thus the rate of reaction at long times varies by many orders of magnitude for small variations around the stoichiometric ratio of concentrations. Although the above results are interesting when applied to simple bimolecular reactions, we have by both analytical and numerical methods shown that similar results are obtained for more complicated mechanisms. Mechanisms consisting of reactions in series and in parallel are considered.

In order to make use of the above principle, it is necessary to be able to measure rates of reaction at fairly long times, where concentrations have decayed considerably from their initial values. One very sensitive method of quantifying reaction rates under such conditions is by observing chemiluminescence from reaction products. If the products decay quickly, chemiluminescent intensity is an instantaneous measurement of reaction rate.

Sharply peaked luminescence provides a general endpoint indicator for gas-phase titration reactions, which can be employed to measure the concentration of reactive species (such as atoms and free radicals) in kinetics studies. If the reactive species (whose concentration cannot be directly measured) undergoes a chemiluminescent reaction with a stable species (whose concentration can be measured), the observation of "persistent" chemiluminescence indicates the stoichiometric proportion of reactants. As one example of this general principle, the sharply peaked luminescence in the $F + NO$ reaction is discussed. Since in this case, the titration is based on a combination reaction, fairly high pressures are needed to achieve a sufficient number of half lives of the reaction. The titration is thus complementary to another fluorine atom titration suggested a number of years ago.^{1,2} That titration, with Cl_2 , works best at low pressures. We believe that titration reactions for many other atoms and radicals will be developed based on this principle of "persistent luminescence".

Besides providing stoichiometric information, the shape of the titration curve gives information concerning the kinetics of the titration reaction. In order to reliably measure rate constants by this method, the kinetic analysis, based on the plug-flow approximation must be extended to include the effect of axial diffusion. The coupled second-order differential equations for a second-order reaction including flow and axial diffusion are solved numerically using a difference equation technique.

1. P. S. Ganguli and M. Kaufman, *Chem. Phys. Lett.* **25**, 22 (1974)
2. P. C. Nordine, *J. Chem. Phys.* **61**, 224 (1974)

Simulation of P-T Explosion Limits and Auto-Ignitions in the $\text{CO} - \text{CH}_3\text{O} - \text{H}_2 - \text{O}_2$ System

U. Maas, J. Warnatz

Physikalisch-Chemisches Institut der Universität Heidelberg
Im Neuenheimer Feld 253, 6900 Heidelberg, West Germany

Since the detection of explosion limits (e.g. of the $\text{H}_2 - \text{O}_2$ system) many efforts have been made to explain the phenomenon quantitatively. But all these attempts had to include some serious simplifications as quasi-steady state assumptions, neglect of reactant consumption, truncation of the reaction mechanism or restriction to homogeneous reaction systems etc. However new numerical methods for the solution of time-dependent stiff partial differential equation systems, the availability of fast computers and a detailed knowledge of the elementary reactions in the $\text{CO} - \text{CH}_3\text{O} - \text{H}_2 - \text{O}_2$ system now allow the simulation of auto-ignitions and explosion limits using one common mechanism (consisting of 37 elementary reactions in the $\text{H}_2 - \text{O}_2$ system and 37 elementary reactions in the $\text{CO} - \text{CH}_3\text{O}$ system), a multi-species transport model (including heat conduction, diffusion and thermal diffusion), and real site surface chemistry based on surface collision numbers and experimentally determined surface destruction efficiencies. None of the simplifications mentioned above has to be applied. The partial differential equation system is solved by spatial discretization using finite differences and integration of the resulting differential/algebraic equation system by implicit methods.

Calculated explosion limits in the $\text{CO} - \text{H}_2 - \text{O}_2$ system as well as in the $\text{CH}_3\text{O} - \text{O}_2$ system are presented. Time and space resolved profiles of temperature and species concentrations in igniting mixtures are calculated for various conditions. Sensitivity analysis (identifying the rate-limiting reactions) together with analysis of the reaction paths reveal insight into the elementary processes in CO and CH_3O auto-ignition.

An example of a simulation of an igniting stoichiometric $\text{CO} - \text{O}_2$ mixture (3% of the carbon monoxide replaced by hydrogen) at an temperature of 803 K and an initial pressure of 120 mbar is shown in Fig. 1. Plotted here is the temperature versus the radius and the reaction time during the time interval where ignition occurs. After the induction period the temperature rises in the vessel centre, and the ignition distributes rapidly over the whole reaction volume due to the relative low pressure (causing fast diffusion) and the high initial temperature. The profiles of the CO_2 mass fractions in the reacting mixture are shown in Fig. 2 (axes are exchanged, and a longer time interval is considered). After the induction time there is a rapid increase of CO_2 . At the end of ignition the content of CO_2 approaches the equilibrium concentration with respect to the temperature of the burnt gas. Then, during the cooling of the burnt gas, the CO_2 content increases again because the equilibrium of CO / CO_2 moves towards a high amount of CO_2 at low temperatures.

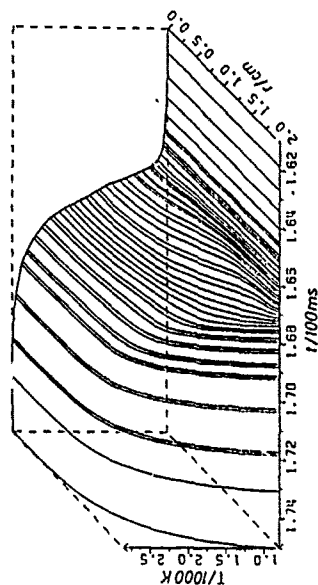


Fig. 1. Calculated profiles of temperature during the auto-ignition of a $\text{CO}/\text{H}_2/\text{O}_2$ mixture (97/3/50), cylindrical geometry.

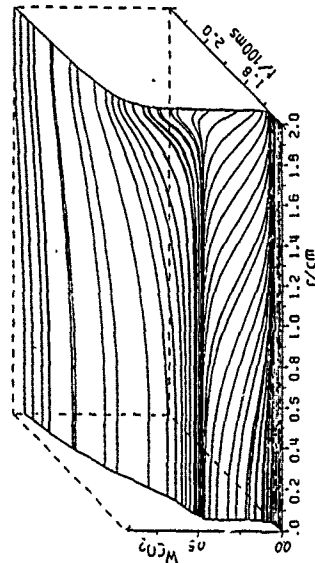


Fig. 2. Calculated profiles of CO_2 mass fraction during the auto-ignition of a $\text{CO} / \text{H}_2 / \text{O}_2$ mixture (97/3/50), cylindrical geometry.

THE MECHANISM OF CHAIN PROPAGATION IN THE
REACTION OF METHANE OXIDATION

V. I. Vedenev, A.A. Mantashyan, M.A. Teitelboim

Institute of Chemical Physics of Academy of
Sciences of USSR (Moscow)

Institute of Chemical Physics of Academy of
Sciences of Armenian SSR, P-Sevac st.5/2, Yerevan

The experimental results on free radical detection in the reaction of simplest hydrocarbons oxidation show that peroxide radicals are stable and are accumulated in high concentrations. In these conditions the role of nonlinear reactions extremely rises and the major conversion of peroxy radicals occurs by the interaction among these radicals. As result more active alkoxy radicals are formed. The reaction of these radicals can be responsible for product formation and further chain propagation. On the basis of direct experimental data on radical behaviour, and using the numerical modelling method, the mechanism of chain propagation in methane oxidation reaction at temperature $T=728K$, $CH_4:O_2=1:2$ is discussed. 70 elementary reactions had been taken into consideration. It is shown that in the process methylperoxy radicals indeed are reacting mainly between each other and with HO_2 and CH_3 radicals, and also with formaldehyde. Methane consumption is mainly connected with OH radicals reactions. The causes of nonlinear dependence observed

both in the experiment and in the numerical modelling, between methane oxidation rate and methylperoxy radicals concentration are discussed. It is shown that the total rate of nonlinear reactions of CH_3O_2 radicals many times exceeds those of linear ones of the same radicals. The analysis of chain propagation mechanism allows to clear up the ways of methane oxidation process control to have a high yield of products, and to approach a problem of hydrocarbon oxidation from a new point of view.

KINETIC MODELLING OF HIGH PRESSURE OXIDATION OF RICH METHAN-OXYGEN MIXTURES

Vedenev V.I., Teitelboim M.A., Goldenberg M.Ya.,
Gorban N.I., Karnaukh A.A.

Inst. of Chemical Physics USSR Ac. Sci.
Kosygin Street 4, Moscow 117334 USSR

Kinetic modelling of methane oxidation mechanism has been carried out. For conditions: high pressures ($p > 50$ atm), $T = 600-800$ K and rich methane-oxygen mixtures the Model involves 63 elementary reactions.

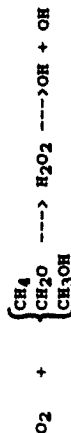
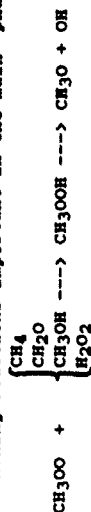
Detailed analysis of the Model has been carried out. The elementary stages determining principle features of kinetics and product composition were fixed. The complicated mechanism of oxidation shows two phases distinctly differing by their time scales: (i) short initial phase is a chain branched process.

Reaction	A	n	E _a
	sm ³ /s.s ⁻¹		kcal/mol
1. CH ₄ + O ₂ → CH ₃ + HO ₂	1.0(-10)	0	56
2. CH ₃ + O ₂ → CH ₃ OO	2.0(-12)	0	0
3. CH ₃ OO + CH ₄ → CH ₃ OOH + CH ₃	8.9(+13)	0	31.3
4. HO ₂ + CH ₄ → H ₂ O ₂ + CH ₃	1.0(-12)	0	21.5
5. CH ₃ OOH → CH ₃ O + OH	4.0(+15)	0	43
6. OH + CH ₄ → H ₂ O + CH ₃	1.32(-17)	1.92	2.69
7. CH ₃ O + CH ₄ → CH ₃ OH + CH ₃	1.0(-12)	0	11
8. CH ₃ O + O ₂ → HO ₂ + CH ₂ O	1.0(-13)	0	2.6
9. CH ₃ OO → wall	<1.0(-1)	0	0
10. 2CH ₃ OO → 2CH ₃ O + O ₂	1.71(-13)	0	0
11. 2CH ₃ OO → CH ₃ OH + CH ₂ O + O ₂	7.4(-14)	0	0
12. CH ₃ OO + HO ₂ → CH ₃ OOH + O ₂	7.7(-14)	0	-2.6
13. HO ₂ + HO ₂ → H ₂ O ₂ + O ₂	2.2(-13)	0	-1.23

Stationary state characterized by approximate equality of the rates of branching and radical combination completes the autoacceleration in this phase. Any reactions of radicals with intermediate products in this phase are unimportant.

(ii) Autoacceleration of main phase of reaction connected with branchings where intermediate products take part in.

Branching reactions important in the main phase:



In this phase reaction proceeds under conditions of approximate equality of the rates of branching and radical combination.

The Model has predicted phenomenon of increasing reaction time with increasing oxygen content in mixture. Melvin² has found experimentally that ignition delays increase with increasing oxygen concentration in rich methane-oxygen mixtures. On the ground of the Model Melvin's results have been quantitatively explained.

The Model has been compared with experimental data existed and proved to be satisfactory in general.

References

1. Vedenev V.I., Goldenberg M.Ya., Gorban N.I., Teitelboim M.A. - Kin. & Cat. 1988, v.29, #1, p. 7
2. Melvin A. - Combust. Flame 1966, v.10, p.10

THERMAL DECOMPOSITION OF DIMETHYLNITRAMINE BY PULSED LASER PYROLYSIS

Paul H. Stewart, S. Esther Migenda, Jean-Michel Zellweger,
Jay B. Jeffries, David M. Golden, and Donald F. McMillen

Department of Chemical Kinetics, Chemical Physics Laboratory
SRI International, Menlo Park, CA 94025

ABSTRACT

As a prototype for more complex nitramines, pyrolysis of dimethylnitramine (DMNA) and dimethylnitrosamine (DMNO) with GC/MS analysis was carried out in a flow system over the temperature range 800 to 900 K using pulsed infrared laser heating, via SF₆ in a 250 torr bath of CO₂ and radical scavenger. Temperature was determined indirectly through use of the comparative rate technique. Arrhenius parameters for DMNO and DMNA decomposition were $\log k(s^{-1}) = 15.8 \pm 1.1 - (50.0 \pm 3.4)/2.3RT$, and $13.5 \pm 0.6 - (37.4 \pm 2.5)/2.3RT$ respectively. The former set of parameters is consistent with simple bond scission as the rate limiting step; the latter set, which was produced with different scavengers, temperature standards, and varying amounts of added NO as a radical trap, is not consistent with simple bond scission. The experimental results can be reproduced via a mechanistic numerical model when N-NO₂ bond scission and nitro-nitrite rearrangement are competitive initial steps and the displacement of NO₂ from DMNA by NO is included as a low temperature route to DMNO. Reaction of dimethylnitramine via a nitro-nitrite rearrangement has not been reported in previous DMNA studies.

In a complementary series of laser pyrolysis experiments, the initial products of DMNA decomposition were observed directly using a molecular-beam/mass spectrometry detection system. The sampling nozzle was positioned immediately adjacent to the laser heated region. Direct detection of initial products at m/z 46 and 30 in the molecular beam revealed that N-NO₂ bond scission was accompanied by a comparable amount of the nitro-nitrite rearrangement (followed by rapid scission of the extremely weak (CH₃)₂NO-NO bond) to produce NO directly. Production of this NO by secondary bimolecular reactions can be ruled out because the time available before the product

mixture was frozen by adiabatic expansion was too short, and because the observed rise times of the NO and NO₂ were identical.

Calibration of the detection system with laser-heated NO and NO₂ at the reaction temperature (900 \pm 50 °C) revealed that the rearrangement/bond-scission branching ratio is $\sim 0.7:1.0$.

In ongoing studies we are probing the laser pyrolysis reactor still more directly, using laser-induced fluorescence (LIF) to determine the nascent NO/NO₂ ratio.

To further establish the significance of the nitro-nitrite rearrangement as an initial step in the decomposition of nitramines we have performed ab-initio calculations for the rearrangement process in the analogous unsubstituted nitramine. With MCSCF calculations employing a 6-31G* basis set, we find a loose rearrangement transition state (N-N bond length 2.85Å) 0.9 kcal mol⁻¹ below the NH₂ + NO₂ asymptote.

Acknowledgement: This work has been supported by the Army Research Office under Contract No. DAAO3-86-K-0030 and by the Air Force Office of Scientific Research under Contract No. F496220-85-K-0006.

References

- (a) Fluornoy, J. M., J. Chem. Phys., 1962, 36, 1106; (b) Korsunskii, B. L., Dubovitskii, F. I., Doklady Akademi Nauk SSSR, 1964, 155(2), 402; (c) McMillen, D. F., Barker, J. R., Lewis, K. E., Trevor, P. L., Golden, D. M., "Mechanisms of Nitramine Decomposition: Very Low-Pressure Pyrolysis of HMX and Dimethylnitramine," Final Report, SRI Project FYU-5787, 18 June 1979 (SAN 0115/117). DOE Contract No. EY-76-C-03-0115; (d) Umstead, M. E., Lloyd, S. A., Lin, M. C., Proc 22nd JANAF Combustion Mtg., CPFA, 1985, p. 512 (e) Wodtke, A. M., private communication.

PYROLYSIS AND IR LASER PHOTOLYSIS OF SiH_4 AND ITS MIXTURES WITH
NON REACTIVE AND REACTIVE ADDITIVES

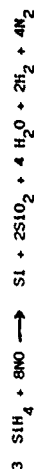
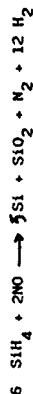
A. Mele and D. Stranges

Dipartimento di Chimica, Università "La Sapienza" P.le A. Moro, 5
Roma, Italy

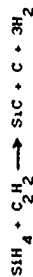
A. Giardini-Guidoni and R. Teghil

Istituto di Chimica, Università di Basilicata,
Via N. Sauro, Potenza, Italy

The possible mechanism of SiH_4 dissociation proposed for pyrolysis and photolysis experiments could be a concerted three center simultaneous bond rupture of two SiH bonds^{2,3}; SiH_2 may be formed in the ground or excited states⁴. The results of CW irradiation agree with the hypothesis of a rapid thermal relaxation process in small reaction volume. This hypothesis is supported by the formation of higher silanes and hydrogenated amorphous silicon. TEA photolysis seems to produce non equilibrium conditions in a very short time. This may lead to formation of electronically excited fragments which predissociate to silicon and hydrogen. A very rapid explosive reaction is ignited by irradiating regardless of the laser employed, mixtures of SiH_4 and NO of various composition and different total pressures. Pressure change and final gaseous and solid products are influenced by the ratio of the initial mixture. The trend of the pressure change agrees with the following simplified reaction scheme:



A radical chain mechanism with branching may account for the explosive character of the reaction. Photolysis of mixtures of SiH_4 and C_2H_2 produces H_2 and solid silicon carbides. Preliminary results show that the stoichiometry of the reaction, whatever the initial composition of the mixture, is the following:



- 1) Y. Hamakawa. Amorphous semiconductors technologies and devices North Holland 1982.
- 2) J.H. Purnell, R. Walsh. Proc. R. Soc. London **A293**, 546 (1966).
- 3) E. Borsella, L. Caneve, A. Giardini-Guidoni and A. Mele. Spectr. Acta **43A**, 277 (1987).
- 4) E. Borsella, L. Caneve. Appl. Phys. B. 1988.

In recent years IR laser induced deposition process have been the subject of growing interest and of intensive experimental research¹. The most suitable laser to be used for IR photolysis is the CO_2 laser, which is line tunable over a reasonably wide frequency range and can be operated both in CW or pulsed mode. Depending upon the nature of excitation and the reaction conditions, different chemistry may follow the initial laser activation of the reaction. In this paper reactions of SiH_4 pure and in mixtures with non reactive and reactive additives, induced by pulsed and CW CO_2 laser irradiation are reported. An outline on the relationship between gas phase SiH_4 dissociation, fragment reaction and thin film or powder production will be provided. Results are compared with pyrolysis studies².

IR laser photolysis experiments were carried out in an apparatus already described³ at different initial pressure in a cell with the laser beam softly focused on the center. The photolysis was monitored by the pressure change. The luminescence accompanying the irradiation was detected by OMA system. Final gaseous products were analyzed by IR spectrophotometry and mass spectrometry. IR spectrophotometry laser ionization mass spectrometry (Lama 500) and X-Rays were employed for the analysis of the solid deposits.

HETEROGENEOUS FACTORS AND THE PHENOMENON OF THE
NEGATIVE TEMPERATURE COEFFICIENT OF THE MAXIMUM
RATE OF PROPIONALDEHYDE OXIDATION
REACTION

Yu. A. Oganesyan, A. P. Jazparyan, I. A. Vardanyan
[A. B. Melbandyan]

Institute of Chemical Physics Armenian Academy of
Sciences, 375044, P. Sevak st. 5/2, Yerevan, USSR

The influence of a nature and the surface to volume ratio (S/V) of a reaction vessel on the kinetics of gas phase C_2H_5CHO oxidation in the pyrex reactors packed and unpacked, coated with boric acid and KCl has been studied at the temperature range 623-803K. Under flow conditions at atmospheric pressure. The phenomenon of NTC is observed beginning from 633K. It has been established that the range of NTC changes dependent on the nature of a surface. The range of NTC in the reactor coated with KCl is displaced to the temperatures (623-653K), being lower than that in boric acid coated vessel (623-683K).

The peroxy radicals are discovered in both of the reactors, but peroxy compounds (RCO_3H , RO_2H , H_2O_2) - only in boric acid coated vessel. The correlation is established between the change of peroxy radical concentration and the rate of C_2H_5CHO consumption. The decrease of the peroxy radical concentration is observed with the decrease of the rate of aldehyde consumption in the range of NTC. It has been shown that in boric acid coated reactors generally RCO_3 radicals are detected in the gas phase, in KCl coated one - RO_2 , and at the higher temperatures - HO_2 - radicals.

It has been established that in boric acid coated vessel the rate of C_2H_5CHO consumption is higher and the amount of peroxy radicals in gas phase is less than that in KCl coated one. It is concluded that there is the heterogeneous way of C_2H_5CHO consumption, and in boric acid coated reactor, being inert with respect to the radical termination, the part of the heterogeneous consumption of aldehyde probably with the participation of the radicals is more.

It has been established that in the range of NTC the surface effects on the rate of the heterogeneous aldehyde consumption, and also on the rate of RCO , RCO_3 and RCO_3H decomposition. It has been shown that as S/V ratio increases, the strong inhibition of the reaction takes place in both of the reactors in the range of NTC. The latter disappeared in KCl coated vessel. As S/V ratio increases in boric acid coated vessel, the yield of H_2O_2 rises at the high temperatures (803K). It is concluded that H_2O_2 is formed by the heterogeneous way with the participation of the peroxy radicals. It has been shown that the addition of the corresponding peroxy compounds to the reaction mixture promotes the reaction in KCl and boric acid coated reactors, and the action of peroxy compounds on the process is mainly conditioned by its heterogeneous radical decomposition. It is concluded also that NTC is conditioned by the competition of the decomposition of RCO and the interaction of the latter with oxygen both in the gas phase and on a surface.

THE REGULARITIES OF NONISOTHERMICAL PROCESSES IN SYSTEMS WITH BRANCHING CHAIN REACTIONS

A. H. Peregudov and V. T. Gontkovskaya

Institute of Structure Makrokinetic
Academy of Sciences of the USSR
Chernogolovka 142432 USSR

The regularities of chain nonisothermal processes development kinetics and mechanism of hydrogen combustion are studied theoretically.

Consideration of branching chain reactions, completely branching chain reactions, reactions with degenerate branching of chains and with direct chains enables to determine some general regularities taking place in all emimerated reaction classes.

In the branching chain processes, in reactions with direct chains and in reactions with degenerate branching of chains the thermal reaction acceleration is the leading one when the thermal explosion takes place. That's why the critical conditions of the thermal explosion are clearly expressed and the induction period as function of the vessel's diameter has maximum when the diameter is equal to critical one.

In branching chain reactions two-stage ignition is observed. Chain and thermal flares are time separated.

rated.

In completely branching reactions the chain process is always leading one. The kinetic induction period is equal to thermal one. The induction period is a monotonous function of the vessel's diameter.

Existence of chain ignition limits in branching chain reactions systems leads to nonuniqueness of critical conditions of the thermal explosion^{1,2}. The existence of thermal ignition semi-island is carried out.

Since the contribution of individual stages in multistaged process is varied with experiment conditions, there exist the dependence of maximal pre-explosion heating's and induction period of these conditions.

In the present time the obtained results are experimentally confirmed.

References

1. Gontkovskaya V. T. On the thermal explosion critical conditions in the systems with branching chain reactions. Dokl. Akad. Nauk, v. 234, 1976, p. 915
2. Gontkovskaya V. T., Ovchinnikov A. A., Peregudov A. H. Some peculiarities of the thermal explosion at the chain ignition semi-island. Kinetica i Kataliz, v. 19, 1978, p. 90.

A MASTER EQUATION STUDY OF THE APPROACH TO EQUILIBRIUM IN
ISOMERISATION AND ADDITION/DISSOCIATION REACTIONS

N.J.B.Green, P.J.Marchant, M.J.Pilling and S.H.Robertson
Physical Chemistry Laboratory, South Parks Road,
Oxford OX1 3QZ, U.K.

Gas phase relaxation experiments on isomerisation reactions:



or association/dissociation reactions



In which the approach to equilibrium is monitored as a function of time, provide two experimental parameters, the relaxation time, τ , and the equilibrium constant, K_C . These parameters may be manipulated to calculate forward and backward rate coefficients k_f^i and k_b^i . Quack¹ pointed out that the relationship between these rate coefficients and those measured under irreversible conditions, k_f^i , k_b^i , is not straight forward.

In order to investigate the problem further, we have set up a time-dependent master equations for model systems for reaction (1) and (2), and determined eigenvalues under both reversible and irreversible conditions. There is close agreement between the values of k_f^i , k_b^i and k_f^e , k_b^e provided provided that both types of energised molecule, A^* and B^* , are included. These rate

coefficients differ considerably from the formal rate coefficients

defined, for example, by

$$k_f = \frac{\sum_i k_i^f n_i^A}{\sum_i n_i^A}$$

where n_i^A is the number of A molecules in energy grain i and k_i^A is the isomerisation rate coefficient from that grain.

Identical behaviour has been established with a simplified 4

state model :-



under steady-state conditions.

An eigenvalue expansion further clarifies the meaning of the steady state in reversible reactions. This expansion also forms the basis of an efficient iterative technique for calculating fall-off behaviour in reversible or irreversible reactions.

References

1. M.Quack, Ber.Bunsenges.Phys.Chem., 1984, 88, 94.

A DETAILED CHEMICAL KINETIC STUDY OF THE OXIDATION OF N-PENTANE

H. J. Pitt and C. K. Westbrook*

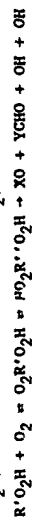
Lawrence Livermore National Laboratory
Livermore, California 94550, U.S.A.

As one proceeds from short to long straight-chain alkanes, n-pentane is the first hydrocarbon whose autoignition characteristics are typical of the long straight-chain alkanes. The dramatic change in autoignition characteristics from smaller n-alkanes to n-pentane can be attributed to the influence of alkylperoxy radical isomerizations. These reactions become more important in n-pentane oxidation due to the increased availability of secondary H-atom sites whose H-atoms are more easily abstracted than primary H-atoms. Also, the longer carbon chain of the n-pentane molecule allows larger ring sizes for the transition state of the peroxy radical isomerizations. The rates of alkylperoxy radical isomerizations increase generally with ring size until the ring size reaches 6 to 7 members.

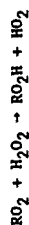
We have developed a detailed chemical kinetic model for n-pentane which includes alkylperoxy radical isomerizations. We compare our computed results to the measurements of Baldwin, Bennett and Walker¹ on n-pentane/H₂/O₂ mixtures in a static reactor at 753 K. We have computed species concentration histories for all the species that they have measured. They have performed a thorough analysis of their experimental data for the single point of 10 percent fuel consumption. Our study extends their results and examines the entire extent of reaction, including the point of 10 percent fuel consumption. Our detailed model takes advantage of the comprehensive set of species concentrations that they have provided from 10 to 90 percent fuel consumption. Also, our model includes secondary processes that are normally neglected in an analysis restricted to low extents of reaction. The model traces the history of secondary products formed from the consumption of the major intermediate products. It includes secondary reactions, such as radical-radical reactions, whose impact on the oxidation process can be assessed with a numerical model.

Our chemical kinetic mechanism for n-pentane includes recently evaluated rate constants, some of which had an impact on the computed results. We have employed the equilibrium constants of the RO₂/RO₂ reaction that have been recently measured by Slagle, Gutsan and coworkers². These equilibrium constants are important in determining the position of the negative temperature coefficient

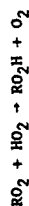
region in n-pentane oxidation. We have modified the rate constants for the alkylperoxy radical isomerizations estimated by Baldwin, Walker and coworkers so that they are consistent with these equilibrium constants. After the alkylperoxy radical isomerizes, RO₂ = R'O₂H, it can react further with O₂,



where R is a pentyl radical, R' and R'' indicate the removal of an H-atom from R, and X and Y are smaller hydrocarbon radicals. We have followed the reaction scheme proposed by Benson³ for the reaction of R'O₂H with O₂. Since this scheme produces two reactive OH radicals, it is chain branching and significantly accelerates the oxidation of n-pentane. We also included two other reaction paths involving alkylperoxy radicals that had a significant effect on our computed results. The first path is reaction with hydrogen peroxide which is present in large concentrations under the current conditions,



where R is an alkyl radical. This reaction converts hydrogen peroxide into alkyl hydroperoxide which decomposes and yields OH radicals more readily than hydrogen peroxide at 753 K. Our calculations show that this path is one of the primary sources of alkyl hydroperoxides under the present conditions. Tsang and Hampson⁴ recently estimated the rate constant for the above reaction when R is methyl. We have used their rate constant for all the analogous RO₂H₂O₂ reactions. The other reaction path involving alkylperoxy radicals that was also one of the main sources of alkyl hydroperoxide in our calculations is:



The alkyl hydroperoxide that is formed decomposes to give an OH radical that accelerates the overall rate of oxidation.

1. R.R. Baldwin, J.P. Bennett, and R.W. Walker, J.C.S. Faraday I **76**, 1075 (1980).
2. I.R. Slagle, E. Ratajczak, and D. Gutsan, J. Phys. Chem. **20**, 402 (1986).
3. S.W. Benson, Prog. Energy Combust. Sci. **7**, 125 (1981).
4. W. Tsang, and R.F. Hampson, J. Phys. Chem. Ref. Data **15**, 1087 (1986).

*This work was performed under the auspices of the U.S. Department of Energy by the Lawrence Livermore National Laboratory Contract No. W-7405-ENG-48.

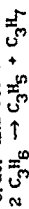
THE PYROLYSIS OF PROPYLENE

Ian Mylie, Clarence S. Rebelro and John M. Roscoe
Department of Chemistry, Acadia University,
Wolfville, Nova Scotia, Canada B0P 1X0

The pyrolysis of propylene has been studied both in static systems at comparatively low temperatures and in shock tubes. The reaction leads to a complex mixture of products at quite small conversions of propylene. In spite of this, the more recent work done in static systems seems to have been able to measure reliable initial rates and to obtain accurate kinetic data. There does, however, continue to be some controversy regarding the nature of the initiation step in this system. The shock tube results are consistent with initiation via



while the results obtained in the static system indicated that initiation was second order and occurred via



The work described here extends the low temperature, static system experiments to lower temperatures in an effort to examine the chemistry at the smallest practical conversions. These results and those in the literature (1) are then used in conjunction with kinetic modelling to deduce a mechanism which provides quantitative agreement with experiment for propylene pyrolysis at small conversions.

The experiments were made in a static reaction vessel with chemical analysis by gas chromatography. The work covered propylene pressures in the range 40 Torr to 750 Torr and temperatures from 630 K to 748 K. Attention focussed on the yields of methane, ethylene, propane, and ethane since these are likely to be characteristic products formed from radicals produced early in the reaction. The reaction orders for production of propane and ethylene were 2, and that for production of methane was approximately 1.7, and that for production of ethane was 1.5. At the very small conversions studied at the lower temperatures, propane yields were masked by a minor propane impurity in the propylene. In all cases the yields were linear with time suggesting that initial rates were being observed. Plots of the log of the reaction rate against the reciprocal of the absolute temperature were linear and

merged smoothly with the results reported in the literature for other static experiments (1) giving activation energies which were in satisfactory agreement with those in the literature.

Kinetic modelling was done with a computer program which has been described elsewhere (2). Approximately 50 chemical reactions were required and their rate constants were taken from critical evaluations of rate data or from recent direct measurements reported in the literature. The experimental data could not be fitted satisfactorily with reasonable rate constants for the unimolecular initiation step. Good agreement with experiment was obtained using bimolecular initiation with an absolute rate constant that was smaller than the experimental one reported in the literature (1). An efficient hydrogen atom chain provides an additional path from propylene to propyl radicals which produce the product, propane, upon which the earlier experimental rate constant calculations were based.

REFERENCES

1. M. Saxon and M. H. Back, *Can. J. Chem.*, **48**, 317-325 (1969).
2. John H. Roscoe and Maria J. Thompson, *Int. J. Chem. Kinet.*, **17**, 967-990 (1985).

OXIDATION REACTION OF HYDROGEN NEAR THE SECOND
IGNITION LIMIT : EVIDENCE FOR
PRESSURE PULSES.

K. SAHETCHIAN, F. JORAND, J. CHAMBOUX, V. VIOSSAT.
Laboratoire de Chimie Générale, C.N.R.S. UA 40870,
Université P. et M. Curie, Tour 55 (6^e Etage)
4 Place Jussieu, 75252 PARIS CEDEX 05

A "semi-static" experimental method has been developed
to study combustibles with three ignition limits (1).

The procedure is as follows :

- first the gaseous mixture flows rapidly (with negligible reaction) through a vessel located in a thermoregulated furnace. The gaseous flow is at the P_0 pressure and T_0 temperature where the experiments will be performed.
- second, the gas is confined instantaneously inside the vessel by closing two electromagnetic valves. Then the reaction is followed by measurement of the pressure change.

Investigation of the second limit and slow reaction was performed in experimental following conditions (2) :

$$H_2/O_2/N_2 : 2/2/1 ; 440 \leq T_0 \leq 530^\circ C ; 60 \leq P_0 \leq 500 \text{ mb.}$$

The vessel is coated with acid boric solution or washed with fluorhydric acid solution, then it is treated by the slow oxidation reaction.

At constant temperature T_0 , a set of experiments was performed at different values of the total initial pressure P_0 .

When P_0 is lowered we observed :

- at $T_0 \leq 500^\circ C$: a slow reaction with a rate increasing when we approach the second ignition limit,
- at $T_0 > 500^\circ C$: the slow reaction, then a zone of pressure pulses near the second limit. By observing the pressure recording we suppose the pulses as isothermal.

These phenomena are explained by the complex part played by radicals and hydrogen peroxide formed during the slow reaction. HO_2 radicals evolution was studied by E.S.R. analysis : their concentration first increases in autocatalytic way, then the accumulation rate slows down, and increases again.

A reaction scheme is proposed, and the pulses are interpreted by an autoinhibition due to radical-radical and radical-peroxide recombination reactions. A reaction simulation is undertaken to reproduce the experimental results.

(1) J. CHAMBOUX, V. VIOSSAT, F. JORAND, K. SAHETCHIAN.
J. Chim. Phys. 1985 82 (5), 499.

(2) K. SAHETCHIAN, F. JORAND, J. CHAMBOUX, V. VIOSSAT.
J. Chim. Phys. 1988 85, (1), 91.

KINETIC AND MECHANISTIC INVESTIGATIONS OF THE REACTIONS OF AROMATIC HYDROCARBONS WITH ATOMIC OXYGEN

Dr. V. Schliephake
M. Tappe
H. Frerichs

Institut für Physikalische Chemie
Tammannstraße 6
D - 3400 Göttingen

Oxydation processes of aromatic hydrocarbons play an important role in combustion as well as in atmospheric chemistry. In this investigation rate constants for the reactions of benzene, toluene, ethylbenzene, the xylenes and some monohalogenated benzenes with atomic oxygen were measured in the temperature range $T = 298 - 870$ K using a quartz flow reactor. Atomic oxygen was produced by microwave discharge of O_2/He mixtures. The kinetic was followed by monitoring the decay of the hydrocarbon using a quadrupole mass spectrometer which was connected to the reactor via a molecular beam sampling device. The O concentration was corrected assuming a first order recombination kinetic. In contrast to previous investigations our study provides a substantial extension in temperature range. Moreover, by the choice of excess O atom conditions the possibility of unwanted formation of tar-like by

products could be significantly reduced. We obtained

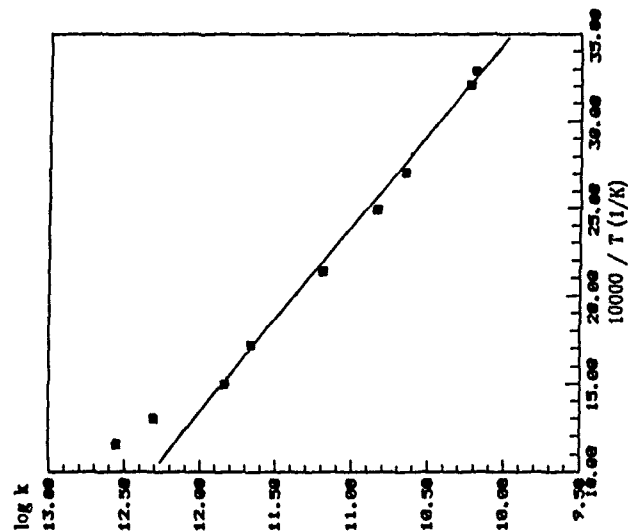


Figure 1: Arrhenius plot for benzene

Arrhenius expressions supporting the proposed mechanisms of electrophilic addition to the aromatic ring and abstraction from the aliphatic side chain. Moreover, evidence is also obtained that H-abstraction from the ring plays no significant role.

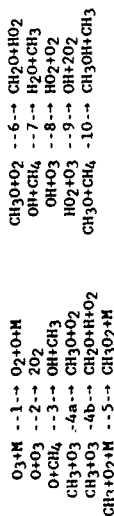
-2-

KINETICS AND CHEMILUMINESCENCE OF THE REACTION OF METHANE WITH OXYGEN ATOMS FROM THE THERMAL DECOMPOSITION OF OZONE

Sidney Toby and Frima S. Toby

Department of Chemistry
Rutgers, The State University of New Jersey
P.O. Box 939
Piscataway, NJ 08855, USA.

A simplified combustion system was generated by reacting methane with decomposing ozone in the temperature range 75-175°C. Experiments were done in static and flow systems and in the presence of added oxygen and carbon dioxide. Under most conditions a period of induction was observed followed by a rapid depletion of O₃. With added O₂ the period of induction disappeared and the reaction slowed. These effects were simulated by a 30-step mechanism which qualitatively accounted for the period of induction. A simpler 11-step mechanism which was more algebraically tractable was used to account quantitatively for the effect of added O₂ over a wide range of conditions



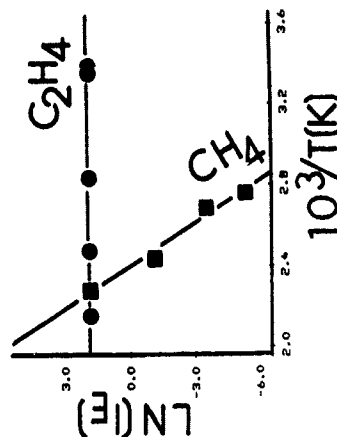
The main ozone-destroying chain is postulated to be steps 4a, 6, 7 and 9, which gives the overall stoichiometry for ozone destruction as $\text{CH}_4 + 2\text{O}_3 \rightarrow \text{CH}_2\text{O} + \text{H}_2\text{O} + 2\text{O}_2$

The simplified mechanism with reasonable assumptions gives $-d[\text{O}_3]/dt = k_1[\text{O}_3][\text{M}]^{1/2} + 4k_1k_4[\text{O}_3]^2/k_5[\text{O}_2]$ where $\alpha = k_3[\text{CH}_4]/(k_2[\text{O}_3] + k_3[\text{CH}_4])$. The kinetics of oxygen inhibition were studied by plotting $-d[\text{O}_3]/dt$ against $1/[\text{O}_2]$. These plots were linear and gave values for k_1k_4/k_5 in good agreement with the literature over the temperature range studied

The reaction was strongly chemiluminescent and the emission was identified as due to Meinel bands, presumably from $\text{H} + \text{O}_3 \rightarrow \text{H}^* + \text{O}_2$, where $\text{H}^* = \text{OH}(^2\Pi, v \leq 9)$. No emission was found when the helium carrier gas was replaced by oxygen. If we add the steps $\text{OH}^* \rightarrow \text{H} + \text{O}_2$ and $\text{H} + \text{O}_2 \rightarrow \text{H}^* + \text{O}_2$ then steps 1-13 with the steady state assumption for intermediates give:

$$\begin{array}{l}
 \text{IE} - \\
 2k_1k_3k_4k_5k_{11}[\text{O}_3]^3[\text{CH}_4] \\
 k_5[\text{O}_2](k_2[\text{O}_3] + k_3[\text{CH}_4])(k_{11}[\text{O}_3] + k_{13}[\text{O}_2][\text{M}])
 \end{array}$$

Under the conditions employed, the activation energy for light emission should be given by $E_a = E_1 + E_3 + E_{4b} + E_{11} - E_5 - E_2 - E_{13} = 29 \pm 0.5 \text{ kcal/mol}$. A plot of $\ln(\text{IE})$ vs $1/T$ is given below for the O_3/CH_4 system and the slope gives $28.7 \pm 0.9 \text{ kcal/mol}$. For comparison the chemiluminescence from ozone with ethylene was measured under similar conditions and shown in the same graph. No temperature dependence was found.



REDUCTION OF LARGE REACTION MECHANISMS

I. Turányi and I. Bérces
Central Research Institute for Chemistry,
Hungarian Academy of Sciences,
Budapest, Hungary

Recently we have used principal component analysis of the relative reaction rate matrix for the identification of reactions which can be omitted from a reaction mechanism constructed with a specific aim.^{1,2} Here we report on the possibilities of mechanism reduction by the omission of certain chemical species.

The objective in modelling is often confined to the reproduction of the concentration profiles for certain selected species. The selected species may consist for example of those which are the characteristic reaction products or those for which experimental data are available. As a first step in mechanism reduction we identify the species of the original scheme whose omission does not influence significantly the calculated concentration profiles of the selected species. The rest may be called the group of the necessary species.

Two methods are proposed for the identification of the necessary species. In the first one all species are probed, one by one, by solving the kinetic differential equations under the conditions where the kinetic parameters for the consuming reactions of the tested species are taken to be zero. The solution differs considerably from the original one for the species which are considered to be necessary ones. The second method identifies the necessary species by analyzing the Jacobian.

In the next step of mechanism reduction, an objective function is formulated by taking into account only the necessary species. Then principal component analysis applied to the relative reaction rate matrix results in a further reduction of the scheme through the identification of the unimportant reaction steps.

The method is used to analyse a 98-step mechanism of low temperature propane pyrolysis³, with 36 reaction species. By mechanism reduction the number of species was decreased to 18 and the number of reactions by a factor of two without significant loss in the accuracy of calculated profiles.

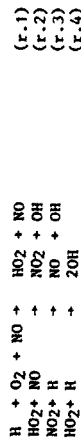
1. I. Turányi, I. Bérces and S. Vajda,
Int.J.Chem.Kinet., submitted for publication.
2. S. Vajda, P. Valkó and I. Turányi,
Int.J.Chem.Kinet., 17, 55(1985)
3. O. Edelson and O.L. Allara
Int.J.Chem.Kinet., 12, 605(1980)

ROLE OF NITRIC OXIDE IN THE H₂-O₂ FLAME

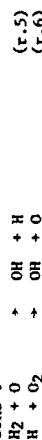
Blam, J., Vandoren, J. and Van Tiggelen, F.
Laboratoire de Physico-Chimie de la Combustion
Université Catholique de Louvain
LOUVAIN-la-NEUVE BELGIUM

The structure of low pressure flames burning in H₂-O₂-Ar mixtures either stoichiometric FS1 (25.4% H₂, 12.7% O₂ and 61.9% Ar) or lean FP1 (18.6% H₂, 76.5% O₂ and 4.9% Ar) have been investigated using a molecular beam sampling coupled with a mass spectrometer analysis.

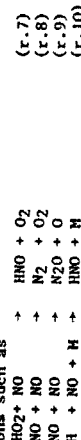
About three percent of NO were added to the reference flames (FS1 and FP1). The figure 1 shows that NO has the behaviour of a diluent such as Ar. This evidence is reinforced by the lack of H₂, H₂O and HNO species in NO containing flames. Nevertheless, the presence of NO in the H₂-O₂ flames induces a drastic increase of the OH concentration, specially in the stoichiometric flame (FS2) as it is noticed in figure 2. In parallel, HO₂ concentration also increases strongly in NO seeded flames. A tentative explanation of these last evidences can be derived from the following reaction mechanism :



where NO is a very efficient third body for the recombination reaction (r.1) producing HO₂ and therefore NO is a catalyst for the OH formation. Such effect is less noticeable in the lean flame as a consequence of the simultaneous large production of OH radical by reactions :



which strongly dilute the OH formation paths (r.2 - r.4). The above mechanism explains why the OH concentration is enhanced by the occurrence of NO without a simultaneous change in the NO profile. The absence of HNO, N₂ and N₂O in these flames indicates that side reactions such as



do not play an important role in the H₂-O₂-NO combustion chemistry, at least in the investigated temperature range (800-1800 K).

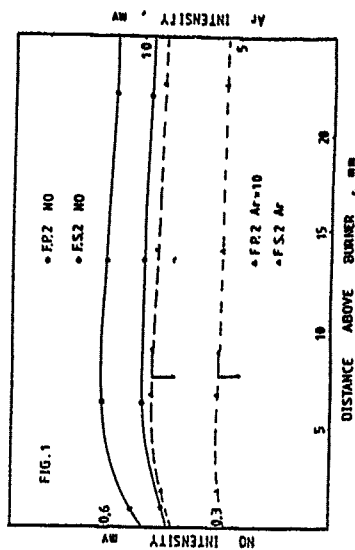


Fig. 1 NO and Ar intensity profiles in NO seeded H₂-O₂-Ar flames (FP2 and FS2).

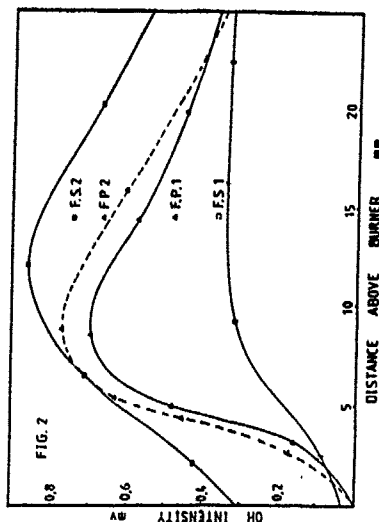


Fig. 2 OH intensity profiles in unseeded (FP1, FS1) and NO seeded (FP2, FS2) flames.

We acknowledge financial support of CEC (grant n° EN3E/0089/8) and FRFC Belgium (grant n° 2-9006-88).

THE HIGH PRESSURE, HIGH TEMPERATURE HYDROGENATION OF BENZENE

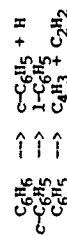
Stephen W. Wood
British Gas plc
Research & Development Division
London Research Station
Michael Road
London SW6 2AD

A high pressure, high temperature flow reactor has been used to study the hydrogenation of benzene over the range of conditions 1000 p/Pascals < 5000, 750 °C < 950. Hydrogen/benzene ratios were kept high (>0.2 w/w) to prevent the formation and deposition of carbon. Gaseous products were analysed by on-line gas chromatography and liquid products by Fourier-Transform-Infrared Spectroscopy (FTIR). The overall loss of benzene can be described by simple first order kinetics with respect to the benzene concentration, with the following rate coefficient:

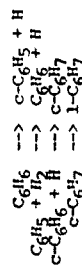
$$k = (2.23 \pm 0.14) \times 10^9 \exp(-(27300 + 1400/T)) \text{ s}^{-1}$$

This value agrees with previous data obtained over a wide range of temperature and pressure. The results indicate that the rate of benzene decomposition is independent of both hydrogen partial pressure and total pressure and suggest destabilisation of the aromatic ring as a common rate controlling step for both hydrogenation and pyrolysis.

A kinetic model has been developed which describes the behaviour of the reaction system over this range of conditions. Two routes to ring opening are invoked to explain the observed product data. Previously it has been proposed that ring opening occurs by the reaction sequence (1):



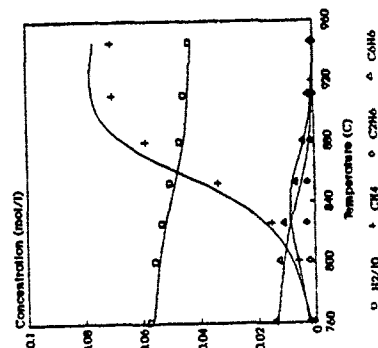
In the presence of the large amounts of hydrogen used in this study, a second ring opening reaction sequence has to be invoked



The predicted product yield ratios are most sensitive to reactions involving the addition of hydrogen to the fragments resulting from the aromatic ring opening reactions. In particular, to obtain the best fit to the experimental data, it is necessary to split the conjugated linear species (ie 1-C₆H₅ and 1-C₆H₇) into C₁ fragments as well as the previously suggested C₂s and C₄s. To achieve this, it is necessary to hydrogenate these linear species to reduce conjugation and ease fragmentation. Evidence for this route is provided by gc analysis of the liquid products which detected the presence of n-pentane.

In the absence of direct measured data for many of the reactions included in the mechanism, some of the relevant rate constants have been adjusted to give the best fit between the experimental and predicted results. Experimental and computed product yield data are compared in figure 1. The model can also be used to predict the behaviour of benzene under low pressure, low temperature pyrolysis conditions.

Figure 1: Experimental & Predicted Data



Luminescences from excited photofragments have been observed during laser bicolor photoexcitation of CF_2Cl_2 by a pulsed ArF laser (6.4 eV) and a CW CO₂ laser (0.11 eV).

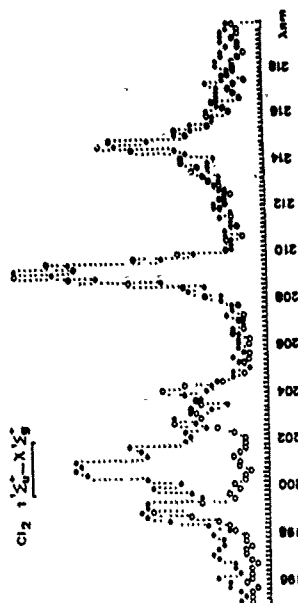
CF_2Cl_2 absorbs the IR radiation and by collisional energy transfers, ground state CF_2Cl_2 are prepared with internal energy; these rotationally excited molecules are photodissociated by UV radiation.

The photodissociation of CF_2Cl_2 with the radiation of the ArF laser leads by a two photons process to a photofragment CF_2 with internal energy, the transient species being radical CF_2Cl .

One observes a fluorescence from CF ($B^2\Delta$, $v' = 2$) prepared from the absorption of another UV quantum at 193.3 nm by rotationally excited CF ($X^2\Pi$, $v = 0$). A fluorescence is also observed from CF ($B^2\Pi$, $v' = 0$) in high rotational levels, the formation of which requires the absorption of one UV quantum by radical CF with vibrational energy up to level $v'' = 1$.

In addition to the luminescences induced by single UV laser irradiation, a fluorescence from Cl_2 ($1^1\Sigma_u^+$) is observed by joint irradiations $\text{UV} + \text{IR}$.

The formation of $\text{Cl}_2(1\ ^1\text{u}_g^*)$ means that an energy gap of at least 0.7 eV is obtained by IR photoexcitation of Cl_2 ; a biphotonic UV dissociation where the transient species is the first excited singlet state of the parent molecule, is then favoured.



Luminescences induced by: o ArF laser irradiation. o UV + IR laser irradiation. Res. : 0.26 nm.

CHLORINE OXIDES IN THE LOW TEMPERATURE PHOTOLYSIS OF ClO_2

A. Reimer and F. Zabel

Physikalische Chemie/FB 9, Bergische Universität-Gesamthochschule Wuppertal, D5600 Wuppertal 1, West Germany

Chlorine oxides, in particular Cl_2O_2 , possibly play an important role in the strong ozone depletion which has been observed in the antarctic stratosphere during spring. For this reason, there is an actual interest in their spectroscopic and kinetic behaviour.

In the present work, $\text{ClO}_2/\text{O}_2/\text{N}_2$ mixtures were photolyzed in a coolable 420 l reaction chamber at temperatures between +20 and -30 °C and total pressures from 0.5 to 1000 mbar. ClO_2 concentrations from 2×10^{-4} to 1×10^{-6} molecules/cm³ were applied. The reaction mixtures were analyzed in situ via long path infrared absorption using a Fourier-transform spectrometer (1 cm resolution). Two sets of strong absorption bands developed in the product spectrum on a time scale of several minutes:

I. High temperatures, high total pressures and, in particular, very low partial pressures (or the absence) of oxygen favoured the formation of three bands centered at 1286, 1041 and 654 cm⁻¹ (fig. 1).

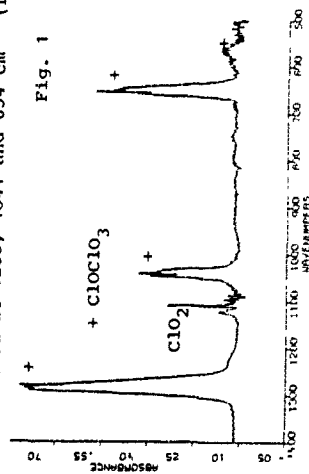


Fig. 1

Both the positions and the relative intensities of these absorption bands agree with those of the three strongest bands in the infrared spectrum of chlorine perchlorate (ClOClO_3), and thus are assigned to this species.

II. Low temperatures, low total pressures and high oxygen partial pressures favour the formation of two strong absorption bands at 1225 and 1057 cm⁻¹ (fig. 2). These bands were first described by Molina and Molina¹, and were assigned by them to a Cl_2O_2 isomer. Weaker, unidentified bands appeared at 740, 653, and 560 cm⁻¹.

The dependence of the intensities of these absorption bands on initial ClO_2 concentrations, their response to NO_2 addition, and the effective reaction mechanisms are discussed.

- (1) K.O. Christe, C.J. Schack, and E.C. Curtis; Inorganic Chemistry 10(1971)1589
- (2) L.T. Molina and M.J. Molina; J. Phys. Chem. 91(1987)433

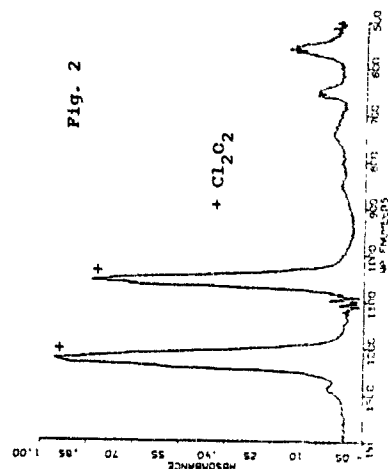


Fig. 2

KINETICS OF THE GAS PHASE REACTION OF Cl ATOMS WITH ORGANIC SPECIES

T.J. Wallington, L.M. Skewes, W.O. Siegl, C.H. Wu, and S.M. Japar

Research Staff
 Ford Motor Company
 P. O. Box 2053
 Dearborn, Michigan 48121

The relative rate technique has been used to determine the rate constants for the reaction of chlorine atoms with a series of alkanes, alkenes, alkynes, alcohols, and ethers. Experiments were performed at 295 ± 2 K and atmospheric pressure of synthetic air or nitrogen. The decay rates of the organic species were measured relative to that of ethane or n-butane. Using rate constants of 9.38×10^{-11} cm³ molecule⁻¹ s⁻¹, and 1.97×10^{-10} cm³ molecule⁻¹ s⁻¹ for the reaction of Cl with ethane and n-butane respectively the following rate constants were derived, in units of 10^{-11} cm³ molecule⁻¹ s⁻¹: propane, (14.0 \pm 0.4); i-butane, (13.2 \pm 0.8); n-pentane, (27.2 \pm 1.4); n-hexane, (30.3 \pm 4.3); cyclohexane, (31.6 \pm 1.3); ethene, (10.6 \pm 0.6); propene, (28.2 \pm 1.2); acetylene, (6.19 \pm 1.00); methylacetylene, (23.4 \pm 1.4); ethylacetylene, (34.0 \pm 1.1); methanol, (5.12 \pm 0.45); ethanol, (9.46 \pm 1.02); n-propanol, (16.1 \pm 1.3); t-butylalcohol, (3.65 \pm 0.22); acetaldehyde, (9.66 \pm 0.88); propionaldehyde, (12.7 \pm 1.02); dimethyl ether, (18.0 \pm 0.7); diethylether, (31.1 \pm 2.5); and methyl-t-butylether, (14.5 \pm 1.1). The results are discussed with respect to the mechanisms of these reactions and to previous literature data.

HCL CATALYSED DECOMPOSITION OF DI-TERTIARY BUTYL PEROXIDE - UNIMOLECULAR REACTIONS OF SURROGATE HYDROPEROXY ALKYL RADICAL

L. Batt, M.A. Khan and T.J. Mitchell,
Department of Chemistry, University of Aberdeen,
Aberdeen AB9 2UZ, Scotland

and

C. Morley,
Shell Research Ltd., Thornton Research Centre, Cheshire.

The HCl catalysed decomposition of di-tertiary butyl peroxide (dtBP) from 90-130°C can be explained by the following mechanism:

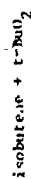
(1)



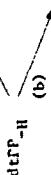
(2)



(3)



(4)



(5)



The last step infers inhibition of the reaction by one or all of the products formed in reactions (2) and (4). RH may also be acetone produced from the decomposition of t-BuO.

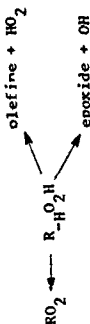
Analysis of this mechanism produces the rate law

$$-\frac{d[\text{dtBP}]}{dt} = \frac{2k_1 k_3 [\text{dtBP}]^2}{k_5 [\text{RH}]}$$

Analysis of the data shows that the rate of reaction is indeed second order with respect to peroxide and is inhibited by the product(s) as predicted by the mechanism. Integration of this expression gives the rate law

$$2k_{\text{obs}} t = \ln \frac{a-x}{a} + \frac{x}{a-x}$$

One of the controversies involved in the mechanism for the oxidation of hydrocarbons is the route for the unimolecular decomposition of the hydroperoxy alkyl radical ($R_{\text{H}}\text{O}_2\cdot$). This would be produced as a result of the isomerisation of the alkyl peroxy radical $\text{RO}_2\cdot$. There are three possible paths for $R_{\text{H}}\text{O}_2\cdot$



In the HCl/dtBP system, dtBP \cdot constitutes a surrogate hydroperoxy alkyl radical. Most importantly this radical is produced in an oxygen free system and only two decomposition paths are available for dtBP \cdot . The relative importance of these two paths may therefore be investigated in isolation. Preliminary analysis of the ratio of the products isobutene and isobutene oxide show that the ratio, k_{4a}/k_{4b} ranges from 0.4 at 90° to 0.1 at 130°.

Direct Observation after IR Multiphoton Absorption of the Dynamics of Excited Molecules near to the Dissociation Threshold.

B. Abel, B. Herzog, H. Hippler and J. Troe
Institut für Physikalische Chemie, Universität Göttingen
Tammannstrasse 6, D-3400 Göttingen

The dynamical behaviour of molecules near to the dissociation threshold is of great interest for the understanding of unimolecular reaction rates. Thermal low pressure limiting rate constants for dissociation or the reverse recombination reaction are governed by collisional energy transfer near to the threshold. Calculations with the statistical adiabatic channel model predict dissociation rate constants and their dependence on total angular momentum. In suitable cases, molecules can be excited to the dissociation threshold using UV absorption followed by internal conversion or overtone absorption. It appears worthwhile to extend these studies by using other excitation techniques. In the present paper CF₃I near to the dissociation threshold is prepared under collision-free conditions using IR multiphoton absorption in short pulses (20 to 50 ns) from a TEA CO₂ laser. Time resolved "hot" UV absorption spectroscopy allows for a characterisation of the resulting dynamics and energy distribution. Dissociation rate constants in the order of 10^5 to 10^6 s⁻¹ are observed for molecules reacting close to the reaction threshold. In the presence of collisions with a heat bath, collisional stabilisation and deactivation is observed directly. The calibrated UV absorption spectrum of CF₃I allows for evaluation of average amounts of energy transferred per collision. This observation is possible not only at reaction threshold but also during the course of deactivation towards thermal equilibrium. Collisions, which during the excitation process perturbed the molecules increased the amount of excited molecules and changed their energy distribution.

COLLISIONAL ENERGY TRANSFER BETWEEN
HIGHLY EXCITED N₂O MOLECULES

H. Tettebaum, University of Ottawa, Dept. of Chemistry and
J. Troe, Inst. für Physikalische Chemie, Universität Göttingen

The rate of low pressure thermal decomposition of N₂O in mixtures with argon was measured in the temperature range 1700-2900 K behind incident and reflected shock waves. The time-resolved absorption of UV radiation (λ=23071 nm) was analysed in accordance with the generally accepted scheme:



After having accounted for the role of secondary reactions as well as of thermal effects on the absorption coefficient and the rate coefficients, we deduced the rate of reaction (1) as a function of mole fraction of N₂O. In our mixtures (0.2%, 2%, 4% and 8% N₂O in Ar) only Ar and N₂O played a major role as collision partners in reaction (1).

Over the short composition range we noticed only a slight deviation from linear dependence of the effective rate coefficient on the mole fraction of N₂O. We also observed that the Arrhenius activation energy for (1) decreased from ~60 Kcal mol⁻¹ (T < 2500 K) by as much as 5 Kcal mol⁻¹ (T > 2500 K) depending on the mole fraction. Both of these observations are indicative of non-equilibrium kinetics.

From the analysis we deduced that N₂O is about 10 times as efficient a collision partner as Ar is. From the decrease in activation energy with temperature and an exponential gap model for energy transfer we could determine that for collisions among highly excited N₂O, <ΔE> down = 6-35 kJ mol⁻¹ over the temperature range 2000-3000 K, in agreement with expectations for triatomic partners.

Compared with the <ΔE>_{down} ≤ 0006 kJ mol⁻¹ obtained from vibrational relaxation studies², the present data indicate a significant dependence of <ΔE> down on vibrational energy, in accord with recent conclusions on the subject³.

1. J. Troe, J. Chem. Phys. 66, 4745 (1977).
2. Z. Baalbaki, H. Tettebaum, Chem. Phys. 104, 83 (1986).
3. M. Heymann, H. Hippler, H.-J. Plach, J. Troe, J. Chem. Phys. 87, 3867 (1987).

AN OSCILLATORY REACTION IN THE GAS PHASE -
THE KINETICS OF HOMOGENEOUS CLUSTER FORMATION

Zhikai Cheng and Heshel Teitelbaum

University of Ottawa
Department of Chemistry
Ottawa, Ont., Canada K1N 6N5

A laser schlieren technique was used to measure density gradients in shock compressed CCl_3F for a narrow range of Mach Nos. 1.09 - 1.63. In this range the pressure of the shock-compressed CCl_3F (initially at or near its vapour pressure) exceeds the thermodynamically specified value for the gas equilibrated at the raised temperature. Hence condensation commences.

We observed signals characteristic of an exothermic chemical process, and we interpreted this to be the nucleation of CCl_3F clusters. We found that at pressures ~ 2 atm. and temperatures in the range 300-340 K the time scale for nucleation is ~ 500 μsec . The rate decreases with increasing temperature.

Unlike previous investigations of shock compressed polyatomic molecules (e.g., vibrational relaxation of pyrolysis of N_2O) where the laser schlieren signals vary smoothly with time, the signals observed here are accompanied by pronounced oscillations. In this study we report on the pressure and temperature dependence of the oscillation frequency and offer a mechanistic explanation for this intriguing phenomenon.

1. Z. Baalbaki, H. Teitelbaum, Chem. Phys. 104, 83 (1986).
2. J.E. Dove, W. NIP, H. Teitelbaum, Fifteenth Symposium International on Combustion, The Combustion Institute, Pittsburgh, p. 903 (1975).

Infrared Multiphoton Dissociation of Dimethylnitramine

Y. Lazarou and P. Papagiannakopoulos

Institute of Electronic Structure and Laser and Department of Chemistry,
Research Center of Crete and University of Crete,
P.O. Box 1470, 714 09 Heraklion, Crete, Greece

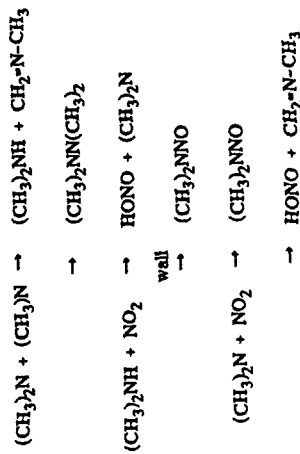
The thermal decomposition and explosion of energetic materials in the gas phase is a complex chemical process with considerable interest and applications in the propellant industry. In particular, the thermal stability of the nitramine group $>\text{NNO}_2$ is of great interest, since it is met in most important energetic materials (RDX, HMX) and plays a significant role in the complex mechanism of their decomposition.

The phenomena of infrared multiphoton absorption (IRMPA) and dissociation (IRMPD) in isolated polyatomic molecules provides a powerful technique for studying the unimolecular decomposition of polyatomic molecules. The main advantages of the technique are, the selective excitation and dissociation of just parent molecules leaving intact the primary photofragments or other added reactants, and the possibility of achieving desirable degrees of vibrational excitation by adjusting the laser fluence or intensity, therefore reaching different channels of unimolecular dissociation. In contrast, in pyrolysis experiments the parent molecules are excited in the same degree as the primary products or other added reactants and the decomposition mechanism becomes complicated.

In this work we studied the infrared multiphoton dissociation of dimethylnitramine (DMNA) by measuring the dependence of the dissociation yield and product formation on the laser fluence and the pressure of different added scavenging gases. The primary dissociation channel of DMNA is the fission of the N-N bond (~ 43 kcal/mol) with no evidence of the HONO elimination channel.

The steady-state rate coefficient for DMNA decay was estimated as $k(\text{st}) \sim 1.7 \times 10^6 (\text{I/MW cm}^{-2}) \text{s}^{-1}$ in the laser intensity range $1\text{--}(3\text{--}1.2)$ MW/cm², which provides a unimolecular dissociation rate constant in the range $k_{\text{uni}} \sim (5\text{--}2) \times 10^6 \text{ s}^{-1}$ respectively. From the RRKM-calculated curve of k_{uni} versus internal energy E^* , the above rate constants correspond to mean internal energies $E^* \sim (50\text{--}45)$ kcal/mol.

The performed scavenging experiments with Cl_2 , NO , NOCl and NO_2 molecules have shown that the overall reaction mechanism following DMNA decomposition involves the reactions:



The formation of dimethylnitrosamine is mainly due to the heterogeneous reaction of dimethylamine with nitrogen dioxide.

I. Y. Lazarou and P. Papagiannakopoulos, Infrared Multiphoton Decomposition of Dimethylnitramine, *J. Phys. Chem.* submitted, (1988).

COMPARISON OF AB INITIO CALCULATIONS,
TRANSITION STATE THEORY AND EXPERIMENT
FOR THE RECOMBINATION OF METHYL RADICALS

Katherine Darvesh, Russell Boyd and Philip Pacey

Department of Chemistry, Dalhousie University,
Halifax, Nova Scotia, Canada, B3H 4J3

Ab initio calculations employing a 6-31G** basis set and the multireference double excitation configuration interaction method have been applied to the recombination of methyl radicals. The methyl radicals have been restricted to a planar equilateral triangular geometry, but the carbon-carbon distance and five angles defining the mutual orientation of the radicals have been varied. Attractions between the radicals appear to be dominated by sigma bonding between the singly occupied orbitals on the two radicals, although pi bonding also appears to contribute in some orientations. At short distances repulsive forces between atoms on adjacent radicals are important. All these interactions have been represented by simple expressions, which have been combined to represent the potential energy as a function of the six coordinates varied. Eight parameters in the potential energy expression have been adjusted by least squares, fitting the ab initio points within about 1 kJ/mol. Canonical variational transition state theory calculations have been performed on the resulting potential energy surface. A Monte Carlo method was used to integrate the Boltzmann factor over the five angles. The critical distance or bottleneck was found to decrease from a carbon-carbon distance of 0.34 nm at 200 K to 0.27 nm at 2000 K. Experimental and theoretical rate constants at high pressures agree; the rate constant decreases with increasing temperature.

CROSS-COMBINATION RATIOS OF METHYL AND C₄-C₆ ALIPHATIC HYDROCARBON RADICALS

L. Seres, A. Macsa, I. Kortvélyesi and M. Görgényi
Institute of General and Physical Chemistry,
A. J. University, Szeged, Hungary.

The methyl radical-initiated thermal reaction of some C₄-C₆ olefins have been investigated.

On the basis of the initial rates of product accumulation, it was possible to check the interesting proposal made by Arthur and Christie¹ that it is simply the ratios of the diameters and masses of radicals which determine the value of the cross-reaction ratio, ϕ . According to their proposal, $\phi > 2$ is expected wherever the diameters and/or masses are different. They found, however, that in systems for which the relation $\phi > 2$ is expected to hold, the available experimental values of ϕ are not well substantiated; accordingly, they emphasized the necessity of obtaining more reliable data to check this approach further.

Allyl radicals have been shown to enter disproportionation reactions reluctantly. Thus, ϕ can only be a little higher than the cross-combination ratio, ϕ , in the reactions of methyl and substituted allyl radicals. Further, $\phi > 2$ is expected if the simple collision model is correct.

Some reactions of the following radicals were investigated: methyl (M), 1-methylallyl (I), 2,3-dimethylpropyl (IV) and 1,1,2,2-tetramethylpropyl (V). The left-hand side subscripts c and t refer to the cis and trans forms of the radical, while the left-hand side superscripts 1 and 3 refer to the terminal and non-terminal reactions, respectively, of a substituted allyl radical e.g. c is a cis-1-methylallyl radical reacting at the terminal position.

The values of ϕ obtained are easily divided into three classes on the basis of the characteristics expected to influence it.

a) In the cross-combination reactions of substituted allyl radicals, the masses and the sizes of the two radicals are identical (or nearly the same if cis and trans isomers are reacting). The cross-combination ratios obtained are:

$$\phi(^1I, ^3I) = 2.03; \quad \phi(^1II, ^3II) = 2.00$$

b) In the cross-combination reactions of methyl and allyl radicals, both the masses and the sizes of the radicals are considerably different, and $\phi > 2$ is predicted. The experimental data seem to contradict this expectation:

$$\phi(M, ^1I) = 1.98 \pm 0.04; \quad \phi(M, ^1II) = 2.22 \pm 0.06;$$

$$\phi(M, ^3II) = 1.97 \pm 0.03$$

c) For the cross-combinations of methyl and alkyl radicals, theory predicts $\phi > 2$, but $\phi(M, t-C_4H_9) \sim 1.3$ has been observed by different authors. The present study does not support the latter finding:

$$\phi(M, III) = 2.26 \pm 0.06; \quad \phi(M, IV) = 2.15 \pm 0.03$$

Conclusions:

- Self-reactions of substituted allyl radicals follow the "cross-combination rule".
- Cross-combinations of methyl and allyl radicals do not follow the pattern predicted on the basis of simple collision theory.
- For the cross-combinations of methyl and alkyl radicals, $\phi > 2$, supporting the theory.

- 1 N.L. Arthur and J.R. Christie, *Int. J. Chem. Kinet.*, **19**, 261 (1987).
- 2 D.L. Boulch, P.K. Chown and D.C. Montague, *Int. J. Chem. Kinet.*, **11**, 1055 (1979).
- 3 C. Anastasi and N.L. Arthur, *J.C.S. Faraday Trans. 2*, **83**, 277 (1987).

GAS PHASE UV PHOTO-CHEMISTRY OF NF_2
DYNAMICS AND KINETICS OF BOTH $\text{NF}(\text{X}^3\Sigma)$ AND $\text{NF}(\text{a}^1\Delta)$ RADICAL
PRODUCTS

H. Heikal, R. F. Heidner III, J. S. Holloway, and J. B. Koffend

Laser Chemistry & Spectroscopy Department
Aerospace Corporation
Los Angeles, California
U.S.A.

The H_2/NF_2 reaction system has been the subject of several studies where particular attention has been paid to the formation of the metastable radical $\text{NF}(\text{a}^1\Delta)$. The $\text{NF}(\text{a}^1\Delta)$ yield from this reaction is crucial to its use as an energy donor in several proposed chemical lasers. In an indirect measurement the $\text{NF}(\text{a}^1\Delta)$ branching fraction was previously determined to be 0.91. In this paper we present the first direct determination of the energy disposal in this reaction. Our technique involves our ability to probe both the $\text{NF}(\text{X}^3\Sigma)$ via $\text{b} \rightarrow \text{X}$ LIF, and the $\text{NF}(\text{a}^1\Delta)$ $\text{a} \rightarrow \text{X}$ emission. Our experiment compares the two emission signals ($\text{NF}(\text{X}^3\Sigma)$, $\text{NF}(\text{a}^1\Delta)$) from 248 nm photolysis of NF_2 with those from the 193 nm photolysis of a HBr/NF_2 mixture. The 193 nm photons are not absorbed by NF_2 but does dissociate HBr with unity quantum yield. The equations describing the four emission signals depend on the photolysis quantum yield and the branching fraction. These equations can be solved under experimental conditions where $[\text{NF}(\text{X}^3\Sigma)]_{\text{total}}$ is known and the two PMT detection geometries are not altered between the two photolysis experiments.

Our experiment utilizes a teflon coated photolysis chamber which can be heated (470 K) and in which we flow the reagent tetrafluorohydrazine (N_2F_4 , 10% mixture in Ar). At the photolysis cell temperature, the N_2F_4 pyrolyzes (98%) to form 2NF_2 . An excimer laser (248 nm, 193 nm) or a tunable UV laser (frequency converted Nd-Yag pumped dye laser) is used as the photolysis source. The Nd-Yag pumped dye laser in the visible also serves as a pump laser for the induced fluorescence (LIF) studies of $\text{NF}(\text{X}^3\Sigma)$. Two PMTs, are simultaneously used to detect the LIF from $\text{NF}(\text{X}^3\Sigma)$ and fluorescence emission from $\text{NF}(\text{a}^1\Delta)$. This capability allows us to simultaneously monitor both ground and excited state products following laser photolysis. Two computers are necessary for the experiment. The first monitors the LIF signal as a function of delay time between photolysis and probe laser, both laser energies, and the probe laser wavelength. The second computer is used to acquire data of the fluorescence emission as digitized by a fast transient recorder. We also monitor all gas mass flow meters, the cell temperature, and pressure.

With the above apparatus we have studied the UV (240–270 nm) photolysis of NF_2 where two possible products can be produced ($\text{NF}(\text{X}^3\Sigma)$, $\text{NF}(\text{a}^1\Delta)$). The absorption cross section of NF_2 and the photolysis quantum yield from the fragment $\text{NF}(\text{a}^1\Delta)$ were measured with 0.25 cm² resolution. Our results show that the $\text{NF}(\text{a}^1\Delta)$ quantum yield decreases at longer wavelengths and is only 1% at 260 nm. This suggests that the first long wavelength band in NF_2 leads primarily to ground state $\text{NF}(\text{X}^3\Sigma)$ and that the existence of a new higher lying NF_2 electronic state is responsible for the $\text{NF}(\text{a}^1\Delta)$ production. Promptly following NF_2 laser photolysis, we observe the ground state $\text{NF}(\text{X}^3\Sigma)$ species. This however is not the case for the excited $\text{NF}(\text{a}^1\Delta)$ radical which has an appearance lifetime of nearly 75 μsec . This observation cannot be reconciled with the fact that the absorption spectrum of NF_2 (240–270 nm) appears as a diffuse continuum. We have yet unknown metastable electronic NF_2 $^3\text{B}_1$ electronic state interconverts to an as yet unknown metastable electronic state from which it dissociates to $\text{NF}(\text{a}^1\Delta) + \text{F}$.

By scanning the LIF pump laser in wavelength, at a fixed delay following photolysis (248 nm) we could measure the nascent vibrational, and rotational population distributions of ground state $\text{NF}(\text{X}^3\Sigma)$ species. This result is the first ever observation of gas phase $\text{NF}(\text{X}^3\Sigma)$ by LIF. The data show that the $\text{NF}(\text{X}^3\Sigma)$ species is produced with considerable internal energy (vibrational $T_v = 2350$ K; rotational $T_r = 1750$ K). For 248 nm photolysis of NF_2 , there is nearly 2 eV available for partitioning between internal and translational degrees of the products $\text{NF}(\text{X}^3\Sigma)$, F , J^* , and F .

For our kinetics studies, we fixed the probe laser wavelength to a particular rovibronic line (v^*, J^*, F^*) and varied the delay between lasers. Using various quenching partners we measured the relaxation of the rotational and the vibrational distributions in $\text{NF}(\text{X}^3\Sigma)$. The rate coefficients for vibrational relaxation of $\text{NF}(\text{X}^3\Sigma)$ with Ar, CO_2 , and SF_6 have been measured. We find both Ar and CO_2 to be poor vibrational quenchers (3×10^{-14} cm³ molec⁻¹ sec⁻¹), relative to SF_6 (1.1×10^{-13} cm³ molec⁻¹ sec⁻¹). We have also observed that $\text{NF}(\text{X}^3\Sigma)$ reacts with its parent NF_2 at a surprisingly fast (2.5×10^{-12} cm³ molec⁻¹ sec⁻¹) rate. In contrast the removal rate of $\text{NF}(\text{a}^1\Delta)$ by NF_2 is slow (2.7×10^{-16} cm³ molec⁻¹ sec⁻¹).

Using all the results above, we performed an experiment to directly measure the $\text{H} + \text{NF}_2 \rightarrow \text{NF}(\text{X}^3\Sigma) + \text{F}$ reaction branching ratio. To date a number of indirect measurements have shown that the addition-elimination reaction between H and NF_2 radicals produces $\text{NF}(\text{a}^1\Delta)$ with high quantum efficiency (>90%). In our experiment we were not able to observe any $\text{NF} \text{ b} \rightarrow \text{X}$ LIF signal from the ArF photolysis of HBr/NF_2 mixtures even at the highest HBr density. By careful signal to noise consideration we can place limits on the branching fraction. Using the values for the NF_2 absorption cross section at 248 nm ($\sigma_{248} = 6.74 \times 10^{-19}$ cm²), and the HBr value at 193 nm ($\sigma_{193} = 1.9 \times 10^{-18}$ cm²) we determine that the branching fraction, b_1 , to form $\text{NF}(\text{a}^1\Delta)$ is > 99%. Our results confirm those from the indirect measurements. Experiments are currently in progress to investigate the kinetics of $\text{NF}(\text{X}^3\Sigma)$ with NF_2 as well as the study of $\text{NF}(\text{X}^3\Sigma)$ disproportionation.

ELECTRONIC QUENCHING OF EXCITED DIATOMIC HYDRIDES

Y.P. Vlahoyannis, E. Hontzopoulos*, A. Vaghi*, S.C. Farantos** and C. Fotakis
F.O.R.T.H.-Research Center of Crete, Institute of Electronic Structure and Laser
Iraklio, Crete, Greece
R.K. Browarzik, P. Heinrich, R.D. Kenner, F. Rohrer and F. Stuhl
Physikalische Chemie I, Ruhr Universität Bochum
Bochum, Federal Republic of Germany

Electronically excited diatomic hydrides are of special interest to scientists of several disciplines, because of their importance in combustion, atmospheric and interstellar chemistry. We present experimental and theoretical results on some aspects of electronic quenching of several of these radicals.

In Bochum, the rates of electronic quenching of the lowest vibrational level of $\text{CH}(\text{A}^2\Delta)$, $\text{NH}(\text{C}^1\Pi)$ and $\text{NH}(\text{A}^3\Pi)$ in a very well defined rotational and translational energy distribution characterized by room temperature have been investigated. The excited radicals were generated in the ArF laser photolysis of $(\text{CH}_3)_2\text{CO}$, HN_3 and NH_3 , respectively, in the presence of a large excess of inert gas and were detected by their fluorescence. Preliminary values of the collisional quenching cross sections for several selected colliders are given below. Included for comparison are literature values for the quenching of $\text{OH}(\text{A}^2\Sigma)$. These values allow comparisons to be made between the quenching rates of three different diatomic hydrides at room temperatures can be extensive set of collision partners. In addition, comparisons can be made between: 1) The values for $\text{CH}(\text{A}^2\Delta)$ and $\text{NH}(\text{A}^3\Pi)$ measured at room and higher temperatures for a number of important colliders and 2) The rates of quenching of four different electronically excited states of the NH radical.

The experimental work in Crete focused on the rotational dependence of the electronic quenching of $\text{CH}(\text{A}^2\Delta)$ in the v=0 vibrational state. Electronically excited CH was produced by KrF excimer laser photolysis of acetone. Spectroscopic measurements revealed the presence of $\text{CH}(\text{A}^2\Delta)$, $\text{B}^2\Sigma^-$ and $\text{C}^2\Sigma^+$. The spectra showed a high degree of vibrational and rotational excitation in the A and B states. Available energy calculations show that the translational temperature has an upper limit of ~340 K. Since the quenching rates of the B and C states of acetone are too fast to be distinguished from the laser pulse (~15 ns) quenching rates of the Q branch and the R(3) to R(7) rotational lines of the v=0 level of $\text{CH}(\text{A}^2\Delta)$ were measured. These measurements show that the quenching efficiency decreases considerably as the rotational excitation increases^{2,3,5}. This result is consistent with measurements on OH¹ and NH^{1,2,3,5} and theoretical predictions. Theoretical calculations in Crete have produced ab initio potential

curves of HeO and potential energy surfaces (PES) of HeOH for the first three states. The PES were found to be repulsive. Close coupling spin averaged cross sections have been calculated for the rotationally inelastic collisions of He with $\text{OH}(\text{A}^2\Sigma^-)$ on this repulsive potential. The partial cross sections show secondary minima, and an explanation is sought by examining the appropriate classical trajectories.

Furthermore, the electronic quenching of $\text{OH}(\text{A}^2\Sigma^-)$ by CO is studied using semiclassical trajectory calculations. The first three PES are represented by analytical functions, calculated by a 3-D cubic spline interpolation of the interaction potential between CO and OH. The dynamics is studied by solving the semiclassical equations of motion. Total electronic quenching cross sections are currently being calculated for several translational, vibrational and rotational temperatures of OH.

TABLE

Quenching cross sections σ at 300 K for the v=0 state of several diatomic hydrides by selected collision partners Q.

Q	$\text{CH}(\text{A}^2\Delta)$	$\text{NH}(\text{C}^1\Pi)$	$\text{NH}(\text{A}^3\Pi)$	$\text{OH}(\text{A}^2\Sigma)$
H_2	0.6	8.0	4.4 ^a	9.2 ⁵
N_2	0.03	1.6	0.006 ^a	4.0 ⁵
CO	6.6	4.2	1.5	4.0 ⁵
CO_2	0.5	2.7	0.8 ^a	5.7 ⁵
CO_2	0.5	2.7	0.8 ^a	9.0 ⁵
H_2O	9.6	8.9	4.2 ^a	

References

- 1) I.S. McDermid and J.B. Landslagler, J. Chem. Phys. 76, 1824 (1982).
- 2) P. Papagiannakopoulos and C. Fotakis, J. Phys. Chem. 89, 3439 (1985).
- 3) A. Hozumehaus and F. Stuhl, J. Chem. Phys. 82, 3152 (1985).
- 4) A. Hozumehaus and F. Stuhl, J. Chem. Phys. 82, 5519 (1985).
- 5) a) R.A. Copeland, M.J. Oger and D.R. Crosley, J. Chem. Phys. 82, 4022 (1985), b) J.B. Jeffries, R.A. Copeland and D.R. Crosley, J. Chem. Phys. 85, 1848 (1986), c) G.P. Smith and D.R. Crosley, J. Chem. Phys. 85, 3896 (1985).

* Also Department of Physics, University of Crete
** Also Department of Chemistry, University of Crete

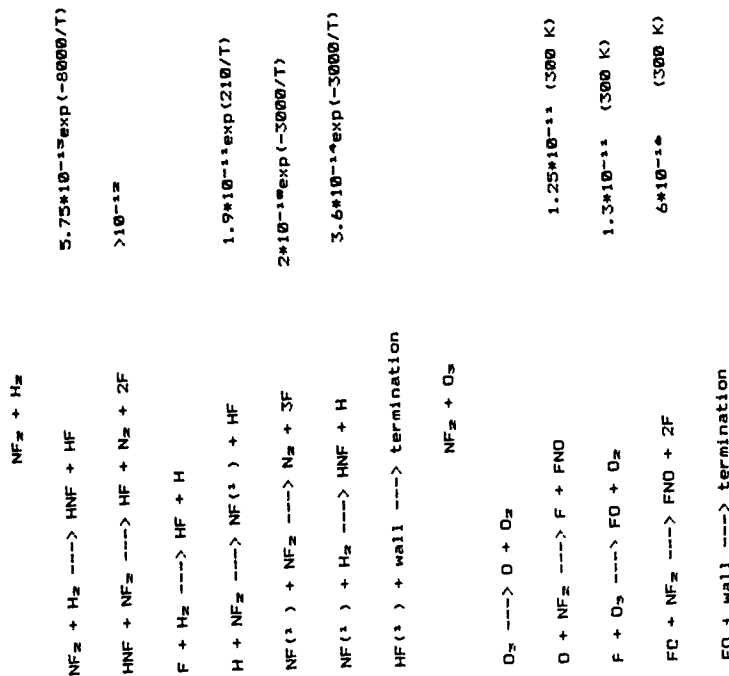
THE BRANCH CHAIN REACTION $\text{NF}_2 + \text{O}_2$ AND THE PROMOTION
OF H_2 , CO AND CH_4 OXIDATION BY NF_2

Yu. M. Gershenzon and V. B. Rozenshtein

Institute of Chemical Physics, Academy of Sciences
Kosygin st. 4, Moscow 117977 USSR

Recently we have discovered the branch chain reactions $\text{NF}_2 + \text{H}_2\text{O}_2$ and $\text{NF}_2 + \text{H}_2$ (1). In this work we obtained the new data on $\text{NF}_2 + \text{H}_2$ reaction and found out that $\text{NF}_2 + \text{O}_2$ was the branch chain reaction. Also it was found that the reaction $\text{NF}_2 + \text{CH}_4$ was a slow process at 300-950 K ($k \sim 10^{-14}$ cm³s⁻¹, T=400-950 K) but a small amount of NF_2 resulted in considerable acceleration of CH_4 oxidation (branching process $\text{CH}_3\text{O}_2 + \text{NF}_2 \rightarrow \text{CH}_3\text{O} + \text{F} + \text{FNO}$) as well as in decrease of inflammation temperature of H_2 - O_2 system (branching process $\text{HO}_2 + \text{NF}_2 \rightarrow \text{OH} + \text{F} + \text{FNO}$). The addition of NF_2 allowed to oxidize CO molecules at room temperature (H_2 present).

The experiments were carried out by means of LMR, EPR, UV and IR absorption and visible chemiluminescence. The temperature and pressure ranges were 250-900 K and 1-700 Torr. The study of macrokinetics and elementary steps led us to the following mechanisms of the branch chain reactions ($\nu = \text{cm}^{-1}$):



REFERENCE

1. Bedjanian Yu. R., Gershenzon Yu. M., Rozenshtein V. B. 9th Int. Symp. Gas. Kinet. Bordeaux 1986 Abstracts, p. E65

AUTHOR INDEX

Abel, B. B51
 Achhammer, G. B29
 Adams, N. G. 17
 Ahlers, G. 37
 Ahonkhal, S. I. A12
 Aleksandrov, E. N. A10
 Al-Yahya, A. B15
 Anastasi, C. A40, A41, B18, B19, B20
 Anderer-Alvarez, J. B18
 Aquilanti, V. A2, B1
 Arutyunov, V. S. A10
 Aschmann, S. M. 52
 Ashfold, M. K. R. 37
 Atkinson, R. 52
 Back, M. H. A12
 Baggott, J. E. 22, A35
 Barnes, R. W. B21
 Baronnat, F. 25, B22, B27
 Barrera, B. 4
 Bartkiewicz, E. A51
 Basevich, V. Y. A11
 Basterrechea, J. B10
 Batt, L. B50
 Baulch, D. L. 29
 Behnke, W. A55
 Beltia, F. A15
 Beneventi, L. B2
 Bennett, P. J. A53
 Berces, T. A13, A14, B44
 Bernard, D. M. 45
 Bian, J. B45
 Blesner, J. 37
 Billaud, F. B27
 Black, G. A37
 Blatt, C. S. A32
 Blitz, M. A. A35
 Boettner, J. C. B23
 Booth, J. P. 21
 Borisov, A. A. B17
 Bourmade, N. A38
 Bowes, C. 34
 Boyd, R. B55
 Brauman, J. I. 42
 Bridier, I. 55
 Brovard, M. 36
 Browarzik, R. K. B58
 Brown, M. J. B19
 Brunetti, B. 39
 Brunning, J. A9
 Buccil, V. B24
 Burrows, J. A29
 Candori, R. B1
 Canosa-Mas, C. E. A44, A45
 Caralp, F. A30
 Carlier, M. 28
 Carpenter, P. J. A44
 Carr, R. W. A50
 Casavecchia, P. B2
 Castano, F. A15, A16, B10
 Cathonnet, M. B23
 Canbet, t. 4
 Cavalli, S. A2
 Chachaty, C. A17
 Chnkir, A. B23
 Chambon, M. B26
 Chamboux, J. A17, B41
 Chasovnikov, S. A. 38
 Cheng, Z. B53
 Cheskis, S. G. A19
 Chichinin, A. I. 38
 Clarke, M. P. A46
 Cohen, N. A43
 Come, G. M. 27, B24, B25, B26
 Contreras, T. 40
 Corthouts, J. A34
 Costes, M. B3
 Couzens, P. J. B19
 Cox, R. A. 53
 Dalgarno, A. 16
 Damm, M. 6
 Darvesh, K. B55
 Davidovits, P. 47
 Davidson, I. M. T. A46
 Demange, E. B24
 Derrick, P. J. 44
 Deson, J. B47
 Devolder, P. 28, A38, A54
 Dillon, M. A46
 Dixon, R. N. 37
 Donlon, M. A39
 Donovan, R. J. 7
 Dorthé, G. 4, B3
 Duguay, B. A7
 Durent, J. L. 2
 Eaton, G. A46
 Elofson, P. A. B4
 Elyahyaoui, K. B27
 Ewig, F. 54
 Fahr, A. A20, A21
 Farantos, S. C. B58
 Ferguson, E. E. 17
 Figuera, J. M. B5
 Fontijn, A. 23
 Forgeteg, S. A13
 Forst, W. A1, A30
 Fors, M. A51
 Fotakis, C. B58
 Frericha, H. B42
 Frey, H. M. 22, A35
 Frost, M. J. A9
 Fuentes, M. B5
 Furue, H. A6
 Gaillard, F. B23
 Gardner, J. 47
 Genske, P. B20
 Gershenzon, Y. M. B59
 Giardini-Guidoni, A. B35
 Gilbert, R. G. 11

Ginty, J. C. B24	Herron, J. T. A24, A25	Kaufmann, M. B30	Lisjanskij, V. V. B17
Giovannucci, P. A. B12, B14	Herzog, B. B53	Kenner, R. D. B58	Liuti, G. B1
Golde, M. F. B6	Heydtmann, H. A26	Kerr, J. A. A53	Louage, F. A5
Golden, D. M. 13, 46, A22, B34	Hippler, H. 6, B51	Keyser, L. F. 48	Lusparyan, A. P. B36
Goldenberg, M. Y. B33	Ho, G. B6	Khan, M. A. B50	Luther, K. 12
Golubkov, G. V. A3	Hoffman, A. 54	King, K. D. 22	
Gontkovskaya, V. T. B37	Holloway, J. S. B57	Klail, S. E. B22	Maas, U. B31
Gonzales, M. D. U. 20	Holmes, A. J. 7	Knjazev, V. D. A10	Maes, D. A31
Gorban, H. 1. B33	Holmild, L. B4	Koffend, J. B. B57	Malacarne, P. A27
Gorgenyi, M. B56	Hontzopoulos, E. B58	Kohse-Höbginghaus, K. B11	Mailard, W. G. A24, A25
Gotts, N. G. 45		Kolb, E. 47	Montashyan, A. A. B32
Gray, P. 24	Ichimura, T. B8	Kortvelyesi, T. B56	Marchais, J. 4
Green, H. J. B. B38	Iogansen, A. A. A19	Kozlov, S. N. A10	Marchant, P. J. B38
Griffiths, J. F. 29	Ivanov, G. K. A3	Krasnoperov, L. N. 38	Marquaire, P. M. 27, B25, B26
Grossi, G. A2	Ivanova, A. V. A4	Kutakov, P. V. A19	Marston, G. 18
Grotheer, H. 9			Marta, F. A14
Gusel'nikov, L. E. B15, B16	Jacobs, A. A27	Lagana, A. 32	Martin, M. P. 27
Gutman, D. 10, A23	Jaegere, S. de A34	Lalo, C. B47	Martinez, E. A15, A16, B10
	Japar, S. M. B49	Langridge-Smith, P. R. R. 7	Martinez, M. T. 36, B10
Halvick, P. A7	Jayne, J. 47	Laszlo, B. A13	Mesamet, J. B47
Hancock, G. 21, B7	Jayawera, I. S. 14	Laufer, A. H. A20	Mesam, R. 43
Hansel, A. 17	Jeffries, J. B. B34	Lazarou, Y. B54	McConstra, M. R. S. B12, B13, B14
Harrison, J. A41	Jenkin, M. E. 51, 53	Le Bec, R. 27	McMillen, D. F. B34
Heard, E. E. B7	Jorand, F. A17, B41	Le Bras, G. A28, A29	Meier, U. B11
Heidner, R. F. B57	Jorg, A. B11	Lesciaux, R. 55, A30, A47	Mele, A. B35
Heinrich, N. A5	Jourdain, J. L. A28	Leu, M-T. 48	Mellouki, A. A28, A29
Heinrich, P. B58	Jowko, A. A51	Levy, M. R. B9	Meriaux, B. A54
Heiss, A. A18	Jusinski, L. E. A37	Lifshitz, C. A5	Mitchell, T. J. B50
Helvajum, H. B57	Just, T. 9, B11	Lightfoot, P. D. 22, A35, A47	Moise, A. 30
Hemberger, H. F. B28		Linn, X. H. A12	Moore, S. B. A50
Henchman, M. 7	Karnaukh, A. A. B33	Lindinger, W. 17	Muortgat, G. K. 51, A29

Morley, C. B50	Pauwels, J. 28, A38	Riehn, C. 6	Siegel, W. O. B49
Morokuma, K. 31	Payne, W. A. A42	Rigny, R. A18	Simon, F. 51
Morris, R. A. 19	Peeters, J. A31	Robertson, R. M. 13	Simon, Y. 25
Muller, C. B24	Peragudov, A. N. B37	Robertson, S. H. B38	Simons, J. P. 36
Muller-Varkgraf, W. A22	Perry, N. 21	Rodriguez, J. C. B5	Simpson, V. J. A40
Munz, J. A40	Pfab, J. B12, B13, B14	Rohrer, F. B58	Sims, J. R. 3
	Pilling, M. J. 8, A56, B38	Rosa, M. A51	Singer, R. A29
Nacsa, A. B56	Pirani, F. B1	Roscoe, J. M. A32, B40	Skachkov, G. I. B17
Naibandyan, A. B. B36	Pitts, J. N. 52	Roscoe, S. G. A32	Skewes, L. M. B49
Naulin, C. B3	Pitz, W. J. 26, B39	Rossi, M. J. 13, 46, A22	Slagle, I. R. 10
Nesbitt, F. L. 18, A42	Plane, J. M. C. 5	Rozenshtein, V. B. B59	Smith, P. 17
Nicovich, J. M. 50	Polanyi, J. C. Polanyi Memorial Lecture	Rusakov, S. A. B17	Smith, D. B. B19
		Russell, J. J. A23	Smith, I. W. M. 3, A8, A9
Nielsen, O. J. A39	Poulet, G. A29		Smith, S. C. 11
Nigenda, S. E. B34	Poxon, M. B20	Sahetchian, K. A. A17, A18, B41	Smith, S. J. A44, A45
Nikitin, E. E. 15	Pratt, G. L. B21	Salouhi, M. B25	Sochet, L. 28
Nishi, N. B8	Preidel M. A52	Sarkisov, O. M. A19	Sperlein, R. P. B6
Nolling, F. A55	Pritchard, H. O. 30	Sawerysyn, J. P. A38, A54	Stace, A. J. 45
Norfolk, D. J. 20	Puyuelo, P. B10	Scacchi, G. 25, B24	Stark, M. A41
		Schillephake, V. B42	Steckler, R. 33
O'Farrell, D. A39	Rabonos, V. S. 40	Schneider, L. 37	Stein, S. E. A21
Oganesyan, E. A. B36	Rajasekhar, B. 5	Schneider, M. B29	Stewart, P. H. B34
O'Mahony, J. 36	Ravishankara, A. R. 49, A48	Schneider, W. 51	Stief, L. J. 18, A42
	Raybone, D. A36	Schwarz, H. A5	Stolte, S. 41
Pacey, P. D. 14, A6, B55	Rayez, J. C. A7, A30	Seakins, P. W. A56	Stranges, D. B35
Pack, K. T. 32	Rayez, M. T. A7, A30	Seetula, J. A. A23	Stuhl, F. B58
Pagsberg, P. A40, B20	Razuvaev, I. Y. A19	Seres, L. B56	Sykes, A. F. 29
Papagiannakopoulos, P. B54	Rebeiro, C. S. B40	Shackelford, C. J. 50	Szmanowicz, M. A51
Peppin, A. J. 29	Rehs, K. 12	Shevelkova, L. V. B16	Symonds, A. 12
Parker, G. A. 32	Reimer, A. B48	Shinohara, H. B8	
Patrick R. A37	Richter, R. 17	Sidebottom, H. W. A39	
Paulson, J. F. 17, 19	Ridley, T. 7		Tao, W. B6

Tappe, M. B42	Veyret, R. 55, A47	Worsdörfer, U. A26
Tardieu de Maleissye, J. B47	Vinckler, C. A34	Worsnop, D. K. 47
Teghil, R. B35	Vigliano, A. A. 19	Wu, C. H. B49
Teitelbaum, H. 34, B52, B53	Viossat, V. A17, B41	Wylie, I. B40
Teitelbaum, M. A. B32, B33	Vlahoyannis, Y. P. B58	
Thang, L. 30	Volkova, V. V. B16	Xie, X. 37
Tighezza, A. A54	Volina, E. A. B15	
Titov, A. A. A19	Volpi, G. G. B2	Yabushita, S. 31
Toby, P. S. B43		Yamashita, K. 31
Tobert, M. A. 46	Waddington, D. J. B19	Yates, A. H. B13
Toogood, M. 21	Wagner, A. F. 10, 33, A49	Young, V. M. B13
Treacy, J. A39	Wahl, M. A27	
Troe, J. 6, B51, B52	Wallington, T. J. B49	Zabel, F. B48
Tully, F. P. 2, A33	Walsh, R. 22, A35	Zahniser, M. S. 47
Turanyi, T. B44	Walter, D. 9	Zalotai, L. A14
Tyndall, G. S. A48	Wardlaw, D. M. A49	Zemanski, V. M. B17
	Warnatz, J. B31	Zarate, A. O. de A16
	Watkinson, T. M. A36	Zare, R. N. 1
Watson, L. 47		Zellner, R. 54, A52
Wanski, S. Y. 15	Watts, I. M. 22	Zellweger, J. M. B34
Urena, A. G. 40	Waygood, S. J. A45	Zetzsch, C. A55
Wayne, R. P. A44, A45		Zewail, A. H. 35
Vandooren, J. B45	Weige, K. H. 37	Ziegler, U. B16
Vnn Doren, J. M. 47	Weller, R. A27	Zimmerman, G. B16
Van Tiggelein, P. J. B45	Westbrook, C. K. 26, B39	
Vardanyan, I. A. B36	Whitehead, J. C. A36	
Vartazaryan, A. S. A3	Wine, P. H. 50	
Vecchiocattivi, F. 39	Winterbottom, F. A36	
Vedenev, V. I. A10, A11, B32, B33	Wojciechowski, K. A51	
Vegiri, A. B58	Wolfrum, J. A27, B28, B29	
Verdasco, E. 40	Wood, S. W. B46	

END